MODULATION OF VIRULENCE FACTORS IN BIOFILM-FORMING *KLEBSIELLA PNEUMONIAE* VIA SELECTED SOUTH AFRICAN MEDICINAL PLANTS AND PHYTOCHEMICAL COMPOUNDS

By

IDOWU JESULAYOMI ADEOSUN

21747050

Supervisor: Dr. Sekelwa Cosa

Submitted in fulfilment (*for Ph.D. by research*) of the requirements for the degree

DOCTOR OF PHILOSOPHY: MICROBIOLOGY

in the

Department of Biochemistry, Genetics, and Microbiology

FACULTY OF NATURAL AND AGRICULTURAL SCIENCES

UNIVERSITY OF PRETORIA

June 2023

DECLARATION

I, Idowu Jesulayomi Adeosun declare that this thesis titled “Modulation of virulence factors in biofilm-forming *Klebsiella pneumoniae* via selected South African medicinal plants and phytochemical compounds”, which I hereby submit for the degree of Doctor of Philosophy in Microbiology at the University of Pretoria, is my own work and has not previously been submitted by me for a degree at this or any other tertiary institution.

Signature: ……

Date: ……

DEDICATION

This research work is dedicated to God Almighty, the giver of strength, courage, and wisdom. Indeed, He is the Alpha and the Omega.

"Patience, persistence and perspiration makes an unbeatable combination for success".

Napoleon Hill.

ACKNOWLEDGEMENTS

First, I would like to acknowledge the Almighty God through whom all blessings flow, for bestowing me with life, strength, wisdom, and an excellent spirit.

I would love to sincerely appreciate my supervisor (Dr. S. Cosa) for the guidance, mentorship, and the great supervisory role she played to ensure the success of my research project. Asides academic mentorship, her sessions of advice on navigating my career path and other phases of life has helped me a great deal. Indeed, working under her supervision has helped me to improve my time management skills, communication skills, resilience, ability to pay attention to details, flexibility, adaptability, stress tolerance and management, as well as leadership skills. I can undoubtedly say that I have successfully grown to be a better version of myself under her mentorship.

I hereby acknowledge the Centre for High Performance Computing (CHPC) for providing the platform for molecular docking and molecular dynamics simulations. Mr. Jason Samspon for assistance with the collection of plant samples and Ms. Magda Nel for assistance with identification of the plants and issuance of voucher specimen numbers. Erna and Charity at the Microscopy unit for assisting me while carrying out my microscopy analysis. Prof. Almuth Hammerbacher for assisting with the chemical profiling of my plants. Prof. Lucy Moleleki, Dr. Jane Chepsergon and Miss Celiwe Innocentia Nxumalo for guidance with molecular assays. Dr. Elliasu Yakubu and Dr. Aimen Aljoundi for assistance with molecular dynamics simulations. NextGen Health Unit at the Council for Scientific and Industrial Research (CSIR), South Africa, for supplying the hypervirulent *Klebsiella pneumoniae* strains used in this study.

A big thank you to Dr. Rebamang Mosa for keeping tabs on my progress and for the timely words of encouragement, also to my lab mates (Lab 9-37) for their support.
To my amazing parents and jewels of inestimable value, Dcn and Dcns. J.O.A Adeosun, thank you so much for being there every step of the way and for your continuous support, timely words of encouragement and ceaseless prayers.

Special thanks to my best friend, lover, encourager and support system, Engr. Victor Oluwatobi Ajayi for being by my side through thick and thin and helping me overcome frustration on days when results seemed not to be forthcoming. For helping me hold

my head high in moments when the chips were down and for constantly reassuring me of my indefatigable strength and worth, you are the best.

My sincere gratitude also goes to my siblings, for believing so much in me, encouraging me at every point in time and always praying for me.

Finally, I would like to acknowledge the South African Medical Research Council (SAMRC) for funding this research and the University of Pretoria for awarding me the prestigious Commonwealth scholarship for my doctoral studies.

RESEARCH OUTPUTS: ARTICLES

1. **Adeosun, I.J.,** Baloyi, I.T, Aljoundi, A. K., Elliasu Y., Ibrahim, M and Cosa, S. (2022). Molecular modelling of SdiA protein by selected flavonoid and terpenes compounds to attenuate virulence in *Klebsiella pneumoniae*. *Journal of Biomolecular Structure and Dynamics*, 0, 1–19**.** *https://doi.org/10.1080/07391102.2022.2148753*

2. **Adeosun, I.J.,** Baloyi, I.T and Cosa, S. (2022). Anti-biofilm and associated anti-virulence activities of selected phytochemical compounds against *Klebsiella pneumoniae. Plants,* 11, 1–20. *https://doi.org/10.3390/plants11111429*

3. **Adeosun, I.J.,** Baloyi, I.T., Moleleki L.N and Cosa, S. Extracts of selected South African medicinal plants mitigate virulence factors in multidrug resistant strains of *Klebsiella pneumoniae.* Currently under review by Evidence-Based Complementary and Alternative Medicine (ID: 3146588).

4. **Adeosun, I.J.,** Baloyi, I.T., Bonvicini, F., Moleleki L.N and Cosa, S. Quantification of virulence gene expression in *Klebsiella pneumoniae* and safety assessment of phytochemical compounds (Manuscript in preparation). To be submitted to Phytotherapy Research.

5. **Adeosun, I.J.,** Baloyi, I.T., Motaung, T.E and Cosa, S. South African medicinal plants: a promising source of mitigating quorum sensing and virulence induced by *Klebsiella pneumoniae* (Manuscript in preparation). To be submitted to Phytochemistry Reviews.

CONFERENCE CONTRIBUTIONS AND WORKSHOPS

1. **Adeosun, I.J**., Baloyi, I.T, Aljoundi, A. K., Elliasu Y., Ibrahim, M. A., and Cosa, S. Molecular modelling of SdiA protein by selected flavonoids and terpenes compounds to attenuate virulence in *Klebsiella pneumoniae* at the 8th Annual International Remote Conference: Science and Society, Toronto, Canada. February 25-26, March 18, 2023 [Virtual presentation].

2. **Adeosun, I.J**., Baloyi, I.T and Cosa, S. Anti-biofilm and associated anti-virulence activities of selected phytochemical compounds against *Klebsiella pneumoniae* at the 1st International conference: Plants research: from phytochemistry to phytoactivity. Kaunas, 21st April 2023 [Oral presentation].

3. Workshop on basic DNA Sanger sequencing. 15th and 17th March 2023.

4. Workshop on basics of computer-aided drug discovery, molecular docking, and biomolecular interactions. 7th -10th June 2021.

5. Workshop on advanced molecular dynamics simulations using AMBER. 16th -19th August 2021.

PREFACE

Prior to this investigation, a foreknowledge of the subject was acquired through a critical review of literature. Thereafter, a good quality research was undertaken to bridge the research gap and augment the knowledge base in this area of research. This study has been meticulously compiled into thesis chapters, which not only elucidate the existing knowledge from literature, but also organize the interesting findings from this research into experimental chapters.

In **chapter one**, a concise summary is provided based on an extensive literature search about the exciting bacterial social media network (quorum sensing) and the systems used for the bacterial cell-to-cell communication. The review further discusses virulence in *K. pneumoniae,* inhibition of quorum sensing and associated virulence factors in *K. pneumoniae,* the potentials of medicinal plants as a source of drugs and quorum sensing inhibitors (QSIs), South African medicinal plants as treatment options for *K. pneumoniae* infections, and *in-silico* techniques for screening and identifying QSIs in medicinal plants.

Chapter two presents an experimental chapter which involves exploring three selected South African medicinal plants (*Lippia javanica, Helichrysum populifolium* and *Carpobrotus dimidiatus),* for their antivirulence activities against two hypervirulent *K. pneumoniae* strains (Carbapenem resistant (CBR) and extended spectrum beta-lactamase (ESBL) producing strains). These plants have received relatively little attention and it is unclear if they contain phytochemicals that could be effective in mitigating virulence factors in hypervirulent *K. pneumoniae*. Thus, they were examined for their inhibitory activities against *K. pneumoniae's* virulence factors. A better understanding of the chemical profiling of the plants was acquired to identify potential bioactive compounds in the plants.

Chapter three explores the structure-activity relationship between the phytochemical compounds profiled from the studied medicinal plants and the transcriptional regulator protein (SdiA) in *K. pneumoniae,* thereby providing answers to the research question of which phytochemical compounds can modulate the virulence-associated protein. This involved the use of computer-based techniques for the virtual screening of the different classes of compounds which employed molecular modelling approach as well as pharmacokinetics study for the assessment of their drug-likeness properties.

Chapter four validates the *in-silico* findings through assessment of the *in-vitro* effect of the phytochemical compounds in inhibiting biofilms and associated virulence factors in CBR and ESBL producing *K. pneumoniae* strains. To further substantiate the findings from traditional techniques, this chapter describes the quantification of virulence genes expression in the studied *K. pneumoniae* strains following treatment with the prospective antivirulence/antipathogenic compounds using molecular techniques. The biosafety of the promising compounds against *K. pneumoniae strains* was also assessed to determine whether the compounds will have any toxic effect on non-malignant mammalian cells.

Chapter five summarizes the findings from the study, achievements of objectives, general conclusions, contribution of the study, the study limitations as well as recommendations. Overall, this study made a valuable contribution to finding solutions to the challenges posed by highly virulent and drug-resistant *K. pneumoniae* strains by exploring plant extracts utilized in traditional medicine and their phytochemical compounds.

ABSTRACT

The emergence of multidrug resistant (MDR) *Klebsiella pneumoniae* has become a growing public health concern across the globe, due to its significant role as a causative agent of severe nosocomial and community acquired infections. Carbapenem-resistant (CBR) and extended spectrum beta lactamase (ESBL) producing *K. pneumoniae* strains, classified as MDR have been identified as the major causes of severe infections in humans. These strains often exhibit hypervirulent characteristics and pose a threat to treatment options due to their resistance to almost all classes of antibiotics, including the last line resorts. The identification of plant-based treatment options to target virulence factors of this pathogen is therefore a priority. Hence, this research was undertaken to explore the antibacterial and antivirulence properties, molecular modelling, virulence gene expression and safety use of bioactive South African medicinal plants and their metabolites against CBR and ESBL producing *K. pneumoniae* strains.

Three South African medicinal plants namely *Carpobrotus dimidiatus, Helichrysum populifolium* and *Lippia javanica* were selected based on their therapeutic use for various *K. pneumoniae* associated infections. The plant extracts (ethyl acetate, dichloromethane, methanol, and water) were validated for their inhibitory activities against bacterial growth and virulence factors such as biofilm formation, exopolysaccharide (EPS) production, curli expression and hypermucoviscosity. The potent extract on *K. pneumoniae* biofilm was observed with a scanning electron microscope (SEM) while exopolysaccharide topography and surface parameters were observed using atomic force microscopy (AFM). Chemical profiling of the potent extract *in-vitro* was analysed using liquid chromatography-mass spectrometry (LC-MS).

Virtual screening of selected compounds from the medicinal plants was carried out to interrupt the QS-associated SdiA transcriptional regulator protein in *K. pneumoniae* and attenuate its virulence. The crystal structure of SdiA, previously reported in *E. coli* as PDB ID: 4LFU was used as a template to model the structure of SdiA, serving as a prototype to search for compounds that could inhibit intercommunication and associated virulence activities. ProCheck, Verify3D, Ramachandran plot scores, and ProSA-Web all attested to the model's good quality. Since SdiA protein in *K. pneumoniae* leads to the expression of virulence, 31 selected prospective bioactive compounds were docked against the SdiA modelled protein for antagonistic potential.

The stability of the protein-ligand complex, atomic motions and inter-atomic interactions were further investigated through molecular dynamics simulations (MDS) at 100 ns production runs. The binding free energy was estimated using the molecular mechanics/poisson-boltzmann surface area (MM/PB-SA). The drug-likeness properties of the studied compounds were also validated.

The promising phytochemical compounds (alpha-terpinene, camphene, fisetin, glycitein and phytol) were further evaluated *in-vitro* for their antibacterial and anti-biofilm associated virulence factors. Furthermore, the expression level of *K. pneumoniae* virulence genes after subjection to treatment with phytochemical compounds was determined using the Quantitative Real-Time PCR (qPCR). Cell viability and cytotoxicity activity of the studied compounds were assessed using African monkey kidney Vero cells.

The antibacterial activity results revealed a noteworthy minimum inhibitory concentration (MIC) value for the *C. dimidiatus* dichloromethane extract at 0.78 mg/mL on CBR-*K. pneumoniae*. With regards to the virulence factors, *L. javanica* (ethyl acetate) showed the highest inhibition (67.25%) of the first biofilm stage-initial cell attachment for CBR-*K. pneumoniae.* Observations from the scanning electron microscope used for the *in-situ* visualization of the biofilms correlated the *in-vitro* findings, evidenced by a significant alteration of the biofilm architecture. Results of the EPS reduction assay, another virulence factor targeted in *K. pneumoniae* revealed the highest reduction of 34.18% for *L. javanica* (ethyl acetate), which was correlated by noticeable changes in the EPS surface topology as observed using atomic force microscope. Hypermucoviscosity, a phenotype which often characterizes hypervirulent *K. pneumoniae* was also reduced by *L. javanica* (ethyl acetate) to the least length mucoid string (1mm - 2mm) at 1mg/mL on both strains. Furthermore, curli expression often implicated with cell aggregation was inhibited by *C. dimidiatus* (aqueous) at 0.5 mg/mL in both *K. pneumoniae* strains. Chemical profiling of *L. javanica* (ethyl acetate), *C. dimidiatus* (aqueous) and *H. populifolium* (aqueous) identified diterpene (10.29%), hydroxy-dimethoxyflavone (10.24%) and 4,5-Dicaffeoylquinic acid (13.41%) respectively as dominant compounds.

Molecular docking studies showed that phytol and glycitein possess the highest binding affinity of -9.205 kcal/mol and -9.752 kcal/mol for terpenes and flavonoids, respectively. The MDS of the protein in complex with the best-docked compounds revealed phytol with the highest binding energy of -44.2625 kcal/mol, a low root-mean-

square deviation (RMSD) value of 1.54 Å and a root-mean-square fluctuation (RMSF) score of 1.78 Å. Analysis of the drug-likeness properties prediction and bioavailability of these compounds revealed their conformed activity to Lipinski's rules with bioavailability scores of 0.55 F.

In-vitro assessment of the compounds revealed fisetin as the best anti-CBR-*K. pneumoniae*, demonstrating MIC value of 0.0625 mg/mL. Phytol, glycitein and α-terpinene showed MIC values of 0.125 mg/mL for both strains. The assessment of the compounds for anti-virulence activity (exopolysaccharide reduction) revealed up to 65.91% reduction in phytol and camphene while phytol also showed the highest antiadhesion activity against CBR and ESBL- *K. pneumoniae* (54.71% and 50.05%), respectively. The expression levels of *mrkA, rcsA* and *luxS* genes in treated *K. pneumoniae* strains revealed fold expression ratio ranging between 0.607 (60.7%) and 1.00 (100%). *MrkA* gene targeted with phytol and *rcsA* gene targeted with camphene in CBR-*K. pneumoniae* strain revealed reduced fold expression values of 0.662 (66.2%) and 0.722 (72.2%), respectively compared to the untreated strain (*16S rRNA* as control) which revealed the value of 1.00 (100%). Phytol was shown to have no cytotoxic effect on the Vero cells whilst maintaining approximately 100% ($p < 0.05$) of the cell's viability even at the highest tested concentration (0.25 mg/mL). The measured lactate dehydrogenase (LDH) activity showed that most of the tested compounds did not cause cell death in a dose-dependent manner.

Overall, findings from this study revealed that the studied medicinal plants are not only rich sources of bioactive compounds but also possess antibacterial and antivirulence activities, with *L. javanica* (ethyl acetate) displaying the most remarkable activity. Secondary metabolites of the studied plants belonging to the terpene and flavonoids classes were also shown to reveal good binding affinities and high binding energies when bound to the transcriptional SdiA receptor which modulates biofilm formation and other virulence factors in *K. pneumoniae*. *In-vitro* antivirulence activities of the compounds revealed phytol to be the most potent antivirulence antibiofilm agent and was observed alongside camphene to downregulate the expression of *mrkA* and *rcsA* genes respectively. Phytol further revealed no cytotoxic effect on Vero cells while camphene revealed significant cell viability. The entire findings from this study presents the potent medicinal plants and compounds as promising leads for the development of novel drugs in the management of hypervirulent *K. pneumoniae* infections.

TABLE OF CONTENT

LIST OF FIGURES

LIST OF TABLES

LIST OF APPENDICES

LIST OF WEBSERVERS

CASTp 3.0	http://sts.bioe.uic.edu/castp/index.html?2r7g
Clustal Omega	https://www.ebi.ac.uk/Tools/msa/clustalo/
NCBI	https://www.ncbi.nlm.nih.gov/cdd/
PDB	https://www.rcsb.org/
PDBsum	http://www.ebi.ac.uk/thornton-srv/databases/pdbsum/
Primer3Plus	https://www.bioinformatics.nl/cgi-bin/primer3plus/primer3plus.cgi
ProsaWeb	https://prosa.services.came.sbg.ac.at/prosa.php
PSVS	http://psvs-1_5-dev.nesg.org/
Pubchem	https://pubchem.ncbi.nlm.nih.gov/
SMS	https://www.bioinformatics.org/sms2/pcr_products.html
SwissADME	http://www.swissadme.ch/index.php
Swiss Model	https://swissmodel.expasy.org/interactive

LIST OF ABBREVIATIONS

AFM	Atomic force microscopy
AHLs	Acyl-homoserine lactones
AIs	Autoinducers
AI-2	Autoinducer-2
ANOVA	Analysis of variance
AQS	Anti-quorum sensing
ATCC	American type culture collection
ATP	Adenosine triphosphate
BA	Blood agar
BHIA	Brain-heart infusion agar
BBB	Blood-brain barrier
CBR	Carbapenem resistant
CCK	Cell counting kit
cDNA	Copy DNA
CFU	Colony forming unit
CHPC	Centre for high performance computing
CLSI	Clinical and laboratory standards institute
CPS	Capsular polysaccharide
CSIR	Council for scientific and industrial research
Ct	Cycle threshold
CV	Crystal violet
DNA	Deoxyribonucleic acid
DCM	Dichloromethane
DMSO	Dimethyl sulfoxide
EPS	Exopolysaccharides
ESBL	Extended spectrum beta lactamase
ESI	Electrospray ionization

ESKAPE	*Enterococcus faecium*, *Staphylococcus aureus*, *Klebsiella pneumoniae*, *Acinetobacter baumannii*, *Pseudomonas aeruginosa*, and *Enterobacter* spp
GI	Gastrointestinal
GNB	Gram-negative bacteria
GPU	Graphic processing unit
HMDS	Hexamethyldisilazane
hvKP	Hypervirulent *Klebsiella pneumoniae*
INT	Iodonitrotetrazolium
LBA	Luria Bertani agar
LBB	Luria Bertani broth
LC-MS	Liquid chromatography-mass spectrophotometry
LDH	Lactate dehydrogenase enzyme
LPS	Lipopolysaccharide
MIC	Minimum inhibitory concentration
MD	Molecular docking
MDS	Molecular dynamics simulation
MDR	Multi-drug resistant
MHB	Mueller Hinton broth
MM/PB-SA	Molecular mechanics/poisson-boltzmann surface area
MMV	Molegro molecular viewer
OD	Optical density
OMPs	Outer membrane proteins
PAINS	Pan assay interference compounds
PDB	Protein data bank
PBS	Phosphate-buffered saline
pH	Potential of hydrogen
QS	Quorum-sensing

QSI	Quorum sensing inhibition
QSIs	Quorum sensing inhibitors
QSS	Quorum-sensing systems
QTOF	Quadrupole time of flight
RNA	Ribonucleic acid
RHC	Ribosylhomocysteine
RMSD	Root-mean-square deviation
RMSF	Root-mean-square fluctuation
SAH	S-adenosylhomocysteine
SAM	S-adenosylmethionine
SAMRC	South African Medical Research Council
SAR	Structure-activity relationship
SAS	Statistical analysis system
SdiA	Suppressor of cell division
SEM	Scanning electron microscope
SI	Selectivity index
SRH	S-ribosylhomocysteine
THMF	Tetrahydroxytetrahydrofuran
TIC	Total ion chromatogram
TPSA	Topological polar surface area
UPLC	Ultra performance liquid chromatography
UTIs	Urinary tract infections
VS	Virtual screening
WST	Water-soluble tetrazolium salt
WHO	World Health Organization

CHAPTER ONE

GENERAL INTRODUCTION AND LITERATURE REVIEW

1.1 Introduction

Klebsiella pneumoniae, a Gram-negative bacteria belonging to the *Enterobacteriaceae* family has emerged as one of the most antibiotic-resistant pathogens responsible for outbreaks in both community and clinical settings (Santajit & Indrawattana, 2016). According to the classification of pathogens by the World Health Organization (WHO) on February 27, 2017, *K. pneumoniae* was categorized under the critical priority list for the research and development of new antibiotics (Talebi et al., 2019). This is because it has been identified as a healthcare and community burden, with a high prevalence of resistance and a leading cause of death (Ventola, 2015). *K. pneumoniae* is usually known for its opportunistic nature and ability to frequently cause nosocomial infections. According to Navon-Venezia et al. (2017), it is implicated in one-third of all Gram-negative infections, which includes urinary tract infections (UTIs), cystitis, pneumonia, surgical site infections, endocarditis, bacteraemia, septicaemia, necrotizing pneumonia, pyogenic liver abscesses, endogenous endophthalmitis, among others (Balestrino et al., 2005). High mortality rates, extended hospitalization, and high costs are often associated with infections caused by this organism (Tumbarello et al., 2006). These infections are attributed to the highly virulent nature of *K. pneumoniae*, enhanced by its quorum sensing ability.

Quorum sensing (QS) is a bacterial cell-to-cell communication which uses signalling molecules in a high bacterial cell population density (Eberl & Riedel, 2011). It modulates several virulence factors in *K. pneumoniae* such as biofilm formation, production of lipopolysaccharides, exopolysaccharides, siderophores and capsule formation (De Araujo et al., 2010). The afore mentioned virulence factors often enhance the degree of pathogenicity in *K. pneumoniae*, thereby posing greater threat to human health. This threat can be attributed to the emergence of MDR strains of *K. pneumoniae* which diminish the effectiveness of antibiotics and exhibit continuous selective pressure due to the continuous exposure to multiple antibiotics (Ashayeri-Panah et al., 2014; Patro & Rathinavelan, 2019). Because of the above-mentioned reasons and other, QS enhances bacterial resistance, thereby enabling a formation of stable communities of microorganisms (Odularu et al., 2022). QS activities of *K. pneumoniae* often modulate its ability to escape the action of almost all available antibiotics, hence, it has been documented as one of the worrying and ESKAPE pathogens (*Enterococcus faecium, Staphylococcus aureus, Klebsiella pneumoniae,*

Acinetobacter baumanni, Pseudomonas aeruginosa and *Enterobacter* species) (Boucher et al., 2009). The alarming rate of antibiotic resistance in *K. pneumoniae* remains a global health threat.

According to WHO in Shaik et al. (2014), medicinal plants and their secondary metabolites can be the best source to obtain a variety of drugs. Natural treatment option such as the use of medicinal plants needs to be evaluated and implemented through clinical and biological trials. Since medicinal plants contain diverse phytochemical compounds belonging to different classes such as flavonoids, terpenoids, tannins, phenolics, alkaloids and saponin glycosides, it has become important to explore their quorum-sensing inhibitory (QSI) potentials. These compounds are abundant in plants, and they have shown antibacterial activities *in-vitro,* hence, suggesting their potentials to thwart virulent factors of *K. pneumoniae.*

1.2 Literature review

Prior to the execution of this research, an in-depth search of related literature was conducted to provide a succinct overview of the bacterial social media network (quorum sensing), particularly in *K. pneumoniae,* the impact of the pathogens' associated virulence factors, and QSI as a plausible strategy to mitigate virulence in *K. pneumoniae.* Moreover, since the South African medicinal plants are implicated and documented in literature as treatment options for *K. pneumoniae* infections, a few of these medicinal plants are reviewed as prospective source of antivirulence drug candidates and QSIs. Furthermore, the *in-silico* techniques for screening and identifying QSIs in medicinal plants were studied.

1.2.1 The bacterial social media network known as quorum sensing

Quorum sensing (QS) can be attributed to bacterial social media networks where signal molecules called autoinducers (AIs) accumulate in the environment based on population density (Quecan et al., 2019). QS is accepted as bacterial social media network due to the coordinated behaviours conducted amongst the bacteria in inter- and or intra- communication. QS not only improves bacterial pathogenicity, but it also improves their ability to infect and harm their host, hence QS disruption has been suggested as a new anti-infective strategy (Defoirdt et al., 2010). Previous authors have reported that QS modulates the expression of virulence factors and the

production of extracellular enzymes in many bacteria (Quecan et al., 2019; Skandamis & Nychas, 2012). QS also controls bioluminescence, plasmid transfer as well as secondary metabolite production in bacteria by regulating gene expression (Aliyu et al., 2016).

QS is frequently connected to antibiotic resistance, biofilm formation, persistent immune system defense, changes in motility as well as production of hydrolytic enzymes, toxins, and polysaccharides (Cadavid et al., 2018). The QS pathways have been classified based on the chemical nature of the signal molecules that operate the system. They include LuxI-LuxR system/autoinducer-1, LuxS/autoinducer 2 system, LuxI-LuxR system/autoinducer-1 and autoinducer 3 system (Al-khayyat, 2018). There are two primary classes of autoinducers, which are described by two systems, Type I QS and Type II QS (Chen et al., 2020; Pereira et al., 2013).

The two primary signaling molecules in the QS system includes the autoinducer-1 N-acyl homoserine lactone (AHL) (Type I QS), commonly utilized by most Gram-negative bacteria (GNB) and the autoinducer-2 (Type II QS), an oligopeptide-based system usually employed by most Gram-positive bacteria (Yunos et al., 2014). The former has been extensively researched, involving LuxR as a transcriptional activator protein that binds to specific AHL molecules produced by LuxI, the autoinducer synthase (Coquant et al., 2020) (Figure 1.1). In this system, AHL molecules exhibit variations in the length of the N-acyl chain (ranging from 4 to 18 carbons), the degree of saturation, and the number of oxygen substitutions. However, all AHLs share a common L-isomeric form of the homoserine lactone ring. The luxI gene, or its similar counterparts, contains the genetic sequences responsible for the synthesis of AHL signaling molecules (Yunos et al., 2014). AHLs are capable of freely traversing cell membranes. When bacterial population densities are low, only small amounts of AHL are present and get diluted away, causing the genes regulated by QS to remain inactive (Asad & Opal, 2008). However, once a critical threshold of population density concentration is reached, an adequate concentration of AHL builds up and the signal transduction cascade is triggered, enabling the modulation of target genes and facilitating collective behavioral adaptation (Yunos et al., 2014; Coquant et al., 2020) (Figure 1.1).

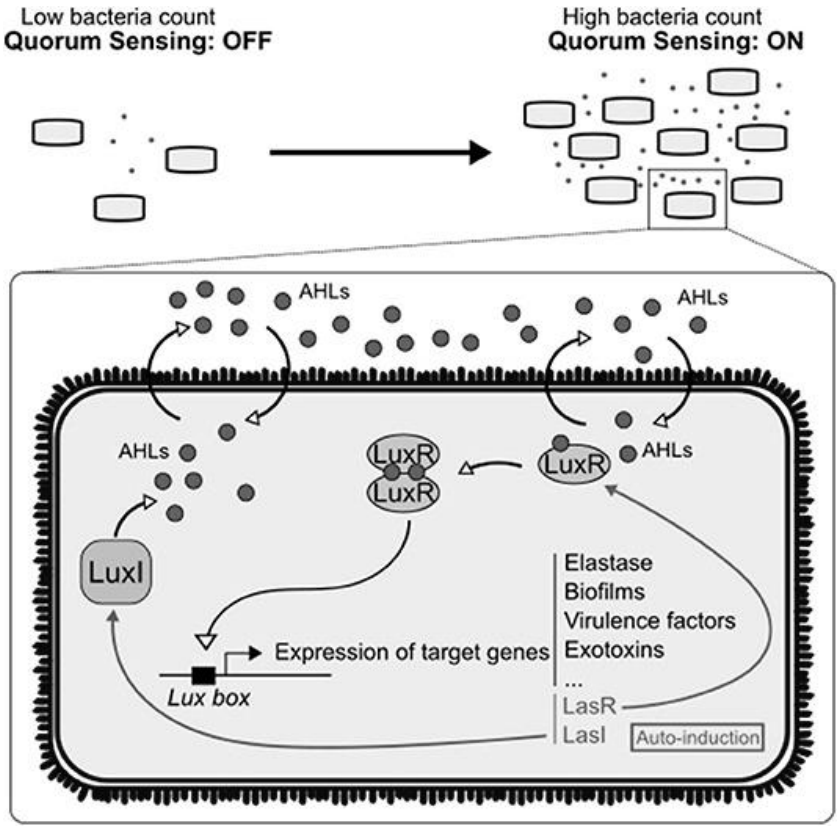

Figure 1.1: LuxR-LuxI/Type I quorum sensing system. Acyl-homomserine lactones (AHLs) are auto-inducers used by Gram-negative bacteria to communicate. The enzyme LuxI synthesizes the AHL, and the latter can diffuse freely through the membrane. Upon reaching a threshold concentration, AHL can bind to its receptor LuxR. The dimerization of the receptor allows it to act as a transcription factor on the Lux box. This triggers not only the expression of target genes involved in the virulence of the bacteria but also the expression of AHL system LuxI/LuxR (Coquant et al., 2020).

On the other hand, the QS Type II functions for interspecies communication, allowing bacteria to respond not only to their AI-2 but also to the AI-2 produced by other species, unlike QS Type I, which is a highly specific system used for intraspecies communication (Chen et al., 2020). The enzyme LuxS produces AI-2, which transforms S-ribosylhomocysteine (SRH) to 4,5-dihydroxy-2,3-pentanedione (DPD). The DPD form is unstable and spontaneously cyclizes to generate the AI-2 molecule (furanosyl borate diester) (Balestrino et al., 2005) which are extracellular signalling molecules that often regulate the quorum sensing system (QSS) (Chen et al., 2020). Because *K. pneumoniae* is a Gram-negative bacterial pathogen, this review will thus focus on the QS in Gram-negative bacteria and further narrow it to discuss the QSS in *Klebsiella pneumoniae* and the associated virulence factors.

In GNB, the transcriptional regulator belonging to the LuxR protein detects the presence of AI known as N-acylhomoserine lactones (AHLs). The AHL molecules are made up of a fatty acid chain connected to a lactone ring by an amide bond. The size and makeup of the fatty acids, which range from 4 to 18 carbons and include various replacements in the chain, are usually the variations that exist between AHL molecules (Quecan et al., 2019; LaSarre & Federle, 2013). QS has been well elucidated in two species of bioluminescent marine bacteria: *Allivibrio fischeri* and *Vibrio harveyi* as well as other model bacteria which include *Chromobacterium violaceum, Pseudomonas aeruginosa, Agrobacterium tumefaciens, Erwinia carotovora,* and *Serratia liquefaciens* (Waters & Bassler, 2005). Some bacteria do not develop AI, yet they can recognize AHLs produced by other bacteria by encoding a LuxR homologue. For example, SdiA (suppressor of cell division inhibition) recognizes AHLs generated by other bacteria. SdiA is a potential therapeutic target because it binds to AHL and causes the transcription of several virulence genes (Pradeep et al., 2018). Because the LuxI homolog is not present in *Klebsiella pneumoniae*, the organism is unable to generate its particular signals and cannot detect signals from other species; but by expressing a LuxR homolog (SdiA), it can detect signal molecules produced by mixed community genera (Tavío et al., 2010). Cell division and the production of virulence factors such as antibiotic resistance, motility, and biofilm formation have been linked to SdiA, a transcriptional regulator in *K. pneumoniae* (Pacheco et al., 2021). There is great interest in studying the QSS of this organism since many of its virulence factors are specifically regulated by QS. Interrupting the QS system in *K. pneumoniae* will render it less or non-virulent and present a novel treatment for various bacterial infections (Cosa et al., 2019).

1.2.2 Signalling communication system in Klebsiella pneumoniae

In recent times, the QSS has unravelled the mechanisms of communication between different bacteria, a mechanism by which these bacteria modulate their activities in their social settings (Cosa et al., 2020; Scoffone et al., 2019). As evidenced by the literature above, the signalling molecules are involved in the regulation of inter and intra-communications between the bacterial cells during the aggregation and formation of biofilm (Pacheco et al., 2021). More so, apart from modulating bacterial behaviours, QS-associated autoinducers may also play a crucial role in the

interactions that exist between the pathogenic microorganisms and their host (Grandclément et al., 2015). Among several pathogenic bacteria, the QSS of *Klebsiella pneumoniae* has received wide attention.

The AI-2 QS system is employed by *K. pneumoniae* (Al-khayyat, 2018), where the communication system responds to cell density via luxS activity to create AI-2. The AI-2 regulates gene expression and other virulence activities such as biofilm development (Chen et al., 2020). *K. pneumoniae* often generates N-octanoylhomoserine lactone (C8-HSL) and N-3-dodecanoyl-L-homoserine lactone (C12-HSL) AHL molecules (Yin et al., 2012). However, *K. pneumoniae* has AI-1-Type QS quenching enzymes and AHL lactonases. The AHL lactonases in prokaryotes are divided into two clusters namely AiiA and AttA. Lactonases from other species share only 30% homology with the *K. pneumoniae* AttA lactonase cluster (Sun et al., 2016). Due to the presence of AHL lactonase in the submerged fermentation of *K. pneumoniae*, AHLs cannot reach the threshold concentration in the culture medium and cannot diffuse back into the cell, hence, cannot be identified by the receptor protein. Therefore, the AHL-receptor protein complex cannot form, and the AHL-mediated QS mechanism in *K. pneumoniae* does not function (Tavío et al., 2010).

However, MetK (which catalyzes the formation of S-adenosylmethionine (AdoMet) from methionine and ATP), pfs (which is involved in methylation processes, polyamine synthesis, vitamin synthesis, and QS pathways), and luxS genes are all found in *K. pneumoniae* (which plays a role in its early stages of biofilm formation) (Al-khayyat, 2018). LuxS is involved in the production of autoinducer 2 (AI-2), a signal molecule secreted by bacterial and used to communicate both cell density and metabolic potential of the environment.

LuxS often catalyzes the conversion of S-ribosylhomocysteine (RHC) to homocysteine (HC) and 4,5-dihydroxy-2,3-pentadione (DPD), all of which encode key enzymes in the synthesis of the signalling molecule AI-2, implying that *K. pneumoniae* uses AI-2 as the signalling molecule in a QS system to regulate group behaviours (Sun et al., 2016). AI-2 is produced from S-adenosylmethionine (SAM) in three stages. In the first stage, SAM acts as a methyl donor for the hazardous intermediate S-adenosylhomocysteine (SAH), which is then hydrolyzed into S-ribosylhomocysteine (SRH) and adenine by the nucleosidase enzyme pfs. LuxS catalyzes the cleavage of SRH to 4,5-dihydroxy 2,3-pentanedione (DPD) and homocysteine in the third step.

DPD is an unstable chemical that recycles, resulting in the formation of the "furanosyl borate diester," which is a group of AI-2 signalling molecules (Al-khayyat, 2018). AI-2 signalling molecules can exist in two isomeric forms of tetrahydroxytetrahydrofuran (THMF) which are R-THMF and S-THMF (Figure 1.2). AI-2 receptor (LuxP) binds to S-THMF-borate, while LsrB (which encodes for autoinducer 2-binding protein) binds to R-THMF, which lacks borate (Torcato et al., 2019).

According to Xavier & Bassler (2003), LuxS is also an essential enzyme involved in the bacterial activated methyl cycle. In this cycle, after methyl transfer from *S-adenosylmethionine* (SAM) to its substrates, S-adenosylhomocysteine (SAH) is produced, which is toxic to the cell thereby, eliminated by Pfs nucleotidase (Figure 1.2). Thereafter, LuxS produces adenine, homocysteine and 4,5-dihydroxy 2,3-pentanedione (DPD), which helps in the formation of the AI-2 signalling molecules (Xue et al., 2016). Thus, the LuxS/AI2 QSS can be said to perform three different functions which include the interspecies cross-talk, modulation of virulence as well as active involvement in metabolic functions (Al-khayyat, 2018).

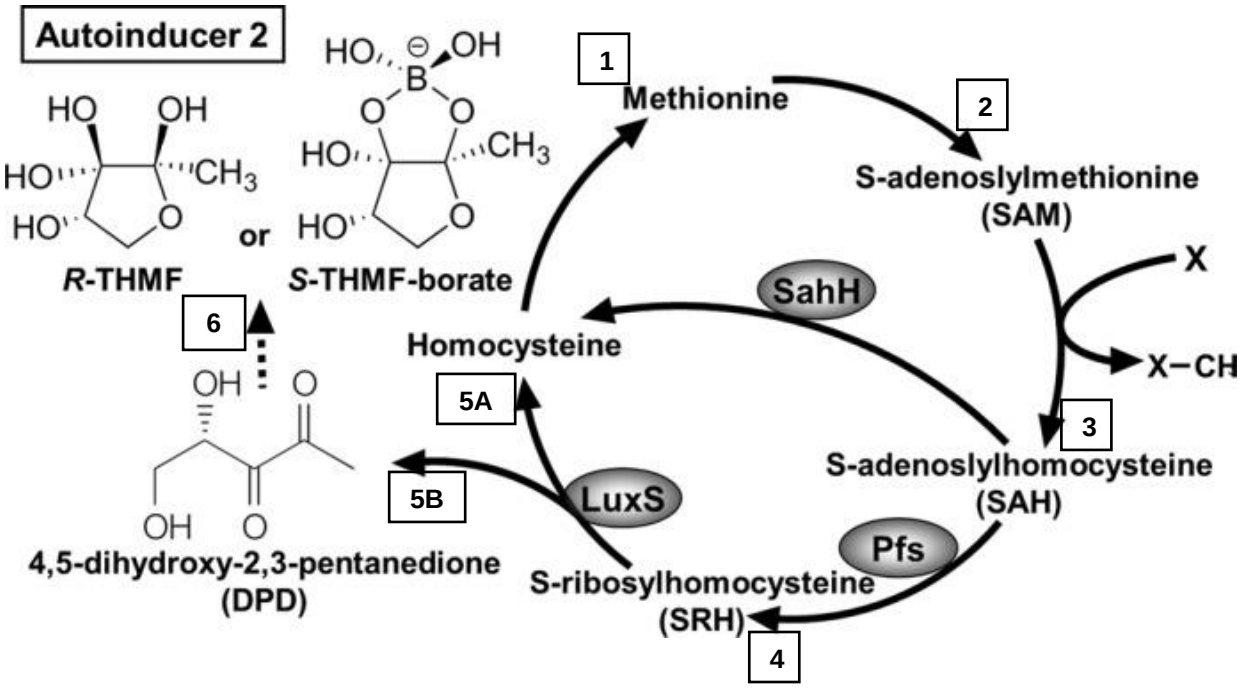

Figure 1.2: Steps involved in AI-2 production. AI-2 signalling molecules can exist in two isomeric forms of tetrahydroxytetrahydrofuran (THMF) which are R-THMF and S-THMF. AI-2 receptor (LuxP) binds to S-THMF-borate, while LsrB (which encodes for autoinducer 2-binding protein) binds to R-THMF, which lacks borate. LuxS is also essential in the bacterial activated methyl cycle. In this cycle, after methyl transfer from *S-adenosylmethionine* (SAM) to its substrates, S-adenosylhomocysteine (SAH) is

produced, which is toxic to the cell thereby, eliminated by Pfs nucleotidase. Thereafter, LuxS produces adenine, homocysteine, and 4,5-dihydroxy 2,3-pentanedione (DPD), which helps in the formation of the AI-2 signalling molecules (Redanz et al., 2012).

In the LuxS/AI-2 QSS, AI-2 enters the cell via an adenosine triphosphate-binding-cassette transporter known as the Lsr transporter. The lsr operon encodes four proteins namely LsrA, LsrB, LsrC, and LsrD, which make up the Lsr transporter (Al-khayyat, 2018). Upon entrance of AI-2 into the bacterial cells, they are phosphorylated by LsrK and modified by LsrF and LsrG. As shown in Figure 1.3, phosphorylated AI-2 binds to the repressor protein LsrR and promotes the transcription of the lsr operon (Al-khayyat, 2018).

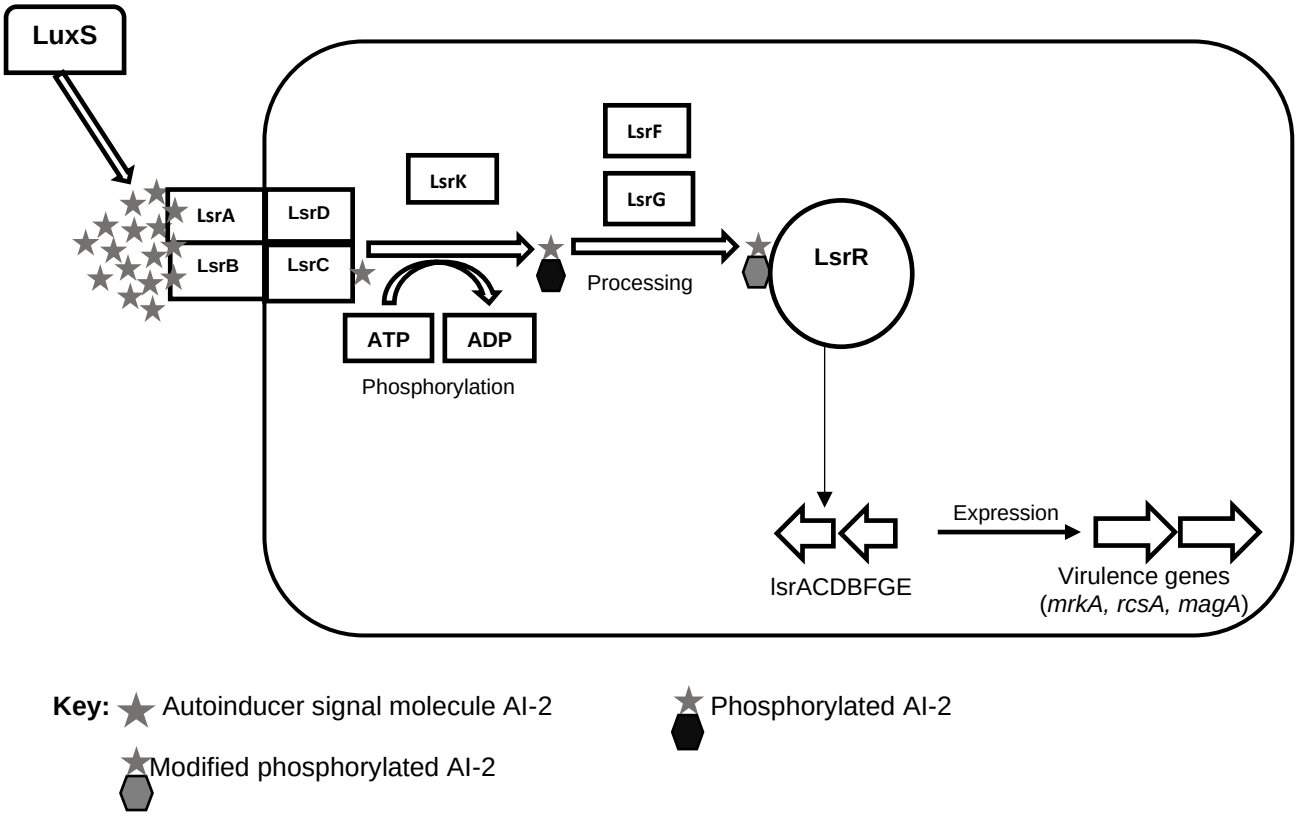

Figure 1.3: Autoinducer-2 System (Modified from Al-khayyat, 2018). Lux S produces autoinducer signal molecule AI-2. When AI-2 reaches a critical extracellular concentration/threshold, it traverses into the cell using the Lsr transporter (constituted by LsrA LsrB, LsrC, and LsrD), where it undergoes phosphorylation by Lsrk. Phosphorylated AI-2 undergoes modification processing by LsrF and LsrG to give a modified phosphorylated AI-2 molecule that binds to the repressor protein LsrR to regulate the Lsr operon, which leads to the expression of virulence genes.

The downstream genes of the Lsr operon (LsrABCD) shown in Figure 1.3 above encodes the Lsr transport apparatus located in the cell membrane, thereby contributing to the overall process of quorum sensing, facilitating intercellular communication and coordination of bacterial behaviours based on cell density (Zuo et al., 2019). While the LsrA helps in coordinating the response of bacterial cells to quorum sensing signals, LsrB is responsible for the uptake and processing of autoinducer molecules from the environment (i.e., the internalization of extracellular AI-2), enabling bacterial cells to sense the presence of other cells and respond accordingly (Taga et al., 2001). Furthermore, LsrC is an autoinducer kinase enzyme which phosphorylates autoinducer molecules, modifying them and preparing them for further processing (Zuo et al., 2019). Moreover, LsrD is involved in the degradation of autoinducer molecules, which helps regulate the quorum sensing response and maintain appropriate autoinducer concentrations in the bacterial environment (Zuo et al., 2019). In addition, during the modification processing (the final step in the processing of the quorum sensing signal AI-2), LsrF gene encodes a coenzyme A-dependent thiolase that catalyzes this step (Taga et al., 2001).

Recent data have confirmed the involvement of the AI-2 QS system in enhancing pathogenicity in *K. pneumoniae* through biofilm formation and other virulence factors (Chen et al., 2020).

1.2.3 Virulence in Klebsiella pneumoniae

Several virulence factors (Figure 1.4) are reported to mediate *K. pneumoniae* infectivity. *K. pneumoniae* also uses these virulence traits to protect itself from the host immune response (Patro & Rathinavelan, 2019). These virulence factors include but are not limited to biofilm formation, adhesins such as pili and fimbriae, antiphagocytic capsule (CPS) production, lipopolysaccharide (LPS), and membrane transporters (Parrott et al., 2021; Clegg & Murphy, 2016), which allows the survival of *K. pneumoniae* and its immune evasion during infection (Vuotto et al., 2017). In addition, hypervirulent strains of *K. pneumoniae* can enhance inherent virulence characteristics by releasing the siderophore enterochelin and aerobactin to fully exploit iron deposits in the surrounding environment (Tay & Yew, 2013). A schematic representation of some virulence factors in *K. pneumoniae* is shown in Figure 1.4. The virulence factors are further discussed below:

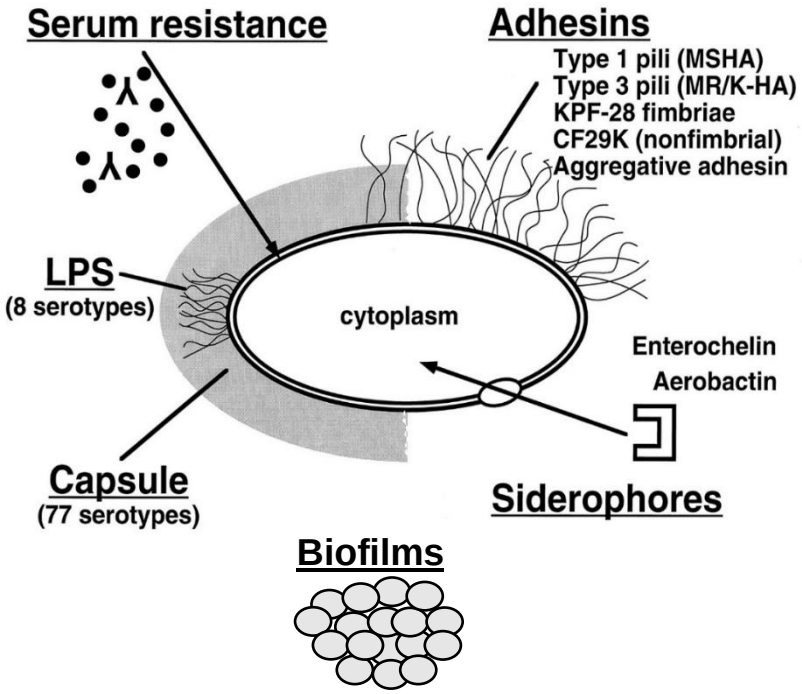

Figure 1.4: Schematic representation of *Klebsiella pneumoniae's* virulence factors. Adapted from Podschun & Ullmann (1998) with slight modification (inclusion of biofilms).

1.2.3.1 The city of microbes: Biofilms

Bacteria do not exist as isolated cells in their natural environment, rather, they develop and survive in structured communities known as biofilms, adhering to solid surfaces and frequently enclosed in an exopolysaccharide matrix (Muhammad et al., 2020; Balestrino et al., 2005). Biofilms are microbial communities made up of one or more bacterial species that have been considered the predominant natural life for most bacteria (Toole et al., 2000). Biofilm-forming bacteria have been reported to often develop antibiotic and host defense resistance (Al-khayyat, 2018) (Götz, 2002), thereby showing higher levels of antibiotic resistance than planktonic cells (Mah & O'Toole, 2001). Biofilm formation is an important resistance mechanism not only because it makes bacterial colonies resistant to antibiotics but also enhances the transmission of resistance genes, boosts the expression of efflux pumps, increases antibiotic metabolism, and favours persistent cells (Vuotto et al., 2017; Soto, 2014).

K. pneumoniae biofilm formation is aided by some of its virulence-related genes. For example, the cps (capsule) gene cluster (Balestrino et al., 2005), mrkA (type 3 fimbriae) genes, (Foroohimanjili et al., 2020), wbbM and wzm (belonging to the six-

gene cluster containing enzymes for the manufacture of O-antigen, which forms part of the LPS) are examples of biofilm-associated virulence genes (Vuotto et al., 2017).

According to Cadavid et al. (2018), biofilm formation is modulated by LuxS/AI 2 QSS, therefore, QS offers a better understanding of the factors that induce biofilm formation. The luxS (AI 2 QSS) and pgaABCD operons (synthesis and translocation of poly-b1,6-N-acetyl-D-glucosamine (PGA) adhesin) affect biofilm development by promoting the cell-to-cell communication process as well as abiotic surface binding and intercellular adhesion, respectively (Balestrino et al., 2005), (Hardie & Heurlier, 2008).

Mutations in LuxS, implicated in the AI 2 QSS cause an increase in the expression of wbbM and wzm (two LPS-synthesis-related genes), which influence *K. pneumoniae* biofilm formation. As a result, the LuxS-dependent signal is critical in the early stages of *K. pneumoniae* biofilm development (De Araujo et al., 2010). Biofilm formation has been reported to occur in different stages.

1.2.3.1.1 *Stages of biofilm formation*

Biofilm formation occurs in a series of phases. With each phase, the biofilm grows more firmly attached and the microorganisms within it become better protected (Hayet et al., 2021). According to Rabin et al. (2015), biofilm formation can be described in three (3) stages (attachment, maturation, and dispersion) however, microcolonies are formed before the maturation stage. A prerequisite to biofilm formation is that bacteria get close to a surface and attach. The bacteria and the surfaces may be attracted by the van der Waals force. This could also possibly be due to the utilization of fimbriae, and flagella as mechanical attachment mechanisms to surfaces (Palmer et al., 2007). The attachment step could be further categorized into two processes: initial reversible attachment and irreversible attachment (Rabin et al., 2015). Flagella and Type IV pili-mediated motilities are critical during the early stages of attachment; however, the cells bind themselves more securely during the irreversible attachment phase by producing exopolymeric material, a stronger adhesive compound. Exopolysaccharide synthesis is required to keep the biofilm's pillars stable (Watnick & Kolter, 2000). The formation of an exopolysaccharide (EPS) matrix marks the start of the irreversible phase of bacterial attachment to a surface, after which microcolonies form and the biofilm matures (Rabin et al., 2015).

During the maturation stage, bacteria within biofilm communities 'talk' to each other and perform specialized functions. Biofilm cells in their mature stage primarily consume energy to generate exopolysaccharides, which the cells use as nutrition (Watnick & Kolter, 2000). As the biofilm matures, more biofilm scaffolds, such as proteins, DNA, polysaccharides, etc. are secreted into biofilms by entrapped bacteria (Rabin et al., 2015).

The dispersal stage, which is equally important for the biofilm life cycle, comes after the biofilm maturation stage. It is the ultimate step in biofilm formation which involves a mature biofilm transitioning to a planktonic state. Dispersal can occur throughout the biofilm, although it is usually limited to a few regions of the biofilm and is a continual process. This stage permits the biofilm to spread to a new surface and colonize it (Rabin et al., 2015). According to Hall-Stoodley & Stoodley (2005), three different dispersal strategies can be observed for biofilm bacteria which are swarming dispersal, clumping dispersal, and surface dispersal. All these dynamic detachment events have the potential to disperse biofilm bacteria to new surfaces or a vulnerable host (Hall-Stoodley & Stoodley, 2005). Factors such as lack of nutrients, intense competition, and outgrown population are reasons for biofilm dispersal. The release of planktonic bacteria (mature bacteria that float or swim as single cells) promotes the initiation of new biofilms at other sites which ultimately enhances bacterial virulence (Rabin et al., 2015).

1.2.3.2 Lipopolysaccharide production

All GNB, including the classical *K. pneumoniae* (cKP) and hypervirulent *K. pneumoniae* (hvKP), produce lipopolysaccharide, which is made up of lipid A, oligosaccharide core, and O antigen (Zhu et al., 2021). Capsular polysaccharide (CPS) and the O-antigen portion of lipopolysaccharide (LPS) are the first bacteria-derived molecules recognized by the host's innate immune system, and they shield the pathogen from complement-mediated death (Hsieh et al., 2012). In *K. pneumoniae*-associated pneumonia and bacteraemia, both CPS and LPS components play a role in pathogenicity (Lugo et al., 2007).

The O antigen binds to a complement component C3b involved in pore development in the outermost subunit of LPS, preventing drilling of the bacterial membrane (Shankar-Sinha et al., 2004). There are eight O serotypes, with the O1 antigen being

the most frequent among clinical *K. pneumoniae* strains (Zhu et al., 2021; Follador et al., 2016). Previous research has suggested that the O-antigen in O1:K2 cKP may play a role in bacterial virulence and fatality by reducing macrophage activation and boosting bacteraemia (Lugo et al., 2007).

1.2.3.3 Siderophore production

Siderophores are ferric ion-specific chelators with a low molecular weight of less than 10 KDa that are secreted by microorganisms when they are iron deficient (Devireddy et al., 2010). They are small iron-binding molecules produced within bacteria and secreted outside the cells, where they attach to ambient iron and bring it back to the cells (Zhu et al., 2021). Following that, outer membrane receptors recognize iron siderophore complexes and transport the corresponding material to the periplasm, where siderophores mix with periplasm proteins to transport them to the inner membrane. Finally, iron goes through an ABC-transporter-mediated route into the bacterial cytoplasm, where ferric iron is converted to ferrous iron that bacteria can use (Brown & Holden, 2002; Khan et al., 2018).

With an increase in iron concentration in the environment, siderophore production diminishes. Enterobactin, yersiniabactin, salmochelin, and aerobactin are four siderophores expressed in hypervirulent *K. pneumoniae* strains that contribute to enhancing the growth and efficiency of *K. pneumoniae* (Zhu et al., 2021). Siderophore is involved in iron acquisition from ferric citrate, ferric phosphate, ferric transferrin, iron attached to plant flavone pigment, sugars, and glycosides, in addition to insoluble hydroxide forms (Khan et al., 2018). Bacteria use a variety of ways to acquire iron from their surroundings, including siderophore-mediated iron uptake. Bacteria solubilize ferric oxides by lowering external pH or converting ferric iron to the more soluble ferrous form to meet iron requirements (Köster, 2001). Iron chelators, such as siderophores, are another option. Specific outer membrane (OM) receptors such FepA, FecA, and FhuA, which bind to their cognate ferrisiderophore complex, are required for siderophore-mediated iron uptake (Köster, 2001). The metal iron siderophore is a crucial element necessary for essential metabolic functions, and the limited availability of iron within extracellular fluid makes bacterial iron acquisition difficult, making it a form of nonspecific immunological response (Zhu et al., 2021).

To survive and thrive, *K. pneumoniae* and other bacteria employ strategies to overcome the difficulty of obtaining iron. As a result, they have a system that has a stronger affinity for iron than the host, which acts as a primary strategy for obtaining iron to compete with hosts (Miethke & Marahiel, 2007; Cassat & Skaar, 2013).

1.2.3.4 Capsule formation / hypermucoviscosity

The virulence factor related to *K. pneumoniae's* viscous phenotype is the capsule that surrounds the bacteria's surface (Zhu et al., 2021). *K. pneumoniae* uses capsules to evade phagocytosis, complement, antimicrobial peptides, and antibodies (Llobet et al., 2011; Paczosa & Mecsas, 2016). Hypervirulent *K. pneumoniae* have thick, hypermucoviscous coats that may help them survive. *K. pneumoniae* can be classified into at least 79 serotypes based on the diversity of the capsule's polysaccharide components as well as the distinct structures and antigens (Pan et al., 2015). Eight types, K1, K2, K5, K16, K20, K54, K57, and KN1 have been described in hvKP with K1 and K2 as the most common (Lee et al., 2016). Several virulence genes, in addition to those found in the cps cluster, have been linked to high capsule productivity, including the regulation of the capsule synthesis B genes (rcsB), a regulator of mucoid phenotype A and A2 (rmpA and rmpA2), and *K. pneumoniae* virulence regulators (kvrA and kvrB) (Palacios et al., 2018; Su et al., 2018).

1.2.3.5 Exopolysaccharide production

The extracellular matrix, a component of *K. pneumoniae* biofilms is made up of proteinaceous adhesins, nucleic acids, and exopolysaccharides (EPS) (Patro & Rathinavelan, 2019). Exopolysaccharides (EPSs) are one of the most common extracellular polymeric substances produced by microorganisms (Zhao et al., 2019), including *K. pneumoniae. K. pneumoniae* generates a thick, mucoid polysaccharide capsule and a variety of adhesion factors, which helps it survive in a variety of conditions, particularly by allowing them to stick to surfaces within biofilm communities (Chen et al., 2020; Paczosa & Mecsas, 2016).

During the biofilm formation phases, irreversible adherence is facilitated by the production of EPS, which is regulated by the QS of the bacterial cell (Muhammad et al., 2020). Through hydrophobic contacts and ion-bridging interactions, EPS can mediate both bacterial cohesion and biofilm attachment to surfaces (Fahs et al., 2014).

Overall, EPS is important for adhesion to surfaces, cell-cell recognition, biofilm development, biofilm structure, water retention, signalling, cell protection, plant symbiosis, nutrient trapping, and genetic exchange (Costa et al., 2018). The primary components of EPS include polysaccharides, proteins, DNAs, lipids, and other polymeric substances (Bacosa et al., 2018; Costa et al., 2018). Polysaccharides, a major component of the EPS matrix are required for biofilm creation and proliferation (Muhammad et al., 2020).

1.2.3.6 Fimbriae, non-fimbrial protein and outer membrane proteins

Fimbriae, which are filamentous organelles found on the surface of GNB, are frequently used to mediate adherence (Struve et al., 2008). The two fimbrial adhesins, type 1 fimbria and type 3 fimbria, are produced by the majority of clinical *K. pneumoniae* isolates. Type 3 fimbriae are well-known bacterial virulence factors that drive improved biofilm formation on abiotic surfaces and mediate adherence to various cell types *in vitro* (Schroll et al., 2010). Type 1 fimbriae are found in many *Enterobacteriaceae* species, and they mediate attachment to mannose-containing sites on host cells and the extracellular matrix (Struve et al., 2008). Despite having the mrkD and fimH genes, which encode type 3 and type 1 fimbriae, hypermucoviscous *K. pneumoniae* with serotype K1 has minimal initial adhesion because hypercapsule might mask these fimbriae (Cubero et al., 2019). Another adhesive structure found in hypervirulent *K. pneumoniae* strains is CF29K, a non-fimbrial protein often involved in pathogenicity (Brisse et al., 2009). OmpA, peptidoglycan-associated lipoprotein (Pal), and murein lipoprotein (LppA) are among the outer membrane proteins (OMPs) that contribute to *K. pneumoniae's* pathogenicity (Zhu et al., 2021).

The above-discussed virulence factors pose a great threat to human health especially as the emergence of multidrug resistant strains of *K. pneumoniae* has been reported. Hence, the exploration of alternative treatment options from natural sources, particularly, medicinal plants to possibly inhibit *K. pneumoniae* QS and its virulence.

1.2.4 Inhibition of QS and associated virulence factors in K. pneumoniae

The continuous emergence of MDR in *K. pneumoniae* has led to the search for new plant-derived antimicrobial substances. Some compounds from plant sources contain anti-pathogenic agents (also known as quorum sensing inhibitors) (Pradeep et al.,

2018). This is because traditional medicine is still recognized as the preferred primary health care system in many communities, with over 60% of the world's population and about 80% in developing countries depending directly on medicinal plants for their medical purposes (Shrestha & Dhillion, 2003). About 80% of these active ingredients indicate a positive correlation between their modern therapeutic use and traditional uses (Sarkar et al., 2015; Ekor, 2014).

Several metabolites are present in medicinal plants which include alkaloids, flavonoids, saponin glycosides, anthraquinones, and sesquiterpenoids to mention a few. Due to the prevalence of abundant bacterial populations in the environments where plants typically grow, plants have developed defense mechanisms against phytopathogens. Consequently, certain plants are believed to produce secondary metabolites that act as inhibitors of quorum sensing (QSIs) or agents with antimicrobial properties against bacterial pathogens.These secondary metabolites mimic bacterial quorum sensing (QS) signal molecules when bound to the regulator protein, competing for the protein active sites in bacteria and lowering bacterial pathogenicity (Koh et al., 2013). The potential of medicinal plants and their phytochemical compounds to inhibit quorum sensing and virulence is intriguing, hence, this study reviewed selected South African medicinal plants that have traditional use/indication for *K. pneumoniae* infections.

1.2.5 South African medicinal plants as treatment options for K. pneumoniae infections

South Africa, a country with a long history of traditional healing, is home to almost 30,000 flowering plant species which accounts for nearly 10% of all higher plant species on the planet (Street & Prinsloo, 2013). Southern Africa has one of the world's highest species diversity indexes, which translates to a large number of medicinal plants, with almost 3000 species used to cure a wide range of diseases (Khumalo et al., 2019). In traditional markets across South Africa, a huge number of medicinal plants are commonly offered as unprocessed pharmaceuticals (Van Wyk, 2011). South Africa's indigenous, traditional plant medicine is being used by an estimated three million people for basic health care (Louw et al., 2002). This diversity and the long-term relationships that South Africans have with their natural environment mean that they use some of this richness as medicine (Cosa et al., 2020).

Of the many South African medicinal plants shown to have ethnobotanical uses, *Lippia javanica, Helichrysum populifolium* and *Carpobrotus dimidiatus* (Figure 1.5) have been reported to possess high therapeutic potential against MDR bacteria and might also play a role in the control of *K. pneumoniae* related infections (Chagonda & Chalchat, 2015; Akinyede et al., 2020). Hence, these plants were selected for this study.

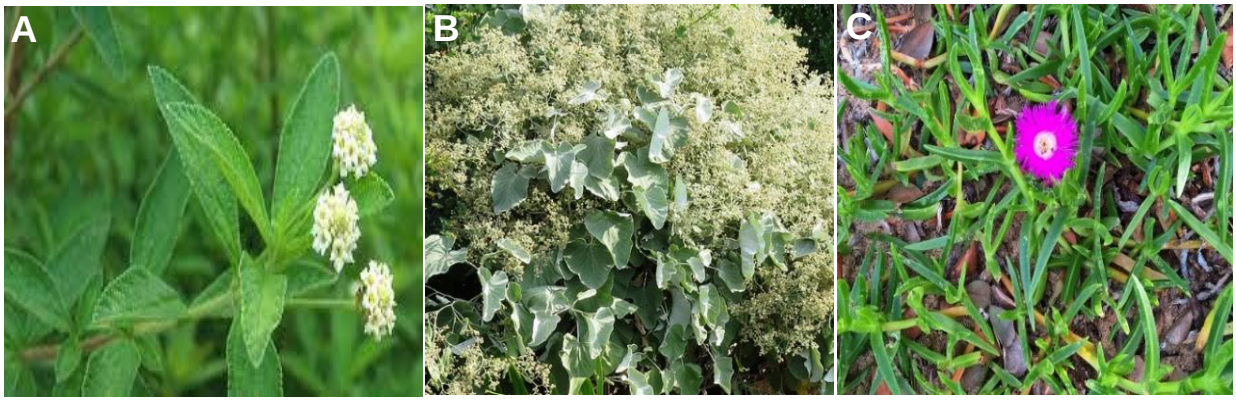

Figure 1.5: South African medicinal plants of interest. **A**: *Lippia javanica*[1], **B**: *Helichrysum populifolium*[2], **C**: *Carpobrotus dimidiatus*[3].

1.2.6 Overview of the medicinal plants of interest

1.2.6.1 Lippia javanica

Lippia javanica (Burm.f.) Spreng, *a Verbenaceae* commonly known as fever tea (Figure 1.5A) is an aromatic, woody shrub with hairy thinly veined leaves which grows up to 2 meters in height (Olivier et al., 2010). It is a multipurpose medicinal plant used since the mid-1990s against numerous ailments such as bronchitis, colds, coughs and fever (Van Wyk, 2011). It's leaves, flowers, and twigs are rich in essential nutrients as well as carbohydrates, proteins, fats, and vitamins (Mahlangeni et al., 2018). Some of these mineral elements are necessary for repairing worn-out tissues, building strong bones and teeth, and producing red blood cells and other related tissues (Maroyi, 2017).

Additionally, Pascual et al. (2001) reported that *L. javanica* contains different classes of phytochemicals, including volatile and non-volatile secondary metabolites, such as alkaloids, amino acids, flavonoids, iridoids, and triterpenes. It's essential oils are highly

[1] *https://southafrica.co.za/lippia-javanica.html* [Accessed on 21st July 2022]
[2] *https://www.theplantlibrary.co.za/plants/Helichrysum-populifolium* [Accessed on 21st July 2022]
[3] *https://pza.sanbi.org/carpobrotus-dimidiatus* [Accessed on 21st July 2022]

variable, having five distinct chemotypes, each with its main compound (myrcenone, carvone, piperitenone, ipsenone or linalool), as described by Viljoen et al. (2005). Previous studies by Maroyi (2017), Viljoen et al. (2005), Philemon et al. (2016) and Chagonda & Chalchat (2015) have confirmed the traditional use and pharmacological (antioxidant, antimalarial, and antibacterial) activities of *L. javanica* and its essential oils.

1.2.6.2 Helichrysum populifolium

Helichrysum populifolium (DC.), commonly known as poplar helichrysum (Figure 1.5B) belongs to the family *Asteraceae*, one of the largest families of flowering plants (Maroyi, 2019). It is a soft, woody shrub that reaches a height and width of approximately two metres. The leaves are large, velvety to the touch, with a round to heart-shape. The leaves upper surface might be virtually dark green, yet it always appears to be covered in grey cobwebs (Maroyi, 2019). It is an aromatic plant widely distributed throughout Southern Africa and is often used in traditional medicine to treat respiratory ailments and wound infections (Malolo et al., 2015). It has also been reported alongside *Helichrysum petiolare*, another specie of *Helichrysum,* to have traditional uses and ethnomedicinal applications in the management of cough, cold, back pain, diabetes, asthma, digestive problems, menstrual pain, chest pain, among others (Lourens et al., 2011; Akinyede et al., 2021; Scott et al., 2004). It has been further characterized by several biological activities, such as antimicrobial, anti-inflammatory, antioxidant, cholagogue, choleretic, hepatoprotective, detoxifying, protease-inhibiting, and antiallergic properties (Malolo et al., 2015). Some of the main active compounds reported to be present among the *Helichrysum* genus include α-pinene, 1, 8-cineole, p-cymene, β-caryophyllene, longipinane, trans-Geranylgeraniol, phytol, geranyllinalool and α-Eicosane (Akinyede et al., 2021).

1.2.6.3 Carpobrotus dimidiatus

Carpobrotus dimidiatus (Haw.) L. Bolus (Figure 1.5C) is an edible, succulent, medicinal plant belonging to the *Aizoaceae* family, which is considered to be South Africa's most diverse and abundant plant family that has been the least studied for medicinal properties (Akinyede et al., 2020). It is commonly called Natal sour fig in English, Natalse suurvy/strandvy in Afrikaans and Ikhambi lamabulawo in Zulu. This

plant mostly grows on dunes along the coast from the Eastern Cape to Mozambique, passing via KwaZulu-Natal (Broomhead et al., 2020).

C. dimidiatus is a strong, trailing plant with threesided leaves that are meaty and green. It has the potential to spread across enormous areas, forming a robust ground cover that is resistant to drought and salt spray (Broomhead et al., 2020). The mauve vygie flowers are huge, glossy, and borne singly on more or less tall blooming branches (Broomhead et al., 2020). It is an economically important Southern African medicinal plant reported to contain active compounds such as isoterpinolene, naphthalene, 1,2-dihydro-2,5,8-tri, N-octanol, nonylaldehyde, 1-octadecene, 2- pentadecanone, phytol, *and t*risiloxane,1,1,1,5,5,5-hexamethyl-3-[(trimethylsilyl)oxy] (Akinyede et al., 2020). Furthermore, it has been used in traditional medicine for the management of diabetes, wounds, high blood pressure, sore throat, diarrhea, digestive problems, and toothaches (Mulaudzi et al., 2019).

The antibacterial activity of the three studied plants (*L. javanica, H. populifolium* and *C. dimidiatus*) against *Klebsiella pneumoniae* have not been previously reported. However, the cut-off points for the classification of antibacterial agents from natural sources (plant crude extracts) have been established and previously reported. According to Mamabolo et al., (2018), minimum inhibitory concentration (MIC) values < 0.1mg/mL indicates significant activity, while values between 0.1 and 0.625mg/mL depicts moderate activity. Values > 0.625mg/mL, however, indicates low activity.

1.2.7 Medicinal plants as a source of drugs and quorum sensing inhibitors

According to the WHO in Shaik et al. (2014) and Douhari et al. (2009), medicinal plants would be the best source to obtain a variety of drugs. Novel antimicrobials are still being sought for treating many *K. pneumoniae* infections, either by developing and synthesizing new agents or by re-searching the repertoire of natural resources for antimicrobials that are yet to be discovered or characterized (Cock & Van Vuuren, 2014). The challenges of drug-resistant microorganisms, side effects of modern drugs and emerging diseases have stimulated renewed interest in medicinal plants as a potential source of new therapies.

In this view, several QSI compounds or enzymes have been discovered in a variety of natural sources, including medicinal plants, common spices, edible fruits, and marine resources (Santhakumari & Ravi, 2019). In recent years, medicinal plant research has gotten a lot of attention around the world. A substantial body of evidence has developed to show the promising potential of medicinal plants employed in many traditional, complementary, and alternative methods of disease treatment (Shaik et al., 2014). Many societies have long recognized medicinal herbs' therapeutic properties and have renewed interest in herbal medications due to their natural endobiotic phytochemicals which are thought to have a lower rate of adverse effects than synthetic xenobiotic drugs, which has sparked recently (Cock & Van Vuuren, 2014).

Natural products are thought to be potential sources of phytochemicals or pharmaceuticals for the development of new lead molecules to treat QS-mediated bacterial pathogenicity (Santhakumari & Ravi, 2019). Secondary metabolites such as tannins, terpenoids, alkaloids, and flavonoids are abundant in plants which have been shown to possess antibacterial activities *in vitro* thereby suggesting their therapeutic properties (Othman et al., 2019). The use of plants or their secondary metabolites could lead to the development of novel anti-QS agents (Asfour, 2018). Some studies have reported the anti-QS activity of organic extracts of medicinal plants (Cosa et al., 2020; Baloyi et al., 2021; Oliveira et al., 2016; Al-Haidari et al., 2016; Vasavi et al., 2016; Thakur et al., 2016). The chemical structure of QS signals can be imitated by phytochemical compounds found in plants extracts, which allows them to function as QS inhibitors (Nazzaro et al., 2013).

Alternatively, these compounds can break down signal receptors (LuxR/LasR) to inhibit QS (Vattem et al., 2007). Bouyahya et al. (2017) reported some phytochemical compounds such as vanillin in *Vanilla planifolia,* naringenin in *Citrus sinensis,* taxifolin in *Cedrus deodara*, eriodictyol in *Eriodictyon californicum*, methyl eugenol in *Cuminum cyminum* to inhibit QS signalling pathways. Figure 1.6 shows examples and structures of some bioactive compounds/secondary metabolites present in plants belonging to the flavonoids, terpenoids, alkaloids, phenolics, tannins and saponin glycosides class of compounds.

Flavonoids

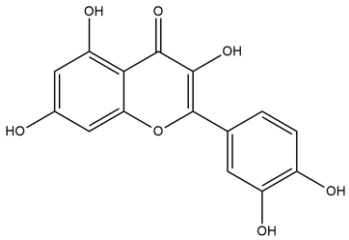
Quercetin

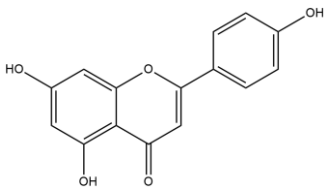
Apigenin

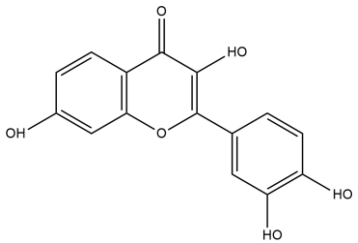
Fisetin

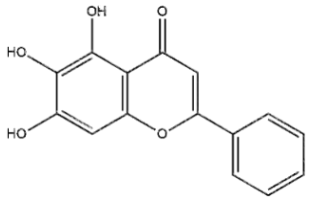
Biacalein

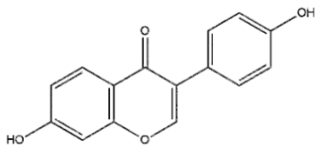
Diadzein

Terpenoids

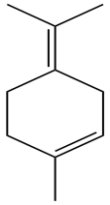
Terpinolene

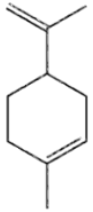
Limonene

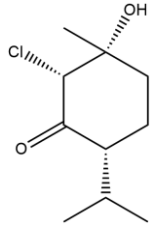
Longifone

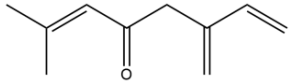
Ipsdienone

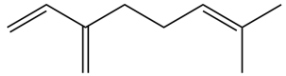
Myrcene

Alkaloids

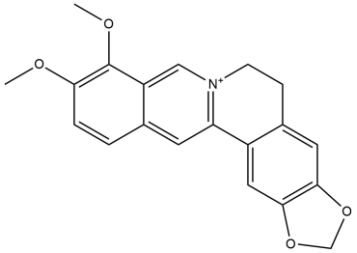
Berberine

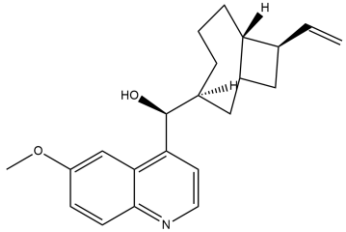
Quinine

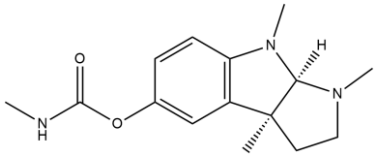
Physostigmine

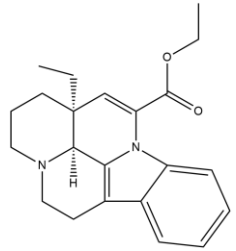
Vinpocetine

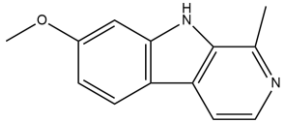
Harmine

Figure 1.6: Selected bioactive compounds present in the studied medicinal plants.

Phenolics

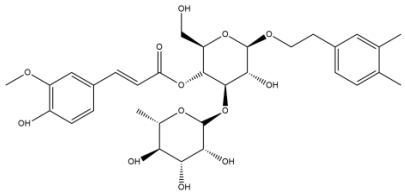

Martynoside

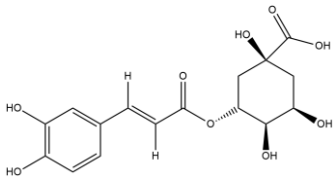

Chlorogenic acid

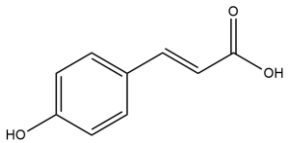

P-coumaric acid

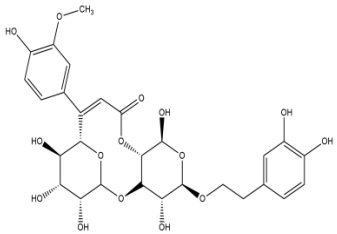

Leucoseptoside A

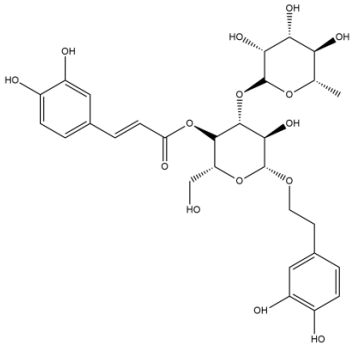

Verbascoside

Tannins and saponin glycosides

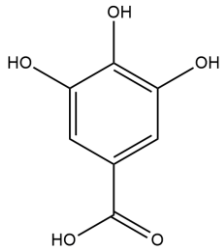

Gallic acid

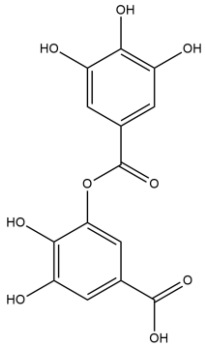

Digallic acid

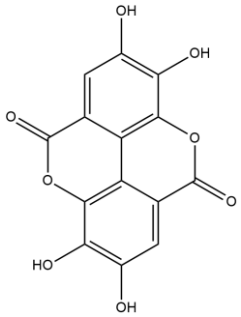

Ellagic acid

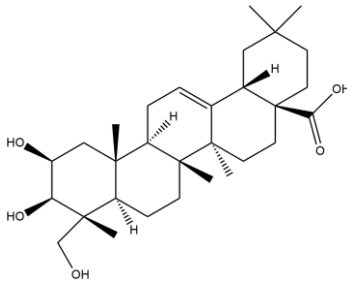

Bayogenin

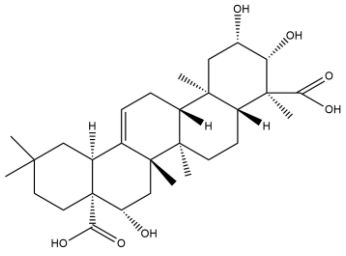

Zanhic acid

Figure 1.6 (Cont'd): Selected bioactive compounds present in the studied medicinal plants.

1.2.8 Anti-quorum sensing strategies of plant compounds

Phytochemical compounds typically hinder QS systems through various methods such as inhibiting the synthesis of signalling molecules by the LuxI synthase, suppressing the activity of enzymes that produces AHLs, secreting signal-degrading enzymes, and/or targeting the LuxR signal receptor using signal mimics or signal blockers (Bodede et al., 2018). Interference in signal communication can arise from either competitive binding where structures similar to AHLs bind to AHL binding sites, or non-competitive binding, where the binding takes place in a site other than the AHL binding site on the receptor, disrupting the binding of AHLs to their corresponding LuxR receptor (Koh et al., 2013). Quorum quenching (QQ) is now known to play a role in the competitive inhibition and degradation of signalling molecules through inhibition of signalling molecule generation, competitive inhibition and degradation signal molecule.

1.2.8.1 **Inhibition of signalling molecule generation**

The formation of signal molecules can be stopped, and QS suppressed by blocking relevant enzymes in the signalling molecule manufacturing pathway. Triclosan, for example, can inhibit the enzyme enoyl-ACP reductase (an important protein in the AHL generation process) (Fischer et al., 2015).

1.2.8.2 **Competitive inhibition**

Structural analogues of signalling molecules can competitively bind with corresponding receptor proteins, and block the binding of signal molecules to receptors, thereby affecting the transmission of signal molecules. For example, halogenated furanone (AHL structural analogues) shown in Figure 1.7 can inhibit QS (Paluch et al., 2020). Acyl homoserine lactones (AHLs) are the most common signal molecules in GNB which are often synthesized by the LuxI homolog proteins. AHL analogs may act as competitive inhibitors, therefore, various QSIs were designed based on this. In different species, the AHLs structures vary, but they have the main features of a lactonized homoserine ring and a hydrocarbon through amide bond (Das & Bengal, 2019).

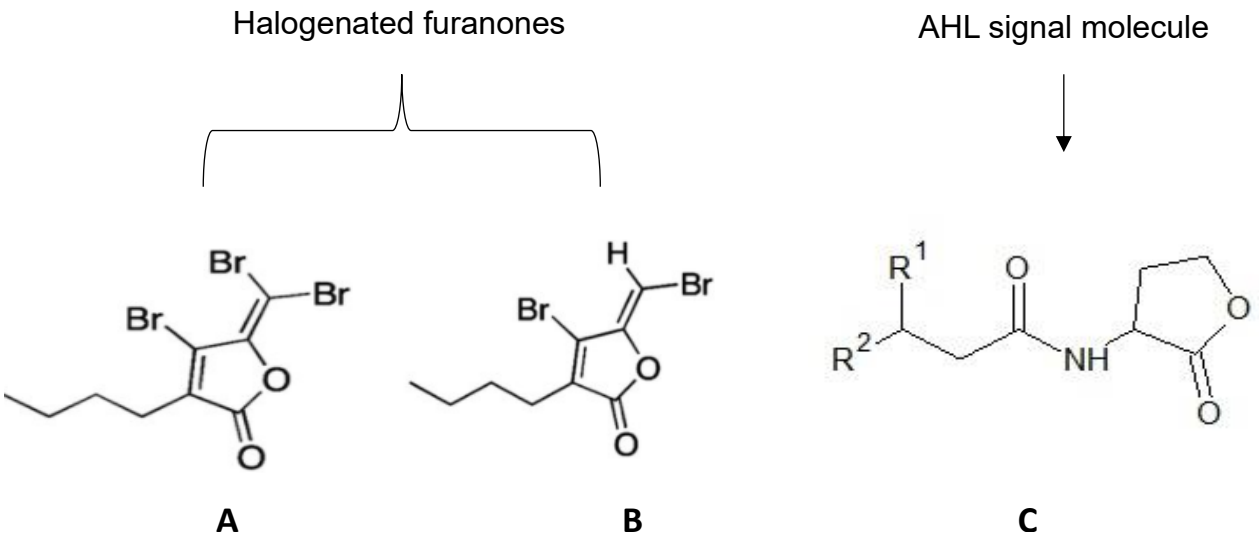

Figure 1.7: (A) Structure of 4-Bromo-3-butyl-5-(dibromomethylene)-2(5H)-furanone (B) Structure of 4-Bromo-5(bromomethylene)-3-butyl-2(5H)-furanone (C) Basic Structure of the AHL Signal molecule (where R^1 = H, OH, or O and R^2 = C1–C18). Adapted from Das & Bengal, (2019) with a slight modification of AHL signal molecule inclusion.

1.2.8.3 Degradation of signal molecules

The concentration of signal molecules is lower than the threshold when degradation enzymes are used to break down signal molecules thereby destroying the QS system. MacQ, for instance, is an AHL acylase, an enzyme that can mediate QQ (Yang et al., 2020).The anti-quorum sensing (AQS) potential of medicinal plants and phytochemical compounds could be the future generation's miracle bullet (Koh et al., 2013).

1.2.9 Screening and identification tools for QSIs in medicinal plants

1.2.9.1 *In vitro* approach

One possible approach to screening local medicinal plants in search of suitable antipathogenic substances and/or QSIs is through *in-vitro* screening (Ram et al., 2004). This approach focuses on pre-clinical studies to understand the basics while ensuring the reliability and reproducibility of results, thereby providing a benchmark for further studies (Sisay et al., 2019). The successful discovery of treatment often uses reliable, predictive *in-vitro* assays and high-throughput screening (Palano et al.,

2021). As such, several medicinal plants and their secondary metabolites have been widely investigated for biological activities using this approach (Lu et al., 2019).

Chromatography analyses such as liquid chromatography-mass spectrometry or high-performance liquid chromatography (HPLC) fractionation have been employed for the extraction or purification of anti-QS compounds for QSI screening (Lu et al., 2022).

Furthermore, previous studies by Gemiarto et al. (2015), Zhu & Sun (2008) and Kong et al. (2017) have used two QS reporter strains namely *Chromobacterium violaceum* (producing violacein pigment) and *Vibrio ha*rveyi (producing bioluminescence) to estimate the anti-QS activity of candidates. However, quantitative analyses of bioluminescence and violacein interference do not seem to adequately demonstrate that these inhibitors specifically disrupt QS signalling pathways (Lu et al., 2022). Hence, due to insufficient conditions, the analysis of QS-controlled phenotypes, such as the virulence factor assays significantly decreases the potential candidates. For example, research conducted by Jordan et al. (2022), Cosa et al. (2020) and Baloyi et al. (2021) have elucidated the discovery of QSIs based on biofilm formation. In such cases, congo red agar, microtiter plate assay, or crystal violet assays were frequently employed as qualitative methods to assess the characteristics of the biofilm (Lu et al., 2022). Aside from biofilm formation, most of the other virulence factors are also regulated by QS systems and may depict QS-controlled phenotypes (Wang et al., 2021), thus, *in-vitro* anti-virulence assessment of potential candidates is essential.

1.2.9.2 Computational techniques

Only limited QSIs have been found using conventional techniques (Lu et al., 2022). Therefore, computational techniques especially structure-based virtual screening have been developed to serve as an effective paradigm for lead discovery that complements existing traditional approaches and facilitates large-scale screenings (Lu et al., 2022; Naqvi et al., 2019). Examples of these computational techniques are molecular docking and molecular dynamics simulations which are discussed below:

1.2.9.2.1 ***Use of molecular docking to identify QSIs***

Molecular docking is a computer-based technique that is commonly utilized to determine the most optimal positioning of one molecule in relation to another molecule, to establish a stable complex with the lowest overall energy after an interaction occurs (Naqvi et al., 2019). This method examines the ligand's conformations within the binding pocket(s) of the macromolecular target and evaluates the ligand-receptor's binding free energy by analysing critical factors involved in the intermolecular recognition process (Therrien et al., 2014). Figure 1.8 shows the molecular docking approach to find protein-ligand interactions.

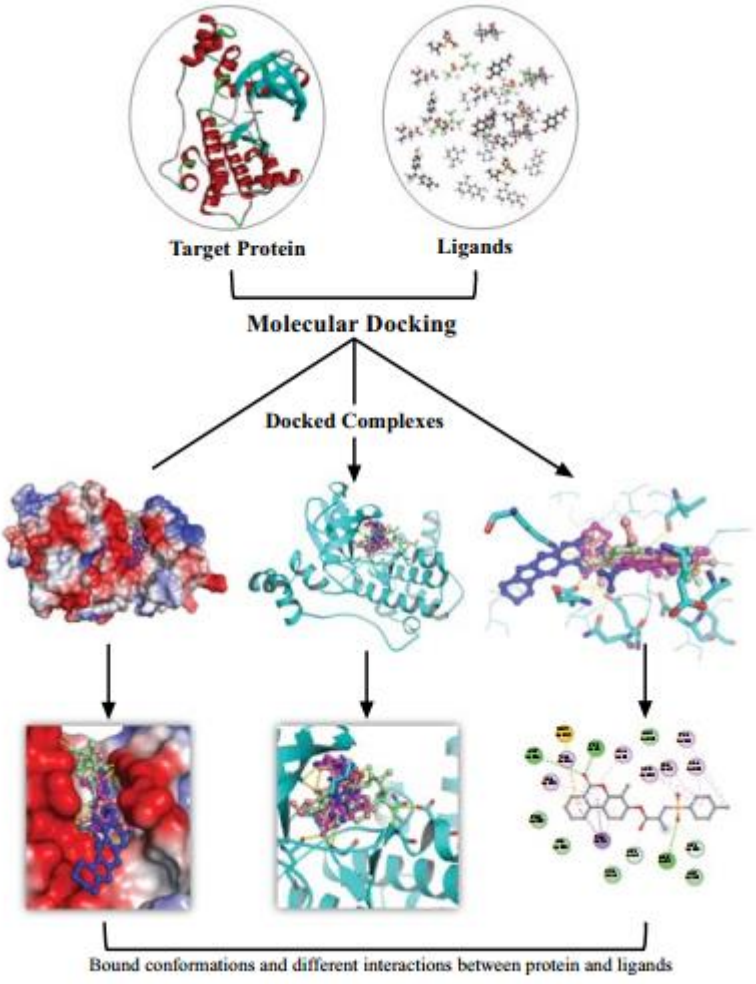

Figure 1.8: Molecular docking approach to find protein-ligand interactions (Naqvi et al., 2019).

Molecular docking is among one of the most popular and successful structure-based *in silico* methods, which helps to predict the interactions occurring between molecules and biological targets (Sliwoski et al., 2014). This process is generally accomplished

by first predicting the molecular orientation of a ligand within a receptor and then estimating its complementarity using a scoring function (Pinzi & Rastelli, 2019).

The use of *in silico* methods allows for the screening of a large number of compounds virtually in a cost-effective manner, thereby minimizing the initial expenses associated with hit identification and enhancing the likelihood of discovering potential drug candidates (Parenti & Rastelli, 2012).

1.2.9.2.2 Molecular dynamics simulations

Structure-based methods, including molecular dynamics simulations (MDS) and binding free energy estimations, have frequently been used in conjunction with molecular docking to enhance virtual screening outcomes (Pinzi & Rastelli, 2019). In particular, MDS provides the ability to assess the flexibility of residues in the target binding site and explore significant conformational changes that a protein may undergo (Salmaso & Moro, 2018). Thus, it is a valuable tool for identifying receptor conformations for docking and evaluating the stability of predicted complexes (De Vivo et al., 2016).

MDS are also employed in search for the most favourable orientation of a ligand compared to a protein target and to calculate the free binding energy (Shukla et al., 2018). This approach has been highly robust in the discovery and development of modern drugs, especially when in association with experimental support (Naqvi et al., 2019).

Virtual screenings speed up and reduce the cost of conventional drug development processes by enabling quick and economical selection of target ligands from enormous libraries of compounds (Mellini et al., 2019). Thus, this study utilized the advantage of virtual screening in evaluating the anti-quorum sensing or antivirulence potential of selected South African medicinal plants and their phytochemical compounds on biofilm-forming *K. pneumoniae.*

1.2.10 Summary

The in-depth literature search was conducted in the quest to review prospective novel therapeutics and promising alternatives in the place of conventional antibiotics, to combat the silent pandemic posed by multidrug resistant and hypervirulent *K.*

pneumoniae strains. According to the literature, *C. dimidiatus, H. populifolium* and *L. javanica* have been used traditionally for ethnomedicinal purposes**.** The pharmacological actions of these plants can be attributed to their vital chemical compounds, essential oils and other secondary metabolites. QS, which often modulates increased pathogenicity in *K. pneumoniae* can be inhibited by phytochemical compounds through several strategies which makes these plants and their compounds of special interest. There is a dire need for more research on South African medicinal plants for the treatment of *K. pneumoniae* infections, as they appear to be prospective sources of beneficial bioactive medicinal compounds that may be utilised in drug development, hence, this study. In addition, a gap in knowledge in the combination use of *in vitro*, computational screening and *in situ* search of antivirulence drug candidates are lagging. Hence, this study took opportunity to employ these tools to screen and validate the selected phytochemicals as prospective antivirulence candidates.

1.3 Research gap and rationale

Conventional antibiotics either kill bacterial cells or prevent bacterial growth by targeting essential biochemical processes, including cell wall, protein and nucleic acid biosynthesis, which ultimately exerts enormous selective pressures leading to the evolution of antibiotic resistance (Fair and Tor, 2014). The alarming rate of antibiotic resistance in *K. pneumoniae* necessitates the need for alternative strategies or target sites, to manage this pathogen. A renewed search for potent plant-based compounds has become more appealing. Since QS system in *K. pneumoniae* controls its associated virulence factors, thereby resulting in its higher degree of pathogenicity; its inhibition (QSI) through medicinal plants and phytochemical compounds should pose a novel intervention strategy to attenuate pathogenicity in *K. pneumoniae*. These phytochemical compounds, however, are enormous, thus involves time consuming and expensive processes for the identification of hit compounds. Virtual screening of individual phytochemical compounds using molecular modelling approach should be useful in identifying specific compounds that may be useful in drug discovery processes.

1.4 Hypotheses

Antivirulence properties in plant extracts and phytochemical compounds of selected South African medicinal plants mitigate QS-controlled virulence factors in MDR *Klebsiella pneumoniae*. Furthermore, virtual screening aids in the quick identification of potential compounds as drug candidates.

1.5 Aim

The aim of this study was to determine the antivirulence (also referred to as anti-quorum sensing) abilities of selected South African medicinal plants used in managing infections caused by *Klebsiella pneumoniae* as well as their phytochemical compounds by employing *in-vitro, in-silico, in-situ* and molecular approaches.

1.6 Research questions

This study sought to answer the following research questions:

- Which South African medicinal plants have potential use for the management of *K. pneumoniae*, through modulating the bacterial virulence factors?
- Using molecular modelling approach, which phytochemical compounds can modulate the SdiA protein in *K. pneumoniae* to attenuate its virulence?
- Following *an in-vitro* approach and *in-situ* visualization techniques, which phytochemical compounds potentially reduce biofilm formation and associated virulence factors in *K. pneumoniae*?
- What impact do the active compounds have on the expression and regulation of virulence genes in *K pneumoniae?*
- Which of the phytochemicals are potentially safe for use, when evaluated for cytotoxic effect on normal epithelial with no malignant cells?

1.7 Objectives

To achieve the aim and answer the research questions raised above, the following specific objectives were met:

- Identification of selected South African medicinal plants and chemical profiling of selected plant extracts, preliminary screening of respective plant extracts for antibacterial, anti-virulence and anti-biofilms activities against *K. pneumoniae* employing *in-vitro* approach and *in-situ* visualization using scanning electron microscopy and atomic force microscopy.
- Molecular modelling of SdiA protein by selected phytochemical compounds to attenuate virulence in *K. pneumoniae:* Sequence retrieval, template identification and homology modelling, molecular docking of phytochemical compounds against SdiA receptor protein of *K. pneumoniae*, confirmation of the stability of the protein-ligand complex, examination of the atomic motions and interactions in the protein-ligand system and estimation of binding interactions of the compounds to the SdiA enzyme using molecular dynamics simulations and validation of drug-likeness properties of the phytochemical compounds.
- *In-vitro* and *in-situ* assessment of phytochemical compounds for antibiofilm and associated antivirulence activities against *K. pneumoniae*.
- Quantification of virulence gene expression in biofilm-forming *K. pneumoniae* strains after treatment with a sub-MIC concentration of phytochemical compounds using quantitative real-time polymerase chain reaction (qPCR).
- Safety assessment of selected bioactive compounds against *K. pneumoniae* through *in-vitro* proof-of-concept cytotoxicity evaluation on normal epithelial cells.

1.8 Concluding remarks

The subsequent chapters will reveal the findings of the antibacterial and antivirulence activities of the selected South African medicinal plants on hypervirulent *K. pneumoniae* strains, profiling of the phytochemical compounds in the bioactive extracts, molecular modelling of SdiA protein (the QS LuxS homologue transcriptional regulator) by selected phytochemical compounds to attenuate virulence in *K.*

pneumoniae, *in-vitro* anti-virulence activities and safety assessment of the compounds, as well as findings of transcriptome measurements to confirm the impact of the compounds on gene expression. The ultimate essence is to investigate safe, potential drug candidates from selected South African medicinal plants as alternative treatment options for *K. pneumoniae* infections.

References

Akinyede, K. A., Cupido, C. N., Hughes, G. D., Oguntibeju, O. O., & Ekpo, O. E. (2021). Medicinal properties and *in vitro* biological activities of selected *Helichrysum* species from South Africa: A review. *Plants*, *10*(8), 1–19. https://doi.org/10.3390/plants10081566

Akinyede, K. A., Ekpo, O. E., & Oguntibeju, O. O. (2020). Ethnopharmacology, therapeutic properties and nutritional potentials of *Carpobrotus edulis*: A comprehensive review. *Scientia Pharmaceutica*, *88*(3), 1–16. https://doi.org/10.3390/scipharm88030039

Al-Haidari, R. A., Shaaban, M. I., Ibrahim, S. R. M., & Mohamed, G. A. (2016). Anti-quorum sensing activity of some medicinal plants. *African Journal of Traditional, Complementary and Alternative Medicines*, *13*(5), 67–71. https://doi.org/10.21010/ajtcam.v13i5.10

Al-khayyat, M. Z. (2018). Quorum sensing in microbial virulence. *International Biological and Biomedical Journal, 4*(3), 127–135.

Aliyu, A. B., Koorbanally, N. A., Moodley, B., Singh, P., & Chenia, H. Y. (2016). Quorum sensing inhibitory potential and molecular docking studies of sesquiterpene lactones from *Vernonia blumeoides. Phytochemistry*, *126*, 23–33. https://doi.org/10.1016/j.phytochem.2016.02.012

Asad, S. & Opal, S.M. 2008. Bench-to-bedside review: Quorum sensing and the role of cell- to-cell communication during invasive bacterial infection. *Critical Care Medicine*. 11:1–11. doi: 10.1186/cc7101

Asfour, H. Z. (2018). Anti-quorum sensing natural compounds. *Journal of Microscopy and Ultrastructure*, 6, 1–10. https://doi.org/10.4103/JMAU.JMAU

Ashayeri-Panah, M., Feizabadi, M. M., & Eftekhar, F. (2014). Correlation of multi-drug resistance, integron and blaESBL gene carriage with genetic fingerprints of extended-spectrum β-lactamase producing *Klebsiella pneumoniae*. *Jundishapur Journal of Microbiology*, *7*(2), 1–5. https://doi.org/10.5812/jjm.8747

Bacosa, H. P., Kamalanathan, M., Chiu, M. H., Tsai, S. M., Sun, L., Labonté, J. M., Schwehr, K. A., Hala, D., Santschi, P. H., Chin, W. C., & Quigg, A. (2018). Extracellular polymeric substances (EPS) producing and oil-degrading bacteria isolated from the northern gulf of Mexico. *PLoS ONE*, *13*(12), 1–19. https://doi.org/10.1371/journal.pone.0208406

Balestrino, D., Haagensen, J. A. J., Rich, C., & Forestier, C. (2005). Characterization of type 2 quorum sensing in *Klebsiella pneumoniae* and relationship with biofilm formation. *Journal of Bacteriology*, *187*(8), 2870–2880. https://doi.org/10.1128/JB.187.8.2870-2880.2005

Baloyi, I. T., Cosa, S., Combrinck, S., Leonard, C. M., & Viljoen, A. M. (2019). Anti-quorum sensing and antimicrobial activities of South African medicinal plants against uropathogens. *South African Journal of Botany*, *122*, 484–491. https://doi.org/10.1016/j.sajb.2019.01.010

Baloyi, I.T., Adeosun, I. J., Yusuf, A. A., & Cosa, S. (2021). *In silico* and *in vitro* screening of antipathogenic properties of *Melianthus comosus* (Vahl) against *Pseudomonas aeruginosa*. *Antibiotics*, *10*(6), 1–23. https://doi.org/10.3390/antibiotics10060679

Bodede, O., Shaik, S., Chenia, H., Singh, P., & Moodley, R. (2018). Quorum sensing inhibitory potential and *in silico* molecular docking of flavonoids and novel terpenoids from *Senegalia nigrescens*. *Journal of Ethnopharmacology*, *216*, 134–146. https://doi.org/10.1016/j.jep.2018.01.031

Boucher, H. W., Talbot, G. H., Bradley, J. S., Edwards, J. E., Gilbert, D., Rice, L. B., Scheld, M., Spellberg, B., & Bartlett, J. (2009). Bad bugs, no drugs: No ESKAPE! An update from the Infectious Diseases Society of America. *Clinical Infectious Diseases*, *48*(1), 1–12. https://doi.org/10.1086/595011

Bouyahya, A., Dakka, N., Et-Touys, A., Abrini, J., & Bakri, Y. (2017). Medicinal plant products targeting quorum sensing for combating bacterial infections. *Asian Pacific Journal of Tropical Medicine*, *10*(8), 729–743. https://doi.org/10.1016/j.apjtm.2017.07.021

Brisse, S., Fevre, C., Passet, V., Issenhuth-Jeanjean, S., Tournebize, R., Diancourt, L., & Grimont, P. (2009). Virulent clones of *Klebsiella pneumoniae*: Identification and evolutionary scenario based on genomic and phenotypic characterization. *PLoS ONE*, *4*(3), 1–13. https://doi.org/10.1371/journal.pone.0004982

Broomhead, N. K., Moodley, R., & Jonnalagadda, S. B. (2020). Elemental analysis of the edible fruit of *Carpobrotus dimidiatus* (from Kwazulu-Natal, South Africa) and the influence of soil quality on its elemental uptake. *Journal of Environmental Science and Health, 55*(4), 406–415. https://doi.org/10.1080/03601234.2019.1707016

Brown, J. S., & Holden, D. W. (2002). Iron acquisition by Gram-positive bacterial pathogens. *Microbes and Infection*, *4*(11), 1149–1156. https://doi.org/10.1016/S1286-4579(02)01640-4

Cadavid, E., Robledo, S. M., Quiñones, W., & Echeverri, F. (2018). Induction of biofilm formation in *Klebsiella pneumoniae* ATCC 13884 by several drugs: The possible role of quorum sensing modulation. *Antibiotics*, *7*(4), 1–14. https://doi.org/10.3390/antibiotics7040103

Cassat, J. E., & Skaar, E. P. (2013). Iron in infection and immunity. *Cell Host & Microbe*, *13*(5), 509–519. https://doi.org/10.1016/j.chom.2013.04.010.Iron

Chagonda, L. S., & Chalchat, J. C. (2015). Essential oil composition of *Lippia javanica* (Burm.f.) spreng chemotype from Western Zimbabwe. *Journal of Essential Oil-Bearing Plants*, *18*(2), 482–485. https://doi.org/10.1080/0972060X.2014.1001140

Chen, L., Wilksch, J. J., Liu, H., Zhang, X., Torres, V. V. L., Bi, W., Mandela, E., Cao, J., Li, J., Lithgow, T., & Zhou, T. (2020). Investigation of Lux S-mediated quorum sensing in *Klebsiella pneumoniae*. *Journal of Medical Microbiology*, *69*(3), 402–413. https://doi.org/10.1099/jmm.0.001148

Clegg, S., & Murphy, C. N. (2016). Epidemiology and virulence of *Klebsiella pneumoniae*. *Urinary Tract Infections: Molecular Pathogenesis and Clinical Management*, 435–457. https://doi.org/10.1128/9781555817404.ch18

Cock, I. E., & Van Vuuren, S. F. (2014). Anti-*Proteus* activity of some South African medicinal plants: Their potential for the prevention of rheumatoid arthritis. *Inflammopharmacology*, *22*(1), 23–36. https://doi.org/10.1007/s10787-013-0179-3

Coquant, G., Grill, J. P., & Seksik, P. (2020). Impact of N-acyl-homoserine lactones, quorum sensing molecules, on gut immunity. *Frontiers in Immunology*, *11*(8), 1–8. https://doi.org/10.3389/fimmu.2020.01827

Cosa, S., Chaudhary, S. K., Chen, W., Combrinck, S., & Viljoen, A. (2019). Exploring common culinary herbs and spices as potential anti-quorum sensing agents. *Nutrients*, *11*(4), 1–17. https://doi.org/10.3390/nu11040739

Cosa, S., Rakoma, J. R., Yusuf, A. A., & Tshikalange, T. E. (2020). *Calpurnia aurea* (Aiton) benth

extracts reduce quorum sensing controlled virulence factors in *Pseudomonas aeruginosa*. *Molecules*, *25*(10),1–21. https://doi.org/10.3390/molecules25102283

Costa, O. Y. A., Raaijmakers, J. M., & Kuramae, E. E. (2018). Microbial extracellular polymeric substances: Ecological function and impact on soil aggregation. *Frontiers in Microbiology*, *9*(7), 1–14. https://doi.org/10.3389/fmicb.2018.01636

Cubero, M., Marti, S., Ángeles Domínguez, M., González-Díaz, A., Berbel, D., & Ardanuy, C. (2019). Hypervirulent *Klebsiella pneumoniae* serotype K1 clinical isolates form robust biofilms at the air-liquid interface. *PLoS ONE*, *14*(9), 1–11. https://doi.org/10.1371/journal.pone.0222628

Das, R. K., & Bengal, W. (2019). A review on quorum sensing inhibitors. *International Journal of Pharmaceutical Sciences and Research,* *10*(12), 5224–5233. https://doi.org/10.13040/IJPSR.0975-8232.10(12).5224-33

De Araujo, C., Balestrino, D., Roth, L., Charbonnel, N., & Forestier, C. (2010). Quorum sensing affects biofilm formation through lipopolysaccharide synthesis in *Klebsiella pneumoniae*. *Research in Microbiology*, *161*(7), 595–603. https://doi.org/10.1016/j.resmic.2010.05.014

De Vivo, M., Masetti, M., Bottegoni, G., & Cavalli, A. (2016). Role of molecular dynamics and related methods in drug discovery. *Journal of Medicinal Chemistry*, *59*(9), 4035–4061. https://doi.org/10.1021/acs.jmedchem.5b01684

Defoirdt, T., Boon, N., & Bossier, P. (2010). Can bacteria evolve resistance to quorum sensing disruption? *PLoS Pathogens*, *6*(7), 1–6. https://doi.org/10.1371/journal.ppat.1000989

Devireddy, L. R., Hart, D. O., Goetz, D. H., & Green, M. R. (2010). A mammalian siderophore synthesized by an enzyme with a bacterial homolog involved in enterobactin production. *Cell*, *141*(6), 1006–1017. https://doi.org/10.1016/j.cell.2010.04.040

Eberl, L., & Riedel, K. (2011). Mining quorum sensing regulated proteins - Role of bacterial cell-to-cell communication in global gene regulation as assessed by proteomics. *Proteomics*, *11*(15), 3070–3085. https://doi.org/10.1002/pmic.201000814

Ekor, M. (2014). The growing use of herbal medicines: Issues relating to adverse reactions and challenges in monitoring safety. *Frontiers in Neurology*, *4*(1), 1–10. https://doi.org/10.3389/fphar.2013.00177

Fahs, A., Quilès, F., Jamal, D., Humbert, F., & Francius, G. (2014). *In situ* analysis of bacterial extracellular polymeric substances from a *Pseudomonas fluorescens* biofilm by combined vibrational and single molecule force spectroscopies. *Journal of Physical Chemistry B*, *118*(24), 6702–6713. https://doi.org/10.1021/jp5030872

Fischer, R., Kontermann, R. E., & Maier, O. (2015). Targeting sTNF/TNFR1 signalling as a new therapeutic strategy. *Antibodies*, *4*(1), 48–70. https://doi.org/10.3390/antib4010048

Follador, R., Heinz, E., Wyres, K. L., Ellington, M. J., Kowarik, M., Holt, K. E., & Thomson, N. R. (2016). The diversity of *Klebsiella pneumoniae* surface polysaccharides. *Microbial Genomics*, *2*(8),1–15. https://doi.org/10.1099/mgen.0.000073

Foroohimanjili, F., Mirzaie, A., Hamdi, S. M. M., Noorbazargan, H., Hedayati Ch, M., Dolatabadi, A., Rezaie, H., & Bishak, F. M. (2020). Antibacterial, antibiofilm, and antiquorum sensing activities of phytosynthesized silver nanoparticles fabricated from *Mespilus germanica* extract against multidrug resistance of *Klebsiella pneumoniae* clinical strains. *Journal of Basic Microbiology*,

60(3), 216–230. https://doi.org/10.1002/jobm.201900511

Gemiarto, A. T., Ninyio, N. N., Lee, S. W., Logis, J., Fatima, A., Chan, E. W. C., & Lim, C. S. Y. (2015). Isoprenyl caffeate, a major compound in manuka propolis, is a quorum-sensing inhibitor in *Chromobacterium violaceum*. *International Journal of General and Molecular Microbiology*, *108*(2), 491–504. https://doi.org/10.1007/s10482-015-0503-6

Gopu, V., Meena, C. K., Murali, A., & Shetty, P. H. (2016). Petunidin as a competitive inhibitor of acylated homoserine lactones in *Klebsiella pneumoniae*. *RSC Advances*, *6*(4), 2592–2601. https://doi.org/10.1039/c5ra20677d

Götz, F. (2002). *Staphylococcus* and biofilms. *Molecular Microbiology*, *43*(6), 1367–1378. https://doi.org/10.1046/j.1365-2958.2002.02827.x

Grandclément, C., Tannières, M., Moréra, S., Dessaux, Y., & Faure, D. (2015). Quorum quenching: Role in nature and applied developments. *FEMS Microbiology Reviews*, *40*(1), 86–116. https://doi.org/10.1093/femsre/fuv038

Hall-Stoodley, L., & Stoodley, P. (2005). Biofilm formation and dispersal and the transmission of human pathogens. *Trends in Microbiology*, *13*(1), 7–10. https://doi.org/10.1016/j.tim.2004.11.004

Hardie, K. R., & Heurlier, K. (2008). Establishing bacterial communities by “word of mouth”: LuxS and autoinducer 2 in biofilm development. *Nature Reviews Microbiology*, *6*(8), 635–643. https://doi.org/10.1038/nrmicro1916

Hayet, S., Sujan, K. M., Mustari, A., & Miah, M. A. (2021). Hemato-biochemical profile of turkey birds selected from Sherpur district of Bangladesh. *International Journal of Advanced Research in Biological Sciences*, *8*(6), 1–5. https://doi.org/10.22192/ijarbs

Hsieh, P. F., Lin, T. L., Yang, F. L., Wu, M. C., Pan, Y. J., Wu, S. H., & Wang, J. T. (2012). Lipopolysaccharide O1 antigen contributes to the virulence in *Klebsiella pneumoniae* causing pyogenic liver abscess. *PLoS ONE*, *7*(3),1–13. https://doi.org/10.1371/journal.pone.0033155

Jiang, Q., Chen, J., Yang, C., Yin, Y., Yao, K., & Song, D. (2019). Quorum Sensing: A prospective therapeutic target for bacterial diseases. *BioMed Research International*, 1–15. https://doi.org/10.1155/2019/2015978

Jordan, S. C., Hall, P. R., & Daly, S. M. (2022). Nonconformity of biofilm formation *in vivo* and *in vitro* based on *Staphylococcus aureus* accessory gene regulator status. *Scientific Reports*, *12*(1), 1–11. https://doi.org/10.1038/s41598-022-05382-w

Khan, A., Singh, P., & Srivastava, A. (2018). Synthesis, nature and utility of universal iron chelator – Siderophore: A review. *Microbiological Research*, *212*(11), 103–111. https://doi.org/10.1016/j.micres.2017.10.012

Khumalo, G. P., Sadgrove, N. J., Van Vuuren, S., & Van Wyk, B. E. (2019). Antimicrobial activity of volatile and non-volatile isolated compounds and extracts from the bark and leaves of *Warburgia salutaris* (*Canellaceae*) against skin and respiratory pathogens. *South African Journal of Botany*, *122*, 547–550. https://doi.org/10.1016/j.sajb.2018.10.018.

Koh, C., Sam, C., Yin, W., Tan, L. Y., Krishnan, T., Chong, Y. M., & Chan, K. (2013). Plant-derived natural products as sources of anti-quorum sensing compounds. *Sensors, 13*(5), 6217–6228. https://doi.org/10.3390/s130506217

Kong, F. D., Zhou, L. M., Ma, Q. Y., Huang, S. Z., Wang, P., Dai, H. F., & Zhao, Y. X. (2017). Metabolites

with Gram-negative bacteria quorum sensing inhibitory activity from the marine animal endogenic fungus *Penicillium* sp. *Archives of Pharmacal Research*, *40*(1), 25–31. https://doi.org/10.1007/s12272-016-0844-3

Köster, W. (2001). ABC transporter-mediated uptake of iron, siderophores, heme and vitamin B12. *Research in Microbiology*, *152*(3), 291–301. https://doi.org/10.1016/S0923-2508(01)01200-1

LaSarre, B., & Federle, M. J. (2013). Exploiting quorum sensing to confuse bacterial pathogens. *Microbiology and Molecular Biology Reviews*, *77*(1), 73–111. https://doi.org/10.1128/mmbr.00046-12

Lee, I. R., Molton, J. S., Wyres, K. L., Gorrie, C., Wong, J., Hoh, C. H., Teo, J., Kalimuddin, S., Lye, D. C., Archuleta, S., Holt, K. E., & Gan, Y. H. (2016). Differential host susceptibility and bacterial virulence factors driving *Klebsiella* liver abscess in an ethnically diverse population. *Scientific Reports*, *6*(7), 1–12. https://doi.org/10.1038/srep29316

Llobet, E., Campos, M. A., Giménez, P., Moranta, D., & Bengoechea, J. A. (2011). Analysis of the networks controlling the antimicrobial-peptide-dependent induction of *Klebsiella pneumoniae* virulence factors. *Infection and Immunity*, *79*(9), 3718–3732. https://doi.org/10.1128/IAI.05226-11

Lourens, A. C. U., Van Vuuren, S. F., Viljoen, A. M., Davids, H., & Van Heerden, F. R. (2011). Antimicrobial activity and *in vitro* cytotoxicity of selected South African *Helichrysum* species. *South African Journal of Botany*, *77*(1), 229–235. https://doi.org/10.1016/j.sajb.2010.05.006

Louw, C. A. M., Regnier, T. J. C., & Korsten, L. (2002). Medicinal bulbous plants of South Africa and their traditional relevance in the control of infectious diseases. *Journal of Ethnopharmacology*, *82*(2), 147–154. https://doi.org/10.1016/S0378-8741(02)00184-8

Lu, L., Hu, W., Tian, Z., Yuan, D., Yi, G., Zhou, Y., Cheng, Q., Zhu, J., & Li, M. (2019). Developing natural products as potential anti-biofilm agents. *Chinese Medicine*, *14*(1), 1–17. https://doi.org/10.1186/s13020-019-0232-2

Lu, L., Li, M., Yi, G., Liao, L., Cheng, Q., Zhu, J., Zhang, B., Wang, Y., Chen, Y., & Zeng, M. (2022). Screening strategies for quorum sensing inhibitors in combating bacterial infections. *Journal of Pharmaceutical Analysis*, *12*(1), 1–14. https://doi.org/10.1016/j.jpha.2021.03.009

Lugo, J. Z., Price, S., Miller, J. E., Ben-David, I., Merrill, V. J., Mancuso, P., Weinberg, J. B., & Younger, J. G. (2007). Lipopolysaccharide O-antigen promotes persistent murine bacteremia. *Shock*, *27*(2), 186–191. https://doi.org/10.1097/01.shk.0000238058.23837.21

Mah, T. F. C., & O'Toole, G. A. (2001). Mechanisms of biofilm resistance to antimicrobial agents. *Trends in Microbiology*, *9*(1), 34–39. https://doi.org/10.1016/S0966-842X(00)01913-2

Mahlangeni, N. T., Moodley, R., & Jonnalagadda, S. B. (2018). Elemental composition of *Cyrtanthus obliquus* and *Lippia javanica* used in South African herbal tonic, Imbiza. *Arabian Journal of Chemistry*, *11*(1), 128–136. https://doi.org/10.1016/j.arabjc.2014.07.007

Malolo, F. A. E., Nouga, A. B., Kakam, A., Franke, K., Ngah, L., Flausino, O., Mpondo, E. M., Ntie-Kang, F., Ndom, J. C., Bolzani, V. da S., & Wessjohann, L. (2015). Protease-inhibiting, molecular modeling and antimicrobial activities of extracts and constituents from *Helichrysum foetidum* and *Helichrysum mechowianum* (*compositae*). *Chemistry Central Journal*, *9*(1), 1–11. https://doi.org/10.1186/s13065-015-0108-1

Mamabolo, M. P., Muganza, F. M., Tabize Olivier, M., Olaokun, O. O., & Nemutavhanani, L. D. (2018). Evaluation of antigonorrhea activity and cytotoxicity of *Helichrysum caespititium* (DC) Harv. whole plant extracts. *Biology and Medicine*, *10*(1), 1–4. https://doi.org/10.4172/0974-8369.1000422

Maroyi, A. (2017). *Lippia javanica* (Burm.f.) Spreng.: Traditional and commercial uses and phytochemical and pharmacological significance in the African and Indian subcontinent. *Evidence-Based Complementary and Alternative Medicine*, 6746071, 1–34. https://doi.org/10.1155/2017/6746071

Maroyi, A. (2019). Medicinal uses, biological and phytochemical properties of *Helichrysum foetidum* (L.) Moench. (*Asteraceae*). *Asian Journal of Pharmaceutical and Clinical Research*, *12*(7), 13–18. https://doi.org/10.22159/ajpcr.2019.v12i7.33607

Mellini, M., Di Muzio, E., D'Angelo, F., Baldelli, V., Ferrillo, S., Visca, P., Leoni, L., Polticelli, F., & Rampioni, G. (2019). *In silico* selection and experimental validation of FDA-approved drugs as anti-quorum sensing agents. *Frontiers in Microbiology*, *10*(10), 1–14. https://doi.org/10.3389/fmicb.2019.02355

Miethke, M., & Marahiel, M. A. (2007). Siderophore-based iron acquisition and pathogen control. *Microbiology and Molecular Biology Reviews*, *71*(3), 413–451. https://doi.org/10.1128/mmbr.00012-07

Muhammad, M. H., Idris, A. L., Fan, X., Guo, Y., Yu, Y., Jin, X., Qiu, J., Guan, X., & Huang, T. (2020). Beyond Risk: Bacterial biofilms and their regulating approaches. *Frontiers in Microbiology*, *11*(5), 1–20. https://doi.org/10.3389/fmicb.2020.00928

Mulaudzi, R. B., Aremu, A. O., Rengasamy, K. R. R., Adebayo, S. A., McGaw, L. J., Amoo, S. O., Van Staden, J., & Du Plooy, C. P. (2019). Antidiabetic, anti-inflammatory, anticholinesterase and cytotoxicity determination of two *Carpobrotus* species. *South African Journal of Botany*, *125*(9), 142–148. https://doi.org/10.1016/j.sajb.2019.07.007

Naqvi, A. A. T., Mohammad, T., Hasan, G. M., & Hassan, M. I. (2019). Advancements in docking and molecular dynamics simulations towards ligand-receptor interactions and structure-function relationships. *Current Topics in Medicinal Chemistry*, *18*(20), 1755–1768. https://doi.org/10.2174/1568026618666181025114157

Navon-Venezia, S., Kondratyeva, K., & Carattoli, A. (2017). *Klebsiella pneumoniae*: A major worldwide source and shuttle for antibiotic resistance. *FEMS Microbiology Reviews*, *41*(3), 252–275. https://doi.org/10.1093/femsre/fux013

Nazzaro, F., Fratianni, F., & Coppola, R. (2013). Quorum sensing and phytochemicals. *International Journal of Molecular Sciences*, *14*(6), 12607–12619. https://doi.org/10.3390/ijms140612607

Odularu, A. T., Afolayan, A. J., Sadimenko, A. P., Ajibade, P. A., & Mbese, J. Z. (2022). Multidrug-resistant biofilm, quorum sensing, quorum quenching, and antibacterial activities of indole derivatives as potential eradication approaches. *BioMed Research International*, 9048245, 1–9. https://doi.org/10.1155/2022/9048245

Oliveira, B. D. Á., Rodrigues, A. C., Cardoso, B. M. I., Ramos, A. L. C. C., Bertoldi, M. C., Taylor, J. G., Cunha, L. R. da, & Pinto, U. M. (2016). Antioxidant, antimicrobial and anti-quorum sensing activities of *Rubus rosaefolius* phenolic extract. *Industrial Crops and Products*, *84*, 59–66. https://doi.org/10.1016/j.indcrop.2016.01.037

Olivier, D. K., Shikanga, E. A., Combrinck, S., Krause, R. W. M., Regnier, T., & Dlamini, T. P. (2010). Phenylethanoid glycosides from *Lippia javanica. South African Journal of Botany*, *76*(1), 58–63. https://doi.org/10.1016/j.sajb.2009.07.002

Othman, L., Sleiman, A., & Abdel-Massih, R. M. (2019). Antimicrobial activity of polyphenols and alkaloids in middle eastern plants. *Frontiers in Microbiology*, *10*(5), 1–28. https://doi.org/10.3389/fmicb.2019.00911

Pacheco, T., Gomes, A. É. I., Siqueira, N. M. G., Assoni, L., Darrieux, M., Venter, H., & Ferraz, L. F. C. (2021). SdiA, a quorum-sensing regulator, suppresses fimbriae expression, biofilm formation, and quorum-sensing signalling molecules production in K*lebsiella pneumoniae*. *Frontiers in Microbiology*, *12*(6), 1–15. https://doi.org/10.3389/fmicb.2021.597735

Paczosa, M. K., & Mecsas, J. (2016). *Klebsiella pneumoniae*: Going on the offense with a strong defense. *Microbiology and Molecular Biology Reviews*, *80*(3), 629–661. https://doi.org/10.1128/mmbr.00078-15

Palacios, M., Miner, T. A., Frederick, D. R., Sepulveda, V. E., Quinn, J. D., Walker, K. A., & Miller, V. L. (2018). Identification of two regulators of virulence that are conserved in *Klebsiella pneumoniae* classical and hypervirulent strains. *American Society for Microbiology MBio*, *9*(4), 1–17. https://doi.org/10.1128/mBio.01443-18

Palano, G., Foinquinos, A., & Müllers, E. (2021). *In vitro* assays and imaging methods for drug discovery for cardiac fibrosis. *Frontiers in Physiology*, *12*(7), 1–11. https://doi.org/10.3389/fphys.2021.697270

Palmer, J., Flint, S., & Brooks, J. (2007). Bacterial cell attachment, the beginning of a biofilm. *Journal of Industrial Microbiology and Biotechnology*, *34*(9), 577–588. https://doi.org/10.1007/s10295-007-0234-4

Paluch, E., Rewak-Soroczyńska, J., Jędrusik, I., Mazurkiewicz, E., & Jermakow, K. (2020). Prevention of biofilm formation by quorum quenching. *Applied Microbiology and Biotechnology*, *104*(5), 1871–1881. https://doi.org/10.1007/s00253-020-10349-w

Pan, Y. J., Lin, T. L., Chen, C. T., Chen, Y. Y., Hsieh, P. F., Hsu, C. R., Wu, M. C., & Wang, J. T. (2015). Genetic analysis of capsular polysaccharide synthesis gene clusters in 79 capsular types of *Klebsiella* spp. *Scientific Reports*, *5*(10), 1–10. https://doi.org/10.1038/srep15573

Parenti, M. D., & Rastelli, G. (2012). Advances and applications of binding affinity prediction methods in drug discovery. *Biotechnology Advances*, *30*(1), 244–250. https://doi.org/10.1016/j.biotechadv.2011.08.003

Parrott, A. M., Shi, J., Aaron, J., Green, D. A., Whittier, S., & Wu, F. (2021). Detection of multiple hypervirulent *Klebsiella pneumoniae* strains in a New York City hospital through screening of virulence genes. *Clinical Microbiology and Infection*, *27*(4), 583–589. https://doi.org/10.1016/j.cmi.2020.05.012

Pascual, M. E., Slowing, K., Carretero, E., Sánchez Mata, D., & Villar, A. (2001). *Lippia*: Traditional uses, chemistry and pharmacology: A review. *Journal of Ethnopharmacology*, *76*(3), 201–214. https://doi.org/10.1016/S0378-8741(01)00234-3

Patro, L. P. P., & Rathinavelan, T. (2019). Targeting the sugary armor of *Klebsiella* species. *Frontiers in Cellular and Infection Microbiology*, *9*(11), 1–23. https://doi: 10.3389/fcimb.2019.00367

Pereira, C. S., Thompson, J. A., & Xavier, K. B. (2013). AI-2-mediated signalling in bacteria. *FEMS Microbiology Reviews*, *37*(2), 156–181. https://doi.org/10.1111/j.1574-6976.2012.00345.x

Philemon, Y. K., Matasyoh, J. C., & Wagara, I. N. (2016). Chemical composition and antifungal activity of the essential oil from *Lippia javanica* (*Verbenaceae*). *International Journal of Biotechnology and Food Science*, *4*(1), 1–6.

Pinzi, L., & Rastelli, G. (2019). Molecular docking: Shifting paradigms in drug discovery. *International Journal of Molecular Sciences*, *20*(18), 1–23. https://doi.org/10.3390/ijms20184331

Podschun, R., & Ullmann, U. (1998). *Klebsiella* spp. as nosocomial pathogens: Epidemiology, taxonomy, typing methods, and pathogenicity factors. *Clinical Microbiology Reviews*, *11*(4), 589–603. https://doi.org/10.1128/cmr.11.4.589

Pradeep, C., Lalitha, S., Rajesh, S. V., & Shanmugam, G. (2018). Comparative modeling and molecular docking studies of quorum sensing transcriptional regulating factor SdiA from *Klebsiella pneumoniae*. *International Journal of Current Research in Science, Engineering & Technology*, *1*(1), 1–8. https://doi.org/10.30967/ijcrset.1.1.2018.9-16

Quecan, B. X. V., Santos, J. T. C., Rivera, M. L. C., Hassimotto, N. M. A., Almeida, F. A., & Pinto, U. M. (2019). Effect of quercetin-rich onion extracts on bacterial quorum sensing. *Frontiers in Microbiology*, *10*(4), 1–16. https://doi.org/10.3389/fmicb.2019.00867

Rabin, N., Zheng, Y., Opoku-Temeng, C., Du, Y., Bonsu, E., & Sintim, H. O. (2015). Biofilm formation mechanisms and targets for developing antibiofilm agents. *Future Medicinal Chemistry*, *7*(4), 493–512. https://doi.org/10.4155/fmc.15.6

Ram, A., Bhakshu, L. M., & Venkata Raju, R. R. (2004). *In vitro* antimicrobial activity of certain medicinal plants from Eastern Ghats, India, used for skin diseases. *Journal of Ethnopharmacology*, *90*(2), 353–357. https://doi.org/10.1016/j.jep.2003.10.013

Redanz, S., Standar, K., Podbielski, A., & Kreikemeyer, B. (2012). Heterologous expression of sahH reveals that biofilm formation is autoinducer-2-independent in *Streptococcus sanguinis* but is associated with an intact activated methionine cycle. *Journal of Biological Chemistry*, *287*(43), 36111–36122. https://doi.org/10.1074/jbc.M112.379230

Salmaso, V., & Moro, S. (2018). Bridging molecular docking to molecular dynamics in exploring ligand-protein recognition process: An overview. *Frontiers in Pharmacology*, *9*(8), 1–16. https://doi.org/10.3389/fphar.2018.00923

Santajit, S., & Indrawattana, N. (2016). Mechanisms of antimicrobial resistance in ESKAPE pathogens. *BioMed Research International*, 1155, 1–8. https://doi.org/10.1155/2016/2475067

Santhakumari, S., & Ravi, A. V. (2019). Targeting quorum sensing mechanism: An alternative anti-virulent strategy for the treatment of bacterial infections. *South African Journal of Botany*, *120*, 81–86. https://doi.org/10.1016/j.sajb.2018.09.028

Sarkar, R., Mondal, C., Bera, R., Chakraborty, S., Barik, R., Roy, P., Kumar, A., Yadav, K. K., Choudhury, J., Chaudhary, S. K., Samanta, S. K., Karmakar, S., Das, S., Mukherjee, P. K., Mukherjee, J., & Sen, T. (2015). Antimicrobial properties of *Kalanchoe blossfeldiana*: A focus on drug resistance with particular reference to quorum sensing-mediated bacterial biofilm formation. *Journal of Pharmacy and Pharmacology*, *67*(7), 951–962. https://doi.org/10.1111/jphp.12397

Schroll, C., Barken, K. B., Krogfelt, K. A., & Struve, C. (2010). Role of type 1 and type 3 fimbriae in

Klebsiella pneumoniae biofilm formation. *BMC Microbiology*, *10,* 1–10. https://doi.org/10.1186/1471-2180-10-179

Scoffone, V. C., Trespidi, G., Chiarelli, L. R., Barbieri, G., & Buroni, S. (2019). Quorum sensing as antivirulence target in cystic fibrosis pathogens. *International Journal of Molecular Sciences*, *20*(8), 1–38. https://doi.org/10.3390/ijms20081838

Scott, G., Springfield, E. P., & Coldrey, N. (2004). A pharmacognostical study of 26 South African plant species used as traditional medicines. *Pharmaceutical Biology*, *42*(3), 186–213. https://doi.org/10.1080/13880200490514032

Shaik, G., Sujatha, N., & Mehar, S. K. (2014). Medicinal plants as a source of antibacterial agents to counter *Klebsiella pneumoniae*. *Journal of Applied Pharmaceutical Science*, *4*(1), 135–147. https://doi.org/10.7324/JAPS.2014.40123

Shankar-Sinha, S., Valencia, G. A., Janes, B. K., Rosenberg, J. K., Whitfield, C., Bender, R. A., Standiford, T. J., & Younger, J. G. (2004). The *Klebsiella pneumoniae* O antigen contributes to bacteremia and lethality during murine pneumonia. *Infection and Immunity*, *72*(3), 1423–1430. https://doi.org/10.1128/IAI.72.3.1423-1430.2004

Shrestha, P. M., & Dhillion, S. S. (2003). Medicinal plant diversity and use in the highlands of Dolakha district, Nepal. *Journal of Ethnopharmacology*, *86*(1), 81–96. https://doi.org/10.1016/S0378-8741(03)00051-5

Shukla, R., Shukla, H., Kalita, P., Sonkar, A., Pandey, T., Singh, D. B., Kumar, A., & Tripathi, T. (2018). Identification of potential inhibitors of *Fasciola gigantica* thioredoxin1: computational screening, molecular dynamics simulation, and binding free energy studies. *Journal of Biomolecular Structure and Dynamics*, *36*(8), 2147–2162. https://doi.org/10.1080/07391102.2017.1344141

Sisay, M., Bussa, N., Gashaw, T., & Mengistu, G. (2019). Investigating *in vitro* antibacterial activities of medicinal plants having folkloric repute in Ethiopian traditional medicine. *Journal of Evidence-Based Integrative Medicine*, *24*, 1–9. https://doi.org/10.1177/2515690X19886276

Skandamis, P. N., & Nychas, G. J. E. (2012). Quorum sensing in the context of food microbiology. *Applied and Environmental Microbiology*, *78*(16), 5473–5482. https://doi.org/10.1128/AEM.00468-12

Sliwoski, G., Kothiwale, S., Meiler, J., & Lowe, E. W. (2014). Computational methods in drug discovery. *Pharmacological Reviews*, *66*(1), 334–395. https://doi.org/10.1124/pr.112.007336

Soto, S. M. (2014). Importance of biofilms in urinary tract infections: New therapeutic approaches. *Advances in Biology*, *2014*, 1–13. https://doi.org/10.1155/2014/543974

Street, R. A., & Prinsloo, G. (2013). Commercially important medicinal plants of South Africa: A review. *Journal of Chemistry*, 205048, 1–16. https://doi.org/10.1155/2013/205048

Struve, C., Bojer, M., & Krogfelt, K. A. (2008). Characterization of *Klebsiella pneumoniae* type 1 fimbriae by detection of phase variation during colonization and infection and impact on virulence. *Infection and Immunity*, *76*(9), 4055–4065. https://doi.org/10.1128/IAI.00494-08

Su, K., Zhou, X., Luo, M., Xu, X., Liu, P., Li, X., Xue, J., Chen, S., Xu, W., Li, Y., & Qiu, J. (2018). Genome-wide identification of genes regulated by *RcsA, RcsB*, and *RcsAB* phosphorelay regulators in *Klebsiella pneumoniae* NTUH-K2044. *Microbial Pathogenesis*, *123*(11), 36–41. https://doi.org/10.1016/j.micpath.2018.06.036

Sun, S., Zhang, H., Lu, S., Lai, C., Liu, H., & Zhu, H. (2016). The metabolic flux regulation of *Klebsiella pneumoniae* based on quorum sensing system. *Scientific Reports*, *6*(12), 1–9. https://doi.org/10.1038/srep38725

Taga, M. E., Semmelhack, J. L., & Bassler, B. L. (2001). The LuxS-dependent autoinducer AI-2 controls the expression of an ABC transporter that functions in AI-2 uptake in *Salmonella typhimurium. Molecular Microbiology*, *42*(3), 777–793. https://doi.org/10.1046/j.1365-2958.2001.02669.x

Talebi, A., Rizvanov, A. A., Haertlé, T., & Blatt, N. L. (2019). World Health Organization report: Current crisis of antibiotic resistance. *BioNanoScience*, *9*(4), 778–788. https://doi.org/10.1007/s12668-019-00658-4

Tavío, M. M., Aquili, V. D., Poveda, J. B., Antunes, N. T., Sánchez-Céspedes, J., & Vila, J. (2010). Quorum-sensing regulator SdiA and MarA overexpression is involved in *in vitro*-selected multidrug resistance of *Escherichia coli. Journal of Antimicrobial Chemotherapy*, *65*(6), 1178–1186. https://doi.org/10.1093/jac/dkq112

Tay, S. B., & Yew, W. S. (2013). Development of quorum-based anti-virulence therapeutics targeting Gram-negative bacterial pathogens. *International Journal of Molecular Sciences*, *14*(8), 16570–16599. https://doi.org/10.3390/ijms140816570

Thakur, P., Chawla, R., Tanwar, A., Chakotiya, A. S., Narula, A., Goel, R., Arora, R., & Sharma, R. K. (2016). Attenuation of adhesion, quorum sensing and biofilm mediated virulence of carbapenem resistant *Escherichia coli* by selected natural plant products. *Microbial Pathogenesis*, *92*, 76–85. https://doi.org/10.1016/j.micpath.2016.01.001

Therrien, E., Weill, N., Tomberg, A., Corbeil, C. R., Lee, D., & Moitessier, N. (2014). Docking ligands into flexible and solvated macromolecules.7.Impact of protein flexibility and water molecules on docking-based virtual screening accuracy. *Journal of Chemical Information and Modeling*, *54*(11), 3198–3210. https://doi.org/10.1021/ci500299h

Toole, G. O., Kaplan, H. B., & Kolter, R. (2000). Biofilm formation as microbial development. *Annual Review of Microbiology*, 49–79.

Torcato, I. M., Kasal, M. R., Brito, P. H., Miller, S. T., & Xavier, K. B. (2019). Identification of novel autoinducer-2 receptors in *Clostridia* reveals plasticity in the binding site of the LsrB receptor family. *Journal of Biological Chemistry*, *294*(12), 4450–4463. https://doi.org/10.1074/jbc.RA118.006938

Tumbarello, M., Spanu, T., Sanguinetti, M., Citton, R., Montuori, E., Leone, F., Fadda, G., & Cauda, R. (2006). Bloodstream infections caused by extended-spectrum-β-lactamase- producing *Klebsiella pneumoniae*: Risk factors, molecular epidemiology, and clinical outcome. *Antimicrobial Agents and Chemotherapy*, *50*(2), 498–504. https://doi.org/10.1128/AAC.50.2.498-504.2006

Van Wyk, B. E. (2011). The potential of South African plants in the development of new medicinal products. *South African Journal of Botany*, *77*(4), 812–829. https://doi.org/10.1016/j.sajb.2011.08.011

Vasavi, H. S., Arun, A. B., & Rekha, P. D. (2016). Anti-quorum sensing activity of flavonoid-rich fraction from *Centella asiatica* L. against *Pseudomonas aeruginosa* PAO1. *Journal of Microbiology, Immunology and Infection*, *49*(1), 8–15. https://doi.org/10.1016/j.jmii.2014.03.012

Vattem, D. A., Mihalik, K., Crixell, S. H., & McLean, R. J. C. (2007). Dietary phytochemicals as quorum

sensing inhibitors. *Fitoterapia*, *78*(4), 302–310. https://doi.org/10.1016/j.fitote.2007.03.009

Ventola, C. L. (2015). The Antibiotics. *Comprehensive Biochemistry*, *11*(4), 181–224. https://doi.org/10.1016/B978-1-4831-9711-1.50022-3

Viljoen, A. M., Subramoney, S., Vuuren, S. F. V., Başer, K. H. C., & Demirci, B. (2005). The composition, geographical variation and antimicrobial activity of *Lippia javanica* (*Verbenaceae*) leaf essential oils. *Journal of Ethnopharmacology*, *96*(1), 271–277. https://doi.org/10.1016/j.jep.2004.09.017

Vuotto, C., Longo, F., Pascolini, C., Donelli, G., Balice, M. P., Libori, M. F., Tiracchia, V., Salvia, A., & Varaldo, P. E. (2017). Biofilm formation and antibiotic resistance in K*lebsiella pneumoniae* urinary strains. *Journal of Applied Microbiology*, *123*(4), 1003–1018. https://doi.org/10.1111/jam.13533

Wang, S., Feng, Y., Han, X., Cai, X., Yang, L., Liu, C., & Shen, L. (2021). Inhibition of virulence factors and biofilm formation by wogonin attenuates pathogenicity of *Pseudomonas aeruginosa* PAO1 via targeting pqs quorum-sensing system. *International Journal of Molecular Sciences*, *22*(23), 1–19. https://doi.org/10.3390/ijms222312699

Waters, C. M., & Bassler, B. L. (2005). Quorum sensing: Cell-to-cell communication in bacteria. *Annual Review of Cell and Developmental Biology*, *21*, 319–346. https://doi.org/10.1146/annurev.cellbio.21.012704.131001

Watnick, P., & Kolter, R. (2000). Biofilm, city of microbes. *Journal of Bacteriology*, *182*(10), 2675–2679. https://doi.org/10.1128/JB.182.10.2675-2679.2000

Xavier, K. B., & Bassler, B. L. (2003). LuxS quorum sensing: More than just a numbers game. *Current Opinion in Microbiology*, *6*(2), 191–197. https://doi.org/10.1016/S1369-5274(03)00028-6

Xue, T., Yu, L., Shang, F., Li, W., Zhang, M., Ni, J., & Chen, X. (2016). Short communication: The role of autoinducer 2 (AI-2) on antibiotic resistance regulation in an *Escherichia coli* strain isolated from a dairy cow with mastitis. *Journal of Dairy Science*, *99*(6), 4693–4698. https://doi.org/10.3168/jds.2015-10543

Yang, M., Meng, F., Gu, W., Li, F., Tao, Y., Zhang, Z., Zhang, F., Yang, X., Li, J., & Yu, J. (2020). Effects of natural products on bacterial communication and network-quorum sensing. *BioMed Research International*, *15*(3), 1–13. https://doi.org/10.1155/2020/8638103

Yin, W. F., Purmal, K., Chin, S., Chan, X. Y., Koh, C. L., Sam, C. K., & Chan, K. G. (2012). N-Acyl homoserine lactone production by *Klebsiella pneumoniae* isolated from human tongue surface. *Sensors*, *12*(3), 3472–3483. https://doi.org/10.3390/s120303472

Yunos, N. Y., Tan, W. S., Mohamad, N. I., Tan, P. W., Adrian, T. G. S., Yin, W. F., & Chan, K. G. (2014). Discovery of *Pantoea rodasii* strain nd03 that produces n-(3-oxo-hexanoyl)-l-homoserine lactone. *Sensors* (Switzerland), *14*(5), 9145–9152. https://doi.org/10.3390/s140509145

Zhao, D., Jiang, J., Du, R., Guo, S., Ping, W., Ling, H., & Ge, J. (2019). Purification and characterization of an exopolysaccharide from *Leuconostoc lactis* L2. *International Journal of Biological Macromolecules*, *139*, 1224–1231. https://doi.org/10.1016/j.ijbiomac.2019.08.114

Zhu, H., & Sun, S. J. (2008). Inhibition of bacterial quorum sensing-regulated behaviors by *Tremella fuciformis* extract. *Current Microbiology*, *57*(5), 418–422. https://doi.org/10.1007/s00284-008-9215-8

Zhu, H. L., Wan, J. B., Wang, Y. T., Li, B. C., Xiang, C., He, J., & Li, P. (2014). Medicinal compounds with antiepileptic/anticonvulsant activities. *Epilepsia*, *55*(1), 3–16.

https://doi.org/10.1111/epi.12463

Zhu, J., Wang, T., Chen, L., & Du, H. (2021). Virulence factors in hypervirulent *Klebsiella pneumoniae*. *Frontiers in Microbiology*, *12*(4), 1–14. https://doi.org/10.3389/fmicb.2021.642484

Zuo, J., Yin, H., Hu, J., Miao, J., Chen, Z., Qi, K., Wang, Z., Gong, J., Phouthapane, V., Jiang, W., Mi, R., Huang, Y., Wang, C., & Han, X. (2019). Lsr operon is associated with AI-2 transfer and pathogenicity in avian pathogenic *Escherichia coli. Veterinary Research*, *50*(1), 1–15. https://doi.org/10.1186/s13567-019-0725-0

CHAPTER TWO

IN-VITRO SCREENING OF SELECTED SOUTH AFRICAN MEDICINAL PLANTS FOR ANTIPATHOGENIC ACTIVITIES AGAINST *K. PNEUMONIAE*

This chapter is submitted for publication in Evidence-Based Complementary and Alternative Medicine: **Adeosun, I.J**., Baloyi, I.T., Moleleki L.N and Cosa, S. Extracts of selected South African medicinal plants mitigate virulence factors in multidrug resistant strains of *Klebsiella pneumoniae.*

2.1 INTRODUCTION

Plants have long been used as medicines to treat a variety of ailments, and approximately 100,000 plant species have been investigated for their medicinal purposes (Uc-Cachón et al., 2021; Górniak et al., 2019). This is based on medicinal plants possessing a diverse range of secondary metabolites such as tannins, terpenoids, alkaloids, and flavonoids, displaying antibacterial activities thereby suggesting their therapeutic properties (Atanasov et al., 2021). As per record, 80% of the emerging world's population relies on traditional medicine for therapy, while the World Health Organization (WHO) documents that ~ 25% of all modern medicines were obtained from medicinal plants (Chintamunnee & Mahomoodally, 2012). This further substantiates medicinal plants as a vital source of both modern and traditional medicine.

South Africans utilize traditional medicine for the management of their physical, psychological and primary healthcare needs (Agbor & Naidoo, 2016). Scott et al. (2004) validate this by documenting that about 70% of South Africans use traditional medicines derived from plant species indigenous to the region. In addition, South Africa has ~30,000 different plant species (~10% of the world's higher plant species) (Cosa et al., 2020). These medicinal plants are, however, rarely explored as prospective drug candidates for the management of MDR pathogens. The pathogenic *Klebsiella pneumoniae* is listed among the most critical priority pathogens by the WHO due to its resistance against almost all available conventional antibiotics (Boucher et al., 2009).

K. pneumoniae, a Gram-negative, non-motile, usually capsulated, facultatively anaerobic bacteria belonging to the family *Enterobacteriaceae* (Kendaganna et al., 2021) is known for its pathogenicity towards humans causing digestive, urinary, and respiratory tract infections (Brisse et al., 2009). It has also been reported to be implicated with septicaemia, soft tissue infections, intra-abdominal infections, wound and blood infections (Adeosun et al., 2022). *K. pneumoniae* possesses virulence factors such as capsular antigens, adherence factors for biofilm formation, O-lipopolysaccharide, exopolysaccharides, and siderophores linked to its infectivity and virulence (Adeosun et al., 2022; Wareth & Neubauer, 2021). Combating its virulence has been challenging due to antibiotic resistance, a phenomenon which has increased dramatically over the last few decades (Adeosun et al., 2019), with resistance to β -

lactams having the greatest impact on treatment efficacy (Martin & Bachman, 2018). Thus, new or alternative therapeutic options other than conventional antibiotics need to be studied to identify unorthodox methods to control antibiotic-resistant bacteria (Bouyahya et al., 2017). As a prospective solution to this global health threat, the WHO recommends the exploration of medicinal plants for their antipathogenic or antivirulence potential as this might be the source of new drugs (Doughari et al., 2009). *Lippia javanica, Helichrysum populifolium* and *Carpobrotus dimidiatus*, the three South African medicinal plants reported to have ethnomedicinal use against MDR bacteria might also play a role in the control of *K. pneumoniae* related infections (Chagonda & Chalchat, 2015; Akinyede et al., 2020).

Lippia javanica, (Burm.f.) Spreng commonly known as the fever tea belongs to the family *Verbenaceae* and has a long history of traditional uses in tropical Africa (Chagonda & Chalchat, 2015). Based on its perceived medicinal characteristics, it is frequently used as an indigenous herbal tea, refreshing beverage, or as culinary addition (Chagonda & Chalchat, 2015). *L. javanica* contains a significant amount of volatile oil, including compounds such as caryophyllene, carvone, ipsenone, ipsdienone, limonene, linalool, myrcene, myrcenone, ocimenone, *p*-cymene, piperitenone, sabinene, tagetenone, and several others (Lukwa et al., 2009), which are contributing factors to its medicinal properties.

Helichrysum populifolium (DC), a member of the *Asteraceae* family, is commonly referred to as poplar helichrysum (Lourens et al., 2008). Generally, plants belonging to the *Helichrysum* genus have long been used in traditional medicine to treat numerous ailments, including liver disorders, gall bladder complications, cystitis, jaundice, stomach pain, allergies, infections, colds, cough, skin infections, inflammation, asthma, arthritis, insomnia, and for wound healing (Akinyede et al., 2021). The health properties of this plant can be attributed to its bioactive compounds which include essential oils such as terpenoids (Mari et al., 2014), as well as flavonoids, phenolic acids, pyrone, benzofurans, and phloroglucinols (Akaberi et al., 2019).

Carpobrotus dimidiatus (Haw.) L. Bolus commonly known as natal sour fig is an indigenous South African species from the *Aizoaceae* family which grows abundantly in the east of the coastal regions in South Africa (Broomhead et al., 2020). It is among the commercially important South African medicinal plants used in traditional medicine

to treat diabetes, wounds, tuberculosis, high blood pressure, sore throat, skin infections, dysentery, digestive ailments and toothaches (Mulaudzi et al., 2019). Bioactive compounds such as flavonoids, tannins, alkaloids, phytosterols, and aromatic acids are found in abundance in the *Carpobrotus* species (Springfield et al., 2003).

Of the three studied plants, only *Lippia javanica* have been previously tested for its anibacterial activity against different pathogens where its essential oil revealed a moderate inhibitory activity on *Klebsiella pneumoniae* and *Streptococcus pneumoniae* (MIC: 0.76 mg/mL), on *Escherichia coli, Staphylococcus aureus*, and *Pseudomonas aeruginosa* (1.50 mg/mL) (Mbayo et al., 2021). However, different *Carpobrotus* species (*C. edulis* and *C. mellei*) have been previously reported to show antibacterial activity against *Staphylococcus aureus, Enterococcus faecalis* and *Pseudomonas aeruginosa* (Springfield and Weitz 2006; Martins et al., 2011) while *Helichrysum* species have been reported for antiviral activities (Emamzadeh et al., 2022).

Even though the medicinal properties and the traditional uses of the studied plants have been documented, their antivirulence activities against hypervirulent *K. pneumoniae* have been less explored with no scientific data available and it is not known if they contain anti-infectious phytochemicals for the management of *K. pneumoniae* infections. This study therefore aimed at studying the effect of *Lippia javanica, Helichrysum populifolium* and *Carpobrotus dimidiatus* extracts on *K. pneumoniae* virulence.

2.2 MATERIALS AND METHODS

2.2.1 Collection and extraction of plant materials

Leaves of three plant species (*L. javanica, H. populifolium* and *C. dimidiatus*) were harvested in June 2021 from the Manie van der Schijff Botanical Garden, University of Pretoria. The identity of the plants was confirmed at the Department of Plant and Soil Sciences, University of Pretoria. Voucher specimen numbers were assigned as PRU 128530 for *Lippia javanica,* PRU 128531 for *Helichrysum populifolium* and PRU 128529 for *Carpobrotus dimidiatus* upon submission at the University of Pretoria H.G.W.J. Schweickerdt Herbarium.

Plant preparation and extractions were carried out according to the method used by Mashamba et al. (2022). The leaves were allowed to dry at room temperature (25 °C), blended and weighed using a weighing balance (Kern 770, Microsep, Johannesburg, South Africa). Extraction was carried out using solvents of varying polarities which include dichloromethane, ethyl acetate, methanol and water. Approximately 30.0 g of each powdered plant material was extracted with 300 mL solvents of methanol and ethyl acetate, while for dichloromethane, 35.0 g of plant powder was used. The mixtures were shaken (Labcon, South Africa) at 140 rpm for 48 hrs. Afterwards, a Whatman no. 1 filter paper (11 µm) was used to filter the extracts. The extracts were concentrated by evaporating the filtrates using a rotatory evaporator (Labotec Buchi Heidolph, Germany) at 45°C under reduced pressure, then dried in a fume hood for 4-5 days until completely dry.

For aqueous extraction, 300 mL of deionized water was added to 30g of the blended plant material and allowed to boil (100°C) for 45 minutes on a hotplate (Labotec, South Africa). After cooling, the mixture was filtered using Whatman no. 1 filter paper (11 µm), transferred to glass jars with screwcaps, frozen at -80 ºC for 3-6 hrs, and subjected to lyophilization using an SP Scientific freeze dryer (Scientific US, USA). Masses of the twelve dried plant extracts (*L. javanica* (aqueous), *L. javanica* (ethyl acetate), *L. javanica* (methanol), *L. javanica* (dichloromethane), *C. dimidiatus* (aqueous), *C. dimidiatus* (ethyl acetate), *C. dimidiatus* (methanol), *C. dimidiatus* (dichloromethane), *H. populifolium* (aqueous), *H. populifolium* (ethyl acetate), *H. populifolium* (methanol) and *H. populifolium* (dichloromethane) were determined, and the extracts were stored at 4°C prior use for biological assays. Subsequently, yield of the extracts were calculated and presented in percentages following equation (1):

$$Percentage\ yield\ (\%) = \frac{dry\ crude\ extract}{dry\ initial\ material\ before\ extraction} \times 100 \qquad (1)$$

2.2.2 Bacterial strains and growth conditions

Two American Type Culture Collection strains of *K. pneumoniae* (ATCC BAA-1705) - CBR and (ATCC 700603) - ESBL producing, were used in this study. Prior to usage, the bacterial strains were stored as glycerol stocks at -80° C. The strains were prepared in Mueller Hinton (MH) medium and incubated at 37°C to obtain active

bacterial cultures. To obtain an absorbance (OD_{600nm}) of 0.1, a few colonies were dissolved in PB solution and resuspended. The bacterial cell suspension was adjusted to obtain an equivalent of 0.5 McFarland standard. Ethics approval (reference number: NAS157/2021) for the use of the *K. pneumoniae* strains was granted by the University of Pretoria, Faculty of Natural and Agricultural Sciences Ethics Committee (Appendix 2.1).

2.2.3 Antibacterial activity of plant extracts against K. pneumoniae strains

The plant extracts were evaluated for their minimum inhibitory concentration (MIC) using the broth microdilution method as described by Alves et al. (2013). A stock concentration of the plant extracts was prepared at approximately 25mg/mL in 1% DMSO and 100 µL of MH broth was added into each well of a 96-well microtiter plate. Then, a 100 µL aliquot of each plant extract was added to the first row of the microtiter plates in triplicates.

Following a series of dilutions in the A to H direction, decreasing values between 6.25–0.048mg/mL were obtained. Approximately, 100 µL of standardized bacterial strains ($OD_{600\ nm}$ = 0.08 – 0.1) were then added to each well. Quercetin (1mg/mL) and ciprofloxacin (0.01mg/mL) were used as the positive controls, while 100 µL of 1% DMSO served as the negative control. Samples were incubated at 37°C for 24 hours. Following incubation, 40 µL of a 0.20 mg/mL solution of p-iodonitrotetrazolium violet (INT) was added to each well and further incubated at 37°C for 30 minutes. Clear wells with no colour change suggested inhibition of bacterial growth. Visual evaluation and recording of the MIC value for each plant extract were done. The MIC was defined as the lowest concentration of plant extracts at which the test strain showed no visible growth. Interpretation of results was done according to the criterion stated by Mamabolo et al. (2018): MIC values < 0.1mg/mL indicates significant activity, while values between 0.1 and 0.625mg/mL depicts moderate activity. Values > 0.625mg/mL, however, indicates low activity.

2.2.4 Effect of plant extracts on biofilm formation stages

The studied plant extracts were assessed for their ability to inhibit three different stages of biofilms namely anti-adhesion (initial cell attachment), preformed biofilm

(biomass measurement) and mature biofilms according to the method described by Baloyi et al. (2021) and Blando et al. (2019). The twelve plant extracts were tested against CBR and ESBL producing *K. pneumoniae* strains for the three biofilm stages. Approximately, 100 µL of standardized bacterial suspension (OD_{600nm} = 0.1), 100 µL of MH broth, and 100 µL of the plant extracts were loaded into the wells for the initial cell attachment inhibition assay and were incubated at 37°C for 24 hours. Quercetin and ciprofloxacin were used as positive controls.

For the preformed and mature biofilm experiments, 100 µL of standardized bacterial suspension and 100 µL of MH broth were loaded into the wells. The samples were incubated at 37°C for 8 hours for preformed biofilm and 24 hours for mature biofilm under static condition and dynamic condition at 180 rpm in a shaker incubator. After incubation, 100 µL of the plant extracts were introduced into each well and further incubated for 24 hours. The modified crystal violet (CV) assay was used to examine initial cell attachment, biofilm biomass, and mature biofilms. The 96-well plates containing formed biofilms were rinsed with sterile distilled water to remove any planktonic cells and media. The plates were dried in an oven at 60°C for 45 minutes. Afterwards, 1% CV solution was applied to the wells and incubated in the dark for 15 minutes. The wells were cleaned with sterile distilled water to remove any remaining stain. Semi-quantitative analysis of biofilm formation was made possible by destaining the wells using 125 µL of 95% ethanol. A fresh plate was coated with approximately 100 µL of the destaining solution, and a multi-mode microplate reader (SpectraMax® paradigm) was used to measure the absorbance ($OD_{585\ nm}$). The percentage inhibition was calculated using equation (2) below:

$$Biofilm\ reduction\ (\%) = \frac{(Control_{585\ nm} - Test_{585\ nm})}{(Control_{585\ nm})} \times 100 \qquad (2)$$

Interpretation of results was done according to the criterion stated by Famuyide et al. (2019). Inhibitory activity was defined by values between 0 and 100%, however, it was further divided into three categories: ≥ 50% (good activity), 0 to 49% (weak activity), and negative values, which showed a rise in biofilm formation rather than its inhibition.

2.2.5 In situ visualization of biofilms using scanning electron microscopy

In order to investigate the morphology and density of *K.pneumoniae* biofilms, sub-inhibitory biofilm inhibitory concentration of the most active plant extract was fixed and visualized using a scanning electron microscope following the protocol outlined by Wijesundara and Rupasinghe (2019). After prompt rinsing in phosphate-buffered saline (PBS), the biofilms were fixed in a microtiter plate with 0.1 M sodium cacodylate buffer (pH 7.2) containing 2% glutaraldehyde for 2 hours. The biofilms were then washed with phosphate washing buffer three more times for 15 minutes each. Afterwards, they were subjected to a series of ethanol gradients at concentrations of 35%, 50%, 75%, 90%, and 100%, which resulted in the dehydration of the samples. All the gradient phases required 15-minute exposure intervals, and the ultimate 100% ethanol treatment was performed three times. An equal volume of hexamethyldisilazane (HMDS) and 100% ethanol was added, and the samples were covered and left to stand for 1 hour. The HMDS-ethanol mixture was withdrawn and fresh HMDS was immediately introduced. Plates were allowed to dry under the fume hood for 2 h. Thereafter, the fixed biofilms were installed on aluminium stubs, coated with gold-palladium (15 nm) and viewed using a Zeiss crossbeam 540 scanning electron microscope.

2.2.6 Inhibition of exopolysaccharide production

The exopolysaccharide reduction assay was done according to the method described by Gopu and Shetty (2016). Approximately, 100 µL of the standardized *K. pneumoniae* strains ($OD_{600\ nm}$ = 0.1) was inoculated in sterile LB broth with plant extracts at their respective MIC values with concentrations ranging from 0.78 - 6.25mg/mL and without plant extracts (as control), thereafter, incubated at 37°C for 24 hours. Biofilms that stuck to the test tube walls were collected to obtain crude exopolysaccharides (EPS). Centrifugation was done briefly at 5000 g for 30 min at 2°C to remove late log phase cells. To precipitate the dislodged EPS, the supernatant was filtered, added to three volumes of chilled ethanol and allowed to incubate overnight at 2 °C. The precipitated EPS was centrifuged at 8000 g for 30 min, dissolved in 1 mL deionized water and kept at -40°C until needed.

EPS quantity was determined by combining 1 mL of EPS solution with an equivalent volume of 5% phenol and 5 mL of concentrated sulfuric acid to produce a red colour.

At concentrations ranging from 0.25 to 1 mg/mL, glucose was utilized as a standard for the determination of the R^2 value used to quantify the crude EPS. The intensity of the colour developed was measured at 490 nm using a Biotek microplate reader.

2.2.7 Atomic force microscopy assessment of exopolysaccharide inhibition

Atomic force microscopy was employed to examine the impact of the best plant extract (*L. javanica*-ethyl acetate) in revealing notable inhibition of exopolysaccharide in *K. pneumoniae* strains following the method described by Santana et al. (2012). The studied *K. pneumoniae* strains were cultured in LB media overnight, centrifuged at room temperature (2,000 x g, 15 min), washed thrice in phosphate buffer (5 mM, pH 6.5), and approximately 10^8 CFU/mL were resuspended into tubes containing the same buffer. Approximately 100 µL of the plant extracts (1mg/mL) were added to 3 mL of the cell suspensions and incubated at 37°C for 4 h. Cell suspensions with no plant extract were used as controls.

Following incubation, 1 mL samples from each treatment were collected, and centrifuged at room temperature for 15 min (6,000 x g,) and a smear of cells was prepared on a glass plate. The slides were allowed to air-dry and viewed using the Veeco Atomic Force Microscope (Dimension icon with Scan Asyst) at a scan frequency of about 300 kHz, a nominal constant of 32 Nm-1, a scan speed of 0.100 Hz, and a scan size of 5.00 µm. Nanoscope Analysis Scan Asyst software (v 8.15) was used for the imaging analysis.

2.2.8 Inhibition of curli expression

Twelve plant extracts were investigated for their effects on curli expression in *K. pneumoniae* strains following the method described by Hammar et al. (1995). For the preparation of the bacterial suspension, 100 µL of *K. pneumoniae* strains (adjusted to optical density 0.1) and plant extracts at their respective MIC values with concentrations ranging from 0.78 - 6.25mg/mL were inoculated in 3 mL of LB broth and were incubated at 37°C for 24 hours.

Following incubation, 3 µL of each bacterial suspension was inoculated onto brain heart infusion (BHI) agar plates supplemented with sucrose and congo red (CRI) dye.

Curli-negative bacteria produced white colonies, which suggested a loss of curli fimbriae, whereas curli-producing *K. pneumoniae* adhered to the congo red dye, thereby appearing as red colonies. The control cultures were not treated with plant extracts.

2.2.9 Hypermucoviscosity reduction assay

To ascertain the impact of the investigated plant extracts on the hypermucoviscous phenotype of *K. pneumoniae* strains, the methodology described by Wiskur et al. (2008) was employed. The pathogen was inoculated on BHI plates with the twelve plant extracts at different concentrations which ranged between 0.125 mg/mL to 1.0 mg/mL, thereafter, incubated at 37°C for 24 h. A mucoviscous string was stretched from a single colony using a conventional bacteriological loop. Each *K. pneumoniae* strain was classified as mucoid or considered to have a hypermucoviscous phenotype if string-like growth or a mucoid string longer than 5 mm was seen, respectively (Wiskur et al., 2008). The control cultures contained no plant extracts.

2.2.10 Liquid chromatography-mass spectrometry analysis of active plant extracts

Chemical constituents of the most active extract from each of the studied plants were determined using liquid chromatography-mass spectrometry **(**LC-MS). Compound separation was performed using a Waters Acquity Ultra Performance Liquid Chromatography (UPLC®) system with ultra-pure LC-grade water and acetonitrile (Romil-UpS™, Microsep, South Africa) acidified with 0.1% formic acid (99+% purity) (Thermo Scientific, South Africa). Compounds were eluted from a Luna® Omega 1.6 µm C18 100 Å (2.1 mm ID x 100 mm length) column using a 17 min gradient from 97% H_2O to 100% acetonitrile with an isocratic wash step with 100% acetonitrile for 1 min and a column reconditioning step with 97% water for 2 min. Volumes of 7.5 µL were injected into the column which was heated to 40 ºC and the flow rate was set at 0.4 mL/min. The UPLC was coupled to a Waters® Synapt G2 high-definition quadrupole-time-of-flight (QTOF) mass spectrometer (Waters Inc., Milford, Massachusetts, USA) operated in negative ionization mode. The electrospray ionization (ESI) capillary voltage was 2.6 kV. The source temperature was set at 120

ºC, the sampling cone voltage at 25 V, the extraction cone voltage at 4.0 V and the cone nitrogen flow at 20 L/h. The desolvation temperature was set at 350 ºC with a nitrogen flow of 600 L/h. Collision-induced fragmentation was performed at 4 V for the trap collision energy and the transfer collision energy was ramped from 20 to 40 V. The instrument's mass axis was continually corrected by infusing 2 ng/µL aqueous leucine enkephalin (m/z 555.2693). Mass spectral scans were collected every 0.3 seconds from 50 to 1 200 Da. MassLynx™ (version 4.1) software (Waters) was used for data acquisition and analysis.

2.2.11 Statistical analysis

Mean standard deviations were computed using the Microsoft Excel Office (2016 version) for all data obtained from the independent experimental repeats in triplicates. Statistical differences were assessed with one-way analysis of variance (ANOVA) for the comparison of the mean differences in the inhibitory activities of extracts and controls using the Statistical Analysis System (SAS) program (v. 9.4). Statistically significant difference was recorded for ρ values < 0.05.

2.3 RESULTS

2.3.1 Plants extracts yield

Leaves of *C. dimidiatus, H. populifolium* and *L. javanica* extracted using four solvents of varying polarities (methanol, dichloromethane, ethyl acetate and water) revealed different percentage yield as shown in Table 2.1. Methanol extracts of *C. dimidiatus* showed the highest yield (36.71%), followed by *L. javanica* (methanol) with a 19.88% yield. The lowest yield was obtained from the dichloromethane extract of *C. dimidiatus* (1.92%).

Table 2.1: Crude extract yield (%) of studied medicinal plants after extraction with solvents of varying polarities

Plant species	Family name	Common name	Voucher specimen number	Extract yield (%)			
				AQ	ME	DCM	EA
Lippia javanica	*Verbenaceae*	Fever Tea, Fever Tree, Lemon Bush, Wild Sage, Wild Tea (E), Beukesbos, Beukesbossie (A).	128530	15.94	19.88	7.36	4.66
Carpobrotus dimidiatus	*Aizoaceae*	Natal sour fig (E), Natalse suurvy/strandvy (A), Ikhambi lamabulawo (Z)	128529	9.07	36.71	1.92	1.99
Helichrysum populifolium	*Asteraceae*	Poplar helichrysum (E), Strooiblom (A)	128531	10.61	10.91	3.18	6.23

Key: E= English, A= Afrikaans, Z= Zulu, AQ= Aqueous, ME= Methanol, DCM= Dichloromethane, EA= Ethyl acetate.

2.3.2 Minimum inhibitory concentration determination of plant extracts on CBR and ESBL producing K. pneumoniae strains

Antibacterial activities of twelve crude extracts against *K. pneumoniae* strains revealed MIC values ranging from 0.78 mg/mL to 6.25 mg/mL (Table 2.2). *C. dimidiatus* (dichloromethane) showed the best MIC value of 0.78 mg/mL on CBR-*K. pneumoniae* exhibiting inhibitory activity on bacterial growth. Other crude extracts tested showed varying MIC values for both strains (Table 2.2). *C. dimidiatus* (methanol) and dichloromethane extracts of *H. populifolium* and *L. javanica* showed higher MIC values of 6.25 mg/mL for CBR and ESBL producing *K. pneumoniae* strains. The positive controls (quercetin and ciprofloxacin) showed significant MIC values of 0.0625 mg/mL and 0.0025 mg/mL, respectively against both strains of *K. pneumoniae*.

Table 2.2: Minimum inhibitory concentration values (mg/mL) of plant extracts tested against *K. pneumoniae* strains

Plant extracts	*K. pneumoniae* strains and MIC (mg/mL) values	
	CBR-*K. pneumoniae*	ESBL-*K. pneumoniae*
Aqueous extracts		
L. javanica	1.56	1.56
C. dimidiatus	6.25	3.12
H. populifolium	1.56	3.12
Dichloromethane extracts		
L. javanica	6.25	6.25
C. dimidiatus	0.78	3.12
H. populifolium	6.25	6.25
Ethyl acetate extracts		
L. javanica	3.12	1.56
C. dimidiatus	3.12	3.12
H. populifolium	3.12	6.25
Methanol extracts		
L. javanica	6.25	1.56
C. dimidiatus	6.25	6.25
H. populifolium	3.12	1.56
Controls		
Quercetin	0.0625	0.0625
Ciprofloxacin	0.0025	0.0025
1% DMSO	6.25	6.25

The MIC values are presented as the mean values of triplicates.

2.3.3 Inhibition of biofilm formation

2.3.3.1 Effect of plant extracts on initial cell attachment

Anti-adhesion (initial attachment) activity of plant extracts against CBR and ESBL producing *K. pneumoniae* strains are shown in Table 2.3. Results of the initial cell attachment inhibition revealed that *L. javanica* (ethyl acetate) and *H. populifolium* (aqueous) had the highest inhibition of cell attachment at 67.25%. Both showed good (above 50% inhibition) anti-adhesion activity for CBR-*K. pneumoniae* similar to the results obtained for ciprofloxacin, while *C. dimidiatus* (aqueous) revealed an inhibitory activity of 45.91%, although the extract was the most prominent for ESBL-*K. pneumoniae* in comparison to the other extracts (Table 2.3).

The least anti-adhesion activity was shown by *C. dimidiatus* (ethyl acetate) (0.07%) and *H. populifolium* (dichloromethane) (0.61%) for CBR-*K. pneumoniae* and ESBL-*K.*

pneumoniae, respectively. No inhibition of initial cell attachment was observed for *H. populifolium* (methanol) and *H. populifolium* (ethyl acetate) for both strains of *K. pneumoniae* tested. Similarly, *L. javanica* (methanol) showed no cell attachment inhibition for CBR-*K. pneumoniae*. Ciprofloxacin exhibited potent inhibitory activity of 69.25% and 62.45% on the initial cell attachment of both strains tested (Table 2.3).

2.3.3.2 Inhibition of preformed biofilms by plant extracts

Inhibition of preformed biofilm in the test strains upon the addition of the studied plant extracts were examined and results are shown in Table 2.3. The inhibition of preformed biofilm by most of the plant extracts were observed to be less potent, with no more than 45% biofilm reduction as compared to the initial attachment that had as high as 67%. The highest percentage inhibition of preformed biofilm by the plant extracts was shown by *L. javanica* (ethyl acetate) for both strains with 45.05% and 20.21% for CBR-*K. pneumoniae* and ESBL-*K. pneumoniae*, respectively (Table 2.3). This was relative to quercetin, which showed inhibitory activity of 35.15% while ciprofloxacin was significantly higher, showing 71.42% inhibition for CBR-*K. pneumoniae*. For ESBL-*K. pneumoniae*, inhibition was recorded at 31.81% and 68.51% for quercetin and ciprofloxacin, respectively.

Table 2.3: Effect of plant extracts on initial cell attachment and biofilm development of *K. pneumoniae* strains

Plant extracts and control	Percentage (%) inhibition of initial cell attachment		Percentage (%) inhibition of biofilm development	
	CBR-*K. pneumoniae*	**ESBL- *K. pneumoniae***	**CBR-*K. pneumoniae***	**ESBL-*K. pneumoniae***
Aqueous extracts				
L. javanica	49.40±0.04 $^{c, d}$	15.17±0.05 $^{a, b, c, d}$	42.37±0.07 ^{c}	13.87±0.01 $^{d, e}$
C. dimidiatus	48.11±0.05 $^{c, d}$	45.91±0.02 ^{d}	11.31±0.03 $^{b, c}$	-45.47±0.01 $^{a, b, c}$
H. populifolium	**67.25±0.06** ^{d}	14.04±0.05 $^{a, b, c, d}$	12.80±0.02 $^{b, c}$	8.25±0.04 $^{c, d, e}$
Dichloromethane extracts				
L. javanica	34.13±0.02 $^{b, c, d}$	28.52±0.04 $^{b, c, d}$	-7.11±0.08 $^{a, b, c}$	8.31±0.02 $^{c, d, e}$
C. dimidiatus	22.81±0.09 $^{b, c, d}$	23.80±0.03 $^{b, c, d}$	11.16±0.07 $^{a, b}$	12.75±0.11 $^{b, c, d}$
H. populifolium	3.33±0.04 $^{a, b, c}$	0.61±0.04 $^{a, b, c}$	-60.29±0.03 ^{a}	-26.85±0.06 $^{a, b, c, d}$
Ethyl acetate extracts				
L. javanica	**67.25±0.01** ^{d}	28.77±0.10 $^{b, c, d}$	45.05±0.08 $^{b, c}$	20.21±0.01 $^{d, e}$
C. dimidiatus	0.07±0.01 $^{a, b, c}$	20.21±0.06 $^{b, c, d}$	9.72±0.05 $^{b, c}$	-59.11±0.14 $^{a, b}$
H. populifolium	-20.58±0.07 $^{a, b}$	-7.93±0.09 $^{a, b}$	-4.02±0.04 $^{a, b, c}$	1.56±0.14 $^{c, d, e}$
Methanol extracts				
L. javanica	-50.31±0.11 ^{a}	12.57±0.02 $^{b, c, d}$	-27.80±0.02 $^{a, b}$	4.64±0.03 $^{c, d, e}$
C. dimidiatus	40.45±0.07 $^{c, d}$	37.41±0.02 $^{c, d}$	-17.98±0.17 $^{a, b, c}$	-39.89±0.05 $^{a, b, c, d}$
H. populifolium	-19.62±0.05 $^{a, b}$	-35.26±0.05 ^{a}	35.15±0.03 $^{b, c}$	19.83±0.04 ^{a}
Controls				
Quercetin	42.57±0.03 $^{c, d}$	40.66±0.01 $^{b, c}$	35.15±0.01 $^{c, d}$	31.81±0.02 $^{a, b}$
Ciprofloxacin	**69.25±0.03** ^{d}	**62.45±0.04** ^{e}	**71.42±0.03** $^{b, c}$	**68.51±0.02** ^{e}
1% DMSO	-3.72±0.04 ^{a}	-9.76±0.01 ^{a}	-5.06±0.03 ^{a}	-8.24±0.02 ^{a}

Mean values are of triplicate independent experiments ± SD. Comparison of percentage inhibition at MIC value per *K. pneumoniae* strain across each treatment. Different letters (a–e) indicate significant differences at $p < 0.05$ between the different treatments (per column) at the same MIC value. Reference control for percentage measurement: ≥ 50% (good activity), 0 to 49% (weak activity), negative values (rise in biofilm formation) (Famuyide *et al.*, 2019).

2.3.3.3 Disruption of K. pneumoniae mature biofilm under dynamic and static conditions

Under static and dynamic conditions, the impact of crude plant extracts on mature biofilms produced by *K. pneumoniae* strains was assessed, as shown in Table 2.4. *L. javanica* (aqueous) and *L. javanica* (ethyl acetate) demonstrated the inhibition of the mature biofilms of both strains under dynamic conditions, each at 20.79% for CBR-*K. pneumoniae* and 21.36% for ESBL-*K. pneumoniae* respectively. However, under the same conditions, *L. javanica* (methanol), *C. dimidiatus* (ethyl acetate), *C. dimidiatus* (methanol), *H. populifolium* (aqueous), and *H. populifolium* (dichloromethane) did not show inhibition but rather enhanced the growth of mature biofilms. Ciprofloxacin inhibited the mature biofilm formed by CBR-*K. pneumoniae* at 42.16%. The mature biofilm inhibitory activity of ciprofloxacin was at 37.72% against ESBL-*K. pneumoniae* with differences found between the plant extracts and positive control (Table 2.4). Statistically significant difference ($p < 0.05$) was observed between the positive control of ciprofloxacin and the treatments.

Similarly, for mature biofilms grown under static conditions, *L. javanica* (aqueous) also revealed the highest inhibitory activity on CBR-*K. pneumoniae* and ESBL-*K. pneumoniae*, at 16.45% and 11.73% respectively (Table 2.4). The extracts showed weak, or no inhibition of mature biofilms formed by both strains tested under static conditions. Only ciprofloxacin showed moderate inhibitory activity at 51.66% and 53.19% for CBR-*K. pneumoniae* and ESBL-*K. pneumoniae,* respectively. Statistical differences were observed for the mature biofilm inhibitory activity of ciprofloxacin when compared with the extracts. Overall, lower inhibition was revealed by the extracts on matured biofilms formed under static conditions than the biofilms formed under dynamic conditions (Table 2.4).

Table 2.4: Effect of plant extracts on disruption of mature biofilms formed by *K. pneumoniae* under dynamic and static conditions

Plant extracts and control	Percentage (%) inhibition of mature biofilm formed under dynamic condition		Percentage (%) inhibition of mature biofilm formed under static condition	
	CBR-*K. pneumoniae*	**ESBL-*K. pneumoniae***	**CBR-*K. pneumoniae***	**ESBL-*K. pneumoniae***
Aqueous extracts				
L. javanica	20.79±0.01 [a, b]	15.90±0.01 [a, b]	16.45±0.01 [b]	11.73±0.02 [a]
C. dimidiatus	13.01±0.01 [a, b]	-55.83±0.01 [a, b]	-25.77±0.03 [a, b]	-37.11±0.04 [a]
H. populifolium	-1.48±0.04 [a, b]	6.51±0.02 [a, b]	-19.89±0.02 [a, b]	7.52±0.01 [a]
Dichloromethane extracts				
L. javanica	17.35±0.03 [a, b]	1.12±0.01 [a, b]	-14.13±0.03 [a, b]	3.63±0.01 [a]
C. dimidiatus	7.57±0.01 [a, b]	-2.37±0.01 [a, b]	11.54±0.02 [a, b]	9.63±0.01 [a]
H. populifolium	-10.19±0.02 [a, b]	-37.67±0.01 [a, b]	-37.45±0.04 [a, b]	-32.79±0.01 [a]
Ethyl acetate extracts				
L. javanica	8.69±0.02 [a, b]	21.36±0.02 [a, b]	6.88±0.07 [a, b]	7.28±0.02 [a]
C. dimidiatus	-20.20±0.12 [a]	-89.23±0.20 [a]	-61.64±0.15 [a, b]	-73.14±0.21 [a]
H. populifolium	9.39±0.04 [a, b]	11.18±0.03 [a, b]	-61.34±0.06 [a, b]	-91.55±0.24 [a]
Methanol extracts				
L. javanica	-7.41±0.01 [a, b]	-26.83±0.01 [a, b]	-46.40±0.05 [a, b]	-18.52±0.02 [a]
C. dimidiatus	-21.99±0.02 [a]	-66.48±0.03 [a, b]	-86.72±0.04 [a]	-67.79±0.05 [a]
H. populifolium	17.17±0.01 [a, b]	-15.73±0.02 [a, b]	11.81±0.02 [a, b]	-84.85±0.26 [a]
Controls				
Quercetin	-27.08±0.01 [a]	-44.55±0.01 [a]	-35.46±0.02 [a]	-52.25±0.02 [a]
Ciprofloxacin	42.16±0.01 [b]	37.72±0.02 [b]	51.66±0.01 [c]	53.19±0.01 [b]
1% DMSO	-39.01±0.01 [a]	-58.35±0.01 [a]	-45.67±0.02 [a]	-68.25±0.02 [a]

Mean values are of triplicate independent experiments ± SD. Comparison of percentage inhibition at MIC value per *K. pneumoniae* strain across each treatment. Different letters (a–c) indicate significant differences at $p < 0.05$ between the different treatments (per column) at the same MIC value. Reference control for percentage measurement: ≥ 50% (good activity), 0 to 49% (weak activity), negative values (rise in biofilm formation) (Famuyide *et al.*, 2019).

2.3.4 *Scanning electron microscopy (SEM) analysis of biofilms*

To gain a detailed view of *K. pneumoniae* biofilms formed after treatment with the most efficient plant extract (*L. javanica*-ethyl acetate), a scanning electron microscopy (SEM) study was carried out. Figure 2.1 displays the SEM micrographs of the untreated biofilms (Figures 2.1A and 2.1E), biofilms developed by the two *K. pneumoniae* strains after exposure to *L. javanica* ethyl acetate extract (Figures 2.1B and 2.1F) and the positive controls: quercetin, 0.1 mg/mL (Figures 2.1C and 2.1G) and ciprofloxacin, 0.001 mg/mL (Figures 2.1D and 2.1H).

L. javanica (ethyl acetate) showed the best antibiofilm activity of all the studied plant extracts for CBR and ESBL-*K. pneumoniae*, as seen in Figures 2.1B and 2.1F respectively. The SEM micrographs revealed fewer clusters of connected microcolonies, indicating a considerable decrease in the number of biofilms. With very few clumps of dispersed cells, ciprofloxacin was found to have a more potent activity (Figures 2.1D and 2.1H).

Comparatively, the untreated biofilms formed by the two strains of *K. pneumoniae* revealed a dense cluster of interconnected *K. pneumoniae* cells that exhibited continuous clumping and substantial aggregates of cells (Figures 2.1A and 2.1E). In comparison to *L. javanica* (ethyl acetate), quercetin was found to be less effective at disrupting the formed biofilms (Figures 2.1C and 2.1G), however, it displayed fewer cell clumps than the untreated biofilms.

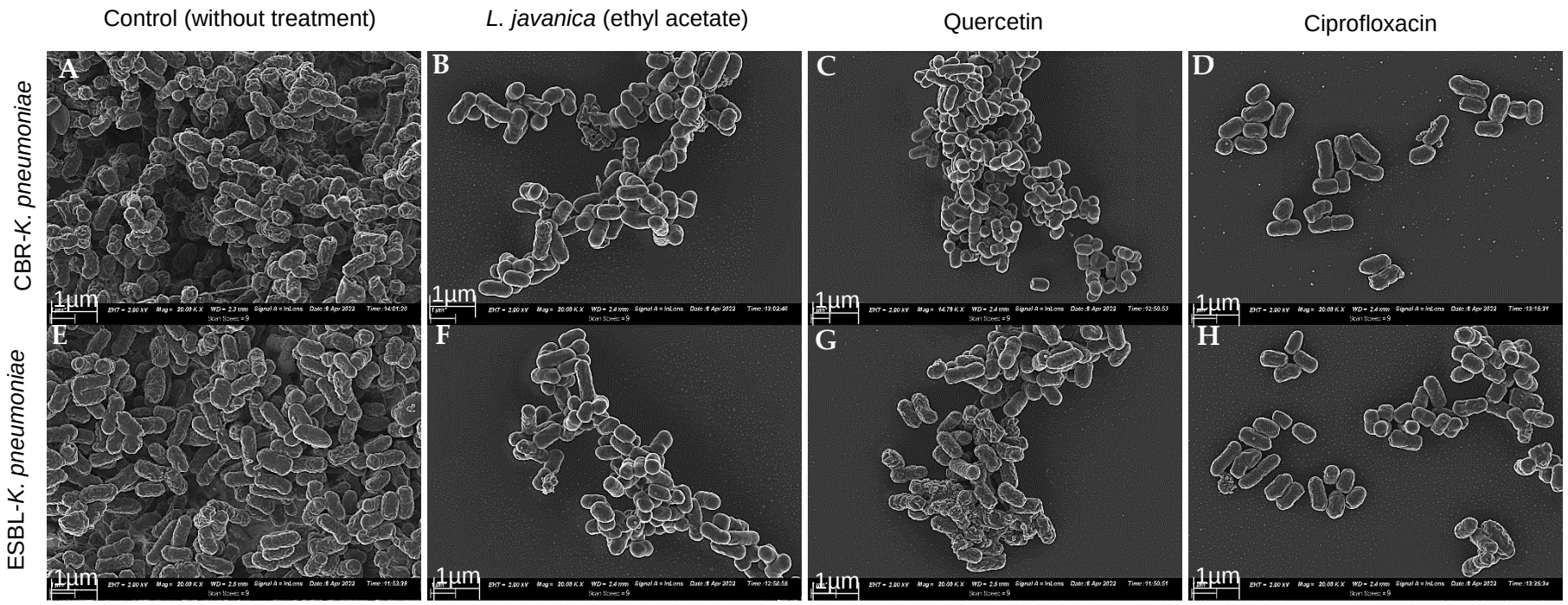

Figure 2.1: SEM micrographs showing biofilm inhibitory activity of *L. javanica* (ethyl acetate extract) against CBR and ESBL producing *K. pneumoniae* at 20 KX magnification. (A) CBR-*K. pneumoniae* (without treatment) (B) CBR-*K. pneumoniae* (treated with *L. javanica* -ethyl acetate extract) (C) CBR-*K. pneumoniae* (treated with quercetin), (D) CBR-*K. pneumoniae* (treated with ciprofloxacin), (E) ESBL-*K. pneumoniae* (without treatment), (F) ESBL-*K. pneumoniae* (treated with *L. javanica* -ethyl acetate extract), (G) ESBL-*K. pneumoniae* (treated with quercetin-positive control), (H) ESBL-*K. pneumoniae* (treated with ciprofloxacin -positive control).

2.3.5 *Inhibition of K. pneumoniae exopolysaccharides (EPS) by plant extracts*

The phenol-sulfuric acid technique was used to determine the quantity of EPS at the corresponding MIC values of test extracts in both pathogen strains. Results revealed that there was good linearity, as evidenced by the correlation coefficient of determination (R^2), with a value of 0.9705, showing how well the data fit the regression model. Following the regression equation derived from the standard curve (Y = 0.348X - 0.074), where Y stands for the absorbance derived from the unknown samples (Figure 2.2), the measurement of EPS was established.

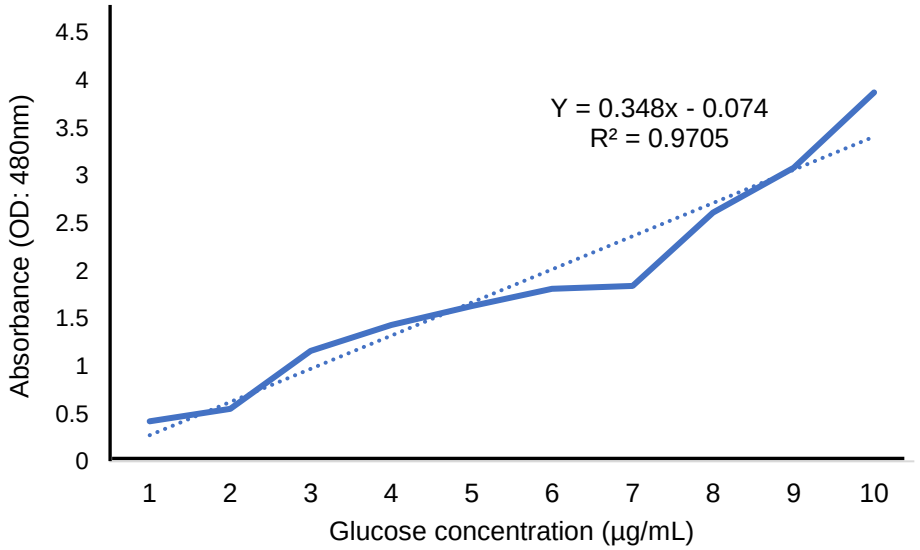

Figure 2.2: Standard curve showing the regression equation for EPS quantification.

EPS percentage inhibition by the plant extracts is shown in Figure 2.3. For ESBL-*K. pneumoniae*, the highest EPS inhibition (%) was observed from *L. javanica* (ethyl acetate) (34.18%) having the least EPS yield while the least EPS inhibition was observed for *L. javanica* (aqueous) at 4.62%. However, *L. javanica* (methanol), *L. javanica* (dichloromethane), *C. dimidiatus* (ethyl acetate), *C. dimidiatus* (methanol), *C. dimidiatus* (dichloromethane), *H. populifolium* (ethyl acetate) and *H. populifolium* (dichloromethane) revealed no inhibition of EPS, rather showing enhanced EPS production. Ciprofloxacin and quercetin revealed EPS inhibition of 38.11% and 24.94%, respectively (Figure 2.3A).

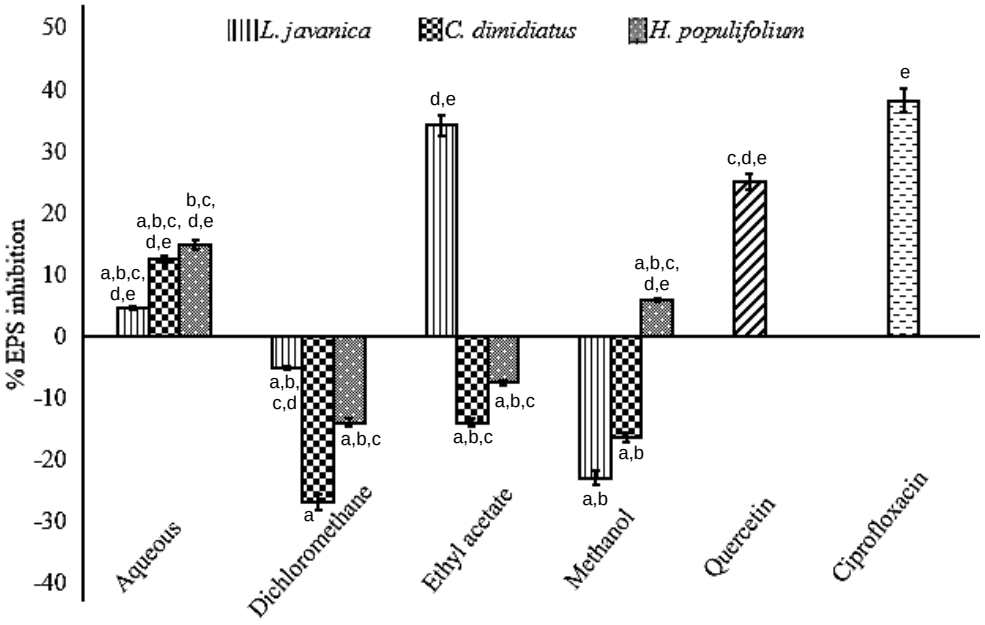

Plant extracts and controls (at MIC values)

(A)

Figure 2.3A: Exopolysaccharide percentage inhibition in ESBL producing *K. pneumoniae* by all plant extracts at respective MIC values. Statistical significance of the test plant extracts and controls are indicated with different letters (a–e) with *p*-value < 0.05 between all the treatments.

Furthermore, *L. javanica* (ethyl acetate) also revealed a percentage of EPS inhibition (36.95%) for CBR-*K. pneumoniae*, followed by *H. populifolium* (aqueous) (27.85%). No EPS inhibitory activity was recorded for *L. javanica* (aqueous), *L. javanica* (methanol), *L. javanica* (dichloromethane), *C. dimidiatus* (ethyl acetate), *C. dimidiatus* (dichloromethane) and *H. populifolium* (methanol). Ciprofloxacin and quercetin revealed EPS inhibition at 51.56% and 34.55% respectively for the two *K. pneumoniae* strains (Figure 2.3B).

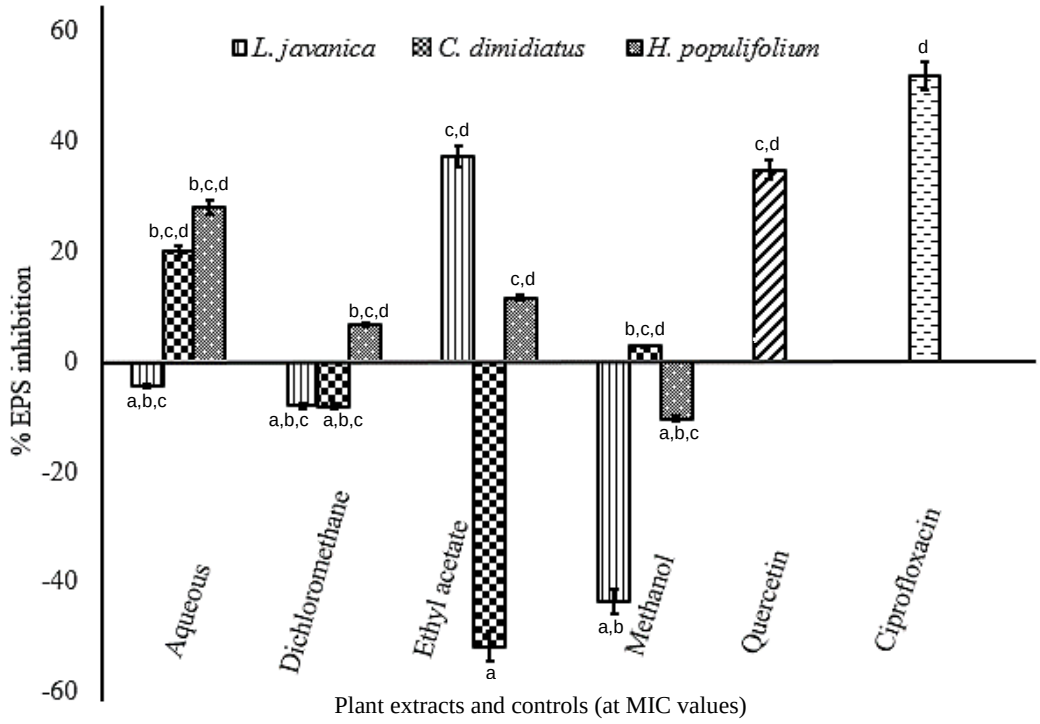

(B)

Figure 2.3B: Exopolysaccharide percentage inhibition in CBR- *K. pneumoniae* by all plant extracts at respective MIC values. Statistical significance of the test plant extracts and controls are indicated with different letters (a–d) with *p*-value < 0.05 between all the treatments.

2.3.6 Microscopic surface topography characterization of K. pneumoniae exopolysaccharides (EPS) using atomic force microscopy (AFM)

Planar (2D) and cubic (3D) views of the surface topography of the examined exopolysaccharides (EPS) of *K. pneumoniae* were captured using AFM. *L. javanica* (ethyl acetate) was selected for AFM due to the above-shown inhibition of EPS as compared to the other plant extracts examined. The AFM results revealed distinct variations between the topographies of EPS that had been treated and the untreated control. Untreated CBR and ESBL producing *K. pneumoniae* produced EPS with irregular shapes and rough surfaces that were primarily made up of unevenly distributed lumps and were easily seen as foggy patches around the cells (Figure 2.4: A1 and E1). The EPS produced by both strains appeared tubular and compact when viewed with the microscope. Furthermore, topological analysis of the EPS indicated a consistent polymer with irregular lumps at a maximum height (h) of 1.4 µm and 1.1 µm for untreated CBR and ESBL producing *K. pneumoniae*, respectively (Figure 2.4: A1

and E1). However, their average roughness (Ra) was measured at 183 nm and 141 nm, respectively. The surface roughness is displayed in the 3D images (Figure 2.4: A2 and E2). The treated EPS at MIC value showed the maximum lump heights of 206.5 nm and 409.8 nm for CBR and ESBL producing *K. pneumoniae,* respectively (Figure 2.4: B1 and F1). The 3D scans revealed a marked decrease in surface roughness (Figure 2.4: B2 and F2). The Ra for CBR and ESBL producing *K. pneumoniae* were 36.9 nm and 123 nm, respectively.

The EPS subjected to treatment with positive controls (Figure 2.4: H1 and H2) also showed reduced surface roughness and height, where ciprofloxacin revealed a better result with a maximum lump height of 104.7 nm and Ra of 8.80 nm for CBR-*K. pneumoniae* (Figure 2.4: D1 and D2). Moreover, for ESBL-*K. pneumoniae*, the height of 156.8 nm and Ra of 27.6 nm were observed for ciprofloxacin (Figure 2.4: H1 and H2).

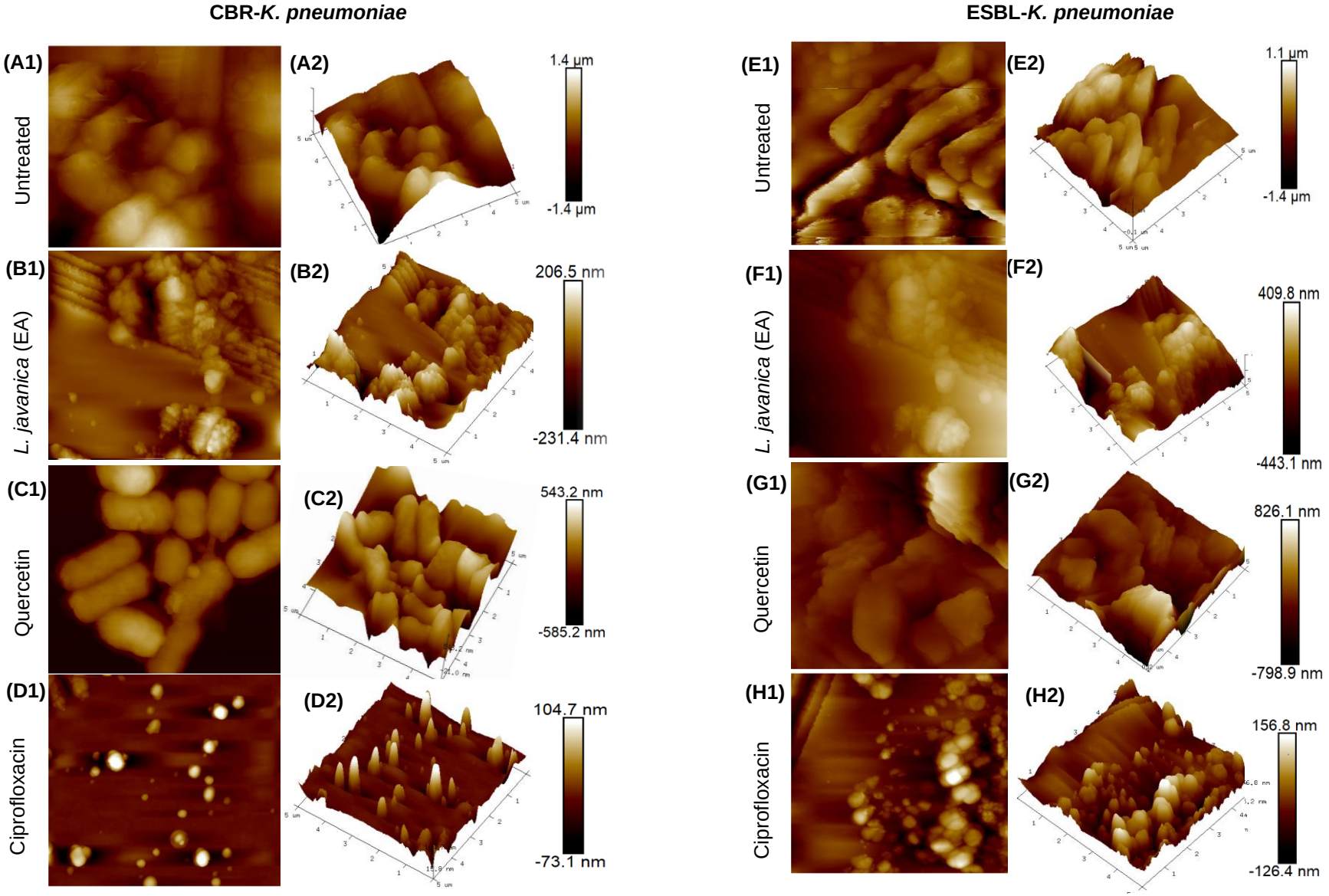

Figure 2.4: AFM micrographs showing two-dimensional (2D) and three-dimensional (3D) surface topography of EPS produced by untreated and *Lippia javanica* (ethyl acetate extract) treated CBR and ESBL producing *K. pneumoniae* strains at a scan size of 5.00µm (5,000nm).

2.3.7 Curli reduction activity in K. pneumoniae strains

The effects of plant extracts on the presence of curli fibres in both strains of *K. pneumoniae* are shown in Table 2.5. According to the findings, curli inhibition was observed in a concentration dependent manner where none of the plant extracts tested at lower concentrations of 0.125 mg/mL and 0.25 mg/mL inhibited the production of curli in the *K. pneumoniae* strains. However, curli expression was reduced by *L. javanica* (ethyl acetate), *L. javanica* (dichloromethane), *C. dimidiatus* (aqueous), and *H. populifolium* (aqueous) extracts at 0.5 mg/mL in both strains. At the same concentration, *L. javanica* (aqueous) and *H. populifolium* (methanol) also inhibited the expression of curli in ESBL-*K. pneumoniae*. Furthermore, at 1.0 mg/mL, 50% of the plant extracts such as *L. javanica* (aqueous), *L. javanica* (ethyl acetate), *L. javanica* (dichloromethane), *C. dimidiatus* (aqueous), *H. populifolium* (aqueous) and *H. populifolium* (methanol) inhibited curli formation in both *K. pneumoniae* strains.

Ciprofloxacin revealed a reduction of curli expression in both strains at varying concentrations (0.125 to 1.0 mg/mL) while quercetin only showed curli reduction at 0.5 and 1.0 mg/mL for both strains. No inhibitory activity was observed for the untreated control tested against both strains (Table 2.5).

Table 2.5: Effect of plant extracts on curli fibre synthesis in *Klebsiella pneumoniae* strains

Plant extracts	Concentration (mg/mL) (A)					Concentration (mg/mL) (B)				
	Control	**0.125**	**0.25**	**0.5**	**1.0**	**Control**	**0.125**	**0.25**	**0.5**	**1.0**
Aqueous extracts										
L. javanica	+	+	+	+	-	+	+	+	-	-
C. dimidiatus	+	+	+	-	-	+	+	+	-	-
H. populifolium	+	+	+	-	-	+	+	+	-	-
Dichloromethane extracts										
L. javanica	+	+	+	-	-	+	+	+	-	-
C. dimidiatus	+	+	+	+	+	+	+	+	+	+
H. populifolium	+	+	+	+	+	+	+	+	+	+
Ethyl acetate extracts										
L. javanica	+	+	+	-	-	+	+	+	-	-
C. dimidiatus	+	+	+	+	+	+	+	+	+	-
H. populifolium	+	+	+	+	+	+	+	+	+	+
Methanol extracts										
L. javanica	+	+	+	+	+	+	+	+	+	+
C. dimidiatus	+	+	+	+	+	+	+	+	+	+
H. populifolium	+	+	+	+	-	+	+	+	-	-
Controls										
Quercetin	+	+	+	-	-	+	+	+	-	-
Ciprofloxacin	+	-	-	-	-	+	-	-	-	-
Untreated	+	+	+	+	+	+	+	+	+	+

Key: A= CBR-*K. pneumoniae,* B= ESBL-*K. pneumoniae, +:* Positive, -: Negative, Control: Untreated *K. pneumoniae* strains.

2.3.8 Reduction in hypermucoviscosity phenotype

The impact of the studied plant extracts on *K. pneumoniae's* hypermucoviscosity was assessed through the use of a string test where the viscosity of the strains gradually decreased as the concentration of most of the studied plant extracts increased. For CBR-*K. pneumoniae* (Figure 2.5A), *L. javanica* (ethyl acetate) showed potent hypermucoviscosity reduction, observed by the least length of mucoid string (1 mm) at 1.0 mg/mL, followed by *L. javanica* (methanol), *H. populifolium* (aqueous), and *H. populifolium* (dichloromethane) (2 mm at 1.0 mg/mL). However, no inhibition was observed for *C. dimidiatus* (dichloromethane) and *H. populifolium* (ethyl acetate) at all the concentrations as observed with the negative control (Figure 2.5A).

Similarly, for ESBL-*K. pneumoniae* (Figure 2.5B), *L. javanica* (ethyl acetate), *C. dimidiatus* (aqueous), *H. populifolium* (aqueous) and *H. populifolium* (dichloromethane) revealed good hypermucoviscosity inhibition, showing the least length of mucoid string (2 mm) at 1.0 mg/mL and 3 mm at 0.5 mg/mL while other plant extracts revealed higher lengths of mucoid strings at those concentrations (Figure 2.5B).

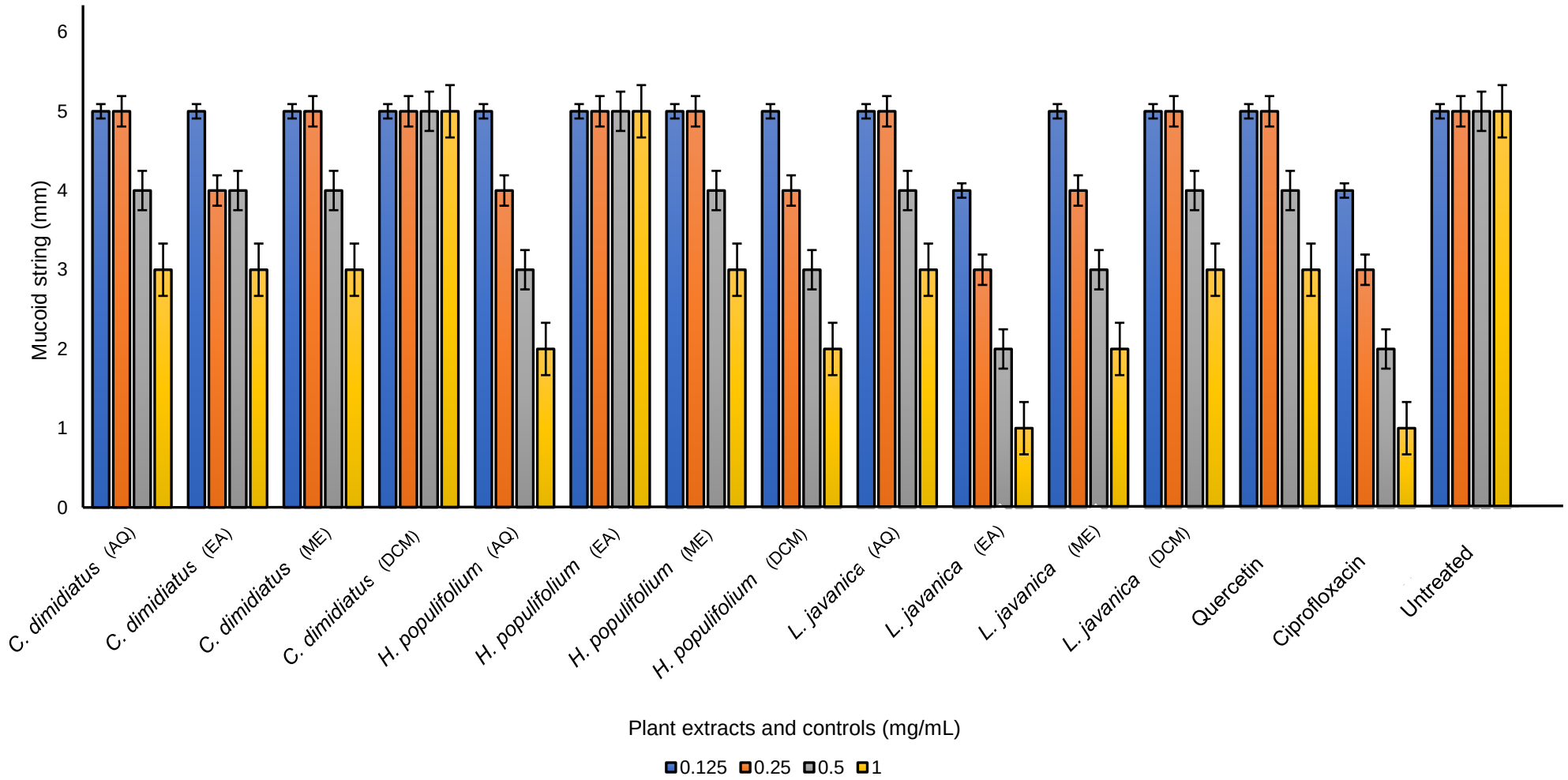

Figure 2.5A: Effect of plant extracts in reducing CBR-*K. pneumoniae* hypermucoviscosity. Means are values of triplicate independent experiments ± SD. AQ: aqueous, EA: ethyl acetate, ME: methanol and DCM: dichloromethane.

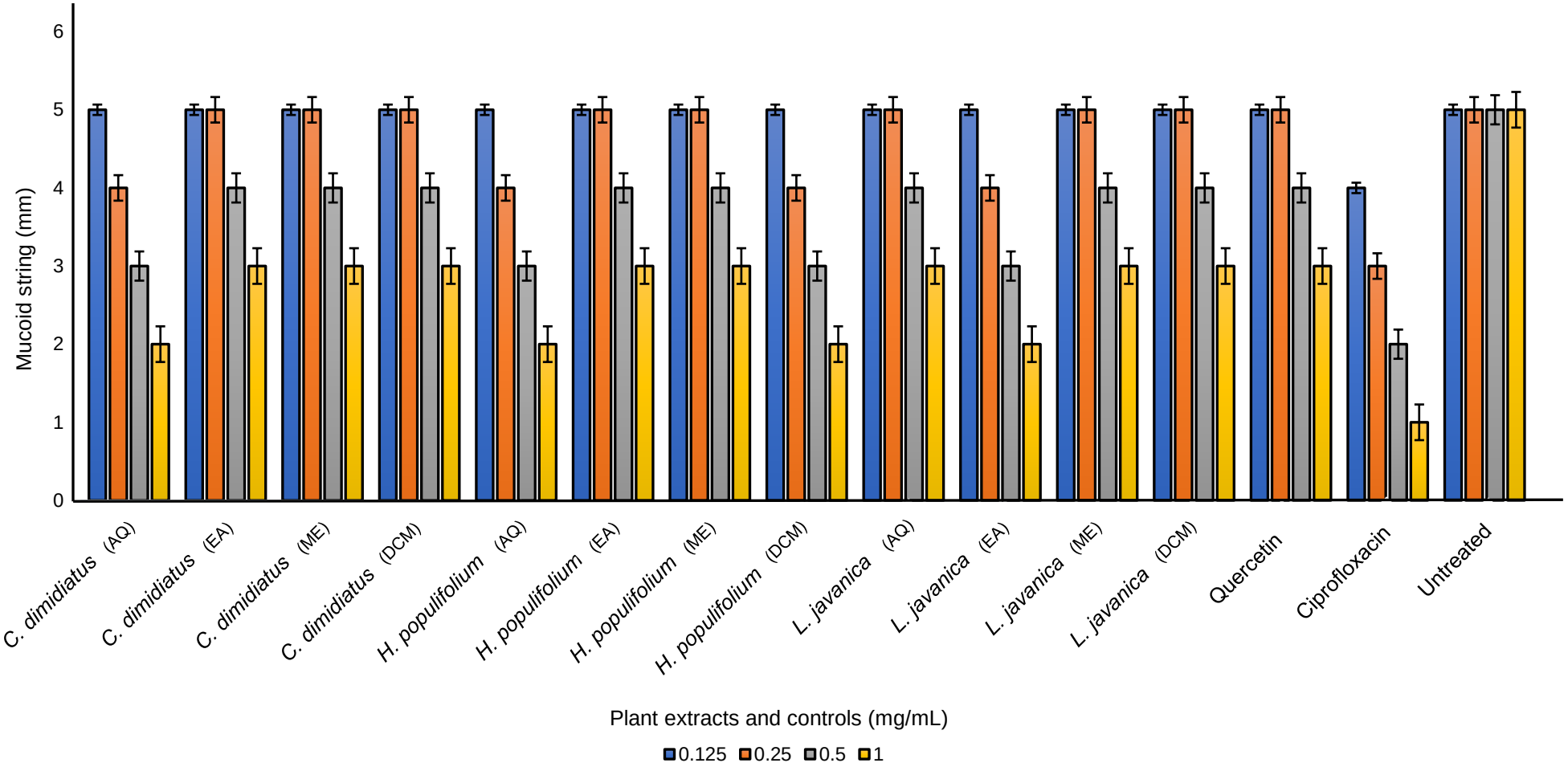

Figure 2.5B: Effect of plant extracts in inhibition of ESBL-*K. pneumoniae* hypermucoviscosity. Means are values of triplicate independent experiments ± SD. AQ: aqueous, EA: ethyl acetate, ME: methanol and DCM: dichloromethane.

2.3.9 Liquid chromatography-mass spectrometry analysis of selected plant extracts

LC-MS chemical profiling was carried out on the most active extract from each of the studied plants, namely *L. javanica* (ethyl acetate), *C. dimidiatus* (aqueous) and *H. populifolium* (aqueous). Identities of the compounds in the three plants of interest are shown in Tables 2.6 - 2.8. Twenty-eight (28) compounds were identified from *L. javanica* (ethyl acetate) at different retention times, the mass-to-charge ratio (m/z) and peak intensities (Table 2.6). For *C. dimidiatus* (aqueous), 30 compounds were distinct, however, the identities of 28 were known while two 2 were unknown (Table 2.7). Furthermore, sixteen (16) compounds were identified from *H. populifolium* (aqueous), however, two (2) were unknown (Table 2.8).

Table 2.6: LC-MS spectral analysis of *Lippia javanica* (ethyl acetate extract)

Peak #	Retention time (min)	m/z	Peak intensity (%)	Identities
1	145.22	461.17	1.56	Caffeoyl-rhamnosyl-glucoside
2	158.02	359.10	1.20	Hydroxy-dimethoxybenzoyl hexopyranose
3	198.20	387.17	2.29	Hydroxy-jasmonic acid-glucoside
4	206.47	419.12	4.29	Afzelechin-rhamnoside
5	221.04	389.11	2.02	Theveside
6	244.06	623.20	3.88	Verbascoside Isomer 1
7	252.31	623.20	6.23	Verbascoside Isomer 2
8	259.92	623.20	8.93	Verbascoside Isomer 3
9	267.71	623.20	7.55	Verbascoside Isomer 4
10	278.40	607.20	2.31	Luteolin-xylosyl-glucoside
11	289.26	637.21	3.00	Quercetin-rutinoside isomer 1
12	297.04	637.21	1.70	Quercetin-rutinoside isomer 2
13	310.33	665.21	1.37	Tetramethyl-quercetin-rutinoside
14	321.18	651.23	3.05	Matairresinol 4'[apiosyl-glucoside]
15	358.13	285.04	1.46	Luteolin
16	393.96	327.22	1.03	Possibly a diterpene
17	400.92	269.05	3.40	Apigenin
18	408.54	299.06	6.67	Diosmethin
19	416.80	329.07	2.94	Tricin
20	421.34	359.08	3.18	Trimethoxyflavone Isomer 1
21	441.76	359.08	0.69	Trimethoxyflavone Isomer 2

Table 2.6 (Cont'd): LC-MS spectral analysis of *Lippia javanica* (ethyl acetate extract)

Peak #	Retention time (min)	m/z	Peak intensity (%)	Identities
22	458.94	299.06	2.31	Chrysoeriol
23	470.45	313.07	8.24	Cirsimaritin
24	483.25	343.08	6.14	Eupatorin
25	499.78	373.09	0.85	Quercetagetin 3,5,6,3'-tetramethyl ether
26	511.94	283.06	1.80	Dihydroxy-methoxy-phenylcoumarin
27	522.80	313.07	1.60	Kaempferol-dimethylether
28	539.64	501.32	10.29	Unknown diterpene

Table 2.7: LC-MS spectral analysis of *Carpobrotus dimidiatus* (aqueous extract)

Peak #	Retention time (min)	m/z	Peak intensity (%)	Identities
1	144.58	153.02	1.89	Dihydroxybenzoic acid
2	151.54	203.08	3.50	Unknown
3	175.85	337.09	6.39	Coumaroyl quinic acid Isomer 1
4	192.38	367.10	1.57	Feruloyl quinic acid
5	202.60	337.09	7.92	Coumaroyl quinic acid Isomer 2
6	209.56	337.09	6.81	Coumaroyl quinic acid Isomer 3
7	222.37	297.06	10.24	Hydroxy-dimethoxyflavone
8	233.87	813.17	2.41	Luteolin triglucoside
9	239.54	683.14	1.72	Trihydroxy-trimethoxy flavone-diglucoside
10	250.40	797.18	2.08	Apigenin-feruloyl-diglucoside
11	259.31	799.23	4.13	Similar to Tricin rutinoside-glucoside
12	262.24	785.21	1.49	Similar to Isorhamnetin rutinoside-glucoside
13	267.75	653.17	2.96	Similar to Syringentin-3-rutinoside
14	279.08	653.17	4.45	Syringentin-rutinoside-like
15	297.08	797.21	3.85	Similar to kaempferol-diglucoside-acetorhamnosyl
16	302.11	651.15	4.17	Similar to kaempferol-acetylglucosyl-glucoside
17	316.85	765.19	3.68	Could be an acetylated pinosylvin-diglucoside
18	323.18	795.20	5.67	Could be catechin-gallate-glucoside-glucuronide
19	330.14	765.19	0.62	Could be another isomer acetylated pinosylvin-diglucoside
20	339.05	619.13	2.34	Similar to Apigenin acetylcoumaroyl glucoside
21	346.84	649.14	4.72	Similar to Pelargonidin-xylosyl-malonyl-glucoside
22	359.47	331.04	0.84	Similar to quercetaggetin-3'-methyl-ether
23	368.39	256.10	0.66	Unknown nitrogen-containing compound

Table 2.7 (Cont'd): LC-MS spectral analysis of *Carpobrotus dimidiatus* (aqueous extract)

Peak #	Retention time (min)	m/z	Peak intensity (%)	Identities
24	373.57	649.14	0.70	Similar to Pelargonidin-xylosyl-malonyl-glucoside
25	393.34	327.22	6.74	Could be an oxygenated diterpene
26	421.38	329.23	3.35	Could be an oxygenated diterpene
27	470.48	313.07	0.92	Similar to kaempferol-dimethyl-ether
28	483.28	343.08	0.88	Dihydroxy-3-methoxyflavonone
29	513.27	293.18	2.28	Unknown
30	524.78	237.11	1.00	Methoxychalcone or cinnamyl-benzoate

Table 2.8: LC-MS spectral analysis of *Helichrysum populifolium* (aqueous extract)

Peak #	Retention time (min)	m/z	Peak intensity (%)	Identities
1	146.58	353.09	2.90	Chlorogenic acid isomer 1
2	166.35	293.12	5.40	Ethyl 3-hydroxybuterate glucoside
3	181.58	353.09	10.80	Chlorogenic acid isomer 2
4	200.70	353.09	5.66	Chlorogenic acid isomer 3
5	218.04	515.12	5.71	4,5-Dicaffeoylquinic acid isomer 1
6	231.98	367.10	2.01	Feruloylquinic acid
7	235.87	463.09	3.73	Hydroxykaempferol glucoside isomer 1
8	243.49	213.12	4.68	Unknown
9	253.69	567.21	2.23	Similar to Citrusin B
10	257.59	463.09	5.78	Hydroxykaempferol glucoside isomer 2
11	268.93	515.12	6.03	4,5-Dicaffeoylquinic acid isomer 2
12	276.07	415.20	2.80	Unknown
13	280.44	515.12	13.41	4,5-Dicaffeoylquinic acid isomer 3
14	287.57	515.12	8.29	4,5-Dicaffeoylquinic acid isomer 4
15	332.79	491.12	2.73	Similar to Lagotiside
16	349.96	677.15	3.67	Pelargonidin di-acetylglucoside
17	393.40	327.22	7.50	Possibly a diterpene
18	422.74	329.23	6.68	Tricin

Based on the mass spectrometry data analysis, different classes of phytochemical compounds were represented which included glucosides, terpenes, flavonoids, quinic acids and derivatives. Among them, 10.29% unknown diterpene, 10.24% hydroxy-dimethoxyflavone (flavonoid) and 13.41% 4,5-dicaffeoylquinic acid isomer (quinic acids and derivatives) were observed as the major constituents, showing the highest peak intensities in *L. javanica* (ethyl acetate), *C. dimidiatus* (aqueous) and *H. populifolium* (aqueous), respectively. The data presented in Tables 2.6 – 2.8 corresponds with the peaks shown in the representative mass spectrometry chromatograms of the analysed extracts as illustrated in Figure 2.6.

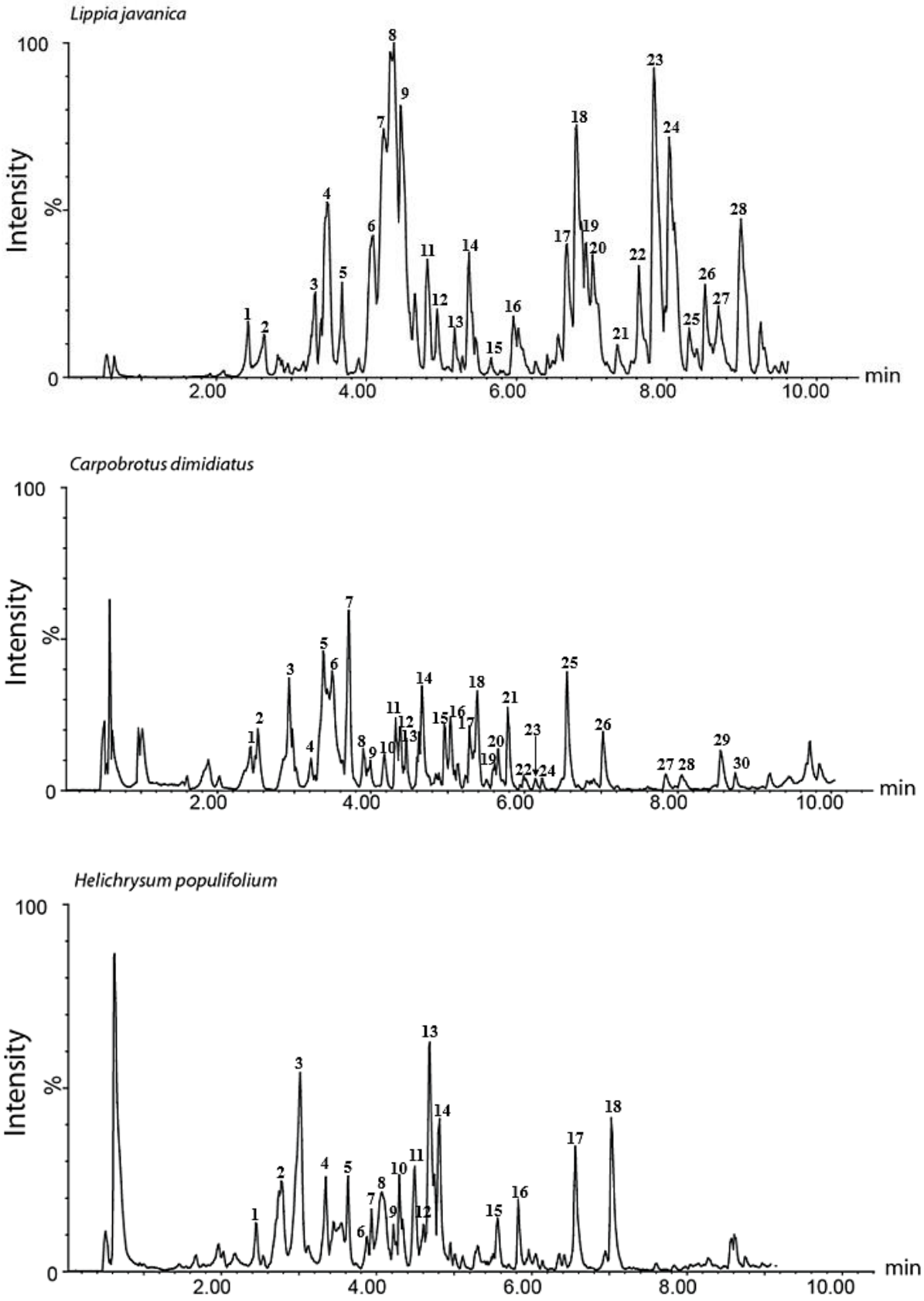

Figure 2.6: LC-MS chromatograms of *L. javanica* (ethyl acetate), *C. dimidiatus* (aqueous) and *H. populifolium* (aqueous) extracts. All peaks correspond to the data presented in Tables 2.6- 2.8.

2.4 DISCUSSION

Over the years, the use of plants in traditional medicine has piqued the attention of several researchers to discover effective plant extracts that can be used in the management of microbial infectious diseases (Baloyi et al., 2021). South African medicinal plants are of great interest because, despite the botanical and cultural diversity of South Africa, only a few plant species have hitherto become fully commercialised as medicinal products (Van Wyk, 2011). Therefore, three medicinal plants (*C. dimidiatus, H. populifolium* and *L. javanica*) indigenous to South Africa, reported to have ethnomedicinal uses against *K. pneumoniae* infections were examined in this study to validate some of their antipathogenic/antivirulence activities.

Since bioactive phytochemicals are vital and responsible for various activities, the extraction process is also crucial (Baloyi et al., 2022). For this reason, varying extractants of different polarities were pivotal to deducing the most potent bioactive components from the plants. Results showed that the methanol extract had the highest yield followed by the aqueous extracts with up to 36.71% for *C. dimidiatus*. Congruent with the findings in this study, Truong et al. (2019), Baloyi et al. (2022), Adam et al. (2019) and Eloff et al. (2018) also reported a higher percentage yield from methanol extracts, followed by aqueous extracts. Highly polar solvents such as methanol and water thus favour extraction efficiency and yield compared to solvents with lesser polarity for plant species containing high levels of phenolic compounds.

The extracts (aqueous, ethyl acetate, methanol and dichloromethane) from the three plant species at varying concentrations were assessed for their MIC activities against *K. pneumoniae*. The MIC determination is considered the gold standard which reveals the lowest concentration of the treatment that inhibits the visible growth of the pathogen (Londonkar et al., 2013). Findings from this study showed the MIC results that ranged from 0.78 mg/mL to 6.25 mg/mL. Van Vuuren and Muhlarhi (2017) defined MIC activities of plant extracts with noteworthy activities as values of 1 mg /mL or lower. Thus, *C. dimidiatus* (dichloromethane) was regarded as the most potent due to its MIC value of 0.78 mg/mL on CBR- *K. pneumoniae,* which was significantly lower than any of the other tested plant extracts. Several literature reports have been documented on the antibacterial properties of various plants against different pathogens such as in Mashamba et al. (2022). However, limited information exists on

the antibacterial activity of *C. dimidiatus.* Variations observed in MIC values of the plant extracts may arise due to the difference in their chemical constituents (Mostafa et al., 2018). The low activity of most of the tested plant extracts can be explained by the fact that *K. pneumoniae,* a GNB has a murein cell wall and an outer membrane, which is a complex barrier system against the permeation of polar plant extracts. Similar results have also been reported by Cosa et al. (2020), Perera et al. (2022) and Mogana et al. (2020). Furthermore, GNB often reduce their outer membrane permeability by reducing the number of porins and inducing drug efflux pumps which transport drug molecules outwardly, making the bacterial cells resistant to treatments (Shriram et al., 2018). For these reasons, further studies using the plant extracts were focused on extracellular bacterial virulence factors of *K. pneumoniae*, including biofilm formation, exopolysaccharide and curli production as well as hypermucoviscosity.

K. pneumoniae is known for its strong propensity to form biofilms which appear as a mucoid, cohesive slime layer, and is considered a major factor in its resistance against antimicrobials and contributes to pathogenicity (Oleksy-Wawrzyniak et al., 2022). Biofilms are extracellular network-like aggregates of bacterial cells adhering to tissues, organs, and medical devices. They are composed of polysaccharides, extracellular DNA and proteins (Huang et al., 2022). The development of *K. pneumoniae* biofilm is initiated by the adhesion of cells, followed by the formation of microcolonies, maturation, and propagation of free-living cells (Wang et al., 2020). The biofilm biomass screening in this study employed the crystal violet staining technique which has been reported by Ramos-Vivas et al. (2019) to be widely accepted and used by many researchers due to the simplicity of its implementation for sessile biofilm detection.

The results of this study showed that *L. javanica* (ethyl acetate) inhibited *K. pneumoniae* biofilm cell attachment, thereby reducing the pathogen's ability to attach and live in a protective scaffold. The ability of *L. javanica* extracts to reduce cell attachment is supported by the findings reported by Shirinda et al. (2019) suggesting that the organic extract of *L. javanica* twigs inhibited the initial cell attachment of biofilm in *Clostridium perfringens.* Furthermore, *L. javanica* (ethyl acetate) also revealed the highest percentage inhibition on preformed and mature biofilm of *K. pneumoniae* strains. Based on documented literature, this could be due to the activity of

verbascoside, a prominent bioactive constituent identified in *L. javanica* as shown in Table 2.6. Shi et al. (2022) have reported that verbascoside is implicated in the eradication of biofilms formed by GNB such as *Pseudomonas aeruginosa.* Congruent to this, findings from Jang et al. (2008) also revealed over 60% inhibition of *E. coli* biofilms by phenylethanoid glycoside (verbascoside). Apigenin, also present in *L. javanica* could be implicated in the antibiofilm activity observed. This can be supported by the findings of Liu et al. (2020), where apigenin was shown to reduce the initial adherence and biofilms formed by *Streptococcus mutans.*

The weak inhibitory activities observed at this stage for the other studied plant extracts could be based on these extracts possessing phytochemicals serving as additional nutrients to promote bacterial growth (Baloyi et al., 2021). Most of the plant extracts studied were observed to be less potent on the mature biofilms with not more than 21.36% biofilm reduction. Previous authors such as Bi et al. (2021) and Mashamba et al. (2022) also reported that eliminating pre-existing biofilms by plant extracts poses a great challenge as several biofilm-forming bacteria have shown resistance. Once mature biofilms are formed, it is more difficult to treat and remove them (Koo & Yamada, 2016). This could be due to the complexity of the physical structure of mature biofilms which makes them difficult to eradicate. Other possible reasons for this can include the presence of persister cells, high volumes of exopolysaccharides as well as phytochemical removal from the matrix by efflux pumps leading to a reduction in the bactericidal efficiency of administered treatments (Koo & Yamada, 2016).

Overall, the antibiofilm experiments revealed that *L. javanica* (ethyl acetate) has the potential to disrupt *K. pneumoniae* cell aggregates before the biofilm fully forms. Based on the efficacy of this extract observed against *K. pneumoniae* biofilms, *in situ* visualization using the scanning electron microscope (SEM) was employed for the qualitative observation of biofilm disruption, as SEM provides an excellent resolution, magnification and actual sample structure preservation (Relucenti et al., 2021; Vyas et al., 2016). SEM analysis confirmed the antibiofilm activity of *L. javanica* (ethyl acetate) against the studied *K. pneumoniae* strains and revealed fewer clumps of attached microcolonies, with a significant reduction in the number of biofilms compared to the untreated cells.

A key component of the biofilm extracellular matrix often produced by a wide range of microorganisms is exopolysaccharide (EPS) (Yamanaka et al., 2011). EPS plays a major role in holding the bacterial community together, attaching the cells to solid surfaces, and ensuring optimum hydration and availability of nutrients (Karygianni et al., 2020). Since EPS aids *K. pneumoniae* immune invasion and increases pathogenicity in biofilm-forming organisms generally, it was assessed as a contributing factor to the pathogenicity of biofilm-forming *K. pneumoniae.* Out of all plant extracts tested for EPS inhibition, *L. javanica* (ethyl acetate) revealed the highest percentage of EPS inhibition. This study marks the first evaluation of the studied plants for EPS reduction. However, extracts of *Mangifera indica* have been reported by Husain et al. (2017) to decrease the production of EPS in a treated culture of *Pseudomonas aeruginosa* where the extract exhibited 50.2% and 58.3% reduction at 400 µg/mL and 800 µg/mL, respectively, which is a significantly higher activity than what we observed for *L. javanica* extracts.

To validate the inhibitory effect of *L. javanica* (ethyl acetate) on EPS production, *in situ* visualization of the EPS was done using the AFM. The AFM allows for the quantification of EPS amount based on height and roughness analyses at the nanometre scale (Relucenti et al., 2021; Ansari et al., 2013). In this study, AFM micrographs of EPS treated with *L. javanica* (ethyl acetate) at MIC value did show distinguishable changes in height and surface roughness when compared to the untreated EPS. This could be due to the presence of camphene, a bioactive constituent in *L. javanica* previously reported by Adeosun et al. (2022) (as part of this research, chapter 4) to show exopolysaccharide inhibitory activity against *K. pneumoniae*. The AFM-based methodology employed in this study was useful to provide surface information regarding the effect of plant extract on *K. pneumoniae* EPS, a major component that makes up its biofilm matrixosome.

Another factor that increases pathogenicity in *K. pneumoniae* is its propensity to generate curli, known as thin aggregative fimbriae (Pacheco et al., 2021). Curli are known for forming interbacterial bundles and interacting directly with the substratum, allowing for a cohesive and stable association of cell aggregates (Besharova et al., 2016). Hence, curli expression in bacteria is linked to biofilm formation, contributing to virulence (Anes et al., 2017). A reduction in curli expression was observed for *L.*

javanica (ethyl acetate), *L. javanica* (dichloromethane) as well as the aqueous extracts of *C. dimidiatus* and *H. populifolium* at 0.5 mg/mL for both *K. pneumoniae* strains. This infers that the plant extracts can efficiently inhibit the formation of curli hence, inhibiting their ability to adhere to host tissue and inhibit biofilm formation. Bioactive compounds such as luteolin, tricin, and quercetin-rutinoside isomer 1 and 2 observed from the chemical profiling of *L. javanica* could have aided the curli reduction since Pruteanu et al. (2020) have reported that the above-mentioned compounds can inhibit the assembly of amyloid curli fibres and interfere with bacterial biofilm formation.

In addition to the aforementioned virulence factors, *K. pneumoniae's* hypermucoviscous nature contributes to its pathogenicity (Yao et al., 2015). This factor is significant since it renders the hypervirulent *K. pneumoniae* strains resistant to macrophage phagocytosis and neutrophil-mediated death, allowing them to spread more efficiently throughout the body of the host (Xu et al., 2021). A hypervirulent *K. pneumoniae* is frequently associated with a hypermucoviscous phenotype, a capsule-associated mucopolysaccharide web (Lin et al., 2011). The results obtained showed a gradual decrease in the viscosity of *K. pneumoniae* strains where *L. javanica* (ethyl acetate) was noted for a strong anti-hypermucoviscosity activity, with the least mucoid string length of less than 2 mm at 1.0 mg/mL concentration for both strains of K. *pneumoniae*. This is significantly lower than the 5 mm standard length defined by a positive string test (Shon et al., 2013). *L. javanica* (ethyl acetate) extracts thus revealed high potential in regulating the hypermucoviscosity phenotype.

For the development, modernisation, and quality control of various formulations from medicinal plants, chemical analysis of plant extracts is crucial (Nile & Park, 2015). Due to high sensitivity and accurate mass spectral detection, coupled with high-resolution chromatographic separation in LC-MS, analysis using this instrument has become more common in medicinal plants research (Parasuraman et al., 2014). For this reason, it was employed in this study for the chemical profiling of the most active extracts (*L. javanica* (ethyl acetate), *C. dimidiatus* (aqueous) and *H. populifolium* (aqueous)). The LC-MS analysis of the selected extracts revealed phytochemical compounds belonging to different classes such as the flavonoids, terpenes, verbascosides, phenolic acids, glycosides, quinic acids and a derivative class of compounds which could contribute to their bioactivities mentioned above. These

classes of compounds are particularly interesting due to their previously reported pharmacological properties. For example, Maroyi (2017) documented apigenin (flavonoid) identified in *L. javanica* (Table 2.6), to possess antibacterial and hepatoprotective properties. Luteolin, another flavonoid shown in the spectra have been reported by Kumar & Pandey (2013) to possess anti-inflammatory and analgesic effects.

Terpenes, also observed as part of the plant's compounds have been recognized as natural antimicrobial compounds (Burt, 2004). Antimicrobial activities of terpenes against *Escherichia coli* O157:H7, *Salmonella typhimurium*, *Clostridium perfringens*, *Campylobacter jejuni* and *Helicobacter pylori* have been reported by Mahizan et al. (2019) and Thapa et al. (2015). Furthermore, Shi et al. (2022) have reported the antibacterial activity of verbascosides against MDR *P. aeruginosa*. This could be due to the presence of the unique multi-hydroxyl group in their chemical structures which could perturb the lipid/water interface. Other possible mechanisms of inhibition by phytochemical compounds include competing and interfering with the activity of the signal molecules, due to their structural similarity or degradation of the signalling molecules (Cosa et al., 2019). *In-silico* and *in-vitro* approaches can be employed to further explore the ability of the profiled compounds to interrupt *K. pneumoniae*'s signalling mechanism which will result in attenuating its virulence thereby providing lead compounds for new drug discoveries.

2.5 CONCLUSION

Findings from this study revealed the three selected South African medicinal plants (*C. dimidiatus, H. populifolium* and *L. javanica*) as prospective antibacterial and anti-virulent agents against carbapenem-resistant and extended-spectrum beta-lactamase positive *K. pneumoniae* strains. A notable antibacterial activity was observed for *C. dimidiatus* (dichloromethane). The plant of *L. javanica* (ethyl acetate extract) decreased virulence factors of *K. pneumoniae* strains, indicating its potential to be used in the development of antipathogenic drugs. The highly complex profile of chemical compounds from *C. dimidiatus, H. populifolium* and *L. javanica* can be further explored for their antivirulence properties against *K. pneumoniae* strains. This

study contributes to the search for solutions to the threats posed by antibiotic resistance through the exploration of plant extracts used in traditional medicine.

To further unravel the next magic bullet from the phytochemical compounds present in the studied plants, the next chapter employed computer-based techniques for the virtual screening of the different classes of compounds. This will aid in assessing their potential to attenuate virulence in *K. pneumoniae* via molecular modelling of *K. pneumoniae's* virulence modulator, the transcriptional regulator SdiA protein.

References

Adam, O. A. O., Abadi, R. S. M., & Ayoub, S. M. H. (2019). Effect of extraction method and solvents on yield and antioxidant activity of certain Sudanese medicinal plant extracts. *The Journal of Phytopharmacology*, *8*(5), 248–252. https://doi.org/10.31254/phyto.2019.8507

Adeosun, I. J., Oladipo, E. K., Ajibade, O. A., Olotu, T. M., Oladipo, A. A., Awoyelu, E. H., Alli, O. A. T., & Oyawoye, O. M. (2019). Antibiotic susceptibility of *Klebsiella pneumoniae* isolated from selected tertiary hospitals in Osun state, Nigeria. *Iraqi Journal of Science*, *60*(7), 1423–1429. https://doi.org/10.24996/ijs.2019.60.7.2

Adeosun, I. J., Baloyi, I. T., & Cosa, S. (2022). Anti-biofilm and associated anti-virulence activities of selected phytochemical compounds against *Klebsiella pneumoniae*. *Plants*, *11*(11), 1–20. https://doi.org/10.3390/plants11111429

Agbor, A. M., & Naidoo, S. (2016). A review of the role of African traditional medicine in the management of oral diseases. *African Journal of Traditional Complementary Alternative Medicine*,13:133–42.

Akaberi, M., Sahebkar, A., Azizi, N., & Emami, S. A. (2019). Everlasting flowers: Phytochemistry and pharmacology of the genus *Helichrysum*. *Industrial Crops and Products*, *138*(4), 1–21. https://doi.org/10.1016/j.indcrop.2019.111471

Akinyede, K. A., Cupido, C. N., Hughes, G. D., Oguntibeju, O. O., & Ekpo, O. E. (2021). Medicinal properties and *in vitro* biological activities of selected *Helichrysum* species from South Africa: A review. *Plants*, *10*(8), 1–19. https://doi.org/10.3390/plants10081566

Akinyede, K. A., Ekpo, O. E., & Oguntibeju, O. O. (2020). Ethnopharmacology, therapeutic properties and nutritional potentials of *Carpobrotus edulis*: A comprehensive review. *Scientia Pharmaceutica*, *88*(3), 1–16. https://doi.org/10.3390/scipharm88030039

Alves, M. J., Ferreira, I. C. F. R., Froufe, H. J. C., Abreu, R. M. V., Martins, A., & Pintado, M. (2013). Antimicrobial activity of phenolic compounds identified in wild mushrooms, SAR analysis and docking studies. *Journal of Applied Microbiology*, *115*(2), 346–357. https://doi.org/10.1111/jam.12196

Anes, J., Hurley, D., Martins, M., & Fanning, S. (2017). Exploring the genome and phenotype of multi-drug resistant *Klebsiella pneumoniae* of clinical origin. *Frontiers in Microbiology*, *8*(10), 1–15. https://doi.org/10.3389/fmicb.2017.01913

Ansari, M. J., Al-Ghamdi, A., Usmani, S., Al-Waili, N. S., Sharma, D., Nuru, A., & Al-Attal, Y. (2013). Effect of jujube honey on *Candida albicans* growth and biofilm formation. *Archives of Medical Research*, *44*(5), 352–360. https://doi.org/10.1016/j.arcmed.2013.06.003

Atanasov, A. G., Zotchev, S. B., Dirsch, V. M., Orhan, I. E., Banach, M., Rollinger, J. M., Barreca, D., Weckwerth, W., Bauer, R., Bayer, E. A., Majeed, M., Bishayee, A., Bochkov, V., Bonn, G. K., Braidy, N., Bucar, F., Cifuentes, A., D'Onofrio, G., Bodkin, M., & Supuran, C. T. (2021). Natural products in drug discovery: advances and opportunities. *Nature Reviews Drug Discovery*, *20*(3), 200–216. https://doi.org/10.1038/s41573-020-00114-z

Baloyi, I. T., Adeosun, I. J., Yusuf, A. A., & Cosa,S. (2021). *In silico* and *in vitro* screening of antipathogenic properties of *Melianthus comosus* (Vahl) against *Pseudomonas aeruginosa*. *Antibiotics*, *10*(6), 1–23. https://doi.org/10.3390/antibiotics10060679

Baloyi, I.T., Adeosun, I. J., Yusuf, A. A., & Cosa, S. (2022). Antibacterial, antiquorum sensing, antibiofilm activities and chemical profiling of selected South African medicinal plants against multi-drug resistant bacteria. *Journal of Medicinal Plants Research*, *16*(2), 52–65. https://doi.org/10.5897/jmpr2021.7192

Besharova, O., Suchanek, V. M., Hartmann, R., Drescher, K., & Sourjik, V. (2016). Diversification of gene expression during formation of static submerged biofilms by *Escherichia coli. Frontiers in Microbiology*, *7*(10), 1–17. https://doi.org/10.3389/fmicb.2016.01568

Bi, Y., Xia, G., Shi, C., Wan, J., Liu, L., Chen, Y., Wu, Y., Zhang, W., Zhou, M., He, H., & Liu, R. (2021). Therapeutic strategies against bacterial biofilms. *Fundamental Research*, *1*(2), 193–212. https://doi.org/10.1016/j.fmre.2021.02.003

Blando, F., Russo, R., Negro, C., De Bellis, L., & Frassinetti, S. (2019). Antimicrobial and antibiofilm activity against *Staphylococcus aureus* of *Opuntia ficus-indica* (L.) mill. cladode polyphenolic extracts. *Antioxidants*, *8*(5), 1–13. https://doi.org/10.3390/antiox8050117

Boucher, H. W., Talbot, G. H., Bradley, J. S., Edwards, J. E., Gilbert, D., Rice, L. B., Scheld, M., Spellberg, B., & Bartlett, J. (2009). Bad bugs, no drugs: No ESKAPE! An update from the Infectious Diseases Society of America. *Clinical Infectious Diseases*, *48*(1), 1–12. https://doi.org/10.1086/595011

Bouyahya, A., Dakka, N., Et-Touys, A., Abrini, J., & Bakri, Y. (2017). Medicinal plant products targeting quorum sensing for combating bacterial infections. *Asian Pacific Journal of Tropical Medicine*, *10*(8), 729–743. https://doi.org/10.1016/j.apjtm.2017.07.021

Brisse, S., Fevre, C., Passet, V., Issenhuth-Jeanjean, S., Tournebize, R., Diancourt, L., & Grimont, P. (2009). Virulent clones of *Klebsiella pneumoniae*: Identification and evolutionary scenario based on genomic and phenotypic characterization. *PLoS ONE*, *4*(3), 1–13. https://doi.org/10.1371/journal.pone.0004982

Broomhead, N. K., Moodley, R., & Jonnalagadda, S. B. (2020). Elemental analysis of the edible fruit of *Carpobrotus dimidiatus* (from Kwazulu-Natal, South Africa) and the influence of soil quality on its elemental uptake. *Journal of Environmental Science and Health, 55*(4), 406–415. https://doi.org/10.1080/03601234.2019.1707016

Burt, S. (2004). Essential oils: Their antibacterial properties and potential applications in foods - A review. *International Journal of Food Microbiology*, *94*(3), 223–253. https://doi.org/10.1016/j.ijfoodmicro.2004.03.022

Chagonda, L. S., & Chalchat, J. C. (2015). Essential oil composition of *Lippia javanica* (Burm.f.) spreng chemotype from Western Zimbabwe. *Journal of Essential Oil-Bearing Plants*, *18*(2), 482–485. https://doi.org/10.1080/0972060X.2014.1001140

Chintamunnee, V., & Mahomoodally, M. F. (2012). Herbal medicine commonly used against non-communicable diseases in the tropical island of Mauritius. *Journal of Herbal Medicine*, *2*(4), 113–125. https://doi.org/10.1016/j.hermed.2012.06.001

Cosa, S., Chaudhary, S. K., Chen, W., Combrinck, S., & Viljoen, A. (2019). Exploring common culinary herbs and spices as potential anti-quorum sensing agents. *Nutrients*, *11*(4), 1–17. https://doi.org/10.3390/nu11040739

Cosa, S., Rakoma, J. R., Yusuf, A. A., & Tshikalange, T. E. (2020). *Calpurnia aurea* (Aiton) Benth extracts reduce quorum sensing controlled virulence factors in *Pseudomonas aeruginosa*. *Molecules*, *25*(10), 1–21. https://doi.org/10.3390/molecules25102283

Doughari, J. H., Human, I. S., Bennade, S., & Ndakidemi, P. A. (2009). Phytochemicals as chemotherapeutic agents and antioxidants: Possible solution to the control of antibiotic-resistant verocytotoxin-producing bacteria. *Journal of Medicinal Plants Research*, *3*(11), 839–848.

Eloff, J. N., Angeh, I. E., & McGaw, L. J. (2018). Solvent-solvent fractionation can increase the antifungal activity of a *Melianthus comosus* (*Melianthaceae*) acetone extract to yield a potentially useful commercial antifungal product. *Industrial Crops and Products*, *111*(3), 69–77. https://doi.org/10.1016/j.indcrop.2017.09.050

Emamzadeh, Y. S., Heyman, H. M., Prinsloo, G., Klimkait, T., & Meyer, J. M. (2022). Identification of anti-HIV biomarkers of *Helichrysum* species by NMR-based metabolomic analysis. *Frontiers in Pharmacology*, *13*(7), 1–11. https://doi.org/10.3389/fphar.2022.904231

Famuyide, I. M., Aro, A. O., Fasina, F. O., Eloff, J. N., & McGaw, L. J. (2019). Antibacterial and antibiofilm activity of acetone leaf extracts of nine under-investigated south African *Eugenia* and *Syzygium* (*Myrtaceae*) species and their selectivity indices. *BMC Complementary and Alternative Medicine*, *19*(1), 1–13. https://doi.org/10.1186/s12906-019-2547-z

Gopu, V., & Shetty, P. H. (2016). Cyanidin inhibits quorum signalling pathway of a food borne opportunistic pathogen. *Journal of Food Science and Technology*, *53*(2), 968–976. https://doi.org/10.1007/s13197-015-2031-9

Górniak, I., Bartoszewski, R., & Króliczewski, J. (2019). Comprehensive review of antimicrobial activities of plant flavonoids. In *Phytochemistry Reviews, 18*(1), 1–21. https://doi.org/10.1007/s11101-018-9591-z

Hammar, M., Arnqvist, A., Bian, Z., Olsén, A., & Normark, S. (1995). Expression of two csg operons is required for production of fibronectin- and congo red-binding curli polymers in *Escherichia coli* K-12. *Molecular Microbiology*, *18*(4), 661–670. https://doi.org/10.1111/j.1365-2958.1995.mmi_18040661.x

Huang, C., Tao, S., Yuan, J., & Li, X. (2022). Effect of sodium hypochlorite on biofilm of *Klebsiella pneumoniae* with different drug resistance. *American Journal of Infection Control*, *0*, 1–7. https://doi.org/10.1016/j.ajic.2021.12.003

Husain, F. M., Ahmad, I., Al-Thubiani, A. S., Abulreesh, H. H., AlHazza, I. M., & Aqil, F. (2017). Leaf extracts of *Mangifera indica* L. inhibit quorum sensing - regulated production of virulence factors and biofilm in test bacteria. *Frontiers in Microbiology*, *8*(4), 1–12. https://doi.org/10.3389/fmicb.2017.00727

Jang, M. H., Piao, X. L., Kim, J. M., Kwon, S. W., & Park, J. H. (2008). Inhibition of cholinesterase and amyloid-&bgr; aggregation by resveratrol oligomers from *Vitis amurensis*. *Phytotherapy Research*, *22*(4), 544–549. https://doi.org/10.1002/ptr

Karygianni, L., Ren, Z., Koo, H., & Thurnheer, T. (2020). Biofilm Matrixome: Extracellular components in structured microbial communities. *Trends in Microbiology*, *28*(8), 668–681. https://doi.org/10.1016/j.tim.2020.03.016

Kendaganna, P., Shivamallu, C., Shruthi, G., Nagabushan, M, Pradeep, S., & Karunakar P. (2021). *In silico* screening and validation of KPHS_00890 protein of *Klebsiella pneumoniae* proteome: an application to bacterial resistance and pathogenesis. *Journal of King Saud University - Science*, 33:1–21.

Koo, H., & Yamada, K. M. (2016). Dynamic cell-matrix interactions modulate microbial biofilm and tissue 3D microenvironments. *Current Opinion in Cell Biology*, *42*(1), 102–112. https://doi.org/10.1016/j.ceb.2016.05.005

Kumar, S., & Pandey, A. K. (2013). Chemistry and biological activities of flavonoids: An overview. *The Scientific World Journal*, *0*, 1–16. https://doi.org/10.1155/2013/162750

Lin, Y. C., Lu, M. C., Tang, H. L., Liu, H. C., Chen, C. H., Liu, K. Sen, Lin, C., Chiou, C. S., Chiang, M. K., Chen, C. M., & Lai, Y. C. (2011). Assessment of hypermucoviscosity as a virulence factor for experimental *Klebsiella pneumoniae* infections: Comparative virulence analysis with hypermucoviscosity-negative strain. *BMC Microbiology*, *11*(1), 1-10. https://doi.org/10.1186/1471-2180-11-50

Liu, Y., Han, L., Yang, H., Liu, S., & Huang, C. (2020). Effect of apigenin on surface-associated characteristics and adherence of *Streptococcus mutans*. *Dental Materials Journal*, *39*(6), 933–940. https://doi.org/10.4012/dmj.2019-255

Londonkar, R. L., Madire Kattegouga, U., Shivsharanappa, K., & Hanchinalmath, J. V. (2013). Phytochemical screening and *in vitro* antimicrobial activity of *Typha angustifolia* Linn leaves extract against pathogenic Gram negative micro organisms. *Journal of Pharmacy Research*, *6*(2), 280–283. https://doi.org/10.1016/j.jopr.2013.02.010

Lourens, A. C. U., Viljoen, A. M., & van Heerden, F. R. (2008). South African *Helichrysum* species: A review of the traditional uses, biological activity and phytochemistry. *Journal of Ethnopharmacology*, *119*(3), 630–652. https://doi.org/10.1016/j.jep.2008.06.011

Lukwa, N., Mølgaard, P., Furu, P., & Bøgh, C. (2009). *Lippia javanica* (Burm F) Spreng: Its general constituents and bioactivity on mosquitoes. *Tropical Biomedicine*, *26*(1), 85–91.

Mahizan, N. A., Yang, S., Moo, C.-L., & Song, A. A.-L. (2019). Terpene derivatives as a potential agent against antimicrobial resistant (AMR) pathogens. *Molecules*, *24*(2631), 1–21.

Mari, A., Napolitano, A., Masullo, M., Pizza, C., & Piacente, S. (2014). Identification and quantitative determination of the polar constituents in *Helichrysum italicum* flowers and derived food supplements. *Journal of Pharmaceutical and Biomedical Analysis*, *96*, 249–255. https://doi.org/10.1016/j.jpba.2014.04.005

Maroyi, A. (2017). *Lippia javanica* (Burm.f.) Spreng.: Traditional and commercial uses and phytochemical and pharmacological significance in the African and Indian subcontinent. *Evidence-Based Complementary and Alternative Medicine*, 0, 1-34. https://doi.org/10.1155/2017/6746071

Martin, R. M., & Bachman, M. A. (2018). Colonization, infection, and the accessory genome of *Klebsiella pneumoniae*. *Frontiers in Cellular and Infection Microbiology*, *8*(1), 1–15. https://doi.org/10.3389/fcimb.2018.00004

Martins, A., Vasas, A., Viveiros, M., Molnár, J., Hohmann, J., & Amaral, L. (2011). Antibacterial properties of compounds isolated from *Carpobrotus edulis*. *International Journal of Antimicrobial*

Agents, *37*(5), 438–444. https://doi.org/10.1016/j.ijantimicag.2011.01.016

Mashamba, T. G., Adeosun, I. J., Baloyi, I. T., Tshikalange, E. T., & Cosa, S. (2022). Quorum sensing modulation and inhibition in biofilm forming foot ulcer pathogens by selected medicinal plants. *Heliyon*, *8*(4), 1–11. https://doi.org/10.1016/j.heliyon.2022.e09303

Mbayo, M.K., Kalonda, M.E., Muhune, K.S., Numbi, W.E., Mulamba, M.J., & Lukusa, K.T.(2021). Investigation of antibacterial and antifungal activities of essential oils of *Lippia javanica* and *Lantana camara* (*Verbenaceae*) harvested in the Haut-Katanga (DRCongo). *International Journal of Advanced Biological and Biomedical Research*, *9*(3), 254–269. https://doi.org/ 10.22034/ijabbr.2021.525721.1353

Mogana, R., Adhikari, A., Tzar, M. N., Ramliza, R., & Wiart, C. (2020). Antibacterial activities of the extracts, fractions and isolated compounds from *Canarium patentinervium* miq. against bacterial clinical isolates. *BMC Complementary Medicine and Therapies*, *20*(1), 1–11. https://doi.org/10.1186/s12906-020-2837-5

Mostafa, A. A., Al-Askar, A. A., Almaary, K. S., Dawoud, T. M., Sholkamy, E. N., & Bakri, M. M. (2018). Antimicrobial activity of some plant extracts against bacterial strains causing food poisoning diseases. *Saudi Journal of Biological Sciences*, *25*(2), 361–366. https://doi.org/10.1016/j.sjbs.2017.02.004

Mulaudzi, R. B., Aremu, A. O., Rengasamy, K. R. R., Adebayo, S. A., McGaw, L. J., Amoo, S. O., Van Staden, J., & Du Plooy, C. P. (2019). Antidiabetic, anti-inflammatory, anticholinesterase and cytotoxicity determination of two *Carpobrotus* species. *South African Journal of Botany*, *125*(9), 142–148. https://doi.org/10.1016/j.sajb.2019.07.007

Nile, S. H., & Park, S. W. (2015). HPTLC densitometry method for simultaneous determination of flavonoids in selected medicinal plants. *Frontiers in Life Science*, *8*(1), 97–103. https://doi.org/10.1080/21553769.2014.969387

Oleksy-Wawrzyniak, M., Junka, A., Brożyna, M., Paweł, M., Kwiek, B., Nowak, M., Mączyńska, B., & Bartoszewicz, M. (2022). The *In vitro* ability of *Klebsiella pneumoniae* to form biofilm and the potential of various compounds to eradicate it from urinary catheters. *Pathogens*, *11*(1), 1–21. https://doi.org/10.3390/pathogens11010042

Pacheco, T., Gomes, A. É. I., Siqueira, N. M. G., Assoni, L., Darrieux, M., Venter, H., & Ferraz, L. F. C. (2021). SdiA, a quorum-sensing regulator, suppresses fimbriae expression, biofilm formation, and quorum-sensing signalling molecules production in *Klebsiella pneumoniae. Frontiers in Microbiology*, *12*(6), 1–15. https://doi.org/10.3389/fmicb.2021.597735

Parasuraman, S., Rao, A., Balamurugan, S., Muralidharan, S., Jayaraj Kumar, K., & Vijayan, V. (n.d.). An overview of liquid chromatography-mass spectroscopy instrumentation. *Pharmaceutical Methods*, *5*(2), 47–55. https://doi.org/10.5530/phm.2014.2.2

Perera, M. M. N., Dighe, S. N., Katavic, P. L., & Collet, T. A. (2022). Antibacterial potential of extracts and phytoconstituents isolated from *Syncarpia hillii* Leaves *in vitro*. *Plants*, *11*(3), 1–16. https://doi.org/10.3390/plants11030283

Pruteanu, M., Hernández Lobato, J. I., Stach, T., & Hengge, R. (2020). Common plant flavonoids prevent the assembly of amyloid curli fibres and can interfere with bacterial biofilm formation.

Environmental Microbiology, *22*(12), 5280–5299. https://doi.org/10.1111/1462-2920.15216

Ramos-Vivas, J., Chapartegui-González, I., Fernández-Martínez, M., González-Rico, C., Fortún, J., Escudero, R., Marco, F., Linares, L., Montejo, M., Aranzamendi, M., Muñoz, P., Valerio, M., Aguado, J. M., Resino, E., Ahufinger, I. G., Vega, A. P., Martínez, L., Fariñas, M. C., Ruiz San Millán, J. C., & de la Torre Cisneros, J. (2019). Biofilm formation by multidrug resistant *Enterobacteriaceae* strains isolated from solid organ transplant recipients. *Scientific Reports*, *9*(1), 1–10. https://doi.org/10.1038/s41598-019-45060-y

Relucenti, M., Familiari, G., Donfrancesco, O., Taurino, M., Li, X., Chen, R., Artini, M., Papa, R., & Selan, L. (2021). Microscopy methods for biofilm imaging: Focus on sem and VP-SEM pros and cons. *Biology*, *10*(1), 1–17. https://doi.org/10.3390/biology10010051

Santana, H. F., Barbosa, A. A. T., Ferreira, S. O., & Mantovani, H. C. (2012). Bactericidal activity of ethanolic extracts of propolis against *Staphylococcus aureus* isolated from mastitic cows. *World Journal of Microbiology and Biotechnology*, *28*(2), 485–491. https://doi.org/10.1007/s11274-011-0839-7

Scott, G., Springfield, E. P., & Coldrey, N. (2004). A pharmacognostical study of 26 South African plant species used as traditional medicines. *Pharmaceutical Biology*, *42*(3), 186–213. https://doi.org/10.1080/13880200490514032

Shi, C., Ma, Y., Tian, L., Li, J., Qiao, G., Liu, C., Cao, W., & Liang, C. (2022). Verbascoside: An efficient and safe natural antibacterial adjuvant for preventing bacterial contamination of fresh meat. *Molecules*, *27*(15), 1–17. https://doi.org/10.3390/molecules27154943

Shirinda, H., Leonard, C., Candy, G., & van Vuuren, S. (2019). Antimicrobial activity and toxicity profile of selected Southern African medicinal plants against neglected gut pathogens. *South African Journal of Science*, *115*(11–12), 1–10. https://doi.org/10.17159/sajs.2019/6199

Shon, A. S., Bajwa, R. P. S., & Russo, T. A. (2013). Hypervirulent (hypermucoviscous) *Klebsiella pneumoniae*: A new and dangerous breed. *Virulence*, *4*(2), 107–118. https://doi.org/10.4161/viru.22718

Shriram, V., Khare, T., Bhagwat, R., Shukla, R., & Kumar, V. (2018). Inhibiting bacterial drug efflux pumps via phyto-therapeutics to combat threatening antimicrobial resistance. *Frontiers in Microbiology*, *9*(12), 1–18. https://doi.org/10.3389/fmicb.2018.02990

Springfield, E. P., Amabeoku, G., Weitz, F., Mabusela, W., & Johnson, Q. (2003). An assessment of two *Carpobrotus* species extracts as potential antimicrobial agents. *Phytomedicine*, *10*(5), 434–439. https://doi.org/10.1078/0944-7113-00263

Springfield, E. P., & Weitz, F. (2006). The scientific merit of *Carpobrotus mellei* L. based on antimicrobial activity and chemical profiling. *African Journal of Biotechnology*, *5*(13), 1289–1293.

Thapa, D., Louis, P., Losa, R., Zweifel, B., & John Wallace, R. (2015). Essential oils have different effects on human pathogenic and commensal bacteria in mixed faecal fermentations compared with pure cultures. *Microbiology*, *161*(2), 441–449. https://doi.org/10.1099/mic.0.000009

Truong, D. H., Nguyen, D. H., Ta, N. T. A., Bui, A. V., Do, T. H., & Nguyen, H. C. (2019). Evaluation of the use of different solvents for phytochemical constituents, antioxidants, and *in vitro* anti-inflammatory activities of *Severinia buxifolia*. *Journal of Food Quality*, 1–9.

https://doi.org/10.1155/2019/8178294

Uc-Cachón, A. H., Dzul-Beh, A. de J., Palma-Pech, G. A., Jiménez-Delgadillo, B., Flores-Guido, J. S., Gracida-Osorno, C., & Molina-Salinas, G. M. (2021). Antibacterial and antibiofilm activities of Mayan medicinal plants against Methicillin-susceptible and -resistant strains of *Staphylococcus aureus*. *Journal of Ethnopharmacology*, *279*(4), 1–10. https://doi.org/10.1016/j.jep.2021.114369

van Vuuren, S., & Muhlarhi, T. (2017). Do South African medicinal plants used traditionally to treat infections respond differently to resistant microbial strains? *South African Journal of Botany*, *112*, 186–192. https://doi.org/10.1016/j.sajb.2017.05.027

Van Wyk, B. E. (2011). The potential of South African plants in the development of new medicinal products. *South African Journal of Botany*, *77*(4), 812–829. https://doi.org/10.1016/j.sajb.2011.08.011

Vyas, N., Sammons, R. L., Addison, O., Dehghani, H., & Walmsley, A. D. (2016). A quantitative method to measure biofilm removal efficiency from complex biomaterial surfaces using SEM and image analysis. *Scientific Reports*, *6*(4), 2–11. https://doi.org/10.1038/srep32694

Wang, J., Liu, Q., Dong, D., Hu, H., Wu, B., & Ren, H. (2020). *In-situ* monitoring of the unstable bacterial adhesion process during wastewater biofilm formation: A comprehensive study. *Environment International*, *140*(4), 1–8. https://doi.org/10.1016/j.envint.2020.105722

Wareth, G., & Neubauer, H. (2021). The Animal-foods-environment interface of *Klebsiella pneumoniae* in Germany: an observational study on pathogenicity, resistance development and the current situation. *Veterinary Research*, *52*(1), 1–14. https://doi.org/10.1186/s13567-020-00875-w

Wijesundara, N. M., & Vasantha Rupasinghe, H. P. (2019). Bactericidal and anti-biofilm activity of ethanol extracts derived from selected medicinal plants against *Streptococcus pyogenes*. *Molecules*, *24*(6), 1–19. https://doi.org/10.3390/molecules24061165

Wiskur, B. J., Hunt, J. J., & Callegan, M. C. (2008). Hypermucoviscosity as a virulence factor in experimental *Klebsiella pneumoniae* endophthalmitis. *Investigative Ophthalmology and Visual Science*, *49*(11), 4931–4938. https://doi.org/10.1167/iovs.08-2276

Xu, Q., Yang, X., Chan, E. W. C., & Chen, S. (2021). The hypermucoviscosity of hypervirulent *K. pneumoniae* confers the ability to evade neutrophil-mediated phagocytosis. *Virulence*, *12*(1), 2050–2059. https://doi.org/10.1080/21505594.2021.1960101

Yamanaka, T., Yamane, K., Furukawa, T., Matsumoto-Mashimo, C., Sugimori, C., Nambu, T., Obata, N., Walker, C. B., Leung, K. P., & Fukushima, H. (2011). Comparison of the virulence of exopolysaccharide-producing *Prevotella intermedia* to exopolysaccharide non-producing periodontopathic organisms. *BMC Infectious Diseases*, *11*(1), 1–10. https://doi.org/10.1186/1471-2334-11-228

Yao, B., Xiao, X., Wang, F., Zhou, L., Zhang, X., & Zhang, J. (2015). Clinical and molecular characteristics of multi-clone carbapenem-resistant hypervirulent (hypermucoviscous) *Klebsiella pneumoniae* isolates in a tertiary hospital in Beijing, China. *International Journal of Infectious Diseases*, *37*, 107–112. *https://doi.org/10.1016/j.ijid.2015.06.023*

CHAPTER THREE

MOLECULAR MODELLING OF SDIA PROTEIN BY SELECTED FLAVONOIDS AND TERPENES COMPOUNDS TO ATTENUATE VIRULENCE IN *KLEBSIELLA PNEUMONIAE*

This chapter has been published in the Journal of Biomolecular Structure and Dynamics: **Adeosun, I.J**., Baloyi, I.T, Aljoundi, A. K., Elliasu Y., Ibrahim, M. A., and Cosa, S. (2022). Molecular modelling of SdiA protein by selected flavonoid and terpenes compounds to attenuate virulence in *Klebsiella pneumoniae*. *Journal of Biomolecular Structure and Dynamics*, vol. 0, no. 0, pp. 1–19, 2022, doi: 10.1080/07391102.2022.2148753.

3.1 INTRODUCTION

Multidrug-resistant (MDR) *K. pneumoniae* remains one of the leading causes of death which continually imposes a healthcare and community burden globally (Ventola, 2015). Recalcitrance to several classes of antibiotics, biofilm-forming ability, persistent immune system defense and chronic infections are often linked to its QS regulatory system (Cadavid et al., 2018). This mechanism not only enhances bacterial pathogenesis but also improves their ability to severely infect and damage their host (Cosa et al., 2019). In GNB, the transcriptional regulators belonging to the LuxR protein plays a pivotal role by detecting the presence of autoinducers (AIs) known as N-acyl-homoserine lactones (AHLs) (Pradeep et al., 2018). Some *Enterobacteriaceae* pathogens such as *Salmonella*, *Escherichia*, including *Klebsiella* do not possess the AHLs-producing enzyme known as LuxI synthase. However, they recognize AHLs produced by other bacteria due to the presence of the SdiA protein which encodes an orphan LuxR homologue (Pacheco et al., 2021). Likewise, in *K. pneumoniae* the LuxI homolog is not found, thus the organism neither generates AHLs signal molecules of their own, however since this pathogen possesses SdiA, rather also senses the AI-2 molecules produced by the mixed community genera (Tavío et al., 2010). A SdiA transcriptional regulator in *K. pneumoniae* has been linked to cell division and the expression of virulence factors such as antibiotic resistance and biofilm formation. In addition, fimbriae and curli have been shown to play a pivotal role in *K. pneumoniae* biofilm development (Pacheco et al., 2021). This consequently marks the SdiA as a potential therapeutic target due to its ability to bind AHL and AI-2 signalling molecules from other pathogens, allowing for the transcription of several virulence genes (Pradeep et al., 2018; Pacheco et al., 2021).

Studies such as Pacheco et al. (2021) and Ahmed et al. (2020) have validated the role of SdiA in the production of QS autoinducers in *K. pneumoniae* and other *Enterobacteriaceae*, as noticed in enterohemorrhagic *Escherichia coli* (EHEC), *Salmonella enteritica* (Cheng et al., 2022). The crystal structure of SdiA has been reported in *E. coli* as PDB ID: 4LFU, 4LGW, 2AVX (Almeida et al., 2016). Since some *Enterobacteriaceae* (except for *Pantoea* and *Erwinia*) encodes the same SdiA protein and are implicated in QS signalling molecule production and modulation of virulence factors, 4LFU was used as a template to model the structure of *K. pneumoniae* SdiA,

thereby serving as a prototype in search for antivirulence or antagonistic compounds to impede the intercommunication and associated virulence activities.

Due to the above-mentioned pathogens' ability to regulate the respective virulence using the signalling mechanism (Gopu & Shetty, 2016), impeding this system hypothetically renders the disease-causing pathogen(s) less or non-virulent, presenting novel management of various bacterial infections (Cadavid et al., 2018). The secondary metabolites from medicinal plants may be the next-generation magic bullet in efficiently modulating QS-associated SdiA protein and the respective virulence factors (Koh et al., 2013). The phenomenon of most plants growing in settings with high bacterial populations fosters them to devise protective mechanisms against phytopathogens. Plants conquer by generating secondary metabolites that mimic microbial signal molecules, to compete for the protein active sites, subsequently impasse the expression of virulence factors and or reduce pathogenicity (Koh et al., 2013). The antivirulence mechanism, therefore, suppresses the expression of key genes vital for infections, rather than exerting bactericidal effect and selective pressure (Cosa et al., 2020). Terpenes, flavonoids, alkaloids, saponins, glycosides, anthraquinones and sesquiterpenoids among others, are all secondary metabolites capable of thwarting signalling mechanisms, hindering the expression of virulence factors (Akinyede et al., 2020; Baloyi et al., 2019; Maroyi, 2017).

In the previous chapter, the chemical profiling analysis of the South African medicinal plants of interest (*L. javanica, H. populifoilum* and *C. dimidiatus*) revealed that they contain different classes of compounds such as the flavonoids, terpenes, verbascosides, phenolic acids, glycosides, quinic acids and a derivative class of compounds which could contribute to their bioactivities. Of these classes of compounds, terpenes and flavonoids possess intriguing characteristics, making them of significant interest. Therefore, they were further investigated in this chapter for their structure-activity relationship to reveal the relationship between their chemical structures and biological activity with *K. pneumoniae*'s transcriptional regulator protein (SdiA).

Terpenes, commonly known as terpenoids, are abundant and diversified natural phytochemicals present in several medicinal plants and are vital component of essential oils. Terpenes of natural products provide medical benefits (Cox-Georgian

et al., 2019) and have proven to be a rich source of medical breakthroughs (Bergman et al., 2019). Flavonoids, on the other hand, are a class of naturally occurring plant compounds from various parts of plants associated with a broad spectrum of health-promoting effects with a wide range of pharmacological effects, including antimicrobial, anti-inflammatory, anti-mutagenic and anti-carcinogenic properties coupled with their capacity to modulate key cellular enzyme functions (Paczkowski et al., 2017; Panche et al., 2016).

The exploration of these bioactive phytochemicals as QS and virulence inhibitors through virtual screenings allows for a rapid and economical selection of prospective target ligands from large libraries of molecules (Huggins et al., 2011). This further accelerates the time and reduces the cost of traditional drug development processes (Naqvi et al., 2019), as well as narrowing the number of potential ligands to be tested *in vitro* for drug screening and drug ability. This study took advantage of computational research tools to evaluate the antivirulence potential of existing plant secondary metabolites known for their medicinal activities against the SdiA transcriptional regulator in *K. pneumoniae.*

3.2 MATERIALS AND METHODS

3.2.1 Sequence retrieval, template identification and homology modelling

A sequence of the SdiA gene was retrieved from the Kyoto Encyclopedia of Genes and Genomes database and searched against Protein Data Bank (PDB) proteins using NCBI-BlastP, following the method described by Ahmed et al. (2020). The SdiA from *Escherichia coli* (A-chain) (PDB ID: 4LFU) was used as a template structure for the generation of the 3D model of *Klebsiella pneumoniae* SdiA by using the Swiss model web server (Arnold et al., 2006).

3.2.2 Validation of the generated model

Protein structure validation suite (PSVS) ver. 1.5 (available at *http://psvs-1_5-dev.nesg.org/*) was used to determine the quality of the generated model, which revealed important validation parameters such as PROCHECK, VERIFY3D and Ramachandran plot. Furthermore, ProSA-Web was used to validate the protein

structure of the modelled SdiA, thereby providing information on the general quality of the input model structure. The secondary structure of the modelled SdiA protein was determined using PDBsum as described by Laskowski et al. (2018).

3.2.3 Prediction of the conserved residues and domains

Following the method described by Ahmed et al. (2020), the conserved residues of SdiA of *K. pneumoniae* was predicted by aligning its sequence with the sequences of the LuxR family proteins. These proteins include the LasR from *Pseudomonas aeruginosa*, CviR from *Chromobacterium violaceum* and SdiA from *Escherichia coli.* The conserved domains of SdiA of *K. pneumoniae* were predicted using the conserved domain and protein classification tool available at the NCBI server (*https://www.ncbi.nlm.nih.gov/cdd/*).

3.2.4 Prediction of the binding site

The CASTp 3.0 server was used for predicting the binding pocket of the modelled SdiA as described by Tian et al. (2018). The pocket with the highest area and largest volume was considered the most probable binding pocket of SdiA.

3.2.5 Molecular docking

Site-specific molecular docking (MD) was carried out following the method previously described by Baloyi et al. (2021) with slight modifications. The two-dimensional structures of the terpenes and flavonoids investigated were retrieved from the PubChem chemical database and sketched using Canvas 3.5 before being exported to Maestro 11.5. Chemically correct models of the ligands and the modelled SdiA receptor structure were built using Schrodinger's ligprep and a protein preparation wizard prior to the docking studies. The glides were then docked using the glide ligand docking module and the glide receptor. For the prepared protein created using the protein grid generation module, all docking calculations were performed using AutoDock 4.0 and Grids (Schrodinger, LLC, New York, NY, USA). Water and metals were removed before optimizing the hydrogen bonds, necessitating minimization and resulting in scores that mimicked the potential energy change when the protein and

the compound became bonded based on hydrogen bonds. MD was carried out on 31 compounds from natural sources which included the terpenes, flavonoids and other classes of compounds against the modelled SdiA protein.

3.2.6 Molecular dynamics simulations

3.2.6.1 System preparation and molecular dynamics simulation

The three-dimensional structures of best-docked terpenes and flavonoids were obtained in SDF format from PubChem, and the structures were optimized using Avogadro software. The modelled SdiA structure was prepared for molecular dynamics simulation (MDS) using the UCSF Chimera software package (Pettersen et al., 2004). MarvinSketch and Molegro Molecular Viewer (MMV) were used for the preparation of the ligand and to ensure that the ligand's proper angles and hybridization state were displayed (Kusumaningrum et al., 2014; Thomsen & Christensen, 2006). AutoDock tools GUI was used to describe the grid box at the catalytic site of the protein (Allouche, 2012). The Lamarckian Genetic algorithm was used to perform docking calculations (Oleg & Arthur, 2010). The prepared systems' protonation states were optimized using Maestro Schrödinger (Madhavi et al., 2013), necessary hydrogen atoms were corrected, and capping neutral residues to ensure protein stability during the simulation. Cumulatively, nine terpenes and eight flavonoids systems of each protein comprising the enzyme were subjected to MDS using the Graphic Process Unit version of the AMBER18 software package (Lee et al., 2018).

The protein was parametized by the FF14SB (Maier et al., 2015) force field integrated into the AMBER18 suit (Wang et al., 2004). The Link Edit and Parm (LEAP) module (Nikitin, 2014) of AMBER18 was then used to add hydrogens that are missing from the systems during preparation. Also, this module neutralizes the system by the addition of counter ions such as Na+ and Cl- after which the systems were solvated by suspending them in Transferable Intermolecular Potential with 3 Point (TIP3P) water box of size 8Å. Complexed coordinates and topology files of the receptor-ligand binding are generated for subsequent processing. The systems were minimized for 2000 energy steps. Initial minimization of 1000 steps with steep descent were performed for all the systems with a restrain potential and then followed by another 1000 steps minimization by conjugate gradient algorithm without restrain. The systems

were then gradually heated from 0K to 300K with a 5kcal/mol A harmonic restraint potential in NTP ensemble using Langevin thermostat of collision frequency of 1/ps. All the systems were then equilibrated at 300K for 500ps without restraint with a constant pressure at 1 bar using Berendsen barostat. SHAKE algorithm was used to restrain all hydrogen bonds (Gonnet, 2007).

MDS production of 100ns was then performed without restrain on the systems with target coupling of 2 ps and constant pressure at 1 bar. Analysis of the trajectories and coordinates generated from the MDS run was carried out through the CPPTRAJ and PTRAJ modules (Roe & Cheatham, 2013) incorporated in AMBER18. The RMSD and RMSF were calculated for all the systems. Discovery studio version v19.10.18289 (Sundaresan & Tharini, 2018) and UCSF chimera were used to visualize the trajectories while the Origin data version 6.0 tool (Seifert, 2014) was used to plot all graphs.

3.2.6.2 Binding free energy calculations

To estimate the binding interactions of the compounds with the modelled SdiA enzyme, binding free energy calculations were carried out using the Molecular Mechanics/Poisson-Boltzmann Surface Area (MM/PB-SA) method (Homeyer & Gohlke, 2012; Hou et al., 2011).

This approach has been widely employed and proven to be reliable in measuring binding free energies involved in protein-ligand complex formation. Moreover, MM/PBSA is mathematically represented as follows:

$$\Delta G_{bind} = G_{complex} - G_{receptor} - G_{ligand} \quad (1)$$

$$E_{gas} = E_{int} + E_{vdw} + E_{ele} \quad (2)$$

$$G_{sol} = G_{GB/PB} + G_{SA} \quad (3)$$

$$G_{SA} = \gamma SASA \quad (4)$$

Where van der Waals and electrostatic interactions are represented as E_{vdw} and E_{ele} while E_{gas} denotes gas-phase energy and E_{int} as internal energy. The solvation free energy denoted by G_{sol} represents the solvation free energy and can be decomposed into polar and nonpolar contribution states. The polar solvation contribution, $G_{GB/PB}$, is determined by solving the GB/PB equation, whereas, G_{SA}, the nonpolar solvation

contribution is estimated from the solvent-accessible surface area determined using a water probe radius of 1.4 Å.

3.2.7 Drug likeness properties of studied terpenes and flavonoids

The physicochemical and pharmacokinetic properties of the hit compounds were analysed using the SwissADME web server (*http://www.swissadme.ch/index.php*) (Daina et al., 2017). The compound's smileys were retrieved from the PubChem database, inserted in the webserver to run and generate the predicted parameters. Lipophilicity, water solubility and medicinal chemistry of the hit compounds were determined. The drug-likeness properties of the compounds (Lipinski's, Ghose's, Veber's, Egan's and Muegge's rules) and the bioavailability scores of the compounds were computed.

3.3 RESULTS

3.3.1 Template identification and homology modelling

BLAST results showed 99.58% sequence similarity between the SdiA protein in *Klebsiella pneumoniae* and the SdiA of the LuxR family transcriptional regulator (Accession number: KMI27310.1). The template 4LFU.1. A showed a low E-value (1e-158) and a sequence identity of 64.58%, hence, it was selected as the template for modelling the SdiA structure. The sequence alignment of the SdiA target protein with the 4LFU template protein and the ribbon structure of the modelled SdiA protein are shown in Figures 3.1A and 3.1B respectively.

```
Model_01    MRDNDFFSWRRDMLHQFQSVAAGEEVYNLLQRETEALEYDYYTLCVRHPVPFTRPRVTFQ   60
4lfu.1.A    MQDKDFFSWRRTMLLRFQRMETAEEVYHEIELQAQQLEYDYYSLCVRHPVPFTRPKVAFY   60
            *:*:******* ** :** : :.****: :: ::: ******:***********:*:*

Model_01    STYPRAWMSHYQAENYFAIDPVLRPENFMRGHLPWEDGLFRDAAALWDGARDHGLKKGVT   120
4lfu.1.A    TNYPEAWVSYYQAKNFLAIDPVLNPENFSQGHLMWNDDLFSEAQPLWEAARAHGLRRGVT   120
            :.**.**:*:***:*::******.**** :*** *:*.** :*  **:.** ***::***

Model_01    QCLTLPNHAQGFLSVSANNRLPGSYPDDELEMRLRMLTELSLLALLRLEDEMVMPPEMKF   180
4lfu.1.A    QYLMLPNRALGFLSFSRCSAREIPILSDELQLKMQLLVRESLMALMRLNDEIVMTPEMNF   180
            * * ***:* ****.*  .       .***::::::*.. **:**:**:**:** ***:*

Model_01    SRRELEILKWTAEGKTSAEVAMILSISENTVNFHQKNMQRKFNAPNKTQIACYAVATGLI   240
4lfu.1.A    SKREKEILRWTAEGKTSAEIAMILSISENTVNFHQKNMQKKINAPNKTQVACYAAATGLI   240
            *:** ***:**********:******************:*:*******:****.*****
```

Figure 3.1A: Alignment of template (4LFU) and model sequences.

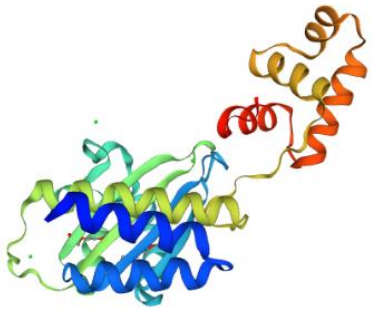

Figure 3.1B: 3D structure of the SdiA model.

3.3.2 Validation of the generated model

The quality of the model was evaluated using PSVS which comprises assessment tools such as Ramachandran score, Verify3D, ProsaWeb and Molprobity Clash score. The raw scores and Z-scores obtained for each parameter are shown in Table 3.1.

Table 3.1: Assessment of the SdiA model structure using protein structure validation suite (PSVS)

Parameter	Raw score	Z-score
Verify 3D	0.22	-3.85
ProsaII (–ve)	0.92	1.12
Procheck (/ – w)	0.25	1.30
Procheck (all)	0.08	0.47
RMSD_bond length (Å)	0.015	-
RMSD_bond angle (°)	1.9	-
Molprobity Clash score	2.21	1.15

Furthermore, Ramachandran plot scores from Procheck and Richardson's lab showed that the selected model had 95.4% and 98.3% residues respectively in the favourable and allowed regions and no residue in the outlier region (Table 3.2).

Table 3.2: Assessment of model quality by Ramachandran plot scores

Ramachandran plot scores	Most favoured regions (%)	Generously and additionally allowed regions (%)	Disallowed regions (%)
Ramachandran plot scores (Procheck)	95.4	4.6	0.0
Ramachandran plot scores (Richardson's lab)	98.3	1.7	0.0

The ProsaWeb also revealed that the SdiA model protein had a Z-score of –7.66, thus confirming the good quality of the model (Figure 3.2).

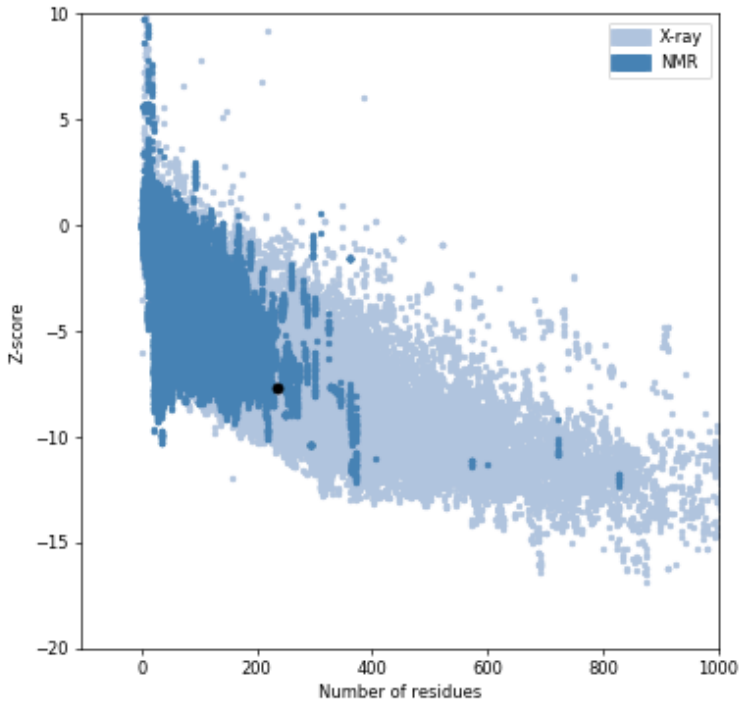

Figure 3.2: Validation of SdiA using ProSA web (Z-score = -7.66).

In addition, validation of the model was performed based on the secondary structure using PDBsum. The result revealed that the SdiA model had 13 a-helices which corresponds with the X-ray crystal structure also having 13 a-helices (Figure 3.3).

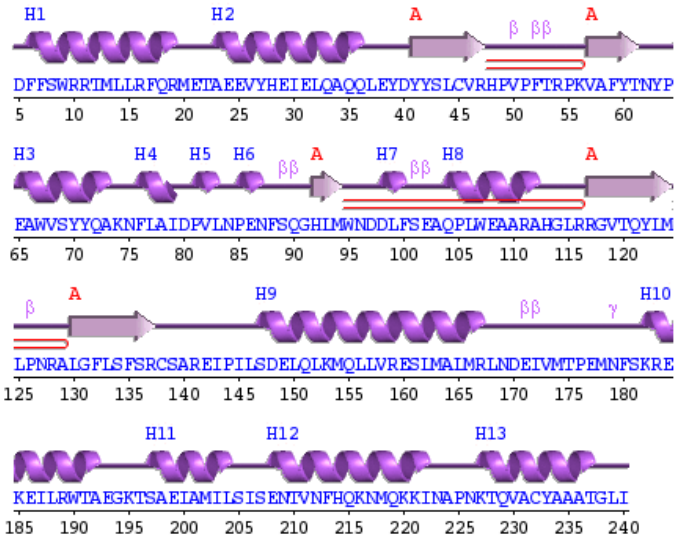

Figure 3.3: Secondary structure prediction of the SdiA model using PDBsum.

3.3.3 Analysis of conserved residues and domains of SdiA

Multiple sequence alignment of SdiA (*Klebsiella pneumoniae*) with the conserved LuxR family proteins (CviR: *Chromobacterium violaceum*, LasR: *Pseudomonas aeruginosa* and SdiA: *Escherichia coli*) revealed that a good number of the amino acid residues in SdiA of *K. pneumoniae* were conserved (conserved areas indicated with asterisk*) (Appendix 3.1). Furthermore, analysis of the conserved domains of SdiA showed that it contains an autoinducer binding domain (24–156), a helix-turn-helix Lux regulon (180–234), C-terminal DNA-binding domain of LuxR-like proteins (180–235), DNA binding transcriptional regulator (180-240), DNA binding response regulator (175-240) and other domain hits (Appendix 3.2).

3.3.4 Analysis of the binding pocket of SdiA

CASTp 3.0 predicted a binding pocket of SdiA with an area of 555.759 Å^2 and a volume of 365.829 Å^3. The amino acid residues lining the binding pocket were Ser43, Cys45, Arg54, Pro55, Lys56, Val57, Phe59, Thr61, Tyr63, Trp67, Val68, Tyr70, Tyr71, Gln72, Asn75, Phe76, Leu77, Asp80, Val82, Leu83, Met94, Trp95, Asn96, Asp97, Phe100, Leu106, Trp107, Ala109, Ala110, Arg111, His113, Leu115, Arg116, Arg117, Gly118, Phe132, Ser134 (Table 3.3).

Table 3.3: Active site prediction of modelled SdiA protein through CASTp

(A)		
Name of the protein	**Surface area (Å²)**	**Volume (Å³)**
Regulatory protein SdiA	555.759	365.829
(B) 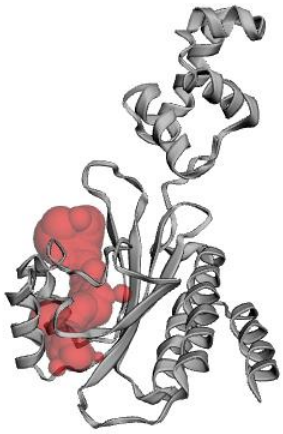	**(C)** Amino acids located at the active site: Ser43, Cys45, Arg54, Pro55, Lys56, Val57, Phe59, Thr61, Tyr63, Trp67, Val68, Tyr70, Tyr71, Gln72, Asn75, Phe76, Leu77, Asp80, Val82, Leu83, Met94, Trp95, Asn96, Asp97, Phe100, Leu106, Trp107, Ala109, Ala110, Arg111, His113, Leu115, Arg116, Arg117, Gly118, Phe132, Ser134	

Key: **(A)** Area and volume of the active site; **(B)** 3D structure of the active site; **(C)** Amino acids located at the active site.

3.3.5 Molecular docking of selected terpenes and flavonoids against SdiA protein

In silico, MD was carried out on 31 compounds from natural sources which included the terpenes, flavonoids and other classes of compounds against the modelled SdiA protein. The binding affinities of all 31 compounds are presented in Table 3.4, alongside their chemical structures, class of compounds, molecular formula, molecular weight and hydrophobic interactions.

Table 3.4: Docking results of 31 selected compounds against the SdiA receptor protein of *K. pneumoniae*

Compound name	Chemical structure	Class	Molecular formula	Molecular weight (g/mol)	Docking score (Kcal/mol)	Hydrophobic interactions
Glycitein	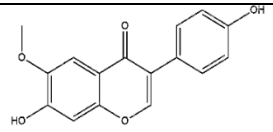	Flavonoids	$C_{16}H_{12}O_5$	284.26	-9.752	Ala110, Trp95, Leu115, Tyr63, Cys45, Tyr71, Leu83, Val82, Pro81, Leu106, Trp107, Phe100
Phloretin	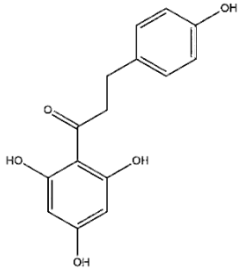	Flavonoids	$C_{15}H_{14}O_5$	274.27	-9.722	Leu115, Leu106, Ala109, Ala110. Tyr63, Phe76, Leu77, Phe59, Val57, Leu83, Cys45, Tyr71, Tyr70, Val68, Trp67
Quercetin	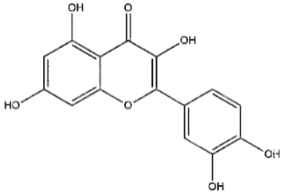	Flavonoids	$C_{15}H_{10}O_7$	302,236	-9.290	Ala109, Ala110, Leu106, Phe76, Trp67, Val68, Tyr70, Tyr71, Phe59, Tyr63, Cys45
3,7,11,15-Tetramethyl-2-hexadecen-1-OL (phytol)	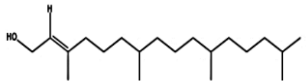	Terpenes	$C_{10}H_{16}$	296.5	-9.205	Leu115, Ala110, Ala109, Leu106, Tyr63, Phe59, Ala58, Val57, Cys45, Leu77, Leu83, Phe76, Tyr71, Tyr70, Val68, Trp67
6,10,14-Trimethylpentadecan-2-one	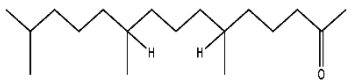	Sesquiterpenoids	$C_{18}H_{36}O$	268.5	-8.977	Trp67, Val68, Tyr70, Tyr71, Tyr63, Phe59, Val57, Cys45, Leu106, Ala109, Leu83, Leu77, Ala110, Phe76, Leu115

Table 3.4 (Cont'd): Docking results of 31 selected compounds against the SdiA receptor protein of *K. pneumoniae*

Compound name	Chemical structure	Class	Molecular formula	Molecular weight (g/mol)	Docking score (Kcal/mol)	Hydrophobic interactions
Fisetin	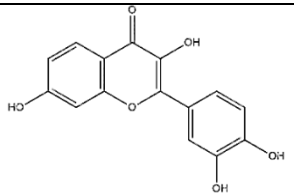	Flavonoids	$C_{15}H_{10}O_6$	286.24	-8.364	Ala110, Trp107, Leu106, Phe100, Leu115, Trp95, Tyr63, Tyr71, Leu83, Val82, Pro81, Phe100, Leu106, Trp107
Genistin	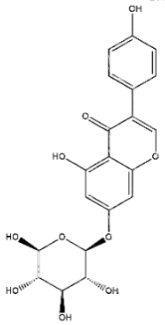	Flavonoids	$C_{21}H_{20}O_{10}$	432.4	-8.337	Phe100, Trp95, Met94, Ala100, Val82, Trp107, Leu106, Tyr63, Tyr71, Leu115
Apigenin	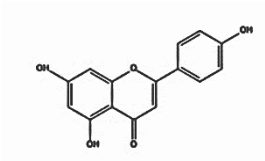	Flavonoids	$C_{15}H_{10}O_5$	270,0528	-8.222	Ala110, Ala109, Leu106, Phe76, Tyr63, Phe59, Cys45, Tyr71, Tyr70, Val68, Trp67
Beta-pinene	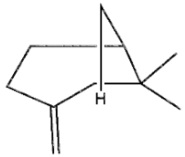	Terpenes	$C_{10}H_{16}$	136,23	-7.473	Leu115, Ala110. Ala109, Leu106, Phe76, Tyr63, Tyr71, Tyr70, Val68, Trp67
Alpha-pinene	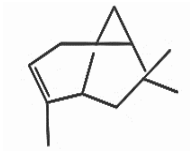	Terpenes	$C_{10}H_{16}$	136,23	-7.343	Ala109, Ala110, Leu106, Phe76, Tyr63, Tyr71, Tyr70, Val68, Trp67, Leu115

Table 3.4 (Cont'd): Docking results of 31 selected compounds against the SdiA receptor protein of *K. pneumoniae*

Compound name	Chemical structure	Class	Molecular formula	Molecular weight (g/mol)	Docking score (Kcal/mol)	Hydrophobic interactions
P-cymene	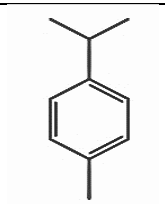	Terpenes	$C_{10}H_{14}$	134,22	-7.277	Ala110, Ala109, Leu106, Tyr71, Tyr70, Val68, Trp67, Tyr63, Phe76, Trp95, Leu115
Alpha-terpinene	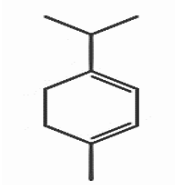	Terpenes	$C_{10}H_{16}$	136.23	-7.245	Leu115, Ala110, Ala109, Leu106, Tyr71, Tyr70, Phe76, Val68, Trp67, Tyr63, Trp95
Isoterpinolene	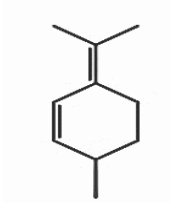	Terpenes	$C_{10}H_{16}$	136.23	-7.235	Tyr71, Tyr70, Val68, Trp67, Ala110, Ala109, Phe76, Leu106, Leu115, Tyr63
3-Carene	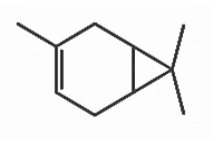	Terpenes	$C_{10}H_{16}$	136.23	-7.226	Ala110, Ala109, Leu106, Phe76, Tyr71, Tyr70, Val68, Trp67, Tyr63, Leu115
Sabinene	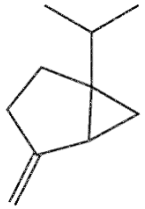	Terpenes	$C_{10}H_{16}$	136.23	-7.209	Leu115, Ala110, Ala109, Trp67, Val68, Leu106, Tyr70, Tyr71, Phe76, Tyr63

Table 3.4 (Cont'd): Docking results of 31 selected compounds against the SdiA receptor protein of *K. pneumoniae*

Compound name	Chemical structure	Class	Molecular formula	Molecular weight (g/mol)	Docking score (Kcal/mol)	Hydrophobic interactions
Octadecane		Alkanes	$C_{18}H_{38}$	254.494	-7.179	Leu77, Phe76, Leu106, Ala109, Ala110, Leu115, Leu77, Phe76, Trp67, Val68, Tyr70, Tyr71, Tyr63, Phe59, Val57, Cys45, Leu83
Camphene	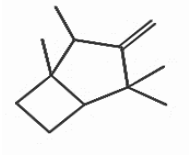	Terpenes	$C_{10}H_{16}$	136.24	-7.039	Ala110, Ala109, Leu106, Tyr71, Tyr70, Val68, Trp67, Phe76, Leu115, Tyr63
Baicalein	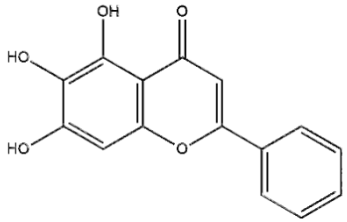	Flavonoids	$C_{15}H_{10}O_5$	270.24	-6.996	Ala110, Phe100, Trp107, Leu106, Val82, Trp95, Tyr63, Leu115
Daidzein	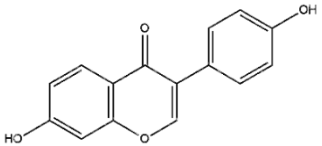	Flavonoids	$C_{15}H_{10}O_4$	254.24	-6.969	Leu115, Ala110, Trp95, Trp107, Leu106, Phe100, Val82, Leu83, Cys45, Tyr71, Tyr63
Acetic acid, [(trimethylsilyl)thio]-, trimethylsilyl ester	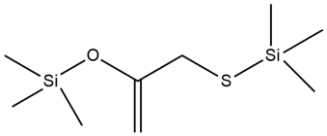	Carboxylic acid	$C_8H_{20}O_2SSi_2$	132.233	-6.896	Ala110, Ala109, Leu106, Phe76, Leu77, Leu83, Phe59, Tyr63, Tyr71, Cys45, Tyr70, Val68, Trp67, Leu115
Terpinolene	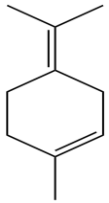	Terpenes	$C_{10}H_{16}$	136,23	-6.812	Ala110, Ala109, Leu106, Phe76, Leu115, Trp67, Val68, Tyr70, Tyr71, Tyr63

Table 3.4 (Cont'd): Docking results of 31 selected compounds against the SdiA receptor protein of *K. pneumoniae*

Compound name	Chemical structure	Class	Molecular formula	Molecular weight (g/mol)	Docking score (Kcal/mol)	Hydrophobic interaction
Carvacrol	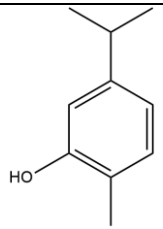	Terpenes	$C_{10}H_{14}O$	150.22	-6.633	Phe76, Ala110, Ala109, Leu106, Trp67, Val68, Tyr70, Tyr71, Tyr63, Leu115
Limonene	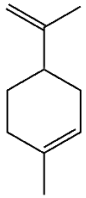	Terpenes	$C_{10}H_{16}$	136.23	-6.633	Tyr63, Ala110, Ala109, Leu106, Phe76, Tyr71, Tyr70, Val68, Trp67
Longifone	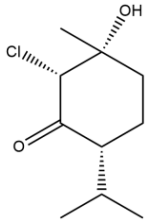	Terpenes	$C_{10}H_{17}ClO_2$	204.69	-6.301	Phe76, Ala110, Ala109, Leu106, Trp67, Val68, Tyr70, Tyr71, Trp95, Tyr63, Leu115
Ipsdienone	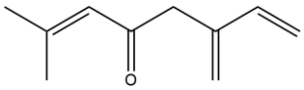	Terpenes	$C_{10}H_{14}O$	150.22	-6.237	Leu106, Ala109, Ala110, Phe76, Leu115, Tyr71, Tyr70, Val68, Trp67, Pro64, Tyr63
Myrcene	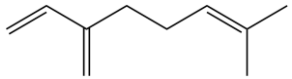	Terpenes	$C_{10}H_{16}$	136,23	-5.768	Leu115, Tyr63, Pro64, Trp67, Val68, Tyr70, Tyr71, Phe76, Leu106, Ala110, Ala109
Ascaridole	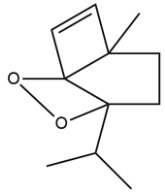	Terpenes	$C_{10}H_{16}O_2$	168.23	-5.385	Trp95, Trp67, Val68, Tyr70, Tyr71, Leu115, Ala110, Ala109, Leu106, Tyr63

Table 3.4 (Cont'd): Docking results of 31 selected compounds against the SdiA receptor protein of *K. pneumoniae*

Compound name	Chemical structure	Class	Molecular formula	Molecular weight (g/mol)	Docking score (Kcal/mol)	Hydrophobic interactions
5-Hydroxylysine	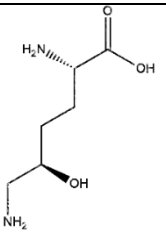	L-alpha amino acid	$C_6H_{14}N_2O_3$	162,187	-5.098	Leu115, Ala110, Tyr63, Phe59, Leu83, Cys45, Tyr71, Val68, Trp67, Phe76, Leu106
Nonanal	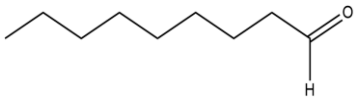	Aldehydes	$C_9H_{18}O$	142,2386	-4.879	Leu106, Ala109, Ala110, Leu115, Trp67, Val68, Phe76, Tyr70, Tyr71, Phe59, Tyr63
1-Octanol		Fatty alcohols	$C_8H_{18}O$ or $CH_3(CH_2)_6CH_2OH$	130,23	-4.676	Tyr71, Tyr70, Trp67, Trp95, Tyr63, Trp67, Leu115, Ala110, Ala109, Leu106, Phe76
Reference compound						
Furanosylborate diester (AI-2 molecule)	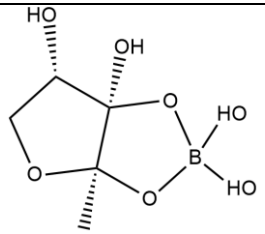	Borates	$C_5H_{10}BO_7$	192.940	-6.081	Leu115, Ala110, Trp107, Leu106, Phe100, Trp95

However, Table 3.5 focused on the MD results of the modelled SdiA protein against selected terpenes and flavonoids alongside their root mean square deviation and fluctuations, binding free energies and conformation to Lipinski's rules for drug-likeness. The results of the docking analysis allowed for the determination of the best binding modes. In particular, terpenes showed good potential as bioactive antagonists or as quorum sensing inhibitors (QSIs) in *K. pneumoniae* SdiA (4LFU) protein.

Based on the findings, terpenes possess high docking scores (Table 3.5) with a maximum score of -9.205kcal/mol achieved by 3,7,11,15-tetramethyl-2-hexadecen-1-ol (phytol) comparable to the scores obtained for SdiA native ligand (AI-2 furanosyl borate diester) with a docking score of -6.081kcal/mol. In addition to 3,7,11,15-tetramethyl-2-hexadecen-1-ol (phytol), eight (8) other terpenes: beta-pinene, alpha-pinene, 3-carene, sabinene, camphene, alpha-terpinene, p-cymene and isoterpinolene showed good docking scores between -7.473 kcal/mol and -7.039 kcal/mol (Table 3.5). These values (> -7 kcal/mol) were comparable to the obtained score of the AI-2 furanosyl borate diester (-6.081kcal/mol), hence, they are regarded as terpenes showing good docking scores.

Flavonoids such as glycitein, phloretin, fisetin, genistin, apigenin, baicalein, daidzein and quercetin against the active site of SdiA protein in *K. pneumoniae* demonstrated improved binding affinities and possessed high docking scores (Table 3.5). The maximum score of -9.752 kcal/mol was achieved by glycitein, which was slightly higher than quercetin (-9.290kcal/mol), a known QSI reference compound (Table 3.5).

Table 3.5: Molecular docking scores, root mean square deviation and fluctuations, binding free energy and drug-likeness prediction of best-docked terpenes and flavonoids

Compound name	Chemical structure	Molecular weight	Docking score (kcal/mol)	RMSD score (Å)	RMSF score (Å)	Binding energy (kcal/mol)	Drug likeness (Lipinski rule)
Glycitein (F)	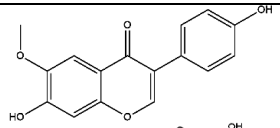	284.26	-9.752	2.23	2.85	- 30.3714	Yes; 0 violation
Phloretin (F)	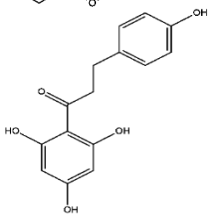	274.27	-9.722	1.96	1.59	-28.8415	Yes; 0 violation
Quercetin (F)	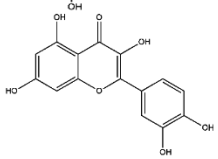	302,236	-9.290	1.57	1.08	-37.1247	Yes; 0 violation
3,7,11,15-Tetramethyl-2-hexadecen-1-ol (phytol) (T)	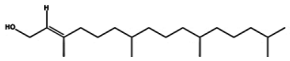	296.5	-9.205	1.54	1.78	-44.2625	Yes; 1 violation: MLOGP>4.15
Fisetin (F)	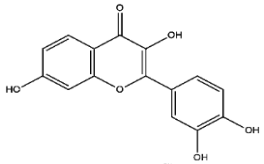	286.24	-8.364	1.71	2.09	-33.4770	Yes; 0 violation
Genistin (F)	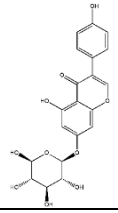	432.4	-8.337	1.44	1.35	-68.1393	Yes; 1 violation: NH or OH>5

Table 3.5 (Cont'd): Molecular docking scores, root mean square deviation and fluctuations, binding free energy and drug-likeness prediction of best-docked terpenes and flavonoids

Compound name	Chemical structure	Molecular weight	Docking score (kcal/mol)	RMSD score (Å)	RMSF score (Å)	Binding energy (kcal/mol)	Drug likeness (Lipinski rule)
Apigenin (F)	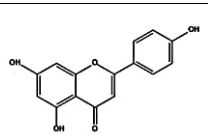	270,0528	-8.222	2.14	1.83	-40.9094	Yes; 0 violation
Beta-pinene (T)	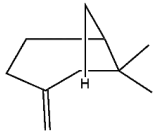	136,23	-7.473	2.58	3.23	-21.4366	Yes; 1 violation: MLOGP>4.15
Alpha-pinene (T)	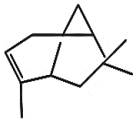	136,23	-7.343	2.14	1.40	-19.1913	Yes; 1 violation: MLOGP>4.15
P-cymene (T)	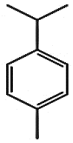	134,22	-7.277	2.21	1.92	-16.6186	Yes; 1 violation: MLOGP>4.15
Alpha-terpinene (T)	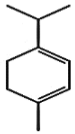	136.23	-7.245	1.73	1.39	-19.2618	Yes; 0 violation
Isoterpinolene (T)	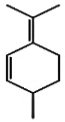	136.23	-7.235	1.61	2.10	-18.8961	Yes; 0 violation
3-Carene (T)	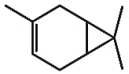	136.23	-7.226	2.09	1.53	-19.2745	Yes; 1 violation: MLOGP>4.15

Table 3.5 (Cont'd): Molecular docking scores, root mean square deviation and fluctuations, binding free energy and drug-likeness prediction of best-docked terpenes and flavonoids

Compound name	Chemical structure	Molecular weight	Docking score (kcal/mol)	RMSD score (Å)	RMSF score (Å)	Binding energy (kcal/mol)	Drug likeness (Lipinski rule)
Sabinene (T)	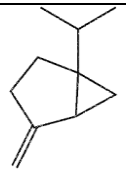	136.23	-7.209	1.48	1.17	-19.3283	Yes; 1 violation: MLOGP>4.15
Camphene (T)	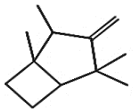	136.24	-7.039	1.86	3.74	-19.8651	Yes; 1 violation: MLOGP>4.15
Biacalein (F)	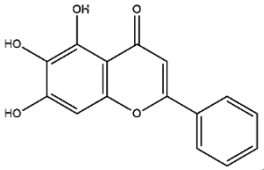	270.24	-6.996	1.54	1.56	-39.1342	Yes; 0 violation
Daidzein (F)	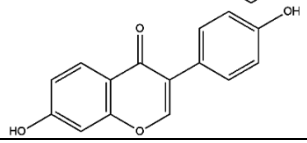	254.24	-6.969	1.69	2.05	-32.7409	Yes; 0 violation

Key: T= Terpene; F= Flavonoid

The interaction networks between the SdiA protein and the terpenes (Figure 3.4) revealed that phytol (3,7,11,15-tetramethyl-2-hexadecen-1-ol) had sixteen hydrophobic interactions and formed hydrogen bonds with Val57 (Figure 3.4A). Whereas beta-pinene formed a polar interaction with HIS 113 and ten hydrophobic interactions (Figure 3.4B). Alpha pinene compound formed a polar interaction with HIS 113 and ten hydrophobic interactions (Figure 4C) while 3-Carene formed ten hydrophobic interactions (Figure 4D). Sabinene also formed polar interaction with HIS 113 (Figure 3.4E). Hydrophobic interactions were also observed in camphene, alpha-terpinene, p-cymene and isoterpinolene as shown in Figure 3.4. The native ligand, AI 2 furanosyl borate diester bound to the active site with hydrogen bonding to amino acids Arg111, Leu115, Arg116 and polar interaction with Asn96, Ser136 (Figure 3.4J).

Docked flavonoid compounds against SdiA protein with respective interactions were as detailed in Figure 3.5. Glycitein had twelve hydrophobic interactions, hydrogen-bonded with Ser43 and a pi-pi stacking with Trp95 (Figure 3.5A) whereas phloretin formed hydrogen bonds with PG4 302 and H_2O, a pi-pi stacking with Tyr71 and Phe59 and fifteen hydrophobic interactions (Figure 3.5B). Fisetin compound was also shown to form hydrogen bonds with Asp80 and Ser13 as well as fourteen hydrophobic interactions (Figure 3.5C) while genistin also formed hydrogen bonds with Asp97 and Trp 95 with ten hydrophobic interactions (Figure 3.5D). Apigenin had eleven hydrophobic interactions (Fig 3.2E) while baicalein had eight hydrophobic interactions, a pi-pi stacking with Trp95, a hydrogen bond with Asp97 and a salt bridge with Arg111 (Figure 3.5F). Daidzein formed a hydrogen bond with Ser43, pi-pi stacking with Trp95 and eleven hydrophobic interactions (Figure 3.5G). Quercetin was shown to actively bind to the protein, forming hydrogen bonds with Trp57, and polar interactions with Gln72, Thr61 and Ser43 (Figure 3.5H).

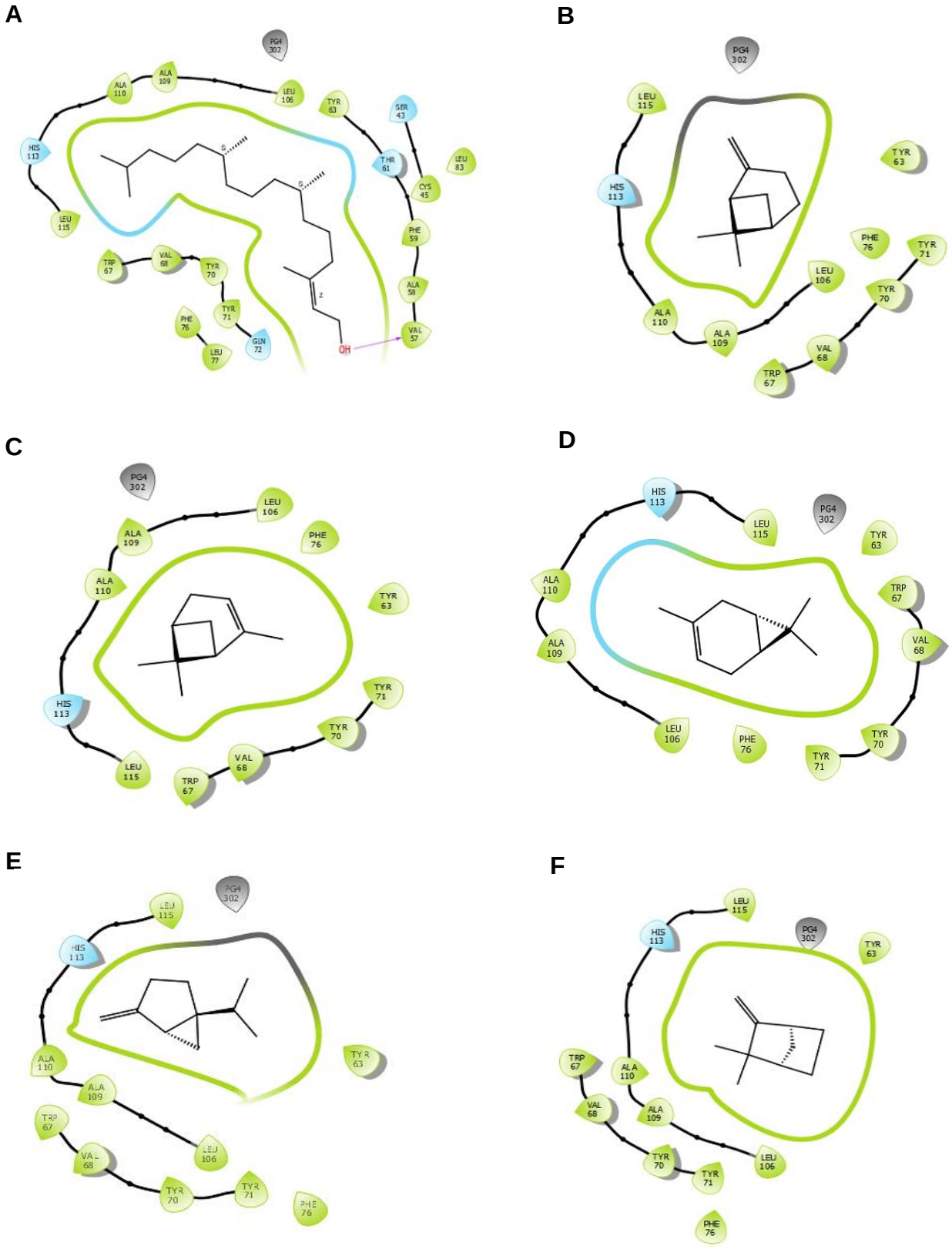

Figure 3.4: Interaction network between SdiA protein and terpenes showing good docking scores. The protein residues with a negative charge are shown in red, positive charge in velvet, polar in cyan, and hydrophobic in parrot green. The H-bond interactions are shown as a purple arrow, and pi-pi stacking as a green line. (A) 3,7,11,15-tetramethyl-2-hexadecen-1-ol (phytol) (B) beta-pinene (C) alpha-pinene (D) 3-carene (E) sabinene (F) camphene.

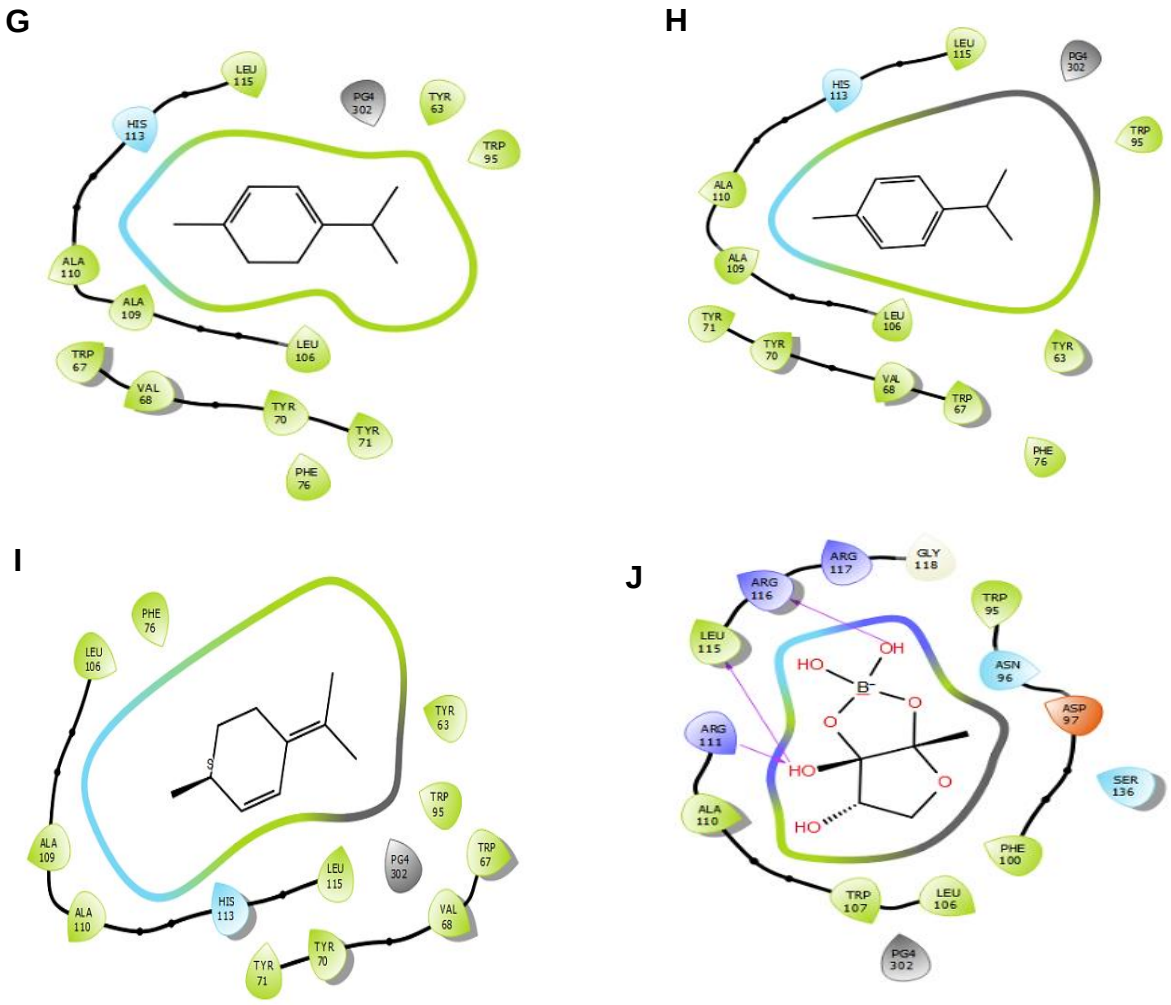

Figure 3.4 (Cont'd): Interaction network between SdiA protein and terpenes showing good docking scores. The protein residues with a negative charge are shown in red, positive charge in velvet, polar in cyan, and hydrophobic in parrot green. The H-bond interactions are shown as a purple arrow, and pi-pi stacking as a green line. (G) alpha-terpinene (H) p-cymene (I) isoterpinolene (J) furanosylborate diester (AI-2 molecule).

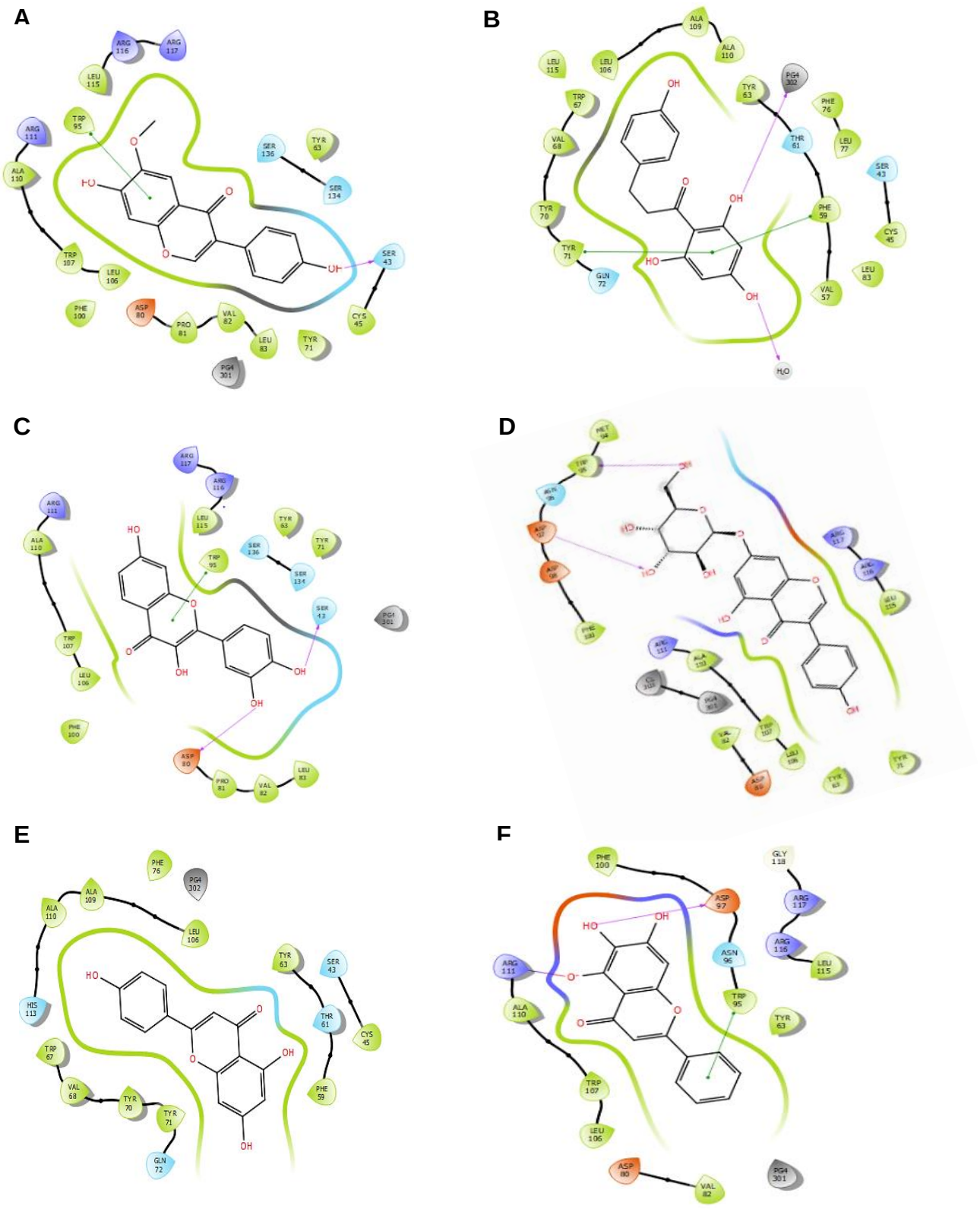

Figure 3.5: Interaction network between SdiA protein and flavonoids showing good docking scores. The protein residues with a negative charge are shown in red, positive charge in velvet, polar in cyan, and hydrophobic in parrot green. The H-bond interactions are shown as a purple arrow, and pi-pi stacking as a green line. (A) Glycitein (B) Phloretin (C) Fisetin (D) Genistin (E) Apigenin (F) Baicalein.

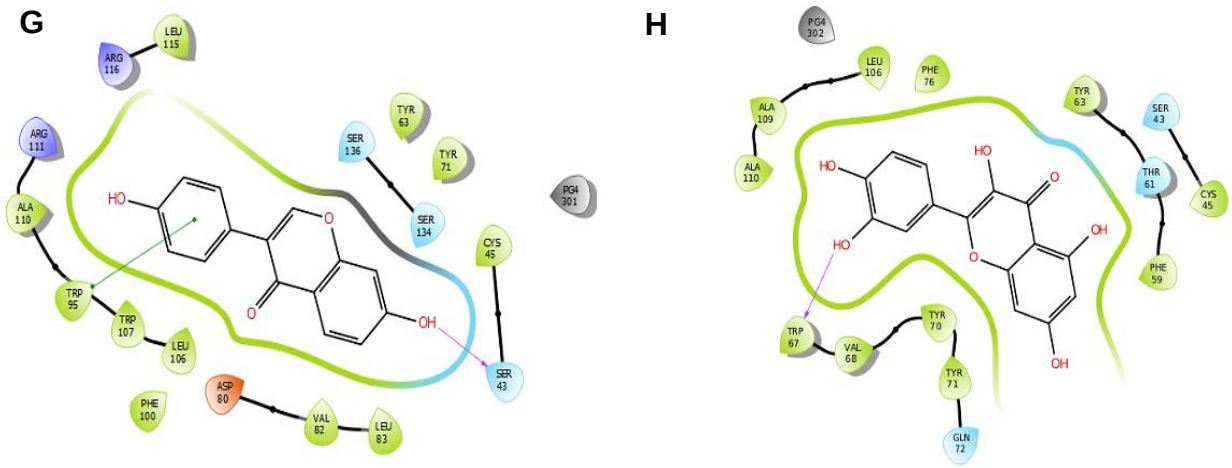

Figure 3.5 (Cont'd): Interaction network between SdiA protein and flavonoids showing good docking scores. The protein residues with a negative charge are shown in red, positive charge in velvet, polar in cyan, and hydrophobic in parrot green. The H-bond interactions are shown as a purple arrow, and pi-pi stacking as a green line. (G) Daidzein (H) Quercetin.

3.3.6 Dynamic conformational stability and fluctuations of the studied terpenes and flavonoid compounds

Further analysis of interactions of terpenes and flavonoids and MDSs were conducted to investigate their respective inhibitory performance on SdiA. Through validation of the system's stability, disrupted motions were deduced and artifacts that may arise during the simulation were avoided. In this study, root-mean-square deviation (RMSD) calculated to measure the systems' stability during the 100ns simulations (Figure 3.6) were recorded as average RMSD values (Table 3.5).

For all frames of SdiA bonded terpene compounds systems, alpha-pinene, alpha-terpinene, beta-pinene, camphene, 3-carene, isoterpinolene, p-cymene, 3,7,11,15-tetramethyl-2-hexadecen-1-ol (phytol), sabinene and the unbound SdiA (Apo) revealed RMSD values of 2.14 Å, 1.73 Å, 2.58 Å, 1.86 Å, 2.09 Å, 1.61 Å, 2.21 Å, 1.54 Å, 1.48 Å, and 2.50 Å, respectively. The comparative C-α RMSD plots showing the degree of stability and convergence of the studied systems over the 100ns MDS time are shown in Figure 3.6A.

On the other hand, the recorded average RMSD values for all frames of SdiA bonded flavonoids which include apigenin, biacalein, diadzein, fisetin, genistin, glycitein, phloretin, quercetin and unbound SdiA (Apo) were 2.14 Å, 1.54 Å, 1.69 Å, 1.71 Å, 1.44 Å, 2.23 Å, 1.96 Å, 1.57 Å, and 2.50 Å respectively (Table 3.5). The comparative C-α RMSD plots showing the degree of stability and convergence of the studied systems over the 100ns MDS time are shown in Figure 3.6B.

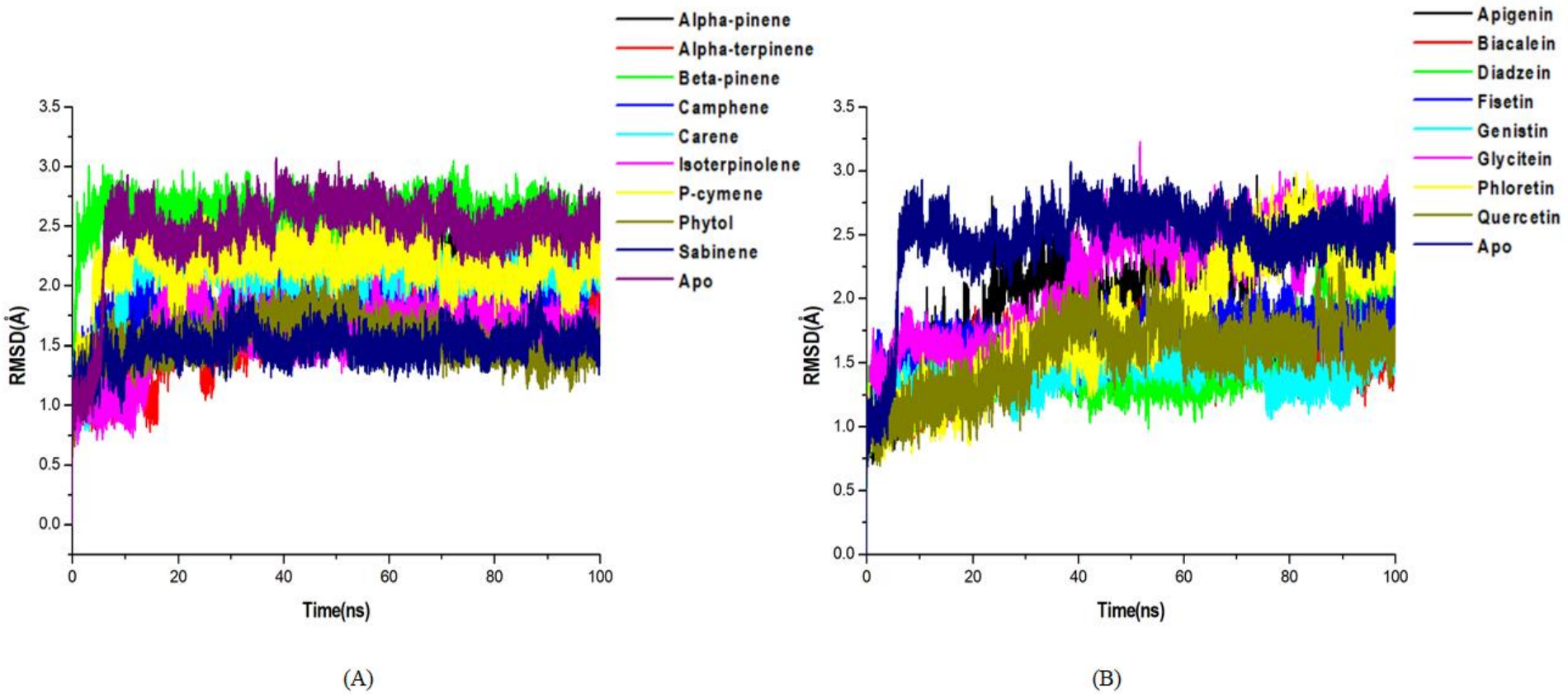

Figure 3.6: Comparative C-α RMSD plots showing the degree of stability and convergence of the studied terpene compounds (A) and flavonoids (B) over the 100ns molecular dynamics simulation time.

The time evolution root-mean-square fluctuation (RMSF) of each residue, indicative of the differences in fluctuations of conformational changes of the protein Cα atom over 100ns for the studied systems (selected terpenes and flavonoids) were superposed on the crystal structures of the studied systems (Figure 3.7).

The evolution of protein structure flexibility upon ligand binding often probes residue performance and their association with the ligand during MDS. The complexes' (SdiA bonded terpenes and flavonoids) residual fluctuations were evaluated using the RMSF algorithm to assess the effect of inhibitor binding towards the respective targets over 100ns simulations. The computed average atomic fluctuation of the terpenes which include alpha-pinene, alpha-terpinene, beta-pinene, camphene, 3-carene, isoterpinolene, p-cymene, 3,7,11,15-tetramethyl-2-hexadecen-1-ol (phytol), sabinene and the unbound SdiA (Apo) were 1.40 Å, 1.39 Å, 3.23 Å, 3.74 Å, 1.53 Å, 2.10 Å, 1.92 Å, 1.78 Å, 1.17 Å and 1.87 Å respectively (Table 3.5, Figure 3.7A). However, the average atomic fluctuations of the flavonoids were also computed which revealed RMSF values for apigenin, biacalein, diadzein, fisetin, genistin, glycitein, phloretin, quercetin and unbound SdiA (Apo) as 1.83 Å, 1.56 Å, 2.05 Å, 2.09 Å, 1.35 Å, 2.85 Å, 1.59 Å, 1.08 Å, and 1.87 respectively (Table 3.5, Figure 3.7B).

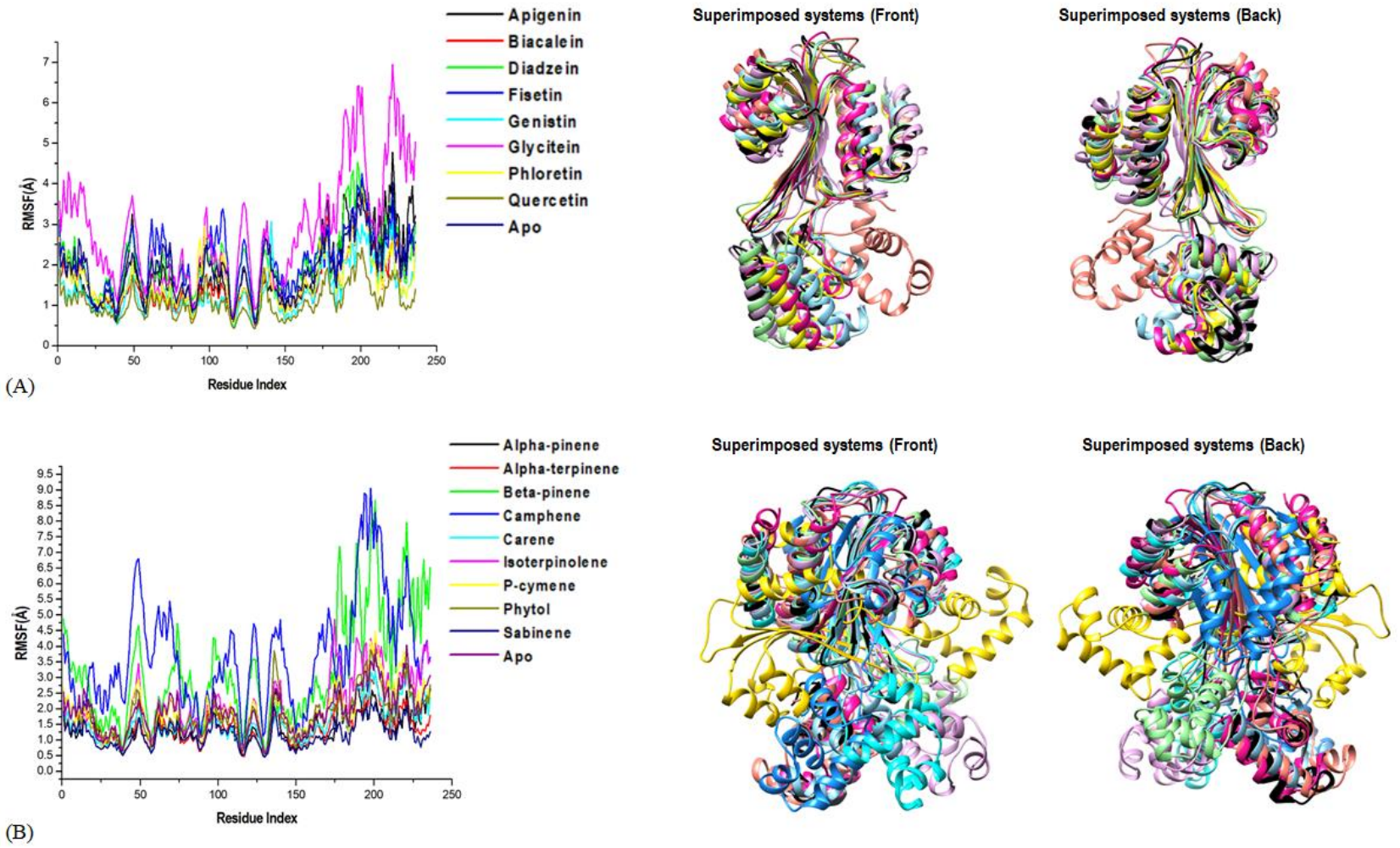

Figure 3.7: The time evolution RMSF of each residue of the protein Cα atom over 100ns for the studied flavonoids (A) and terpenes (B) superposed on the crystal structures of the studied systems to show differences in fluctuations and conformational changes. Comparative Cα RMSF plot showing the degree of major flexibility of certain loops and helixes at the highest fluctuation during the simulation.

3.3.7 Binding free energy landscape of SdiA bonded terpene and flavonoid compounds

The binding free energy of the studied SdiA bonded terpenes ranged from -16.6186kcal/mol to as high as -44.2625kcal/mol (Table 3.5). Results revealed that 3,7,11,15-tetramethyl-2-hexadecen-1-ol (phytol) had the highest binding energy of -44.2625kcal/mol while the least binding energy was observed in p-cymene (-16.6186kcal/mol) (Table 3.5). For the SdiA-bound flavonoids, their binding free energy ranged from -28.8415kcal/mol to -68.1393kcal/mol. Genistin showed the highest binding energy of -68.1393kcal/mol while the least binding energy was observed in phloretin (-28.8415kcal/mol) (Table 3.5).

Results of MM/GBSA-based binding free energy profile of SdiA bonded terpenes and flavonoids revealing other energy components (electrostatic energy, van der Waals energy, solvation free energy and gas-phase free energy) are shown in Table 3.6.

Table 3.6: MM/GBSA-based binding free energy profile of SdiA bonded terpenes and flavonoids

S/N	Terpenes	Energy components (kcal/mol)					Flavonoids	Energy components (kcal/mol)				
		ΔE_{vdw}	ΔE_{ele}	ΔG_{gas}	ΔG_{sol}	ΔG_{bind}		ΔE_{vdw}	ΔE_{ele}	ΔG_{gas}	ΔG_{sol}	ΔG_{bind}
1	P-cymene	-24.7764	0.6310	-24.1454	5.7552	-18.3902	Fisetin	-23.8535	-22.5346	-46.3881	24.1463	-22.2418
2	3,7,11,15-Tetramethyl-2-hexadecen-1-OL (phytol)	-48.8645	-4.6792	-53.5437	10.2756	-43.2680	Genistin	-24.8153	-34.2254	-59.0407	36.5112	-22.5295
3	Alpha-pinene	-24.8209	0.0145	-24.8064	4.4408	-20.3656	Diadzein	-28.5005	-14.3454	-42.8459	18.0030	-24.8429
4	Alpha-terpinene	-25.1307	0.5571	-24.5736	4.5242	-20.0495	Quercetin	-42.3552	-12.2763	-54.6315	22.4873	-32.1442
5	3 - Carene	-23.7216	-1.0117	-24.7333	4.8996	-19.8336	Glycitein	-31.2432	-19.8918	-51.1351	24.2802	-26.8549
6	Camphene	-22.5031	-22.5031	-22.9386	4.7237	-18.2148	Phloretin	-37.0394	-21.3957	-58.4350	26.5341	-31.9010
7	Sabinene	-6.6711	-0.0279	-6.6990	1.8893	-4.8097	Apigenin	-22.7803	-11.3078	-34.0881	15.0348	-19.0533
8	Beta-pinene	-13.1169	-0.3701	-13.4871	3.1648	-10.3223	Biacalein	-30.0588	-33.4847	-63.5436	29.2440	-34.2996
9	Isoterpinolene	-24.5669	-0.2579	-24.8248	5.1453	-19.6795						

All energies are in kcal/mol.
ΔEele = electrostatic energy; **ΔEvdW** = van der Waals energy; **ΔGbind** = total binding free energy; **ΔGsol** = solvation free energy **ΔG** = gas phase free energy

3.3.8 Validation of drug-likeness properties of the studied terpenes and flavonoids

The drug-likeness properties of the studied compounds revealed information on their physicochemical properties, lipophilicity, water solubility, pharmacokinetics and medicinal chemistry. All the studied terpenes were shown to have 10 heavy atoms (except phytol which had 21), 0 aromatic heavy atoms (except p-cymene which had 6) and Csp3 fractions of 0.80 (Table 3.7). The compounds, except for phytol (with higher values) had 0 number of H-bond acceptors and donors with molar refractivity ≥ 45.22 and TPSA of 0 $Å^2$. On the other hand, flavonoids had heavy atoms and heavy aromatic atoms > 10 with a higher number of hydrogen-bond acceptors and donors, Molar refractivity and TPSA≥ 4, 73 and 70$Å^2$ respectively. Additionally, the terpenes had low gastrointestinal (GI) absorption and can permeate the blood-brain barrier (BBB), except phytol with Log K_P≥ 4.0 cm/s although phytol and α-pinene had values of -2.29 cm/s and -3.95 cm/s respectively (Table 3.7). Also, the terpenes had zero alert PAINS with zero or one alert brenk and synthetic availabilities of ≥ 1.00. In the case of flavonoids, the compounds fisetin, baicalein and quercetin had 1 alert PAINS and brenk with catechol A. Other compounds showed zero alert PAINS and zero alert brenk respectively (Table 3.7). In addition, the consensus Log Po/w of the terpenes was predicted to be ≥ 3.0 with phytol having 6.21 while the flavonoids had a value ranging from 0.42- 2.3 (Table 3.7).

Furthermore, Table 3.8 revealed the different solubility classes of the tested compounds where the compounds were classified as either insoluble, poorly soluble, moderately soluble, soluble, very soluble or highly soluble. For Log S (Esol and SILICOS-IT), all the terpenes appeared to be soluble in water except phytol which showed moderate solubility. In the case of Log S (Ali), α-pinene and 3-carene revealed moderate solubility while poor solubility was predicted for phytol. For the flavonoids, all the compounds were soluble (except baicalein) by the Log S (Esol) parameter while baicalein, apigenin, genistin, glycitein and daidzein compounds showed moderate solubility for Log S (Ali and SILICOS-IT) (Table 3.8).

Table 3.7: Drug likeness properties of studied terpenes and flavonoids

Compounds	Physico-chemical properties						Lipophilicity	Water Solubility		Pharmacokinetics			Medicinal Chemistry	
	No. heavy atoms	No. rotatable bonds	No. H-bond acceptors	No. H-bond donors	Molar Refractivity	TPSA (Å^2)	Consensus Log Po/w	Log S (ESOL)	Class	GI absorption	BBB permeation	Log Kp (Skin permeation) (cm/s)	PAINS	Brenk
Phytol	21	13	1	1	98.94	20.23	6.21	-5.98	Moderately soluble	Low	No	-2.29	0 alert	1 alert: isolated_alkene
Beta-pinene	10	0	0	0	45.22	0.00	3.44	-3.31	Soluble	Low	Yes	-4.18	0 alert	1 alert: isolated_alkene
Alpha-pinene	10	0	0	0	45.22	0.00	3.42	-3.51	Soluble	Low	Yes	-3.95	0 alert	1 alert: isolated_alkene
P-cymene	10	1	0	0	45.99	0.00	3.50	-3.63	Soluble	Low	Yes	-4.21	0 alert	0 alert
Alpha-terpinene	10	1	0	0	47.12	0.00	3.30-	-3.30	Soluble	Low	Yes	-4.11	0 alert	0 alert
Isoterpinolene	10	0	0	0	47.12	0.00	3.09	-2.90	Soluble	Low	Yes	-4.64	0 alert	0 alert
3-Carene	10	0	0	0	45.22	0.00	3.42	-3.44	Soluble	Low	Yes	-4.02	0 alert	1 alert: isolated_alkene
Sabinene	10	1	0	0	45.22	0.00	3.25	-2.57	Soluble	Low	Yes	-4.94	0 alert	1 alert: isolated_alkene
Camphene	10	0	0	0	45.22	0.00	3.43	-3.34	Soluble	Low	Yes	-4.13	0 alert	1 alert: isolated_alkene
Glycitein	21	2	4	2	78.46	79.90	2.30	-3.57	Soluble	High	No	-6.30	0 alert	0 alert
Phloretin	20	4	5	4	74.02	97.99	1.93	-3.38	Soluble	High	No	-6.11	0 alert	0 alert
Fisetin	21	1	6	4	76.01	111.13	1.55	-3.35	Soluble	High	No	-6,65	1 alert: catechol_A	1 alert: catechol_A
Genistin	31	4	10	6	106.11	170.05	0.42	-3.18	Soluble	Low	No	-8.33	0 alert	0 alert
Apigenin	20	1	5	3	73.99	90.90	2.11	-3.94	Soluble	High	No	-5.80	0 alert	0 alert

Table 3.7 (Cont'd): Drug likeness properties of studied terpenes and flavonoids

Compounds	Physico-chemical properties						Lipophilicity	Water Solubility		Pharmacokinetics			Medicinal Chemistry	
	No. heavy atoms	No. rotatable bonds	No. H-bond acceptors	No. H-bond donors	Molar Refractivity	TPSA (Å^2)	Consensus Log Po/w	Log S (ESOL)	Class	GI absorption	BBB permeation	Log Kp (Skin permeation) (cm/s)	PAINS	Brenk
Baicalein	20	1	5	3	73.99	90.90	2.24	-4.03	Moderately soluble	High	No	-5.70	1 alert: catechol_A	1 alert: catechol_A
Daidzein	19	1	4	2	71.97	70.67	2.24	-3.53	Soluble	High	Yes	-6.10	0 alert	0 alert
Quercetin	22	1	7	5	78.03	131.36	1.23	-3.16	Soluble	High	No	-7.05	1 alert: catechol_A	1 alert: catechol_A
Furanosylboratediester	13	0	7	4	37.77	108.61	-2-32	0.48	Highly soluble	Low	No	-9.18	0 alert	1 alert: heavy_metal

Table 3.8: Water Solubility

Compounds	Log S (ESOL)	Solubility (mg/mL)	Class	Log S (Ali)	Solubility (mg/mL)	Class	Log S (SILICOS-IT)	Solubility (mg/mL)	Class
3,7,11,15-Tetramethyl-2-hexadecen-1-OL(Phytol)	-5.98	3.10e-04	Moderately soluble	-8.47	9.94e-07	Poorly soluble	-5.51	9.06e-04	Moderately soluble
Beta-pinene	-3.31	$6.74e^{-02}$	soluble	-3.87	1.85^{e-02}	Soluble	- 2.48	4.55e-01	soluble
Alpha-pinene	-3.51	4.24e-02	soluble	-4.20	8.59e-03	Moderately soluble	-2.23	8.06e-01	soluble
P-cymene	-3.63	3.12e-02	soluble	-3.81	2.10e-02	Soluble	-3.57	3.58e-02	soluble
Alpha-terpinene	-3.30	6.89e-02	soluble	-3.96	1.49e-02	Soluble	-2.23	8.06e-01	soluble
Isoterpinolene	-2.90	1.73e-01	soluble	-3.19	8.72e-02	Soluble	-2.01	1.33e+00	soluble
3-Carene	-3.44	4.90e-02	soluble	-4.10	1.09e-02	Moderately soluble	-2.33	8.06e-01	soluble
Sabinene	-2.57	3.71e-01	soluble	-2.76	2.38e-01	Soluble	-2.48	2.38e-01	soluble
Camphene	-3.34	6.18e-02	soluble	-3.93	1.60e-02	Soluble	-2.48	4.55e-01	soluble
Glycitein	-3.57	7.63e-02	Soluble	-3.76	4.93e-02	Soluble	-5.10	2.25e-03	Moderately soluble
Phloretin	-3.38	1.15e-01	soluble	-4.34	1.26e-02	Moderately soluble	-3.37	1.16e-01	soluble
Fisetin	-3.35	1.27e-01	soluble	-3.93	3.37e-02	Soluble	-3.82	4.29e-02	soluble
Genistin	-3.18	2.85e-01	soluble	-4.01	4.18e-02	Moderately soluble	-2.69	8.77e-01	soluble
Apigenin	-3.94	3.07e-02	soluble	-4.59	6.88e-03	Moderately soluble	-4.40	1.07e-02	Moderately soluble

Table 3.8 (Cont'd): Water Solubility

Compounds	Log S (ESOL)	Solubility (mg/mL)	Class	Log S (Ali)	Solubility (mg/mL)	Class	Log S (SILICOS-IT)	Solubility (mg/mL)	Class
Baicalein	-4.03	2.51e-02	Moderately soluble	-4.74	4.93e-03	Moderately soluble	-4.40	1.07e-02	Moderately soluble
Daidzein	-3.53	7.51e-02	Soluble	-3.60	6.41e-02	Soluble	-4.98	2.64e-03	Moderately soluble
Quercetin	-3.16	2.11e-01	Soluble	-3.91	3.74e-02	Soluble	-3.24	1.73e-01	Soluble
Furanosylboratediester	0.48	5.77e+02	Highly soluble	0.66	8.79e+02	Highly soluble	1.91	1.58e+04	Soluble

Solubility class (Log S scale): Insoluble <-10 < Poorly <-6 < Moderately <-4 < Soluble < -2 Very < Highly.

Results of the conformation of the studied terpenes and flavonoids to other pharmacokinetic principles such as ghose filter, veber filter, egan filter and muegge filter are shown in Table 3.9. Besides phytol that disobeyed the Veber and Egan rule, all the terpenes obeyed the rules in addition to Lipinski's although they disobeyed the Ghose and Muegge rules. The flavonoids, on the other hand, obeyed all the rules except for genistin which violated the Veber, Egan and Muegge rules respectively. Overall, the bioavailability scores of both terpenes and flavonoids were found to be 0.55 F (Table 3.9).

Table 3.9: Conformation of studied terpenes and flavonoids to other pharmacokinetic rules

Compounds	Lipinski	Ghose	Veber	Egan	Muegge	Bioavailability score
3,7,11,15-Tetramethyl-2-hexadecen-1-OL(Phytol)	Yes; 1 violation: MLOGP>4.15	No; 1 violation: WLOGP>5.6	No; 1 violation: Rotors>10	No; 1 violation: WLOGP>5.88	No; 2 violations: XLOGP3>5, Heteroatoms<2	0.55
Beta-pinene	Yes; 1 violation: MLOGP>4.15	No; 1 violation: MW<160	Yes	Yes	No; 2 violations: MW<200, Heteroatoms<2	0.55
Alpha-pinene	Yes; 1 violation: MLOGP>4.15	No; 1 violation: MW<160	Yes	Yes	No; 2 violations: MW<200, Heteroatoms<2	0.55
P-cymene	Yes; 1 violation: MLOGP>4.15	No; 1 violation: MW<160	Yes	Yes	No; 2 violations: MW<200, Heteroatoms<2	0.55
Alpha-terpinene	Yes; 0 violation	No; 1 violation: MW<160	Yes	Yes	No; 2 violations: MW<200, Heteroatoms<2	0.55
Isoterpinolene	Yes; 0 violation	No; 1 violation: MW<160	Yes	Yes	No; 2 violations: MW<200, Heteroatoms<2	0.55
3-Carene	Yes; 1 violation: MLOGP>4.15	No; 1 violation: MW<160	Yes	Yes	No; 2 violations: MW<200, Heteroatoms<2	0.55

Table 3.9 (Cont'd): Conformation of studied terpenes and flavonoids to other pharmacokinetic rules

Compounds	Lipinski	Ghose	Veber	Egan	Muegge	Bioavailability score
Sabinene	Yes; 1 violation: MLOGP>4.15	No; 1 violation: MW<160	Yes	Yes	No; 2 violations: MW<200, Heteroatoms <2	0.55
Camphene	Yes; 1 violation: MLOGP>4.15	No; 1 violation: MW<160	Yes	Yes	No; 2 violations: MW<200, Heteroatoms <2	0.55
Glycitein	Yes; 0 violation	Yes	Yes	Yes	Yes	0.55
Phloretin	Yes; 0 violation	Yes	Yes	Yes	Yes	0.55
Fisetin	Yes; 0 violation	Yes	Yes	Yes	Yes	0.55
Genistin	Yes; 1 violation: NHorOH>5	Yes	No; 1 violation: TPSA>140	No; 1 violation: TPSA>131.6	No; 2 violations: TPSA>150, H-don>5	0.55
Apigenin	Yes; 0 violation	Yes	Yes	Yes	Yes	0.55
Baicalein	Yes; 0 violation	Yes	Yes	Yes	Yes	0.55
Daidzein	Yes; 0 violation	Yes	Yes	Yes	Yes	0.55
Quercetin	Yes; 0 violation	Yes	Yes	Yes	Yes	0.55
Furanosylboratediester	Yes; 0 violation	No; 2 violations: WLOGP<-0.4, MR<40	Yes	Yes	No; 2 violations: MW<200, XLOGP3<-2	0.56

Lipinski: Hydrogen bond donors ≤ 5, hydrogen bond acceptors ≤ 10, molecular weight ≤ 500, Log P (CLog P) ≤ 5, No of rotatable bonds ≤ 10. **Ghose filter**: 160 ≤ MW ≤ 480; -0.4 ≤WLOGP≤ 5.6, 40 ≤ MR ≤ 130; 20 ≤ atoms ≤ 70. **Veber**: Rotatable bonds ≤ 10; TPSA**:** ≤ 140. **Egan:** WLOGP ≤ 5.88. TPSA**:** ≤ 131.6. **Muegge:** 200 ≤ MW ≤ 600; -2 ≤ XLOGP ≤ 5; TPSA**:** ≤ 150, Num. rings ≤ 7; Num. carbon > 4; Num. heteroatoms > 1; Num. rotatable bonds ≤ 15; H-bond acc. ≤ 10; H-bond don. ≤ 5.

3.4 DISCUSSION

K. pneumoniae was studied due to its ability to become progressively resistant to almost all classes of conventional antibiotics (Adeosun et al., 2022). For example, in a study conducted by Nirwati et al., (2019), *K. pneumoniae* clinical isolates revealed resistance to various antibiotics including ampicillin (97.90%), cefazolin (65.2%), ceftriaxone (56.64%), cefepime (56.34%), trimethoprim-sulfamethoxazole (53.13%), tobramycin (46.15%) among others, showing a 54.49% overall proportion of multidrug-resistant *K. pneumoniae* isolates. In another study by Ballen et al., (2021), 40.16% of *K. pneumoniae* isolated from clinical sources were identified as multi-drug resistant. As such, the highly resistant and virulent nature of this pathogen poses threat to global health, hence, the need to explore the potentials of bioactive compounds as alternative treatment remedies. This study explored new targets within the bacterial cell that could be modulated by bioactive compounds as potential therapeutic targets and inhibitors to attenuate mild to severe infections (Gorlenko et al., 2020). Since terpenes, commonly found in essential oils and flavonoids possess antimicrobial actions of bacteriostatic and bactericidal effects (Mahizan et al., 2019), they were explored to inhibit virulence factors in *K. pneumoniae*, which is often modulated by SdiA protein. Due to the unavailability of the crystal structure of the SdiA protein from *K. pneumoniae* in the structural databases, its 3D model was built using the Swiss model workspace and the quality of the built model was validated. Currently, *in silico* pharmacology paradigm is being explored as a result of its wide range of prospects which speeds up the identification of new targets and eventually result in the development of drugs with anticipated biological activity for these novel targets (Ekins et al., 2007).

Virtual screening strategies such as MD and MDS are often employed for the prediction of the preferred binding orientation of ligands into receptors (Ramírez & Caballero, 2018). These approaches provide quick insights into the specific targets and compounds that are likely to move from the laboratory to the clinic and eventually to the market as rapidly as possible given the amount of information that needs to be processed for drug discovery (Swaan & Ekins, 2005).

MD is a technique in drug discovery which is useful in estimating the binding and fitting of two molecular structures. In addition, it reveals the molecular recognition pattern between the protein and ligands (Naqvi et al., 2019), hence, it was employed in this

study. Findings from this docking studies presented insightful interactions between the test phytocompounds and the SdiA receptor protein, implicated in the expression of virulence in *K. pneumoniae*. Ligand interactions were shown in Figures 3.4 and 3.5. Docking results confirmed nine (9) terpenes and eight (8) flavonoids as competitive inhibitors of virulence, vital in the development of therapeutic agents for the management of *K. pneumoniae* infections. Of the studied chemical groups, phytol (-9.205 kcal/mol) and glycitein (-9.752 kcal/mol) had the best docking scores, displaying the highest binding affinity.

The improved binding affinities can be attributed to the test compounds' ability to fit well in the receptor's pocket (Baloyi et al., 2021). Good docking scores observed for these compounds suggest that they are better QSIs which can be characterized by the presence of functional groups. The presence of methoxy and hydroxyl functional groups in the glycitein structure could have contributed to its good binding property, thereby making it a better QSI as per the criteria stated by Qin et al. (2020). The hydroxyl group is also found in phytol which consists of an oxygen atom covalently linked to a hydrogen atom. The link between oxygen and hydrogen is extremely polar due to the strong electronegativity of the oxygen atom (Swaan & Ekins, 2005). Resulting from this, water molecules are drawn to the hydroxyl group, generating hydrogen bonds which in turn improves the binding affinity (Chen et al., 2016). Oyewole et al. (2020) documented that "the higher the binding affinity as observed for phytol and genistin in this study, the more improved the inhibitory effect of the compound". This presents them as the most potent of all the terpene and flavonoid compounds considered in this study.

Good docking scores were also reported for apigenin (-8.222kcal/mol), quercetin (-9.290 kcal/mol) and phloretin (-9.722kcal/mol) in this study. Congruent to the findings of this study, Vikram et al. (2010) have previously reported apigenin and quercetin as effective antagonists of QS, inhibiting virulence in other GNB such as *Vibrio harveyi* and *Escherichia coli* 0157:H7. The good docking scores observed for the tested terpenes and flavonoids imply that they have inhibitory actions that are linked to SdiA binding mechanisms. This also suggests that they may be physiologically active as well as highly efficient molecules, as they provide energy to promote the protein-ligand binding interaction (Gupta & Bajaj, 2018). The direct binding of virulence-associated proteins as observed in this study can be added as a potent therapeutic target of flavonoids, in

addition to the antibacterial mechanism of action, as also noted by Donadio et al. (2021).

Furthermore, the hydrogen bond interactions observed in some compounds like phytol against the SdiA protein were comparable to furanosyl borate diester (A1-2 molecule) which formed hydrogen bonds with Val57, Arg111, Leu115, and Arg116. Glycitein formed hydrogen bonds with Ser43, phloretin with PG4 302 and H_2O, fisetin with Asp80 and Ser13, genistin with Asp97 and Trp 95, baicalein with Asp97, daidzein with Ser43 and quercetin with Trp57. According to Ahmed et al. (2020), the hydrogen bond between a protein and a ligand plays a significant role in their recognition and is often useful in investigating the stability, directionality, and specificity of polar interactions.
Another vital virtual screening tool employed in this study is MDS. MDS helps to study the atomic movements of biological systems and to understand molecular interaction mechanisms (Naqvi et al., 2019). The RMSD and RMSF are the two most widely used metrics of structural fluctuations in MDS which provides insight into inter-atomic motions and stability of the protein-ligand complex (Kuzmanic & Zagrovic, 2010).

RMSD is important for analysing time-dependent structural motions as well as determining the structure's inability to drift away from the initial coordinates over time in simulations (Martínez, 2015). This study ascertained the overall conformational stability of SdiA protein upon binding to the test compounds by monitoring the RMSD, where the RMSD of the bound systems were measured relative to the unbound SdiA structure. Results revealed varying stability of the compounds with RMSD scores ranging between 1.48 Å to 2.58 Å for terpenes and 1.44 Å to 2.50 Å for flavonoids (Table 3.5). Overall, all the bound compounds (terpenes and flavonoids) stabilized the SdiA conformation as evidenced by the estimated RMSD averages in the range of 1.44 Å to 2.58 Å for all bound systems in contrast to the unbound SdiA system after the 100ns simulation. Notably, sabinene and genistin had the lowest RMSD averages of 1.48Å and 1.44Å respectively for the terpenes and flavonoids, correlating to the compounds that enacted the most structural stability. In most structural studies, higher average RMSD correlates to a less stable structural conformation and vice versa as employed in various studies (Salifu et al., 2019; Abdullahi et al., 2018). According to Ramírez & Caballero (2018), RMSD < 2.0 Å corresponds to good docking solutions. Moreover, RMSD scores between 2.0 and 3.0 Å may have deviated from the position of the reference, but they

keep the desired orientation. Corroborative to the set rules by Qin et al. (2020), none of the studied terpenes and flavonoids had RMSD score >3.0 Å.

Furthermore, the displacement of a single atom, or a group of atoms, relative to the reference structure is measured by RMSF, which is averaged across the number of atoms (Farmer et al., 2017). RMSF was calculated in this study to elucidate the flexibility and motion of individual residues in the protein.

The average deviation of the systems was monitored by the RMSF from a reference point over 100 ns. Findings revealed RMSF scores ranging from 1.08 Å to 3.74 Å for the studied terpenes and flavonoids (Table 3.5). Overall, quercetin revealed the least RMSF score (1.08 Å), which corresponds with the RMSD to depict high stability. The good RMSF score observed may imply that the catalytic machinery in the SdiA active site was not altered by its binding (Martínez, 2015).

The assessment of the flexibility of the studied compounds indicates a diverse activity associated with the binding of each compound. This is in reference to some of the compounds (alpha-pinene, alpha-terpinene, 3-carene, phytol, sabinene, apigenin, biacelein, genistin, phloretin and quercetin) exhibiting less flexibility on the SdiA structure while other compounds such as beta-pinene, camphene, isoterpinene, p-cymene, diadzein, fisetin and glycitein proved to be highly flexible relative to the unbound SdiA state. The substantial difference in structural flexibility of the bound terpenes and flavonoids in contrast to the unbound SdiA could play a crucial role in the biological activity of the protein (Salifu et al., 2019), as the binding of the compounds may result in a more flexible or more rigid SdiA structure which directly impacts the native state of the protein.

The molecular mechanics/poisson boltzmann surface area (MM/PBSA) and the molecular mechanics/generalized-born surface area (MM/GBSA) combine molecular mechanics computations with continuum solvation models to derive binding free energies for macromolecules (Hou et al., 2011). They serve as powerful tools in drug design where a correct ranking of inhibitors is often emphasized (Hou et al., 2011). Hence, this approach, which represents a higher-level scoring theory than docking was used to estimate the aggregate binding free energy of the compound complexes as presented in Table 3.6. Genistin revealed the highest binding free energy score of -68.1393 kcal/mol for flavonoids while phytol revealed -44.2625 kcal/mol as the highest

for terpenes. These calculated energies provide comprehensive molecular-level evidence that could be useful to design a drug by creating better ligand binding.

In addition, certain parameters of the selected terpenes and flavonoids were predicted for their physicochemical properties, lipophilicity, water-solubility, pharmacokinetics, drug-likeness and medicinal chemistry. In this study, the drug-likeness properties were characterized to determine the pharmacokinetics of the test compounds, by testing for favorable ADME (absorption, distribution, metabolism, and excretion) properties. A major criterion employed for the characterization was hinged on the Lipinski rule of five. This rule predicts the poor absorption or permeation of a drug when there are more than 5 hydrogen bond donors, 10 hydrogen bond acceptors, molecular weight larger than 500, and an estimated Log P (CLog P) value greater than 5 (Benet et al., 2016). The results of this assessment revealed that the test compounds obeyed the rules, with glycitein, phloretin, quercetin, fisetin, apigenin, alpha-terpinene, isoterpinolene, biacalein and diadzein having no violation. However, phytol, genistin, beta-pinene, alpha-pinene, p-cymene, 3-carene, sabinene and camphene only showed one violation each, which is considered acceptable since the violation does not exceed one, a submission opined by Pathania & Singh (2021). This result suggests the potential drug-likeness features of the compounds. Drug likeness can often be used as a proxy for oral bioavailability especially because bioavailability is amongst the most prominent criteria of a drug (Bickerton et al., 2012). Heavy atoms were also observed in the test compounds. The presence of heavy atoms in compounds is an important chemical structure-related character linked to their physiochemical properties and drug-likeness properties (Mao et al., 2016). Other pharmacokinetic principles such as ghose filter, veber filter, egan filter and muegge filter also supported the drug-likeness characteristics of the test compounds as shown in Table 3.9. These principles are accepted by researchers as one of the key evaluation parameters for the drug-likeness of any virtually screened molecule (Pathania & Singh, 2021).

Another interesting finding from this study is that all the terpenes studied but phytol can permeate the blood-brain barrier (BBB) (Table 3.7), suggesting their potential to permeate the central nervous system (CNS) which is indicative of therapeutic ability. This corroborates the submission of Agatonovic-Kustrin et al. (2019) who opined that many terpenes could cross the BBB. From the flavonoids tested, daidzein revealed the ability to permeate the BBB, possibly due to its broad therapeutic activities which

include cardioprotective, anticancer, anti-allergic, antidiabetic, anti-inflammatory and anti-oxidative properties as reported by Kwiecień et al. (2020). Stout et al. (2013) corroborate that daidzein can cross the BBB in mice, and improve cognition, reduce anxiety, and aggression, and increase locomotory movement.

In medicinal chemistry, the Brenk and pan assay interference compounds (PAINS) structural alerts predict unstable, reactive, toxic fragments present in the structure (Sultan et al., 2020). All active compounds, except fisetin, baicalein and quercetin had zero alerts in PAINS descriptors (Table 3.7), providing added promising indicators as drug candidates. Physicochemical characteristics are critical in the efficiency, care, and absorption of compounds (Meanwell, 2011).

Thus far, the *in-silico* results demonstrate phytol, genistin and glycitein as the best compounds bound to the modelled SdiA receptor protein, revealed high binding energies, demonstrated stability and less fluctuation in the atomic and inter-atomic interactions in the protein-ligand system, showed drug-like properties as well as moderate solubility in water. The ability of the studied compounds to inhibit virulence activities in *K. pneumoniae* has been elucidated *in vitro.* Results of the *in vitro* studies in the next chapter validated the *in-silico* findings, proving the compounds to be promising in the development of drugs against *K. pneumoniae* infections.

3.5 CONCLUSION

The continuous emergence of MDR *K. pneumoniae* necessitates the search to explore natural products of plant origin as pivotal in the management of its infections. This study validated p-cymene, alpha-pinene, isoterpinolene, alpha-terpinene, phytol, 3-carene, beta-pinene, sabinene, camphene, fisetin, genistin, diadzein, quercetin, glycitein, phloretin, apigenin and biacalein (terpenes and flavonoids) bound SdiA's autoinducer binding site forming critical interactions with the binding site's key residues. The MDS established the inhibitory performance and interactions revealing high free binding energies for genistin (flavonoid) and phytol (terpene). The drug-likeness prediction of the selected compounds validated their drug potential conferring them as promising QSI drugs for *K. pneumoniae.* Therefore, the study further suggests the exploration of terpenes and flavonoids as alternative QSIs, other than the known antibacterial target sites.

Having established that some of the tested terpenes and flavonoids revealed good binding affinities and high binding energies when bound to the transcriptional SdiA receptor which modulates biofilm formation and other virulence factors in *K. pneumoniae*, the next chapter focused on the *in-vitro* evaluation of the inhibitory potential of selected promising phytochemical compounds on biofilm-associated virulence factors in *K. pneumoniae*, as well as authenticating their antibiofilm activity.

References

Abdullahi, M., Olotu, F. A., & Soliman, M. E. (2018). Allosteric inhibition abrogates dysregulated LFA-1 activation: structural insight into mechanisms of diminished immunologic disease. *Computational Biology and Chemistry*, *73*, 49–56. https://doi.org/10.1016/j.compbiolchem.2018.02.002

Adeosun, I. J., Baloyi, I. T., & Cosa, S. (2022). Anti-biofilm and associated anti-virulence activities of selected phytochemical compounds against *Klebsiella pneumoniae. Plants*, *11*(11), 1–20. https://doi.org/10.3390/plants11111429

Agatonovic-Kustrin, S., Kustrin, E., & Morton, D. W. (2019). Essential oils and functional herbs for healthy aging. *Neural Regeneration Research*, *14*(3), 441–445. https://doi.org/10.4103/1673-5374.245467

Ahmed, M. Z., Muteeb, G., Khan, S., Alqahtani, A. S., Somvanshi, P., Alqahtani, M. S., Ameta, K. L., & Haque, S. (2020). Identifying novel inhibitor of quorum sensing transcriptional regulator (SdiA) of *Klebsiella pneumoniae* through modelling, docking and molecular dynamics simulation. *Journal of Biomolecular Structure and Dynamics*, *0*(0), 1–11. https://doi.org/10.1080/07391102.2020.1767209

Akinyede, K. A., Ekpo, O. E., & Oguntibeju, O. O. (2020). Ethnopharmacology, therapeutic properties and nutritional potentials of *Carpobrotus edulis*: A comprehensive review. *Scientia Pharmaceutica*, *88*(3), 1–16. https://doi.org/10.3390/scipharm88030039

Allouche, A. (2012). Software News and Updates Gabedit - A Graphical User Interface for Computational Chemistry Softwares. *Journal of Computational Chemistry*, *32*, 174–182. https://doi.org/10.1002/jcc

Almeida, F. A. de, Pinto, U. M., & Vanetti, M. C. D. (2016). Novel insights from molecular docking of SdiA from *Salmonella enteritidis* and *Escherichia coli* with quorum sensing and quorum quenching molecules. *Microbial Pathogenesis*, *99*, 178–190. https://doi.org/10.1016/j.micpath.2016.08.024

Arnold, K., Bordoli, L., Kopp, J., & Schwede, T. (2006). The SWISS-MODEL workspace: A web-based environment for protein structure homology modelling. *Bioinformatics*, *22*(2), 195–201. https://doi.org/10.1093/bioinformatics/bti770

Ballén, V., Gabasa, Y., Ratia, C., Ortega, R., Tejero, M., & Soto, S. (2021). Antibiotic resistance and virulence profiles of *Klebsiella pneumoniae* strains isolated from different clinical sources. *Frontiers in Cellular and Infection Microbiology*, *11*(9), 1–11. https://doi.org/10.3389/fcimb.2021.738223

Baloyi, I. T., Cosa, S., Combrinck, S., Leonard, C. M., & Viljoen, A. M. (2019). Anti-quorum sensing and antimicrobial activities of South African medicinal plants against uropathogens. *South African Journal of Botany*, *122*, 484–491. https://doi.org/10.1016/j.sajb.2019.01.010

Baloyi, I. T., Adeosun, I. J., Yusuf, A. A., & Cosa, S. (2021). *In silico* and *in vitro* screening of antipathogenic properties of *Melianthus comosus* (Vahl) against *Pseudomonas aeruginosa*. *Antibiotics*, *10*(6), 1–23. https://doi.org/10.3390/antibiotics10060679

Benet, L. Z., Hosey, C. M., Ursu, O., & Oprea, T. I. (2016). BDDCS, the Rule of 5 and drugability. *Advanced Drug Delivery Reviews*, *101*, 89–98. https://doi.org/10.1016/j.addr.2016.05.007

Bergman, M. E., Davis, B., & Phillips, M. A. (2019). Medicinal useful plant terpenoids: biosynthesis, occurrence, and mechanism of action. *Molecules, 24*(21), 1–23.

Bickerton, G. R., Paolini, G. V, Besnard, J., Muresan, S., & Hopkins, A. L. (2012). Quantifying the chemical beauty of drugs Europe PMC Funders Group. *Nature Chemistry*, *4*(2), 90–98. https://doi.org/10.1038/nchem.1243

Cadavid, E., Robledo, S. M., Quiñones, W., & Echeverri, F. (2018). Induction of biofilm formation in *Klebsiella pneumoniae* ATCC 13884 by several drugs: The possible role of quorum sensing modulation. *Antibiotics*, *7*(4), 1–14. https://doi.org/10.3390/antibiotics7040103

Chen, D., Oezguen, N., Urvil, P., Ferguson, C., Dann, S. M., & Savidge, T. C. (2016). Regulation of protein-ligand binding affinity by hydrogen bond pairing. *Science Advances*, *2*(3), 1–16. https://doi.org/10.1126/sciadv.1501240

Cheng, C., Yan, X., Liu, B., Jiang, T., Zhou, Z., Zhang, D., Wang, H., Chen, D., Li, C., Fang, T., Agriculture, F., & Province, F. (2022). SdiA, a quorum-sensing transcriptional regulator, enhanced the drug resistance of *Cronobacter sakazakii* and suppressed its motility, adhesion, and biofilm formation. *Frontiers in Microbiology,* 13, 1–14.

Cosa, S., Chaudhary, S. K., Chen, W., Combrinck, S., & Viljoen, A. (2019). Exploring common culinary herbs and spices as potential anti-quorum sensing agents. *Nutrients*, *11*(4), 1–17. https://doi.org/10.3390/nu11040739

Cosa, S., Rakoma, J. R., Yusuf, A. A., & Tshikalange, T. E. (2020). *Calpurnia aurea* (Aiton) Benth extracts reduce quorum sensing controlled virulence factors in *Pseudomonas aeruginosa. Molecules*, *25*(10), 1–21. https://doi.org/10.3390/molecules25102283

Cox-Georgian, D., Ramadoss, N., Dona, C., & Basu, C. (2019). Therapeutic and medicinal uses of terpenes. *Medicinal Plants: From Farm to Pharmacy*, 333–359. https://doi.org/10.1007/978-3-030-31269-5_15

Daina, A., Michielin, O., & Zoete, V. (2017). SwissADME: A free web tool to evaluate pharmacokinetics, drug-likeness and medicinal chemistry friendliness of small molecules. *Scientific Reports*, *7*, 1–13. https://doi.org/10.1038/srep42717

Donadio, G., Mensitieri, F., Santoro, V., Parisi, V., Bellone, M. L., De Tommasi, N., Izzo, V., & Piaz, F. D. (2021). Interactions with microbial proteins driving the antibacterial activity of flavonoids. *Pharmaceutics*, *13*(5), 1–23. https://doi.org/10.3390/pharmaceutics13050660

Ekins, S., Mestres, J., & Testa, B. (2007). *In silico* pharmacology for drug discovery: Applications to targets and beyond. *British Journal of Pharmacology*, *152*(1), 21–37. https://doi.org/10.1038/sj.bjp.0707306

Farmer, J., Kanwal, F., Nikulsin, N., Tsilimigras, M. C. B., & Jacobs, D. J. (2017). Statistical measures to quantify similarity between molecular dynamics simulation trajectories. *Entropy*, *19*(12), 1–17. https://doi.org/10.3390/e19120646

Gonnet, P. (2007). P-SHAKE: A quadratically convergent SHAKE in O (n2). *Journal of Computational Physics*, *220*(2), 740–750. https://doi.org/10.1016/j.jcp.2006.05.032

Gopu, V., & Shetty, P. H. (2016). Cyanidin inhibits quorum signalling pathway of a food borne opportunistic pathogen. *Journal of Food Science and Technology*, *53*(2), 968–976. https://doi.org/10.1007/s13197-015-2031-9

Gorlenko, C. L., Kiselev, H. Y., Budanova, E. V., Zamyatnin, A. A., & Ikryannikova, L. N. (2020). Plant secondary metabolites in the battle of drugs and drug-resistant bacteria: New heroes or worse clones of antibiotics? *Antibiotics*, *9*(4), 1–19. https://doi.org/10.3390/antibiotics9040170

Gupta, S., & Bajaj, A. V. (2018). Extra precision glide docking, free energy calculation and molecular dynamics studies of 1,2-diarylethane derivatives as potent urease inhibitors. *Journal of Molecular Modeling*, *24*(9), 1–27. https://doi.org/10.1007/s00894-018-3787-4

Homeyer, N., & Gohlke, H. (2012). Free energy calculations by the molecular mechanics poisson-boltzmann surface area method. *Molecular Informatics*, *31*(2), 114–122. https://doi.org/10.1002/minf.201100135

Hou, T., Wang, J., Li, Y., & Wang, W. (2011). Assessing the performance of the MM/PBSA and MM/GBSA methods. 1. The accuracy of binding free energy calculations based on molecular dynamics simulations. *Journal of Chemical Information and Modeling*, *51*(1), 69–82. https://doi.org/10.1021/ci100275a

Huggins, D. J., Venkitaraman, A. R., & Spring, D. R. (2011). Rational methods for the selection of diverse screening compounds. *ACS Chemical Biology*, *6*(3), 208–217. https://doi.org/10.1021/cb100420r

Koh, C., Sam, C., Yin, W., Tan, L. Y., Krishnan, T., Chong, Y. M., & Chan, K. (2013). Plant-derived natural products as sources of anti-quorum sensing compounds. *Sensors, 13*(5) 6217–6228. https://doi.org/10.3390/s130506217

Kusumaningrum, S., Budianto, E., Kosela, S., Sumaryono, W., & Juniarti, F. (2014). The molecular docking of 1,4-naphthoquinone derivatives as inhibitors of Polo-like kinase 1 using molegro virtual docker. *Journal of Applied Pharmaceutical Science*, *4*(11), 47–53. https://doi.org/10.7324/JAPS.2014.4119

Kuzmanic, A., & Zagrovic, B. (2010). Determination of ensemble-average pairwise root mean-square deviation from experimental B-factors. *Biophysical Journal*, *98*(5), 861–871. https://doi.org/10.1016/j.bpj.2009.11.011

Kwiecień, A., Ruda-Kucerova, J., Kamiński, K., Babinska, Z., Popiołek, I., Szczubiałka, K., Nowakowska, M., & Walczak, M. (2020). Improved pharmacokinetics and tissue uptake of complexed daidzein in rats. *Pharmaceutics*, *12*(2), 1–12. https://doi.org/10.3390/pharmaceutics12020162

Laskowski, R. A., Jabłońska, J., Pravda, L., Vařeková, R. S., & Thornton, J. M. (2018). PDBsum: Structural summaries of PDB entries. *Protein Science*, *27*(1), 129–134. https://doi.org/10.1002/pro.3289

Lee, T. S., Cerutti, D. S., Mermelstein, D., Lin, C., Legrand, S., Giese, T. J., Roitberg, A., Case, D. A., Walker, R. C., & York, D. M. (2018). GPU-accelerated molecular dynamics and free energy methods in amber18: performance enhancements and new features. *Journal of Chemical Information and Modeling*, *58*(10), 2043–2050. https://doi.org/10.1021/acs.jcim.8b00462

Madhavi, G., Adzhigirey, M., Day, T., Annabhimoju, R., & Sherman, W. (2013). Protein and ligand preparation: parameters, protocols, and influence on virtual screening enrichments. *Journal of Computer-Aided Molecular Design*, *27*(3), 221–234. https://doi.org/10.1007/s10822-013-9644-8

Mahizan, N. A., Yang, S., Moo, C.-L., & Song, A. A.-L. (2019). Terpene derivatives as a potential agent against antimicrobial resistance. *Molecules*, *24*(2631), 1–21.

Maier, J. A., Martinez, C., Kasavajhala, K., Wickstrom, L., Hauser, K. E., & Simmerling, C. (2015). ff14SB: Improving the accuracy of protein side chain and backbone parameters from ff99SB. *Journal of Chemical Theory and Computation*, *11*(8), 3696–3713. https://doi.org/10.1021/acs.jctc.5b00255

Mao, F., Ni, W., Xu, X., Wang, H., Wang, J., Ji, M., & Li, J. (2016). Chemical structure-related drug-like criteria of global approved drugs. *Molecules*, *21*(1), 1–18. https://doi.org/10.3390/molecules21010075

Maroyi, A. (2017). Review of ethnomedicinal uses, phytochemistry and pharmacological properties of *Euclea natalensis* A. DC. *Molecules*, *22*(12), 1–34. https://doi.org/10.3390/molecules22122128

Martínez, L. (2015). Automatic identification of mobile and rigid substructures in molecular dynamics simulations and fractional structural fluctuation analysis. *PLoS ONE*, *10*(3), 1–10. https://doi.org/10.1371/journal.pone.0119264

Meanwell, N. A. (2011). Improving drug candidates by design: A focus on physicochemical properties as a means of improving compound disposition and safety. *Chemical Research in Toxicology*, *24*(9), 1420–1456. https://doi.org/10.1021/tx200211v

Naqvi, A. A. T., Mohammad, T., Hasan, G. M., & Hassan, M. I. (2019). Advancements in docking and molecular dynamics simulations towards ligand-receptor interactions and structure-function relationships. *Current Topics in Medicinal Chemistry*, *18*(20), 1755–1768. https://doi.org/10.2174/1568026618666181025114157

Nikitin, S. (2014). Leap Gradient Algorithm. *ArXiv preprint,* 1–24. http://arxiv.org/abs/1405.5548

Nirwati, H., Sinanjung, K., Fahrunissa, F., Wijaya, F., Napitupulu, S., Hati, V. P., Hakim, M. S., Meliala, A., Aman, A. T., & Nuryastuti, T. (2019). Biofilm formation and antibiotic resistance of *Klebsiella pneumoniae* isolated from clinical samples in a tertiary care hospital, Klaten, Indonesia. *BMC Proceedings*, *13*(11), 1–8. https://doi.org/10.1186/s12919-019-0176-7

Oleg, T., & Arthur, O. (2010). Software news and updates gabedit — a graphical user interface for computational chemistry softwares. *Journal of Computational Chemistry*, *32*, 174–182. https://doi.org/10.1002/jcc

Oyewole, R. O., Oyebamiji, A. K., & Semire, B. (2020). Theoretical calculations of molecular descriptors for anticancer activities of 1, 2, 3-triazole-pyrimidine derivatives against gastric cancer cell line (MGC-803): DFT, QSAR and docking approaches. *Heliyon*, *6*(5), 1–13. https://doi.org/10.1016/j.heliyon.2020.e03926

Pacheco, T., Gomes, A. É. I., Siqueira, N. M. G., Assoni, L., Darrieux, M., Venter, H., & Ferraz, L. F. C. (2021). SdiA, a quorum-sensing regulator, suppresses fimbriae expression, biofilm formation, and quorum-sensing signalling molecules production in *Klebsiella pneumoniae*. *Frontiers in Microbiology*, *12*, 1–15. https://doi.org/10.3389/fmicb.2021.597735

Paczkowski, J. E., Mukherjee, S., McCready, A. R., Cong, J. P., Aquino, C. J., Kim, H., Henke, B. R., Smith, C. D., & Bassler, B. L. (2017). Flavonoids suppress *Pseudomonas aeruginosa* virulence through allosteric inhibition of quorum-sensing receptors. *Journal of Biological Chemistry*, *292*(10), 4064–4076. https://doi.org/10.1074/jbc.M116.770552

Panche, A. N., Diwan, A. D., & Chandra, S. R. (2016). Flavonoids: an overview. *Journal of Nutritional Science*, *5*, 1–15. https://doi.org/10.1017/jns.2016.41

Pathania, S., & Singh, P. K. (2021). Analyzing FDA-approved drugs for compliance of pharmacokinetic principles: should there be a critical screening parameter in drug designing protocols? *Expert*

Opinion on Drug Metabolism and Toxicology, *17*(4), 351–354. https://doi.org/10.1080/17425255.2021.1865309

Pettersen, E. F., Goddard, T. D., Huang, C. C., Couch, G. S., Greenblatt, D. M., Meng, E. C., & Ferrin, T. E. (2004). UCSF Chimera - a visualization system for exploratory research and analysis. *Journal of Computational Chemistry*, *25*(13), 1605–1612. https://doi.org/10.1002/jcc.20084

Pradeep, C., Lalitha, S., Rajesh, S. V., & Shanmugam, G. (2018). Comparative modelling and molecular docking studies of quorum sensing transcriptional regulating factor SdiA from *Klebsiella pneumoniae*. *International Journal of Current Research in Science, Engineering & Technology*, *1*(1), 1–8. https://doi.org/10.30967/ijcrset.1.1.2018.9-16

Qin, X., Vila-Sanjurjo, C., Singh, R., Philipp, B., & Goycoolea, F. M. (2020). Screening of bacterial quorum sensing inhibitors in a *Vibrio fischeri* LuxR-based synthetic fluorescent *E. coli* biosensor. *Pharmaceuticals*, *13*(9), 1–25. https://doi.org/10.3390/ph13090263

Ramírez, D., & Caballero, J. (2018). Is it reliable to take the molecular docking top scoring position as the best solution without considering available structural data? *Molecules*, *23*(5), 1–17. https://doi.org/10.3390/molecules23051038

Roe, D. R., & Cheatham, T. E. (2013). PTRAJ and CPPTRAJ: Software for processing and analysis of molecular dynamics trajectory data. *Journal of Chemical Theory and Computation*, *9*(7), 3084–3095. https://doi.org/10.1021/ct400341p

Salifu, E. Y., Agoni, C., Olotu, F. A., Dokurugu, Y. M., & Soliman, M. E. S. (2019). Halting ionic shuttle to disrupt the synthetic machinery—structural and molecular insights into the inhibitory roles of bedaquiline towards *Mycobacterium tuberculosis* ATP synthase in the treatment of tuberculosis. *Journal of Cellular Biochemistry*, *120*(9), 16108–16119. https://doi.org/10.1002/jcb.28891

Seifert, E. (2014). OriginPro 9.1: Scientific data analysis and graphing software - software review. *Journal of Chemical Information and Modeling*, *54*(5), 1–15. https://doi.org/10.1021/ci500161d

Stout, J. M., Knapp, A. N., Banz, W. J., Wallace, D. G., & Cheatwood, J. L. (2013). Subcutaneous daidzein administration enhances recovery of skilled ladder rung walking performance following stroke in rats. *Behavioural Brain Research*, *256*, 428–431. https://doi.org/10.1016/j.bbr.2013.08.027

Sultan, M. A., Galil, M. S. A., Al-Qubati, M., Omar, M. M., & Barakat, A. (2020). Synthesis, molecular docking, drug-likeness analysis, and admet prediction of the chlorinated ethanoanthracene derivatives as possible antidepressant agents. *Applied Sciences,* *10*(21), 1–23. https://doi.org/10.3390/app10217727

Sundaresan, K., & Tharini, K. (2018). Identification of potent Cyanoacetylhydrazone derivatives as antidiabetic activity by *in silico* method. *Asian Journal of Pharmacy and Pharmacology*, *4*(6), 771–776. https://doi.org/10.31024/ajpp.2018.4.6.8

Swaan, P. W., & Ekins, S. (2005). Reengineering the pharmaceutical industry by crash-testing molecules. *Drug Discovery Today*, *10*(17), 1191–1200. https://doi.org/10.1016/S1359-6446(05)03557-9

Tavío, M. M., Aquili, V. D., Poveda, J. B., Antunes, N. T., Sánchez-Céspedes, J., & Vila, J. (2010). Quorum-sensing regulator sdiA and marA overexpression is involved in *in vitro*-selected multidrug resistance of *Escherichia coli. Journal of Antimicrobial Chemotherapy*, *65*(6), 1178–1186. https://doi.org/10.1093/jac/dkq112

Thomsen, R., & Christensen, M. H. (2006). MolDock: A new technique for high-accuracy molecular docking. *Journal of Medicinal Chemistry*, *49*(11), 3315–3321. https://doi.org/10.1021/jm051197e

Tian, W., Chen, C., Lei, X., Zhao, J., & Liang, J. (2018). CASTp 3.0: Computed atlas of surface topography of proteins. *Nucleic Acids Research*, *46*(1), 363–367. https://doi.org/10.1093/nar/gky473

Ventola, C. L. (2015). The Antibiotics. *Comprehensive Biochemistry*, *11*(4), 181–224. https://doi.org/10.1016/B978-1-4831-9711-1.50022-3

Vikram, A., Jayaprakasha, G. K., Jesudhasan, P. R., Pillai, S. D., & Patil, B. S. (2010). Suppression of bacterial cell-cell signalling, biofilm formation and type III secretion system by citrus flavonoids. *Journal of Applied Microbiology*, *109*(2), 515–527. https://doi.org/10.1111/j.1365-2672.2010.04677.x

Wang, J., Wolf, R. M., Caldwell, J. W., Kollman, P. A., & Case, D. A. (2004). Development and testing of a general Amber force field. *Journal of Computational Chemistry*, *25*(9), 1157–1174. https://doi.org/10.1002/jcc.20035

CHAPTER FOUR

ANTIBIOFILM AND ASSOCIATED ANTIVIRULENCE ACTIVITIES OF SELECTED PHYTOCHEMICAL COMPOUNDS AGAINST *K. PNEUMONIAE* STRAINS

Parts of this chapter have been published in Plants Journal**:** **Adeosun, I.J**., Baloyi, I.T and Cosa, S. (2022). Anti-biofilm and associated anti-virulence activities of selected phytochemical compounds against *Klebsiella pneumoniae. Plants.* 11, 1-20, 1429. *https://doi.org/10.3390/plants11111429*

4.1 INTRODUCTION

Biofilms are typical forms of bacterial communities that grow on living and non-living solid surfaces, which are often immersed in a self-producing matrix (Camele et al., 2019; Sánchez et al., 2016). Biofilm-associated cells can attach irreversibly to several surfaces and have become a critical worldwide health concern because of their ability to withstand antibiotics, human defense mechanisms, and other external stimuli, contributing to persistent chronic infections (De la Fuente-Núñez et al., 2013). The growth pattern of biofilm-forming bacteria allows for a noticeable decrease in their vulnerability to antimicrobial agents (Khan et al., 2021). For instance, in a study documented by Donlan (2021), biofilm-forming *Escherichia coli* necessitated more than 500 times the MIC of ampicillin to achieve a 3-log reduction. *Staphylococcus aureus* biofilms also required over 10 times the minimum bactericidal concentration (MBC) of vancomycin to provide a 3-log reduction. These further highlights biofilm formation as a survival strategy for most bacteria (Vestby et al., 2020).The adsorption of molecules to surfaces, bacterial adherence to the surface, the release of extracellular polymeric substances (EPS), microcolony formation, and biofilm maturation are all stages involved in biofilm formation (Divakar et al., 2019) which have been reported in several bacteria communities.

Klebsiella pneumoniae, a Gram-negative bacterium belonging to the family *Enterobacteriaceae*, has been reported to form biofilms that often adhere to surfaces such as lungs, livers, and central venous catheters which are implicated in prominent nosocomial and community-acquired infections (Mombeshora et al., 2021). The interest in studying CBR-*K. pneumoniae* (ATCC BAA-1705) was contingent on its ability to produce carbapenemases (KPC), which is a prevalent mechanism of resistance generated by *Klebsiella pneumoniae,* resulting in increased therapeutic dilemma and a global health threat linked to high rates of mortality (Yao et al., 2015). Carbapenem-resistant (CBR) *K. pneumoniae* is often characterized by its capacity to spread rapidly, having extensive antibiotic resistance phenotypes, yet only a few treatment options exist (Yao et al., 2015). Furthermore, ESBL-*K. pneumoniae* (ATCC 700603) was also studied because it produces extended-spectrum beta-lactamases (ESBL). According to Fils et al. (2021), the global spread of *K. pneumoniae*-producing extended-spectrum lactamase (ESBL-Kp) is a serious issue; hence, the World Health Organization (WHO)

categorized it alongside other ESBL-producing *Enterobacteriaceae* as a priority pathogen listed for the research and development of new antibiotics. Several antimicrobial treatments are critical in lowering the global burden imposed by this pathogen, but the evolution of antibiotic-resistant *K. pneumoniae* strains has become a serious public health concern (Adeosun et al., 2019). *K. pneumoniae* can elude the effects of antimicrobial treatment due to the acquisition of resistance genes and the production of biofilms facilitated by EPS, making them exceedingly difficult to manage or control (De Paula Ramos et al., 2016).

Antibiotic-resistant *K. pneumoniae*, which often forms biofilms, is associated with high virulence due to the nature of biofilm populations (Divakar et al., 2019). Biofilm-associated virulence factors such as exopolysaccharide production, hypermucoviscosity, and the formation of curli and fimbriae also enhance the pathogenicity of this organism (Chung, 2016). Bacteria protected by biofilm exopolysaccharides are up to 1000 times more resistant to antibiotics than planktonic cells (Sánchez et al., 2016), posing substantial therapeutic challenges and complicating treatment options.

Hypervirulent strains of *K. pneumoniae,* especially hypermucoviscous strains, also have capsule polysaccharides (CPS) for survival and immune evasion during infection, which allows them to consistently escape neutrophil-mediated intracellular killing and form abscesses at various sites, including the liver (Li et al., 2014). Fimbriae, another major virulence component that contributes to biofilm development in *K. pneumoniae*, consists of *MrkA* (capable of initiating biofilm formation) and *MrkD* subunits which control the binding capability and confer adhesive properties (Chung, 2016). Furthermore, curli known as thin aggregative fimbriae connect directly to the substratum, which produces interbacterial bundles, allowing a cohesive and stable attachment of cells in biofilm, thereby playing an important role in biofilm development (Kikuchi et al., 2005).

Since biofilm formation has been reported to increase virulence in *K. pneumoniae*, posing a remarkable therapeutic challenge and having developed resistance to almost all classes of conventional antibiotics (Boucher et al., 2009), the development of alternative treatment options which target biofilms and related virulence factors in this pathogen is paramount. This, therefore, necessitates the exploration of promising alternatives, which includes the search for naturally occurring compounds of plant origin capable of disrupting biofilms and their associated virulence activities. Historically,

biologically active phytochemical compounds have been a valuable source of natural products, which are prominent in the prevention and treatment of diseases, helping to maintain human health (Karuppiah & Mustaffa, 2013).

In the previous chapter, selected phytochemical compounds belonging to the terpene and flavonoid classes were shown to bind to the transcriptional SdiA receptor protein which modulates biofilm formation and associated virulence factors in *K. pneumoniae.* Furtherance to these findings, this chapter sought to validate the *in-silico* findings by assessing the *in-vitro* effect of the phytochemical compounds in inhibiting biofilms and associated virulence factors in CBR and ESBL producing *K. pneumoniae* strains. The expression level of virulence genes in the studied *K. pneumoniae* strains following treatment with the prospective antivirulence/antipathogenic compounds was also quantified using molecular diagnostic techniques. This is crucial to further substantiate the findings from traditional techniques. Hence, quantitative real-time PCR (qPCR) was employed to study this phenomenon at transcript level gene expression. Thereafter, the biosafety of the promising compounds against *K. pneumoniae* was assessed through *in-vitro* proof-of-concept cytotoxicity evaluation on non-malignant epithelial cells.

The phytochemical compounds considered in this chapter were selected based on good docking scores and improved binding energy when bound to the SdiA protein in *K. pneumoniae,* as well as their drug-likeness properties which were obtained in the previous chapter. The research of phytochemicals for antibacterial action, particularly against multidrug-resistant GNB, has received a lot of attention in the last ten years, especially as these organisms are posing a global health challenge as well as significant economic concerns due to the rising healthcare costs (Barbieri et al., 2017).

This chapter, therefore, assessed the antibacterial activity and the effect of phytochemical compounds (alpha-terpinene, camphene, fisetin, glycitein and phytol) in disrupting biofilm at different stages, as well as biofilm-related virulence factors for the development of new therapeutic strategies in place of the existing conventional antibiotics.

4.2 MATERIALS AND METHODS

4.2.1 Chemicals, media and compounds used in assays

Chemicals used in the study, including dimethyl sulfoxide (DMSO), iodonitrotetrazolium (INT), hexamethyldisilazane (HMDS), congo red and crystal violet were purchased from Sigma-Aldrich (Johannesburg, South Africa). Luria Bertani (LB) agar, Luria Bertani (LB) broth, Brain-Heart Infusion (BHI agar), Blood agar (BA) and Muller-Hinton (MH) broth were purchased from Lasec (Johannesburg, South Africa). Compounds and positive controls used in the study, including phytol (lot no: 0001452396), glycitein (lot no: MFCD00016679), camphene (lot no: MKCL4074), fisetin (lot no: 82542), alpha-terpinene (lot no: BCCD2529), quercetin (lot no: LRAB7760) and ciprofloxacin (lot no: 098M4006V), were purchased from Sigma-Aldrich (Johannesburg, South Africa). The compounds were dissolved in 1% DMSO and a 1mg/mL stock concentration of each compound was prepared for further assays.

4.2.2 Bacterial strains and growth conditions

American Type Culture Collection (ATCC) strains of CBR *K. pneumoniae* (ATCC BAA-1705) and ESBL *K. pneumoniae* (ATCC 700603) were obtained from the NextGen Health Unit at the Council for Scientific and Industrial Research (CSIR), South Africa. The bacterial strains were kept as glycerol stocks at −80°C until required for use. The two strains of *K. pneumoniae* used in this study were prepared in Mueller-Hinton (MH) medium during a minimum inhibitory concentration (MIC) assay and incubated at 37°C to obtain active bacterial cultures. One or two colonies were often transferred to sterile PB solution to obtain an absorbance ($OD_{600\ nm}$) of 0.1. The cell suspension was adjusted to achieve a 0.5 McFarland standard equivalent.

Ethics approval for the use of the *K. pneumoniae* strains was sought and obtained from the University of Pretoria, Faculty of Natural and Agricultural Sciences Ethics Committee (reference number: NAS157/2021) (Appendix 2.1).

4.2.3 Antibacterial activity of phytochemical compounds against *K. pneumoniae* strains

The MIC of the phytochemical compounds dissolved in 1% DMSO was determined following the broth dilution method as described by Alves et al. (2013), with slight modifications. Stock concentrations (1 mg/mL) of alpha-terpinene, camphene, fisetin, glycitein and phytol compounds were prepared and 100 µL of MH broth was transferred into each well of a 96-well microtiter plate. A 100 µL aliquot of each phytochemical compound (in triplicate) was transferred into the first row of microtiter plates. Serial dilutions were performed in the direction from A to H, resulting in decreasing concentrations over the range of 0.25 – 0.0019 mg/mL. Subsequently, 100 µL of the standardized bacterial strains ($OD_{600\ nm}$ = 0.08 – 0.1) was transferred into each well. Each plate was prepared with a set of positive and negative controls. Quercetin and ciprofloxacin were used as the positive controls at a concentration of 1 mg/mL and 0.01 mg/mL, respectively, while 100 µL of 1% DMSO was used as the negative control. Following incubation at 37°C for 24 h, 40 µL of a 0.20 mg/mL solution of *p*-iodonitrotetrazolium violet (INT) was added to each well and incubated at 37°C for 30 min. The MIC value for each phytochemical compound was visually assessed and recorded. The MIC was recorded as the minimum concentration of the compounds at which there was no visible growth of the test strain. The antibacterial assay was carried out in triplicate.

4.2.4 Inhibition of biofilm-associated virulence factor – Exopolysaccharide (EPS)

Reduction in EPS was carried out according to the method described by Gopu and Shetty (2016). A sterile LB broth with and without alpha-terpinene, camphene, fisetin, glycitein and phytol compounds was inoculated with 100 µL of the standardized *K. pneumoniae* strains ($OD_{600\ nm}$ = 0.1) and incubated at 37 °C. Biofilms that adhered to the walls of the test tubes were harvested to obtain crude EPS. Briefly, late log phase cells were removed by centrifugation at 5000×g for 30 min at 2 °C. The filtered supernatant was added to three volumes of chilled ethanol and incubated overnight at 2°C to precipitate the dislodged EPS. Precipitated EPS was collected by centrifugation at 8000×g for 30 min then dissolved in 1 mL of deionized water and stored at −40°C

until further use. EPS was quantified by mixing 1 mL of EPS solution with an equal volume of 5% phenol and 5 mL of concentrated sulfuric acid to develop a red colour. Glucose with a concentration range between 0.25 and 1 mg/mL was used as a standard to determine the R^2 value in the calibration and for the quantification of crude EPS. The intensity of the colour developed was measured using a microplate reader (Biotek, United States of America) at 490 nm.

4.2.5 Assessment of EPS inhibition using atomic force microscopy (AFM)

The effect of the best two compounds (phytol and camphene) shown to reveal noteworthy exopolysaccharide inhibition in *K. pneumoniae* strains were monitored using AFM following the method described by Santana et al. (2012). The CBR and ESBL producing *K. pneumoniae* strains were grown overnight in LB media, centrifuged (2000× *g*, room temperature, 15 min), washed three times in phosphate buffer (5 mM, pH 6.5), and approximately 10^8 CFU/mL were resuspended into tubes containing the same buffer. The phytochemical compounds were diluted to 1mg/mL and 100 µL of compounds were added to 3 mL of the cell suspensions. The samples were incubated for 4 h at 37 °C. Cell suspensions without the addition of the compounds were used as controls.

After incubation, samples of 1 mL were collected from each treatment, centrifuged (6000×g, at room temperature for 15 min) and a smear of cells was prepared in a glass slide (191cm). The slides were air-dried and viewed using the AFM at the Microscopy Unit, University of Pretoria, South Africa.

Samples were observed in a contact imaging mode using a Veeco atomic force microscope (Dimension icon with Scan Asyst) and silicon tip on nitride lever (cantilever 0.55–0.75 µm). A nominal constant of 32 Nm-1 and resonance frequency of ≈ 300 kHz were used with a scan rate of 0.100 Hz and scan size of 5.00 µm. Imaging analysis was performed using the Nanoscope analysis Scan Asyst software (Nanoscope version 8.15).

4.2.6 Inhibition of curli expression

The effect of the five test compounds (alpha-terpinene, camphene, fisetin, glycitein and phytol) and controls (quercetin and ciprofloxacin) on curli expression was assessed according to the method described by Jabuk (2016) with slight modifications. The

bacterial suspension was prepared by inoculating 100 µL of standardized *K. pneumoniae* strains and 100 µL of the compounds in 3 mL of LB broth. The suspension was incubated at 37°C for 24 h. After incubation, 3 µL of the bacterial suspension was inoculated onto plates containing BHI agar supplemented with congo red dye and sucrose. Curli-producing *K. pneumoniae* bound to congo red dye and formed red colonies, whereas curli-negative bacteria formed white colonies, which indicated a loss of curli fimbriae. Control cultures contained no compounds.

4.2.7 Reduction in hypermucoviscosity using the string test

A variation of the string test was used to determine the effect of the studied compounds on the hypermucoviscosity (HMV) phenotype of CBR and ESBL *K. pneumoniae* strains according to the method described by Wiskur et al. (2008) and Jabuk (2016). *K. pneumoniae* strains were inoculated on BHI agar plates containing the five phytochemical compounds with varying concentrations (0.125-1.0 mg/mL) and incubated overnight at 37 °C. A standard bacteriological loop was used to vertically stretch a mucoviscous string from a single colony. Each strain was defined as mucoid or regarded as a hypermucoviscous (HMV+) when string-like growth or a mucoid string of >5 mm was observed, respectively. The control culture contained no compounds.

4.2.8 Effect of phytochemical compounds on biofilm formation

Anti-adhesion (initial cell attachment), preformed biofilm (biomass measurement) and mature biofilms were assessed for inhibition by the phytochemical compounds, following the method described by Baloyi et al. (2021) and Blando et al. (2019), with slight modifications.

Five phytochemical compounds (alpha-terpinene, camphene, fisetin, glycitein and phytol) were tested against CBR and ESBL *K. pneumoniae* strains for initial cell attachment, preformed and mature biofilm inhibition. For the initial cell attachment inhibition assay, 100 µL of standardized bacterial suspension ($OD_{600\ nm}$ = 0.1), 100 µL of MH broth and 100 µL of the compound were added to the wells. The positive controls (quercetin 0.1 mg/mL and ciprofloxacin, 0.001 mg/mL) and negative control (1% DMSO) were also added into the wells, which were then incubated at 37°C for 24 h.

For preformed and mature biofilm assays, 100 µL of standardized bacterial suspension and 100 µL of MH broth were added to the wells and incubated at 37°C for 8 h for preformed biofilm, while for mature biofilm, wells were incubated at 37°C with and without shaking for 24 h. Following incubation, 100 µL of the compounds was transferred to individual wells and incubated for another 24 h. The modified crystal violet (CV) assay was used to analyze initial cell attachment, biofilm biomass, and mature biofilms. To eliminate planktonic cells and medium, the 96-well plates containing developed biofilm were rinsed with sterile distilled water. Afterwards, the plates were dried in the oven for 45 min at 60 °C. After drying, the remaining biofilm was stained for 15 min in the dark with a 1% CV solution (Sigma-Aldrich, Johannesburg, South Africa). To eliminate any unabsorbed stain, the wells were washed with sterile distilled water. Destaining the wells with 125 µL of 95% ethanol allowed for the semiquantitative measurement of biofilm formation. Approximately 100 µL of the destaining solution was transferred to a new plate and the absorbance (OD $_{585\ nm}$) was read using a multi-mode microplate reader (SpectraMax® paradigm). The percentage (%) inhibition of test compounds was calculated from the untreated broth culture. The formula below was used in calculating the percentage of inhibition where the control is the untreated biofilm:

$$\text{Biofilm reduction}\ (\%) = (\text{Control}_{585\text{nm}} - \text{Test}_{585\text{nm}})/(\text{Control}_{585\text{nm}}) \times 100$$

Results were interpreted following the criterion described by Famuyide et al. (2019). Values between 0 and 100% were interpreted as inhibitory activity; however, it was further broken down as follows: ≥ 50% was interpreted as good activity, and values between 0 and 49% were interpreted as weak activity, while negative values indicated a growth increase rather than the inhibition of biofilm.

4.2.9 *In situ* visualization of biofilms using scanning electron microscopy (SEM)

Sub-inhibitory biofilm inhibitory concentrations of the two most active compounds (phytol and glycitein) were fixed and visualized in a field emission gun SEM to observe the cell density and morphology of biofilms following the method described by Wijesundara & Rupasinghe (2018) with slight modifications. Biofilms were fixed (while still in a microtiter plate) over a minimum of 2 h in 0.1 M sodium cacodylate buffer (pH

7.2) containing 2% glutaraldehyde immediately after being rinsed in PBS. The biofilms were further rinsed three times with phosphate washing buffer 3 times for 15 minutes each. Then, the samples were dehydrated through an ethanol gradient series (35%, 50%, 75%, 90% and 100%).

All the steps in the gradient involved 15 min exposure times, with the final 100% ethanol treatment being repeated three times. Drying of samples was achieved through an ethanol gradient series (25:75, 50:50, 75:25 and 100:0) for 15 min at each concentration. The 100:0 dilution step was repeated three times. A 50:50 mixture of hexamethyldisilazane (HMDS) and 100% ethanol was added and allowed to stay for 1 h with the samples covered. The HMDS-ethanol mixture was removed and fresh HMDS was added. Plates were air-dried under the fume hood for 2 h. Finally, fixed biofilms were mounted on aluminum stubs. Then, sputters were coated with gold-palladium (15 nm) and visualized using a Zeiss crossbeam 540 SEM with operational conditions of an acceleration voltage of 10 kV, emission current of 14–16 µA, the working distance of 10–12 mm and analysis lens mode.

4.2.10 DNA extraction

Deoxyribonucleic acid (DNA) was extracted from the CBR and ESBL producing *K. pneumoniae* strains following the manufacturer's instruction in the GeneJET genomic DNA purification kit (Thermofisher scientific). This procedure involved steps such as cell harvesting, addition of digestion solution, proteinase K solution, lysis solution, wash buffer and elution buffer with intermittent centrifugation steps as specified in the GeneJET kit. Afterwards, the purified DNA was stored immediately at -20°C for further use.

4.2.11 Primer design

The primer sequences used for amplification of the virulence genes (Table 4.1) were generated using Primer3 plus bioinformatics online tool (https://www.bioinformatics.nl/cgi-bin/primer3plus/primer3plus.cgi). The product sizes (Table 4.1) were also determined using the PCR test bioinformatics tool (https://www.bioinformatics.org/sms2/pcr_products.html). Primer efficiencies were determined by performing a temperature gradient reaction from 45°C to 50°C. The optimal annealing temperature for each gene is shown in Table 4.1.

Table 4.1: Sequences of oligonucleotide primers used for PCR and qPCR

Gene function/ description	GenBank accession number of templates	Gene	Nucleotide sequence of primers [5^{l} -3^{l}]	Size of amplicon/ product size	Annealing temperature (°C)
Fimbrial protein for biofilm formation	KPHS_43470	*mrkA-F*	ACGTCTCTAACTGCCAGGC	115bp	48
		mrkA-R	TAGCCCTGTTGTTTGCTGGT		
S-Ribosylhomocysteinase protein coding gene	KPHS_40930	*luxS-F*	GGCGTGGAAATTATCGACAT	180bp	47
		luxS-R	GTAGGTCCCGCACTGGTAGA		
Positive regulator of ctr capsule/ extracellular polysaccharide biosynthesis	KPHS_34420	*rcsA-F*	ACGGGATATCTGACCAGTCG	180bp	49
		rcsA-R	CGGGTTTTGCGTAATGATCT		
16S rRNA-processing protein	KPHS_40460	*16S rRNA-F*	CCACCACAATCAGGACATCA	161bp	49
		16S rRNA-R	TAACTACCTGGCAGCCCATC		

4.2.12 PCR detection of virulence genes in *K. pneumoniae* strains

Polymerase chain reaction (PCR) was used to detect *mrkA, luxS,* and *rcsA* virulence *K. pneumoniae* strains following the method described by Foroohimanjili et al. (2020) with slight modification. The presence of the *16srRNA* housekeeping gene was also confirmed. Prior to conducting the PCR assay, the concentration of the extracted DNA was determined using a NanoDrop spectrophotometer (ThermoScientific). For the amplification of the selected virulence genes, a PCR reaction was carried out in a final volume of 25 µL, which comprised of 1 µL of extracted DNA (with concentrations ranging between 25-30 ng/µL) as the template, 0.5 µL of forward primer, 0.5 µL of reverse primer (10 pmol), 12.5 µL of Master Mix (CinnaGen, Iran), and 10.5 µL of double-distilled water. PCR was performed using a Bio-Rad T100 thermal cycler, following the ThermoScientific recommended thermal cycling conditions (Table 4.2).

Table 4.2: PCR thermal cycling conditions

Steps	Temperature (°C)	Time	Number of cycles
Initial denaturation	95	1-3 min	1
Denaturation	95	30 secs	35
Annealing	46	30 secs	
Extension	72	1 min	
Final extension	72	5-15 min	1

4.2.13 RNA isolation

For ribonucleic acid (RNA) isolation, the same culture plate model and growth conditions employed during the phenotypic assays for antibiofilm activity and exopolysaccharide reduction as described above were used. *K. pneumoniae* strains were treated with the phytochemical compounds that revealed the best result for each assay such as phytol for biofilm inhibition and camphene for exopolysaccharide reduction before RNA extraction. Strains were also treated with ciprofloxacin and quercetin as the positive controls while the untreated strains were used as the negative control.

RNA extraction was carried out following the method described by Patole et al. (2021). The treated and untreated cultures were incubated at 37 °C, 220 rpm for 24 hours, after which the cells were harvested by centrifugation, resuspended and then diluted with two volumes of RNAProtect Bacterial Reagent (QIAGEN) to stabilize the RNA. The cells were progressively lysed using lysozyme and proteinase-K. The RNA was extracted using the RNeasy Mini Kit (QIAGEN) with on-column DNase-I digestion performed using the RNase-free DNAse-I Kit (QIAGEN) and was eluted using nuclease-free water.

4.2.14 RNA quality determination

RNA quantity and quality (concentration and purity of the total RNA) were spectrometrically determined using a NanoDrop 1000TM (Thermo Scientific) following the method described by França et al. (2012). Three independent measurements of the same sample were performed. The absorbance ratio at 260nm and 280nm were used as an indicator of protein contamination while the absorbance ratio at 260nm and 230nm were used as an indicator of polysaccharide, phenol, and/or chaotropic salt contamination. The integrity of the total RNA was assessed to ensure the absence of

contaminating DNA by visualization of the RNA gene banding pattern. Gel electrophoresis was carried out at 80 V for 60 minutes using a 1.5% agarose gel. The gel was stained with ethidium bromide and visualized using a GelDoc2000 (Bio-Rad, Hercules, CA, US).

4.2.15 cDNA synthesis

Purified RNA was immediately converted to copy DNA (cDNA) to avoid RNA degradation following the manufacturer's instructions in the Super Script (Invitrogen) kit. The primers listed in Table 4.1 above were also used for the cDNA synthesis. Similarly to the method described by França et al. (2012), the same amount of total RNA (500 ng/20 mL) was reversely transcribed following the manufacturer's protocol.

4.2.16 Quantitative real-time PCR

To determine the kind of gene expression events that are correlated with phenotypic differences, the transcript levels of the three selected virulence genes present in the studied *K. pneumoniae* strains were measured using qPCR following the method described by Foroohimanjili et al. (2020) with slight modifications.

qPCR was performed using a SYBR Green-containing Master Mix (Powerup, applied biosystems) to evaluate the expression level of the virulence genes in *K. pneumoniae*. A reaction volume of 20 µL of was set up for each sample, comprising 2 µL of cDNA, 10 µL of SYBR Green Master Mix, 0.5 µL of 100 µM of each primer, and 7 µL of sterile double RNase treated water. The reaction was started with an initial denaturation at 95°C for 3 min and 35 amplification cycles of 95°C for 30 s, 46°C for 30 s and 72°C for 2 min. The *16S rRNA* gene was used as an internal control. Finally, the relative expression of the virulence genes was calculated by the ΔΔCt method. The data were analyzed using the $2^{-\Delta\Delta Ct}$ equation where:

$\Delta\Delta C_t = (C_t, \text{Target} - C_t, \textit{16S rRNA})_{\text{Time } x} - (C_t, \text{Target} - C_t, \textit{16S rRNA})_{\text{Time 0.}}$

Time *x* is each sample's treatment time and Time 0 represents the untreated control sample. The fold change in the target gene, normalized to the reference gene (*16S rRNA*) and relative to the expression in the untreated sample, were calculated for each sample using the $2^{-\Delta\Delta Ct}$ equation.

4.2.17 Cell viability and cytotoxicity assays

Water-soluble tetrazolium salt (WST-8) was used to evaluate the metabolic activity of cells as an indicator of cell viability using the cell counting kit-8 (CCK-8; Dojindo Molecular 150 Technologies, Italy). The cytotoxicity activity was determined using the lactate dehydrogenase enzyme (LDH Assay kit-WST, Dojindo Molecular Technologies, Italy). LDH is a firm cytoplasmic enzyme released into the cell culture medium because of the loss of membrane integrity (Kamiloglu et al., 2020).

Bioactive compounds were evaluated for their cytotoxic effects on epithelial African green monkey kidney cells (Vero ATCC CCL-81) following the method described by Bonvicini et al. (2021) with slight modifications. CCK-8 and LDH release were assessed on mammalian cells after 48 h of treatment. An aliquot of 100 µL cell suspension was seeded into 96-well microplates at 10^4 cells/well and incubated in 5% CO_2 at 37°C for 24h. After incubation, the exhausted medium was replaced with the renewal of a complete medium supplemented with varying concentrations of compounds (0.25 mg/mL – 0.0019 mg/mL) and doxorubicin (0.025 – 0.00019 mg/mL), a cytotoxic antineoplastic agent used as clinical drug control. All experiments included wells with untreated Vero cells (positive control), background medium of the compounds and a range of 0.1 – 0.0008% DMSO. These varying concentrations of DMSO relative to the redissolved compounds were added to verify that the DMSO does not have any influence on the Vero cells. After 48 h incubation, cellular morphology evaluation of the micro-wells containing cells with treatment was visualised at a 10X magnification and captured using the Hamamatsu corporation image software (Olympus i73 mic). Subsequently, 10 µL of lysis buffer was transferred to several wells of Vero cells representing the positive control in the LDH and incubated for 10 min at 37°C. All supernatants were removed from the 96-well plate and stored for LDH measurements. Approximately, 100 µL of fresh medium containing 10 µL of CCK-8 solution were added to the cell monolayer and incubated for 2 h. The optical density (OD) values at 450 nm were measured after 2 h of incubation and data were expressed as percentage values of cell viability relative to the untreated controls using the equation below:

$$\text{Cell viability} = \text{OD}\,(450\text{ nm})\ \text{untreated cells}/\text{OD}\,(450\text{nm})\ \text{treated cells} \times 100$$

In parallel, the collected cell-free supernatants were assayed for LDH released through damaged plasma membranes by adding a volume of the reconstituted working solution.

After 30 min of incubation at room temperature in the dark, the stop solution was added, and absorbance was measured at 490 nm using a Multiskan Ascent Microplate Reader (Thermo Fischer, Italy). Data were expressed as percentage values relative to both the 100% lysis controls, included in the test, and untreated controls using the equation below:

$$\text{Cytotoxicity}\ (\%) = (\mathrm{A} - \mathrm{C})/(\mathrm{B} - \mathrm{C}) \times 100$$

Where: A indicates treated cells (test samples), B: high control (lysed Vero cells) and C: low control (untreated Vero cells).

4.2.18 Statistical analysis

All results were presented as mean ± standard deviations for each sample and treatment. Data were generated in independent experimental repeats with each sample in triplicates. The ANOVA generalized linear model (Proc GLM) was used to analyze the means of inhibitory activities of the compounds and controls. All statistical analyses were carried out using the Statistical Analysis System (SAS) program version 9.4 from Stats Inc., 100 SAS Campus Drive, Cary, NC, USA, with $p < 0.05$ values considered statistically significant. The qPCR data were analyzed using the $2^{-\Delta\Delta Ct}$ method, where the data were expressed as the fold change in gene expression normalized to the housekeeping gene (*16S rRNA*).

4.3 RESULTS

4.3.1 *In vitro* antibacterial validation of selected compounds

The antibacterial activities of five phytochemical compounds (alpha-terpinene, camphene, fisetin, glycitein and phytol) against *K. pneumoniae* strains showed MIC values ranging from 0.0625 mg/mL to 0.250 mg/mL (Table 4.3). The best MIC value was shown by fisetin (0.0625 mg/mL) for CBR-*K. pneumoniae*. Phytol, glycitein and alpha-terpinene showed MIC values of 0.125 mg/mL for both strains; however, camphene revealed a higher MIC value of 0.250 mg/mL. The positive controls, quercetin and ciprofloxacin, revealed significant MIC values of 0.0625 mg/mL and 0.0025 mg/mL, respectively, against both strains of *K. pneumoniae* (Table 4.3). The negative control showed no inhibitory activity against both strains of *K. pneumoniae.*

Table 4.3: MIC values of selected phytochemical compounds on *K. pneumoniae* strains

Compounds	*K. pneumoniae* strains and MIC (mg/mL) values	
	CBR-*K. pneumoniae*	ESBL-*K. pneumoniae*
Alpha-terpinene	0.125	0.125
Camphene	0.250	0.250
Fisetin	0.0625	0.125
Glycitein	0.125	0.125
Phytol	0.125	0.125
Controls		
Ciprofloxacin	0.0025	0.0025
Quercetin	0.0625	0.0625

The MIC values are presented as the mean values of triplicates.

4.3.2 Inhibition of *K. pneumoniae* EPS

The quantity of EPS observed following the phenol-sulfuric acid method depicted a decrease at respective MIC values in both test pathogens. Good linearity was indicated by the correlation coefficient (R^2), which yielded a value of 0.9705. The quantification of EPS was determined following the regression equation obtained from the standard curve $Y = 0.348X - 0.074$, where Y represents the absorbance obtained from the unknown samples. Figure 4.1 presents the EPS quantification and percentage inhibition of ESBL- *K. pneumoniae* EPS by the compounds. Out of all the compounds active against the EPS production in ESBL- *K. pneumoniae*, the highest percentage of EPS inhibition was shown by phytol and camphene (65.91%) (Figure 4.1). This percentage can be compared with the result obtained for the positive control ciprofloxacin (68.45%), although quercetin (the QSI control) showed a low percentage reduction of EPS (23.21%) (Figure 4.1). Furthermore, of all the active compounds against EPS production in CBR-*K. pneumoniae*, camphene showed the highest percentage inhibition and/or anti-slime activity (43.80%) (Figure 4.1), having the lowest EPS yield (OD value = 2.22) (Table 4.4), similar to the results observed for ciprofloxacin (EPS inhibition at 46.26%) (Figure 4.1). Conversely, the untreated EPS showed enhanced production for both strains of *K. pneumoniae.*

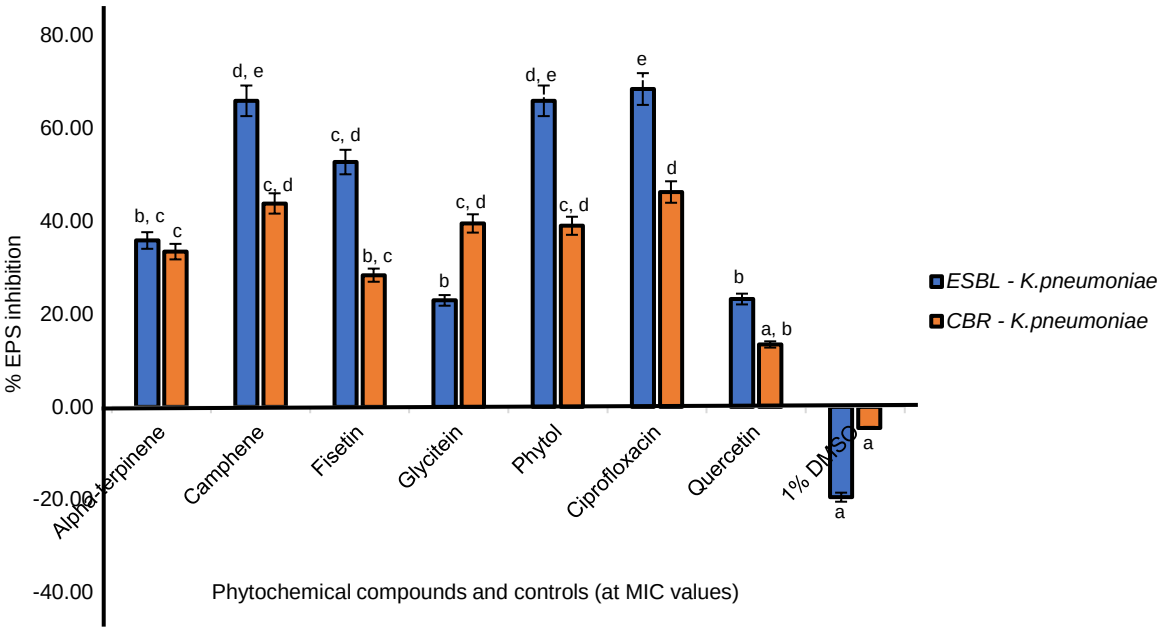

Figure 4.1: Quantification and percentage inhibition of EPS present in ESBL and CBR- *K. pneumoniae* treated with phytochemical compounds at respective MIC values. Statistical significance of the test compounds and controls are indicated with different letters (a–e) with *p*-value < 0.05 between the different treatments.

The highest percentage of ESBL- *K. pneumoniae* EPS inhibition shown by phytol and camphene can be correlated with their low EPS yield (OD value = 1.91) observed in Table 4.4. The positive control ciprofloxacin revealed a lower EPS yield (OD value of 1.05), although quercetin (the QSI control) treated EPS showed a higher yield with an OD value of 2.68 (Table 4.4).

Table 4.4: Exopolysaccharide reduction in ESBL and CBR-*K. pneumoniae* by the studied phytochemical compounds

Compounds	**ESBL-*K. pneumoniae***		**CBR-*K. pneumoniae***	
	EPS quantity (OD_{480nm})	**% of EPS quantity**	**EPS quantity (OD_{480nm})**	**% of EPS quantity**
Alpha-terpinene	2.24	64.18	2.63	66.58
Camphene	1.19	34.09	2.22	56.20
Fisetin	1.65	47.28	2.83	71.65
Glycitein	2.69	77.08	2.39	60.51
Phytol	1.19	34.09	2.41	61.01
Controls				
Ciprofloxacin	1.05	31.55	2.01	53.74
Quercetin	2.68	76.79	3.42	86.58
1% DMSO	4.17	119.48	4.13	104.56

4.3.3 Microscopic surface topography characterization of EPS using AFM

The planar (2D) and cubic (3D) views of the surface topography of studied *K. pneumoniae* EPS are shown in Figure 4.2. AFM detected marked differences between the topographies of untreated and treated (camphene and phytol) EPS, selected due to the significant reduction in EPS.

The AFM analysis revealed the irregularity and surface roughness of the EPS produced by untreated CBR and ESBL-*K. pneumoniae* strains, mainly composed of unevenly distributed lumps which were visible as cloudy areas around the cells (Figure 4.2A1, F1). Microscopically, the exopolysaccharides of both test strains exhibited a compact and tubular structure. Topologically, the EPS revealed a consistent polymer with a maximum height of the irregular lumps at 1.4 µm and 1.1 µm for untreated CBR and ESBL-*K. pneumoniae*, respectively, as shown in the 2D images (Figure 2A1, F1), while the average roughness (Ra) was recorded at 183 nm and 141 nm for CBR and ESBL producing *K. pneumoniae*, respectively. The roughness parameters were obtained using the nanoscope analysis (v 8.15) software. The surface roughness is shown in the 3D images (Figure 4.2A2, F2).

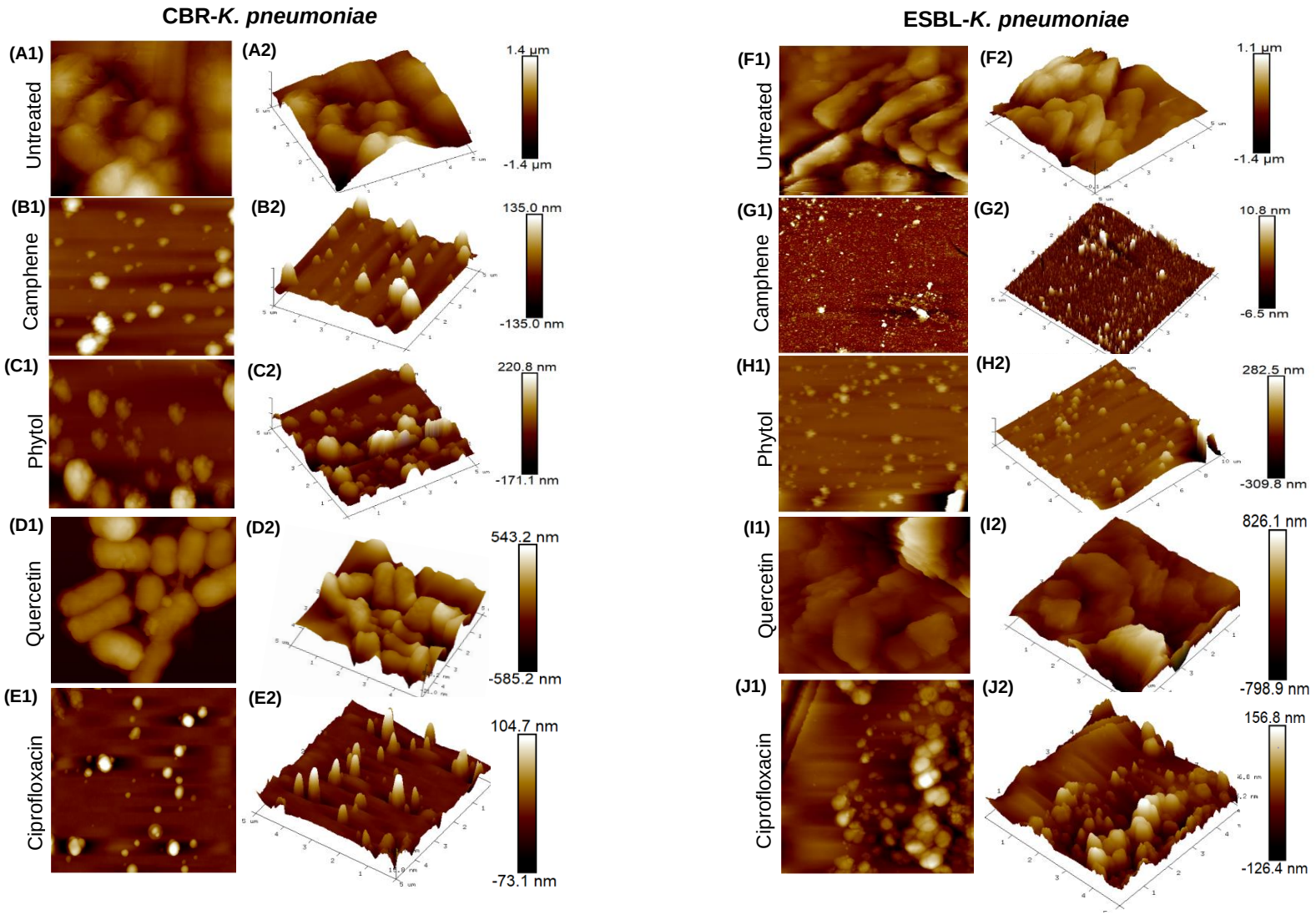

Figure 4.2. AFM images showing two-dimensional (2D) and three-dimensional (3D) surface topography of EPS produced by untreated and treated CBR and ESBL producing *K. pneumoniae* strains at a scan size of 5.00µm (5,000nm). 2D images of untreated and treated *K. pneumoniae* EPS are shown in A1-J1. Corresponding 3D images are shown in A2-J2.

The EPS treated with camphene and phytol at the MIC value revealed visible differences in height and surface roughness in comparison with the untreated EPS. The camphene-treated EPS showed maximum lump heights of 135 nm and 10.8 nm for CBR and ESBL-*K. pneumoniae,* respectively (Figure 4.2B1, G1). A significantly reduced surface roughness is shown in the 3D images (Figure 4.2B2, G2). The average roughness (Ra) was recorded at 15.6 nm for CBR-*K. pneumoniae* and 1.25 nm for ESBL-*K. pneumoniae*.

On the other hand, EPS treated with phytol had a maximum height of 220.8 nm and 282.5 nm for CBR and ESBL-*K. pneumoniae*, respectively (Figure 4.2C1, H1). The average roughness (Ra) for phytol-treated EPS was 34.8 nm for CBR-*K. pneumoniae* and 25.0 nm for ESBL-*K. pneumoniae*. Figure 4.2C2, H2 revealed a reduction in surface roughness when compared with the untreated EPS.

The EPS treated with the positive controls (quercetin and ciprofloxacin) also revealed a significant reduction in the surface roughness and height, although ciprofloxacin showed improved results with a maximum lump height at 104.7 nm and average roughness at 8.80 nm for CBR-*K. pneumoniae* (Figure 4.2E1, E2). Moreover, ciprofloxacin-treated ESBL-*K. pneumoniae* had a maximum height of 156.8 nm and average roughness of 27.6 nm (Figure 4.2J1, J2).

4.3.4 Curli expression reduction by phytochemical compounds

The impact of alpha-terpinene, camphene, fisetin, glycitein and phytol compounds on the occurrence of curli fibers in both strains of *K. pneumoniae* is shown in Table 4.5. The results showed that all compounds tested at 0.125 mg/mL and 0.250 mg/mL did not inhibit curli expression in the *K. pneumoniae* strains. However, phytol, glycitein, fisetin and quercetin (positive control) at concentrations of 0.5 and 1.0 mg/mL reduced the curli expression of both strains. In addition, ciprofloxacin showed a reduction in curli expression for both strains at varying concentrations (0.125 to 1.0 mg/mL) (Table 4.5).

On the contrary, no inhibition was shown by camphene and alpha-terpinene at all concentrations. No changes were observed in bacterial colonies (which appeared red in the presence of these compounds), similar to the negative control.

Table 4.5: Effect of compounds on curli fiber synthesis in *Klebsiella pneumoniae* strains

Compounds	Concentration (mg/mL) (A)					Concentration (mg/mL) (B)				
	Control	0.125	0.250	0.5	1.0	Control	0.125	0.250	0.5	1.0
Alpha-terpinene	+	+	+	+	+	+	+	+	+	+
Camphene	+	+	+	+	+	+	+	+	+	+
Fisetin	+	+	+	-	-	+	+	+	-	-
Glycitein	+	+	+	-	-	+	+	+	-	-
Phytol	+	+	+	-	-	+	+	+	-	-
Controls										
Ciprofloxacin	+	-	-	-	-	+	-	-	-	-
Quercetin	+	+	+	-	-	+	+	+	-	-
Untreated	+	+	+	+	+	+	+	+	+	+

Key: + (Present), - (Absent), A = CBR-*K. pneumoniae*, B = ESBL-*K. pneumoniae*

Figure 4.3 shows the representative images where no inhibition of curli expression was observed for the negative control (Figure 4.3A) versus the observed inhibition for the phytol compound (Figure 4.3B).

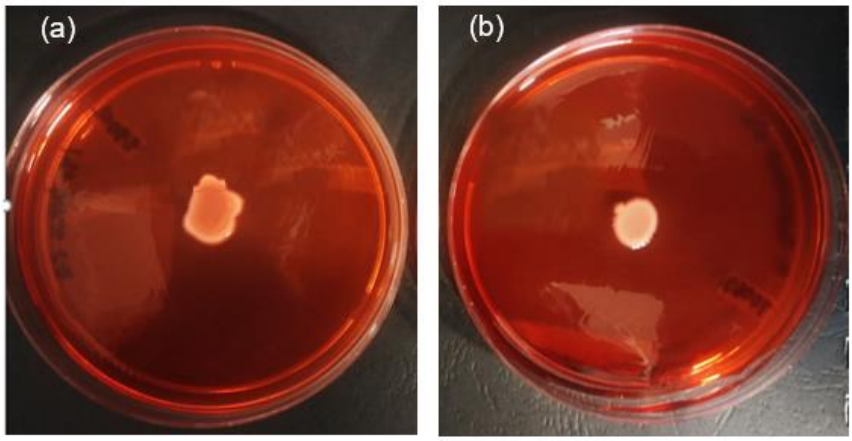

Figure 4.3: Representative images of curli expression in *K. pneumoniae*. (**a**) Negative control (untreated), showing curli-producing *K. pneumoniae*, which binds congo red dye (**b**) Inhibition of curli expression in *K. pneumoniae* subjected to phytol, as indicated by the appearance of white colonies on the BHI agar plates supplemented with congo red dye.

4.3.5 *K. pneumoniae* hypermucoviscosity reduction using the string test

The effect of the test compounds on hypermucoviscosity is shown in Figure 4.4. The string test showed that an increase in compound concentration led to a gradual decrease in the viscosity of the test strains.

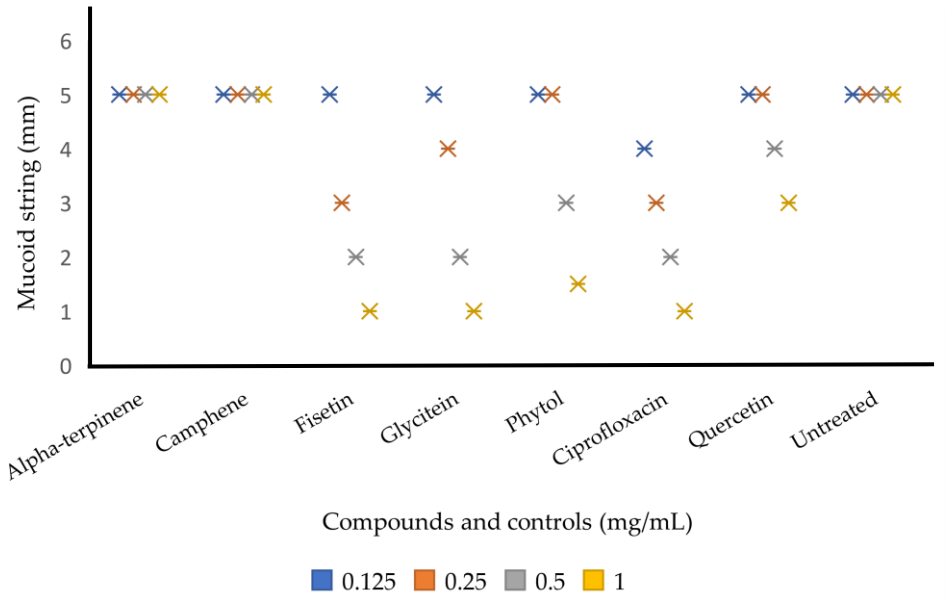

(A)

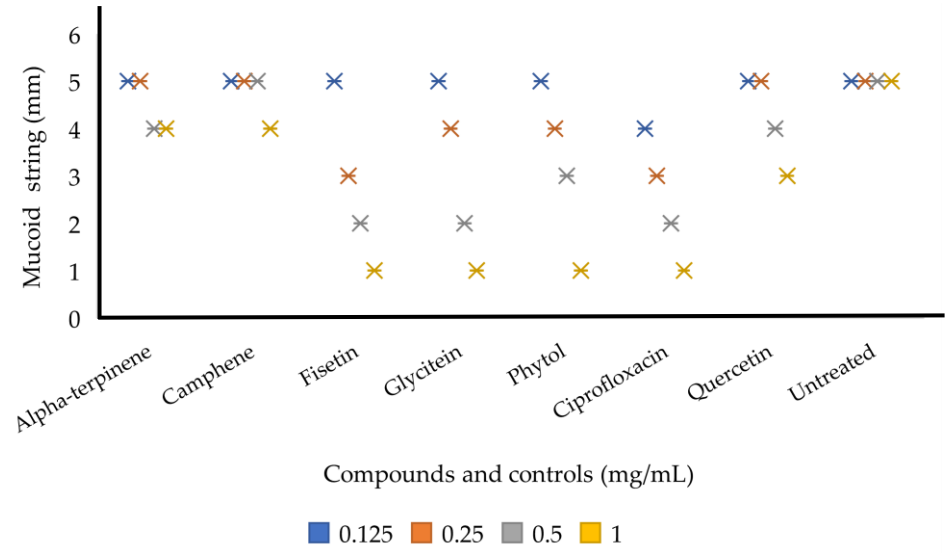

(B)

Figure 4.4. Effect of compounds on the inhibition of *K. pneumoniae* hypermucoviscosity (**A**) For CBR-*K. pneumoniae* (**B**) For ESBL-*K. pneumoniae*.

For CBR-*K. pneumoniae* (Figure 4.4A), glycitein and fisetin revealed the potent hypermucoviscosity inhibitory activity, both showing the shortest mucoid string (1 mm) at 1.0 mg/mL (represented by the yellow *), followed by phytol (1.5 mm at 1.0 mg/mL), while no inhibitory activity was observed for camphene and alpha-terpinene for all the concentrations tested, as seen in the negative control. Furthermore, none of the

compounds showed a reduction in the hypermucoviscosity phenotype at the lowest concentration (0.125 mg/mL) tested.

Similarly, for ESBL- *K. pneumoniae* (Figure 4.4B), glycitein, fisetin and phytol revealed potent hypermucoviscosity inhibitory activity, showing the shortest mucoid string (1 mm) at 1.0 mg/mL. However, at 0.5 mg/mL, the prominent viscosity reduction activity was shown by glycitein and fisetin, both having a mucoid string length of 2 mm. In addition, fisetin showed a potent result at the lowest concentration of 0.25 mg/mL in terms of mucoid string length reduction (3 mm), compared to the other compounds.

For CBR-*K. pneumoniae*, no reduction in the hypermucoviscosity phenotype was shown by all the compounds at the lowest concentration tested (0.125 mg/mL), similar to the negative control. In contrast, the positive controls (quercetin and ciprofloxacin) revealed a good reduction, with ciprofloxacin showing the highest reduction in the mucoid string length at varying concentrations for both strains (Figure 4.4A, B).

4.3.6 Inhibition of biofilm formation

4.3.6.1 Effect of phytochemical compounds on initial cell attachment

The results of the anti-adhesion (initial attachment) assay against CBR and ESBL-*K. pneumoniae* treated with test compounds are shown in Table 4.6. The results showed that phytol had the highest inhibition of initial cell attachment for both strains tested, with 54.71% and 50.05%, respectively, followed by glycitein, which showed inhibition at 48.35% and 44.34%, respectively for both strains (Table 4.6).

Table 4.6: Effect of phytochemical compounds on initial cell attachment (anti-adhesion) and biofilm development of *K. pneumoniae* strains

Compounds	Percentage (%) inhibition of initial cell attachment		Percentage (%) inhibition of biofilm development	
	CBR-*K. pneumoniae*	**ESBL-*K. pneumoniae***	**CBR-*K. pneumoniae***	**ESBL-*K. pneumoniae***
Alpha-terpinene	33.71 ± 0.01 ^{a,b}	37.05 ± 0.00 ^{a,b}	17.23 ± 0.04 ^{b,c}	19.04 ± 0.03 ^{a,b}
Camphene	22.27 ± 0.08 ^{a}	18.53 ± 0.01 ^{a}	14.58 ± 0.04 ^{a}	11.08 ± 0.02 ^{a}
Fisetin	39.81 ± 0.01 ^{a,b}	32.59 ± 0.04 ^{a}	25.79 ± 0.00 ^{a,b}	29.93 ± 0.02 ^{a,b}
Glycitein	48.35 ± 0.02 ^{b,c}	44.34 ± 0.02 ^{c}	39.61 ± 0.01 ^{d}	32.77 ± 0.04 ^{b}
Phytol	**54.71** ± 0.01 ^{c}	**50.05** ± 0.00 ^{c}	43.81 ± 0.01 ^{e}	40.02 ± 0.01 ^{b}
Controls				
Ciprofloxacin	69.25 ± 0.03 ^{d}	62.45 ± 0.04 ^{d}	56.42 ± 0.03 ^{f}	51.77 ± 0.03 ^{c}
Quercetin	42.57 ± 0.03 ^{b,c}	40.66 ± 0.01 ^{b,c}	35.15 ± 0.01 ^{c,d}	31.81 ± 0.02 ^{a,b}
1% DMSO	−3.72 ± 0.04 ^{a}	−9.76 ± 0.01 ^{a}	−5.06 ± 0.03 ^{a}	−8.24 ± 0.02 ^{a}

Mean values of triplicate independent experiments ± SD. Comparison of percentage inhibition at MIC value for each treatment against *K. pneumoniae*. Different letters (^{a}-^{f}) indicate a significant difference at $p < 0.05$ between the different treatments (per column) at the same MIC value. Reference control for percentage measurement: ≥ 50% (good activity), 0 to 49% (weak activity), negative values (rise in biofilm formation) (Famuyide *et al.*, 2019).

The least anti-adhesion activity was shown by camphene at 22.27% for CBR-*K. pneumoniae* and 18.53% for ESBL-*K. pneumoniae* (Table 4.6). Quercetin and ciprofloxacin revealed an initial cell attachment inhibition at 42.57% and 69.25% for CBR-*K. pneumoniae*, while for ESBL-*K. pneumoniae*, 40.66% and 62.45% were observed for quercetin and ciprofloxacin, respectively. No inhibition was revealed by the negative control (Table 4.6). A statistically significant difference was observed between phytol and the other compounds tested ($p < 0.05$). Phytol showed potent activity since it revealed >50% inhibition, while glycitein, camphene, fisetin and alpha-terpinene showed weak activity, having percentage inhibition values between 0 and 49% (Table 4.6).

4.3.6.2 Effect of phytochemical compounds on preformed biofilm inhibition: biomass measurement

The inhibition of biofilm microcolonies formed by the test strains upon treatment with the phytochemical compounds was assessed, and the results are shown in Table 4.7. The percentage inhibition of preformed biofilm by the compounds was observed to be slightly less compared with the initial cell attachment, with the highest biofilm reduction of 43.81% shown by phytol for CBR-*K. pneumoniae*. Glycitein also revealed 39.61% inhibition for CBR-*K. pneumoniae* and 32.77% inhibition for ESBL-*K. pneumoniae*, which is slightly higher than the results obtained for quercetin, showing 35.15% and 31.81% inhibition for CBR-*K. pneumoniae* and ESBL-*K. pneumoniae*, respectively. However, the highest percentage inhibition was observed for ciprofloxacin at 56.42% and 51.77% for CBR and ESBL-*K. pneumoniae*, respectively (Table 4.7). The negative control did not reveal any inhibitory effect on biofilm development, except for a slightly enhanced biofilm formation.

4.3.6.3 Disruption of mature biofilm by phytochemical compounds

Mature biofilms formed by *K. pneumoniae* strains determined under dynamic and static conditions are shown in Table 4.7. The highest disruption of mature biofilms under dynamic conditions was shown by phytol at 24.94% and 25.88% for CBR and ESBL-*K. pneumoniae*, respectively. The least inhibition was shown by camphene at 5.24% for CBR-*K. pneumoniae* and 2.06% for ESBL-*K. pneumoniae* (Table 4.7).

Table 4.7: Disruption of mature *K. pneumoniae* biofilms formed by various compounds under dynamic and static conditions

Compounds	Percentage (%) inhibition of mature biofilm formed under dynamic condition		Percentage (%) inhibition of mature biofilm formed under static condition	
	CBR-*K. pneumoniae*	**ESBL-*K. pneumoniae***	**CBR-*K. pneumoniae***	**ESBL-*K. pneumoniae***
Alpha-terpinene	18.55 ± 0.02 ^{b}	17.22 ± 0.13 ^{b}	15.18 ± 0.05 ^{b}	12.15 ± 0.03 ^{c,d}
Camphene	5.24 ± 0.01 ^{a,b}	2.06 ± 0.05 ^{b}	4.56 ± 0.01 ^{a,b}	4.08 ± 0.05 $^{b, d}$
Fisetin	14.83 ± 0.02 ^{a,b}	12.33 ± 0.02 ^{b}	−8.52 ± 0.01 ^{a,b}	−32.43 ± 0.02 ^{a,b}
Glycitein	8.89 ± 0.01 ^{a,b}	−5.71 ± 0.01 ^{b}	6.89 ± 0.01 ^{a,b}	−12.53 ± 0.01 ^{b,c}
Phytol	24.94 ± 0.04 ^{b}	25.88 ± 0.00 ^{b}	20.32 ± 0.02 ^{b}	18.07 ± 0.01 ^{d}
Controls				
Ciprofloxacin	44.73 ± 0.04 ^{c}	51.88 ± 0.00 ^{c}	42.24 ± 0.02 ^{b}	39.15 ± 0.01 ^{e}
Quercetin	−27.08 ± 0.01 ^{a}	−44.55 ± 0.01 ^{a}	−35.46 ± 0.02 ^{a}	−52.25 ± 0.02 ^{a}
1% DMSO	−39.01 ± 0.01 ^{a}	−58.35 ± 0.01 ^{a}	−45.67 ± 0.02 ^{a}	−68.25 ± 0.02 ^{a}

Mean values are of triplicate independent experiments ± SD. Comparison of percentage inhibition at MIC value for each treatment against *K. pneumoniae*. Different letters (^{a}-^{e}) indicate a significant difference at $p < 0.05$ between the different treatments (per column) at the same MIC value. Reference control for percentage measurement: ≥ 50% (good activity), 0 to 49% (weak activity), negative values (rise in biofilm formation) (Famuyide *et al.*, 2019).

Under static conditions, phytol again revealed higher inhibitory activity (20.32% and 18.07% for both strains), followed by alpha-terpinene (Table 4.7), with statistical differences found between the compounds ($p < 0.05$). The least inhibitory activity for this group was also shown by camphene at 4.56% for CBR-*K. pneumoniae* and 4.08% for ESBL-*K. pneumoniae*. Moreover, fisetin and quercetin showed no inhibitory activity on mature biofilms formed by both strains under static conditions.

Overall, a notable difference was observed between the two tested conditions with less inhibitory activity shown by the compounds on mature biofilms under static conditions when compared to the dynamic condition. This was also observed for the positive control of ciprofloxacin (Table 4.7).

4.3.7 In situ visualisation of biofilms using SEM

To further investigate the detailed effects of the *K. pneumoniae* biofilms formed after treatment with the best active or potent compounds (phytol and glycitein) on antibiofilm assay results, a SEM analysis was carried out. Figure 4.5 shows the SEM micrographs of the biofilms formed by the two *K. pneumoniae* strains upon exposure to phytol and glycitein (0.1 mg/mL), the positive controls (quercetin; 0.1 mg/mL and ciprofloxacin; 0.001 mg/mL), and the untreated biofilms.

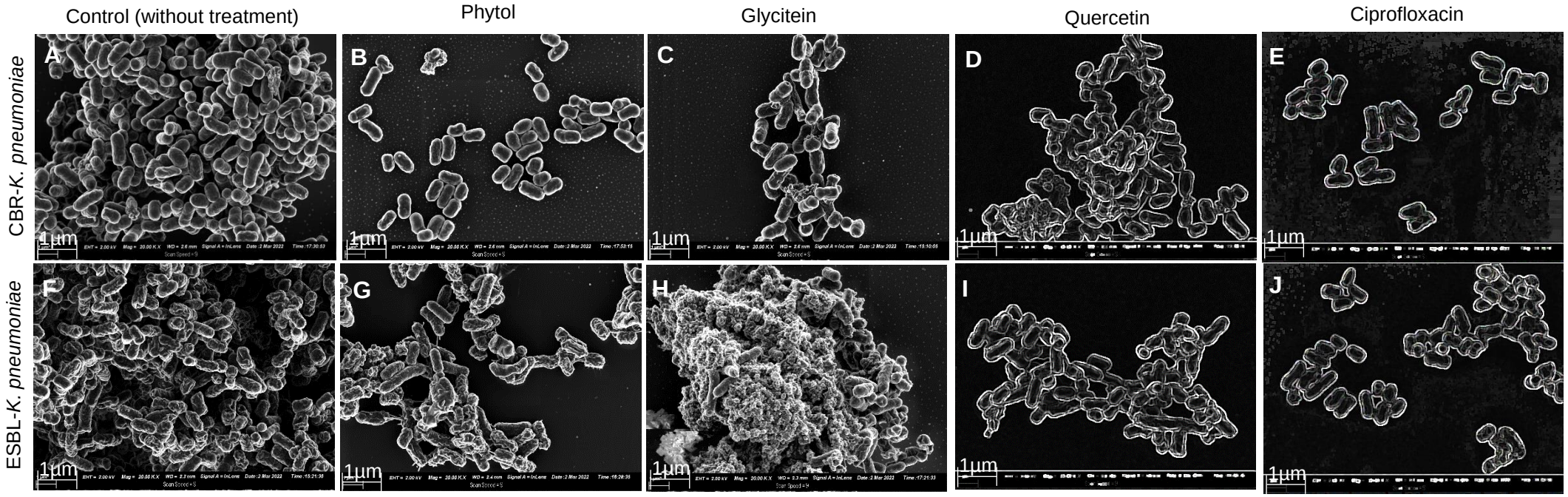

Figure 4.5: SEM micrographs showing the biofilm inhibitory activity of phytol and glycitein against CBR and ESBL-*K. pneumoniae* at ×20,000 magnification. (**A**) CBR-*K. pneumoniae* (without treatment), (**B**) CBR-*K. pneumoniae* (treated with phytol), (**C**) CBR-*K. pneumoniae* (treated with glycitein), (**D**) CBR-*K. pneumoniae* (treated with quercetin), (**E**) CBR-*K. pneumoniae* (treated with ciprofloxacin), (**F**) ESBL-*K. pneumoniae* (without treatment), (**G**) ESBL-*K. pneumoniae* (treated with phytol), (**H**) ESBL-*K. pneumoniae* (treated with glycitein), (**I**) ESBL-*K. pneumoniae* (treated with quercetin), (**J**) ESBL-*K. pneumoniae* (treated with ciprofloxacin).

Phytol revealed potent antibiofilm activity for CBR and ESBL-*K. pneumoniae*, as evidenced in Figures 4.5B, G, where fewer clumps of attached microcolonies were observed, revealing a notable lessening in the quantity of biofilms with some of the cells being distances apart. A similar observation was recorded for ciprofloxacin, showing very few clumps of scattered cells (Figures 4.5E, J).

In comparison, the untreated biofilms formed by the two strains of *K. pneumoniae* revealed a compact arrangement of interconnected *K. pneumoniae* cells, thereby presenting continuous clumps and large aggregates of cells (Figures 4.5A, F). However, biofilms treated with glycitein only revealed a slight distance amongst the cells of CBR-*K. pneumoniae* (Figure 4.5C), while the treatment was shown to shrink and disrupt cells of ESBL-*K. pneumoniae* with extruding materials and cell debris (Figure 4.5H). Quercetin was less effective compared with phytol and glycitein (Figures 4.5D, I); moreover, it showed lesser clumps of cells than the untreated biofilms.

4.3.8 PCR detection of virulence genes in *K. pneumoniae* strains

Gel electrophoresis of PCR products validated the presence of virulence genes such as *mrkA*, *luxS, rcsA* and the housekeeping gene (*16srRNA*) in CBR and ESBL producing *K. pneumoniae*. Sizes of the genes were also indicated as 115 bp for *mrkA*, 180 bp for *luxS* and *rcsA* and 161 bp for *16srRNA.* A representative gel electrophoresis image showing the four selected genes is shown in Appendix 4.1.

4.3.9 RNA quality determination

The integrity of the total RNA isolated from the treated and untreated *K. pneumoniae* strains was assessed by visualization of the 23S/16S banding pattern on a gel and shown to be intact (Appendix 4.2). The 260/280nm and 260/230nm absorbance ratios of the extracted RNA samples as determined spectrophotometrically ranged between 1.80nm and 2.50nm.

4.3.10 Expression levels of *mrkA*, *rcsA* and *luxS* genes quantified by qPCR

4.3.10.1 Fold change of genes due to treatment

The expressions of *mrkA* (biofilm-associated gene), *rcsA* (exopolysaccharide biosynthesis gene) and *luxS* (AI-2 quorum sensing S-ribosylhomocysteinase protein-coding gene) in CBR and ESBL-*K. pneumoniae* strains were compared using the cycle threshold (Ct) values. Differences in Ct values were observed among the genes subjected to treatment with selected phytochemicals and controls showing mean Ct values ranging from 20.477 to 30.186 for the two *K. pneumoniae* strains (Table 4.8).

Table 4.8: Ct values obtained for the genes subjected to treatment with selected phytochemicals and controls in the *K. pneumoniae* strains

Samples	Ct values	
	CBR-*K. pneumoniae*	**ESBL-*K. pneumoniae***
Phytol-*Mrk A*	24.780	26.012
Camphene-*RcsA*	27.699	27.658
Ciprofloxacin-*LuxS*	25.134	25.782
Ciprofloxacin-*MrkA*	24.187	26.323
Ciprofloxacin-*RcsA*	27.422	27.435
Quercetin-*LuxS*	25.414	25.001
Quercetin-*MrkA*	20.477	24.914
Quercetin-*RcsA*	26.278	30.186

Results of the comparative relative expression of the genes targeted with different treatments on *K. pneumoniae* strains calculated relative to the untreated *K. pneumoniae* strains are illustrated in Figure 4.6. The results revealed that the mRNA levels of *mrkA* and *rcsA* genes were significantly downregulated after treatment with a subminimum inhibitory concentration of phytol and camphene respectively (Figure 4.6).

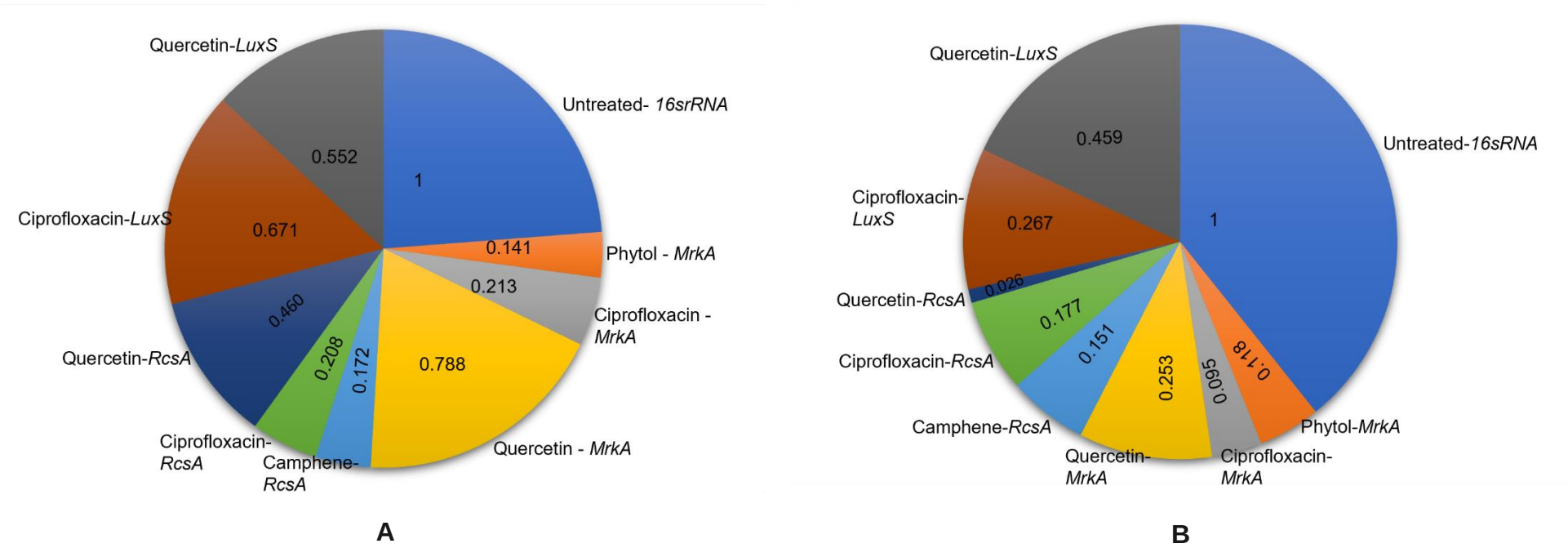

Figure 4.6: Fold change in mRNA levels of *mrkA, rcsA* and *luxS* target genes in treated *K. pneumoniae* strains. **A**: CBR-*K. pneumoniae*, **B**: ESBL-*K. pneumoniae*.

4.3.10.2 Fold expression ratio relative to control

The fold expression ratio relative to control revealed varying values between 0.607 (60.7%) and 1.00 (100%). For CBR-*K. pneumoniae*, *mrkA* gene targeted with phytol revealed a fold expression value of 0.662 (66.2%), compared to the untreated strain (*16SrRNA* as control) which had the value of 1.00 (100%) (Figure 4.7A), indicating the antibiofilm activity of phytol at the transcriptional level.

Phytol showed a better reduction in the expression level of *mrkA* compared to ciprofloxacin and quercetin which revealed fold expression values of 0.776 (77.6%) and 0.983 (98.3%) respectively (Figure 4.7A). Furthermore, the *rcsA* gene targeted with camphene showed a reduced fold expression value of 0.722 (72.2%), while ciprofloxacin and quercetin had 0.770 (77%) and 0.896 (89.6%) respectively (Figure 4.7A). *LuxS* gene targeted with ciprofloxacin and quercetin revealed a slight downregulation with fold expression values of 0.929 (92.9%) and 0.913 (91.3%) respectively compared to the control (Figure 4.7A).

Similarly, for ESBL-*K. pneumoniae*, phytol revealed downregulation of the *mrkA* gene with a fold expression value of 0.607 (60.7%) as compared to quercetin (0.816; 81.6%) (Figure 4.7B). *RcsA* gene targeted with camphene was also shown to be downregulated (fold expression value of 0.693; 69.3%), which revealed a slightly better result in comparison to ciprofloxacin (0.737; 73.7%). However, quercetin revealed a negative fold expression value of -0.771 (-77.1%) (Figure 4.7B). Ciprofloxacin and quercetin which targeted the *luxS* gene showed slight downregulation when compared to the control sample with values of 0.826 (82.6%) and 0.899 (89.9%) respectively (Figure 4.7B).

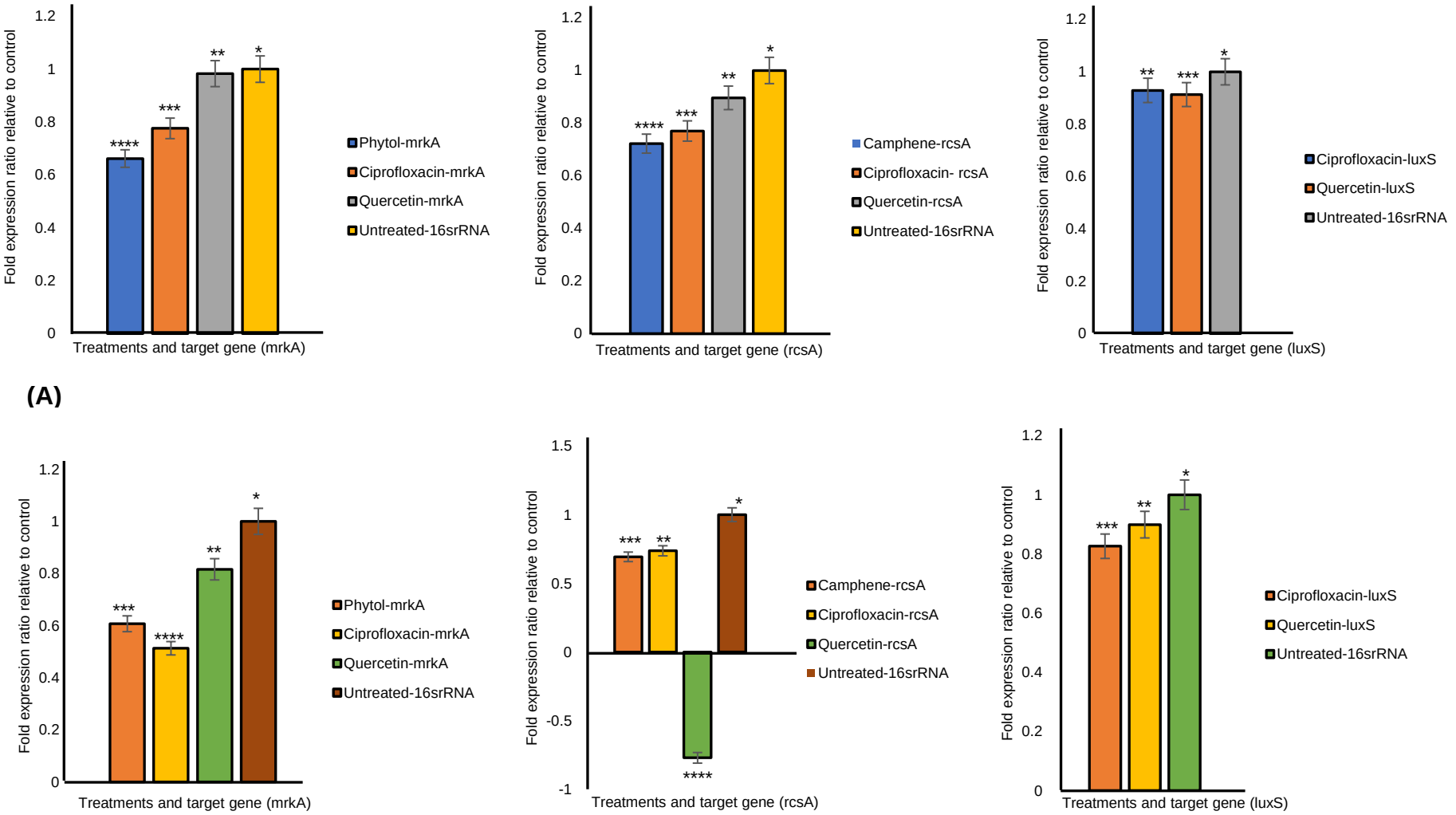

Figure 4.7: Relative gene expression of **(A)**: CBR-*K. pneumoniae* and **(B):** ESBL-*K. pneumoniae* following treatment with a subminimum inhibitory concentration of phytochemical compounds and positive controls, represented as fold difference between treated samples targeting *mrkA, rcsA* and *luxS* gene. Transcripts were normalized to *16S rRNA* and results were calculated as fold change relative to gene expression values obtained for untreated ESBL-*K. pneumoniae* strain. Data are mean ± standard deviation of three independent experiments performed with four technical replicates.

4.3.11 Cytotoxicity activity of phytochemical compounds

The cytotoxicity test was carried out on Vero cells as these epithelial non-malignant cells are a well-defined experimental setting for cytotoxicity studies. Treatment with compounds exhibited a decrease in cell viability in a dose-dependent manner, whereby the compounds had a cytostatic effect on the cells at a higher concentration as presented in Table 4.9. Experiments included DMSO at different concentrations (range 0.1 – 0.008%) and it didn't interfere with cell metabolism. The principles of cell viability and cytotoxicity assays are based on various cell functions such as enzyme activity, cell membrane permeability, cell adherence, ATP production, co-enzyme production and nucleotide uptake ability, resulting in either cytotoxic effect (destroying/killing of cells) or cytostatic effect (prevention/inhibition of cells).

Based on the results, phytol exhibited no cytotoxic effect on the Vero cells, approximately 100% ($p < 0.05$) of the cell's viability was maintained even at the highest tested concentration (0.25 mg/mL), as presented in Table 4.9. Camphene showed above 60% cell viability at a concentration of 0.25 mg/mL. The positive controls, doxorubicin and quercetin reduced cell viability by 43.18% and 10.23%, particularly at higher concentrations of 0.25 mg/mL. All compounds maintained the cell's viability above 50% at 0.125 mg/mL as presented in Table 4.9 except for quercetin which showed 50% cell viability at a concentration of 0.0312 mg/mL.

Lactate dehydrogenase (LDH) is a firm cytoplasmic enzyme demonstrated in all types of cells and released into the cell culture medium due to the damaged plasma membrane. Therefore, the cytotoxicity activity (LDH) of compounds was measured and is presented in Table 4.9. The findings indicated that the compounds exerted a cytostatic effect on Vero metabolism rather than a cytotoxic effect. Compounds of camphene and phytol had no cytotoxic effect in all tested concentrations on mammalian cells. Doxorubicin had a cytotoxic effect on Vero cells with maximum LDH activity at 33.20% and 22.63% respectively at the highest concentration of 0.25 mg/mL (Table 4.9).

The micrograph images revealing the morphological changes of the Vero cells after being treated with compounds are shown in Appendix 4.3. Appendix 4.3B represent camphene at 0.062 mg/mL concentration, where it was shown that cells maintained their cellular morphology. Whereas doxorubicin showed high cell confluency at

concentrations of 0.062 mg/mL and 0.125 mg/mL (Appendix 4.3E). Phytol showed higher confluency of cells even at a lower concentration of 0.002 mg/mL as presented in Appendix 4.3C. Quercetin maintained the cell's morphology even at the highest concentration as shown in Appendix 4.

Table 4.9: Percentage (%) cell viability and lactate dehydrogenase (LDH) activity on Vero cells (ATCC CCL81) at different concentrations (mg/mL) of the compounds

Concentrations (mg/mL)	Percentage (%) cell viability relative to the untreated Vero cells (ATCC CCL81) at different concentrations (mg/mL) of the compounds				Lactate dehydrogenase (LDH) activity on Vero cells (ATCC CCL81) at different concentrations (mg/mL) of the compounds			
	Camphene	Phytol	Quercetin	Doxorubicin	Camphene	Phytol	Quercetin	Doxorubicin
0.002	71.50±1.94 [b, c]	106.56±8.49 [a]	82.70±4.07 [a]	79,04±17,31 [a, b]	2,52±4,18[a]	2.08±1.17 [c]	-10,95±1,92 [c]	-4.44±3,24 [b]
0.004	68.94±9.56 [b]	106.27±2.08 [a]	80.15±21.53 [a, b]	74,16±24,02 [a, b]	-2,00±4,53 [a]	-1.43±0.26 [b]	-6,71±3,35 [b]	1,29±3,44 [a]
0.007	68.59±1.61 [b]	102.58±4.03 [a]	66.60±12.08 [b]	71,73±13,59 [a, b]	-4,16±1,14 [b]	-1.61±0.45 [c]	-8,18±3,19 [c]	8,90±1,90 [a]
0.016	68.37±5.19 [b]	101.24±7.47 [a]	63.85±17.10 [b]	69,90±16,38 [b]	-5,10±1,37 [b]	-4.85±0.16 [c]	-7,98±3,33 [d]	9,82±1,77 [a]
0.031	68.00±4.66 [b]	98.61±5.61 [a]	63.81±1.85 [b]	69,05±11,69 [b]	0,00±6,02 [a]	-1.63±0.35 [b]	-11,35±1,47 [b]	8,73±0,84 [a]
0.062	66.89±3.22 [b]	96.72±10.53 [a]	49.83±31.57 [b]	59,72±3,86 [b]	-0,37±4,40 [b]	-1.69±0.18 [c]	-6,54±1,84 [c]	16,50±5,43 [a]
0.125	66.00±4.35 [a, b]	92.72±2.16 [a]	42.11±8.16 [b]	56,27±8,26 [b]	-5,49±2,41 [b]	-0.75±0.27 [c]	-3,38±2,59 [c]	22,53±3,93 [a]
0.25	63.43±0.78 [a]	92.28±5.24 [a]	10.23±4.93 [c]	43,18±2,83 [b]	-4,03±8,95 [a]	-4.13±0.99 [b]	-4,02±2,00 [b]	33,20±3,39 [a]

Means are values of triplicate independent experiments ± SD. Treatments with phytochemical compounds were compared based on concentrations. Means that do not share a letter are statistically significant. Comparison for each concentration of the compounds is presented with different letters (a–d) and are significantly different ($p \leq 0.05$).

4.4 DISCUSSION

Phytochemicals have vast advantages over synthetic compounds, including green status and unique modes of action, which could aid in the fight against antibiotic resistance. Hence, they are emphasized as a valuable source of novel bioactive compounds that is both sustainable and abundant (Borges et al., 2015). Furthermore, they have been identified as a promising source of quorum-sensing inhibitors, disrupting bacterial cell-to-cell communication, which enables pathogenicity and for bacteria to withstand antimicrobial substances through biofilm formation and other virulence factors (Borges et al., 2016). These phytochemicals often have a wide range of chemical variety, structural complexity, and biological activity (Borges et al., 2016), making them promising tools for the management of illnesses, especially biofilm-related infections in an era where the supply of effective antibiotics is no longer guaranteed (Monte et al., 2014). New sources of antimicrobials and tactics for effective biofilm inhibition and/or eradication are unquestionably necessary. Therefore, the discovery of phytochemicals targeting distinct stages of biofilm formation, such as adhesion, motility and EPS generation, including other biofilm-related virulence factors, is imperative (Barbieri et al., 2017). As such, the effects of phytochemical compounds at different stages of biofilm formation and associated virulence factors in CBR and ESBL-*K. pneumoniae* were explored in this chapter.

The five studied compounds (alpha-terpinene, camphene, fisetin, glycitein and phytol) were first validated for their antibacterial effect on the growth of CBR and ESBL-*K. pneumoniae* strains. The findings revealed MIC values ranging from 0.0625 to 0.25 mg/mL (Table 4.3). Of the five compounds, fisetin showed a MIC value of 0.0625 mg/mL for CBR-*K. pneumoniae,* as well as quercetin and ciprofloxacin (the positive controls), indicative of significant activity. This suggests that fisetin and quercetin are potential antibacterial agents against the studied pathogen. Their potent activity can be attributed to the mode of action of flavonoids, which includes the interaction of phytochemical compounds with bacterial proteins and cell wall structures (Lahiri et al., 2019). This is congruent with the suggestions of Gibbons (2004) and Mamabolo et al. (2018), where the antimicrobial activity of a phytochemical compound or single entity compound is defined as significant when the MIC value is ≤ 0.064mg/mL or ≤ 0.01mg/mL, respectively.

Other tested compounds revealed MIC values greater than 0.1 mg/mL; hence, they are regarded as compounds with low antibacterial activity. According to Mbaveng et al. (2015), the MIC activity of a compound is considered low when it is greater than 100 µg/mL or 0.1 mg/mL. The low MIC values obtained may be due to the protective outer membrane present in *K. pneumoniae*, being a GNB (Cosa et al., 2020). In addition, they can also be attributed to the ability of *K. pneumoniae* to actively efflux the compounds from the cell, forming a capsule that shields the cell from being penetrated by the compounds or changing its phytocompound target. The low MIC values, however, do not completely rule out the bioactive potentials of these compounds as they possess a broad range of biological activities. Cosa et al. (2019) and Vasavi et al. (2016) reported that in some cases, compounds of natural origin may yield poor MIC values, but they can interfere with the QS signalling mechanism and inhibit virulence at sub-MIC concentrations. Hence, the compounds were further assessed for their biofilm-associated anti-virulence activities.

Because biofilms are supported by a matrix of polymeric compounds known as extracellular polymeric substances (EPS), often composed of exopolysaccharides that are secreted into the environment (Rabin et al., 2015), it was assessed as one of the contributing virulence factors. *Klebsiella pneumoniae*'s exopolysaccharides generally contain rare sugars such as L-fucose, L-rhamnose, or uronic acids (Kumar et al., 2007; Patro & Rathinavelan, 2019). Based on the findings, the exopolysaccharide reduction assay revealed that both phytol and camphene showed the highest percentage inhibition of EPS (65.91%) for ESBL-*K. pneumoniae*, while camphene revealed the greatest reduction in exopolysaccharide production (43.80%) in CBR-*K. pneumoniae* (Figure 4.1).

Similar findings were reported by Srinivasan et al. (2017), where phytol significantly inhibited the EPS production in *Serratia marcescens* to the level of 32% and 39% at 5 and 10 µg/mL concentrations, respectively, while no significant level of EPS inhibition was shown by the control. The bioactive potential of camphene observed in this study is congruent with the submission of Hachlafi et al. (2021), where camphene inhibited pathogenicity in a wide range of pathogenic bacteria, such as *Klebsiella pneumoniae, Staphylococcus aureus* and *Escherichia coli.* Based on the findings, the reduction in EPS in *K. pneumoniae* by the active phytochemical compounds suggests their

potential to disrupt biofilm-associated virulence factors. This is because EPS production is a key factor which forms the framework in microbial biofilms.

The validation of reduced exopolysaccharides in *K. pneumoniae* was performed using AFM, a powerful technique for imaging the surfaces of microbial cells (Huang et al., 2015). It has been reported as a vital tool in characterizing the topographic features of microbial exopolysaccharides (Zhao et al., 2019). Dufrêne (2014) also confirmed that AFM imaging allows the observation of cell wall components directly on live cells, such as polysaccharides, peptidoglycan, teichoic acids, among others, and has aided in elucidating their roles in cellular processes such as adhesion. When AFM imaging was employed in this study to analyse the surface topology of treated and untreated *K. pneumoniae* exopolysaccharides, the untreated strains resulted in the formation of a clear detectable EPS network composed of unevenly distributed and compact lumps (Figure 4.2A1, F1). The lumps may be formed due to the intra- and intermolecular aggregation of polysaccharide macromolecules (Banerjee et al., 2020). This high conformational rigidity of EPS might function as a polymeric scaffold used by bacteria to build biofilms (Foschiatti et al., 2009). The surface topography of EPS treated with phytol and camphene on the other hand revealed scarce EPS polymers which were generally thinner and often showed irregular shapes, similar to the positive control (ciprofloxacin) (Figure 4.2B1, C1, G1, H1). These compounds showed a significant reduction in the height and surface roughness of *K. pneumoniae* EPS. This validates the results obtained from the *in-vitro* phenol sulfuric acid method of EPS biomass measurement.

Curli, a type of fimbriae composed of proteins called curlins and functional amyloid surface fiber, is another prominent virulence factor in *K. pneumoniae* known to be involved in cell attachment to surfaces, as well as cell aggregation, which allows the formation of biofilms (Anes et al., 2017). Curli are effective inducers of the host inflammatory response and often mediate host cell adhesion and invasion (Chaudhary & Payasi, 2012). The results demonstrated that phytochemicals such as phytol, glycitein, fisetin and quercetin (0.5 and 1.0 mg/mL) efficiently inhibited the formation of curli in the *K. pneumoniae* strains (Table 4.5). According to a study by Gupta et al. (2012), cranberry, which contains diverse bioactive phytochemical compounds, inhibited the expression of curli in *Escherichia coli* and resulted in a loss of epithelial cell colonization. This suggests that certain phytochemical compounds can bind to

curli, and fimbriae as observed in this study, thereby preventing them from attaching to the host tissue. According to Kikuchi et al. (2005), studies have shown that curli and other cell surface structures play a significant role in the development of biofilm in *E. coli*, an *Enterobacteriaceae* similar to *K. pneumoniae*. Understanding and inhibiting biofilm-forming structures such as curli are crucial for the development of therapeutics that can reduce biofilm formation and host colonization (Barnhart & Chapman, 2010).

Furthermore, virulence in *K. pneumoniae* can also be attributed to efficient iron uptake, poor sedimentation, and the copious synthesis of a capsule, which confers a hypermucoviscous phenotype (Sánchez-López et al., 2019; Mikei et al., 2021). The effect of the studied phytochemical compounds on the hypermucoviscosity of *K. pneumoniae* was examined using the string test. The results reveal glycitein and fisetin as the compounds showing the best inhibition at 1.0 mg/mL for both strains, alongside phytol for ESBL-*K. pneumoniae* (Figure 4.4). The viscosity-lowering effect of the compounds, as seen in this study, is proportional to their concentrations, as none of the compounds examined at the lowest concentration (0.125 mg/mL) showed any reduction in the hypermucoviscosity phenotype. A similar observation was also recorded in the study of Jabuk (2016), where viscosity inhibition was observed in a dose-dependent manner. Lin et al. (2013) reported a decrease in *K. pneumoniae* mucoviscosity, and capsular polysaccharide production by *Fructus mume* in a dose-dependent manner, thereby reducing the resistance of *K. pneumoniae* to serum killing.

K. pneumoniae can produce a thick extracellular matrix that promotes bacterial adhesion to living or non-living surfaces, preventing antibiotic penetration and lowering the effects of treatments (Nirwati et al., 2019). Again, the host defenses may be improved if any stage in the formation of the biofilm's structure is interrupted, resulting in better treatment outcomes. Hence, this study examined the effect of phytochemical compounds on initial cell attachment, preformed biofilm, and mature biofilm formation.

The results of the initial cell attachment inhibition reveal that phytol showed good activity on both strains of *K. pneumoniae* tested following the criteria stated by Famuyide et al. (2019), having >50% inhibition (Table 4.6). Reports on the anti-adhesion activity of the studied compounds on *K. pneumoniae* are limited; however, Ramanathan et al. (2018) reported a good anti-biofilm activity of phytol, showing up to 60% biofilm inhibition in another notorious biofilm former, *Acinetobacter baumannii,* at concentrations ranging from 5 to 640 µg/mL. Congruent to the findings in this chapter,

Srinivasan et al. (2017) also reported a decrease in the level of metabolically active cells involved in biofilm formation in phytol treatment compared with their respective controls. This corroborates the submission of Ramanathan et al. (2018), that phytol is a potential anti-biofilm agent, as it can inhibit or halt the formation of biofilms, making them more receptive to treatments. On the other hand, glycitein, camphene, fisetin, alpha-terpinene and quercetin showed weak anti-adhesion activity, having percentage inhibition values <49%. The weak activity observed might be attributed to the interference of the hydrogen bonds, electrostatic forces, and van der Waals forces of interaction within the biofilm, which often mediates the initial attachment of the sessile group of cells to solid surfaces (Lahiri et al., 2019).

Furthermore, the results revealed a reduced inhibition of the microcolony formation stage by the compounds (Table 4.6). This suggests that biofilms can be better inhibited during the initial cell attachment stage than when they begin to develop. A similar trend was observed for the inhibition of mature biofilm, where the biofilms had accumulated biomass. These findings are in tandem with results obtained in a study carried out by Mombeshora et al. (2021), where the compound tested did not have any disruptive effect on mature (72 h) biofilms of *P. aeruginosa*, a Gram-negative bacterium like *K. pneumoniae*. This can also be attributed to the opinion of Kelmanson et al. (2000), who noted that more resistance to external agents is often shown once biofilms have been fully established; therefore, the disruption of mature biofilms tends to require higher doses of disrupting agents than those needed to destroy planktonic cells. Additionally, difficulty in the disruption of mature biofilms might result from the slow or incomplete penetration of the treatments to the established biofilm population or an altered biochemical microenvironment within the biofilm (Lebeaux et al., 2014). Other studies by Baloyi et al. (2021) and Sarkar et al. (2014) have also shown that eradicating biofilms is challenging, as various biofilm-forming microorganisms have demonstrated resilience.

The effect of the phytochemical compounds on the inhibition of mature *K. pneumoniae* biofilm was assessed under both static and dynamic conditions. The results revealed that *K. pneumoniae* biofilms formed under static (non-shaking) conditions had lower inhibition percentages compared with the mature biofilm formed under dynamic conditions (Table 4.7). This could be because more mature biofilms were formed without shaking compared with the biofilms formed while shaking; hence, the

treatment showed higher inhibitory activity on less mature biofilms formed while shaking. This result corroborates the findings of Wang et al. (2020), where a decrease was observed in the biofilm biomass attached to substratum surfaces under dynamic conditions compared with the static condition. The difference in mature biofilms generated with and without shaking can be attributed to shear force, which is one of the most decisive factors in the formation of biofilms in hydrodynamic conditions (Wang et al., 2020). Due to shear forces, bacteria that settled but could not adhere securely to the substratum surface might have been resuspended in the bulk liquid, resulting in relatively low levels of adherent biomass under dynamic conditions. Bacterial adhesion, which contributes to mature biofilm formation, is often inhibited when there is an increase in shear stress (Moreira et al., 2013).

An additional remarkable mechanism in biofilm formation is the distinctive biofilm architecture (Ramanathan et al., 2018). SEM micrographs of the structurally complex matrix architecture and the bacteria in that matrix were used to visually validate the inhibitory effect of phytol and glycitein against biofilms formed by the two *K. pneumoniae* strains. Exceptionally, phytol treatment led to a huge collapse in the extracellular matrix architecture of CBR-*K. pneumoniae* biofilms, resulting in individual cells and loose microcolonies adhering to the coverslip (Figure 4.5B). The images correlated well with the quantitative results of the crystal violet staining assay, which indicated that phytol possessed good antibiofilm activity against *K. pneumoniae*. Furthermore, glycitein influenced the integrity of the ESBL-*K. pneumoniae* cell wall (Figure 4.5F), making the cells incapable of maintaining their typical morphology in the presence of the treatment. Damaged cell walls and cellular leakages resulting from phytochemical compound treatment can eventually cause the death of microbial cells (Wijesinghe et al., 2021). The inhibition of the biofilm-forming ability and associated virulence factors in *K. pneumoniae* by selected phytochemical compounds could be an effective approach in controlling pathogenicity in this pathogen, hence, researchers are delving more into unravelling this science of survival.

Studies on the expression profiles of genes involved in biofilm formation (*mrkA*), exopolysaccharide production (*rcsA*) and quorum sensing (*luxS*) in *K. pneumoniae* after treatment with phytochemical compounds are however still limited in number. Therefore, this study further assessed the inhibitory effect of selected phytochemical compounds (phytol and camphene) and controls (quercetin and ciprofloxacin) on *K.*

pneumoniae's biofilm formation, exopolysaccharide production and AI-2 quorum sensing through the expression level of selected virulence genes (*rcsA, mrkA* and *luxS*) using a molecular approach. A molecular approach such as quantitative PCR (qPCR) is a prominent technique to understand fundamental cellular mechanisms and identify changes in gene expression levels in response to specific biological stimuli such as pharmacological agents (Yilmaz et al., 2012), hence, it was employed in this study.

The expression levels of *mrkA, rcsA* and *luxS* genes were quantified by qPCR. The fold change of the genes due to treatment by compounds and controls (phytol, camphene, quercetin and ciprofloxacin) were observed. Results revealed that the mRNA levels of *mrkA* and *rcsA* genes were significantly downregulated after treatment with a subminimum inhibitory concentration of phytol and camphene, respectively. This corroborates the *in-vitro* findings where phytol and camphene significantly inhibited biofilm formation and exopolysaccharide production respectively in ESBL and CBR *K. pneumoniae* strains. The fold expression ratio of the *mrkA* gene in CBR-*K. pneumoniae* relative to control was 0.662 (66.2%) to the ratio of 1.00 (100%) (Figure 4.6A), further indicating the antibiofilm activity of phytol at the transcriptional level.

After noting the downregulatory expression of selected virulence genes in *K. pneumoniae* strains by the studied phytochemical compounds, this study constituted an *in vitro* proof-of-concept on the cytotoxicity activities of the compounds. This is imperative because pharmaceutical safety is an essential factor in the development of every medicament (Bácskay et al., 2018), and should be evaluated before their impact in drug discovery is taken into consideration (Tshikalange & Hussein, 2010).

The cytotoxic effects of the compounds were investigated to ensure their safety using epithelial African green monkey kidney cells (Vero ATCC CCL-81), a cell line routinely used for *in vitro* cytotoxicity assessments. The results showed that phytol exhibited no cytotoxic effect on the Vero cells maintaining approximately 100% of the cell's viability at all the concentrations tested (Appendix 4.3). Findings also revealed that the phytochemical compounds of camphene, fisetin and alpha-terpenine showed above 60% cell viability at the concentration of 0.25 mg/mL which indicates that the majority of the cells are viable. Furthermore, the compounds had a concentration-dependent effect on the viability of cells and revealed a cytostatic effect on the cells at a higher concentration. A similar observation was recorded in a study conducted by Borges et

al. (2014), where the tested compounds had a concentration-dependent effect on the viability of cells. Higher doses of the phytochemical compounds were less toxic to the cells, which had a favourable impact on the viability of the cells. This supports the compounds' lack of cytotoxic effects and suggests their potential application for therapeutic purposes (Borges et al., 2014). The measured LDH activity showed that most of the tested compounds did not cause cell death in a dose-dependent manner (Table 4.9), hence revealing these compounds as promising leads for the development of novel drugs. Future studies can include investigating the activity of the compounds on human-associated cell lines and conducting *in vivo* biological assessments to validate their significance in manufacturing new pharmaceuticals (Asong et al., 2019).

4.5 CONCLUSION

In this chapter, a better knowledge of the efficacy of selected phytochemical compounds was acquired by investigating their antivirulence and antibiofilm activities where phytol proved to be the most potent antivirulence antibiofilm agent, inhibiting initial cell attachment as well as exopolysaccharide production, curli expression and hypermucoviscosity. AFM proved to be a useful tool for visualizing the effect of compounds on EPS production to corroborate the *in vitro* findings. The expression level of selected virulence genes in hypervirulent *K. pneumoniae* strains following treatment with selected phytochemical compounds was quantified using the quantitative real-time polymerase chain reaction (qPCR) assay. Findings revealed that phytol and camphene downregulated the expression of *mrkA* and *rcsA* genes, respectively, which are responsible for biofilm formation and exopolysaccharide production in *K. pneumoniae.* Furthermore, when the promising compounds were examined for safety through cell viability and cytotoxicity assessment, phytol further revealed no cytotoxic effect on the Vero cells while camphene revealed significant cell viability. Consequently, these intriguing compounds can be employed as a model in the search for new medications or as an alternative in regulating the pathogenicity of *K. pneumoniae*.

References

Adeosun, I. J., Oladipo, E. K., Ajibade, O. A., Olotu, T. M., Oladipo, A. A., Awoyelu, E. H., Alli, O. A. T., & Oyawoye, O. M. (2019). Antibiotic susceptibility of *Klebsiella pneumoniae* isolated from selected tertiary hospitals in Osun state, Nigeria. *Iraqi Journal of Science*, *60*(7), 1423–1429. *https://doi.org/10.24996/ijs.2019.60.7.2*

Adeosun, I. J., Baloyi, I. T., & Cosa, S. (2022). Anti-biofilm and associated anti-virulence activities of selected phytochemical compounds against *Klebsiella pneumoniae*. *Plants*, *11*(11),1–20. https://doi.org/10.3390/plants11111429

Alves, M. J., Ferreira, I. C. F. R., Froufe, H. J. C., Abreu, R. M. V., Martins, A., & Pintado, M. (2013). Antimicrobial activity of phenolic compounds identified in wild mushrooms, SAR analysis and docking studies. *Journal of Applied Microbiology*, *115*(2), 346–357. https://doi.org/10.1111/jam.12196

Anes, J., Hurley, D., Martins, M., & Fanning, S. (2017). Exploring the genome and phenotype of multi-drug resistant *Klebsiella pneumoniae* of clinical origin. *Frontiers in Microbiology*, *8*(10), 1–15. *https://doi.org/10.3389/fmicb.2017.01913*

Asong, J. A., Amoo, S. O., McGaw, L. J., Nkadimeng, S. M., Aremu, A. O., & Otang-Mbeng, W. (2019). Antimicrobial activity, antioxidant potential, cytotoxicity and phytochemical profiling of four plants locally used against skin diseases. *Plants*, *8*(9), 1–19.https://doi.org/10.3390/plants8090350

Baloyi, I. T., Adeosun, I. J., Yusuf, A. A., & Cosa, S. (2021). *In silico* and *in vitro* screening of antipathogenic properties of *Melianthus comosus* (Vahl) against *Pseudomonas aeruginosa*. *Antibiotics*, *10*(6), 1–23. *https://doi.org/10.3390/antibiotics10060679*

Bácskay, I., Nemes, D., Fenyvesi, F., Váradi, J., Vasvári, G., Fehér, P., Vecsernyés, M., & Ujhelyi, Z. (2018). Role of cytotoxicity experiments in pharmaceutical development. *Cytotoxicity,* 1–16. https://doi.org/10.5772/intechopen.72539

Banerjee, A., Das, D., Rudra, S. G., Mazumder, K., Andler, R., & Bandopadhyay, R. (2020). Characterization of exopolysaccharide produced by *Pseudomonas* sp. PFAB4 for synthesis of EPS-Coated AgNPs with antimicrobial properties. *Journal of Polymers and the Environment*, *28*(1), 242–256. https://doi.org/10.1007/s10924-019-01602-z

Barbieri, R., Coppo, E., Marchese, A., Daglia, M., Sobarzo-Sánchez, E., Nabavi, S. F., & Nabavi, S. M. (2017). Phytochemicals for human disease: An update on plant-derived compounds antibacterial activity. *Microbiological Research*, *196*, 44–68. https://doi.org/10.1016/j.micres.2016.12.003

Barnhart, M. M., & Chapman, M. R. (2010). Plaque assay for detecting lysogeny. *Annual Review of Microbiology*, *60*, 131–147. https://doi.org/10.1146/annurev.micro.60.080805.142106.Curli

Blando, F., Russo, R., Negro, C., De Bellis, L., & Frassinetti, S. (2019). Antimicrobial and antibiofilm activity against *Staphylococcus aureus* of *Opuntia ficus-indica* (L.) mill. cladode polyphenolic extracts. *Antioxidants*, *8*(5), 1–13. *https://doi.org/10.3390/antiox8050117*

Bonvicini, F., Belluti, F., Bisi, A., Gobbi, S., Manet, I., & Gentilomi, G. A. (2021). Improved eradication efficacy of a combination of newly identified antimicrobial agents in *C. albicans* and *S. aureus* mixed-species biofilm. *Research in Microbiology*, *172*(6), 1–8. https://doi.org/10.1016/j.resmic.2021.103873

Borges, A., Abreu, A. C., Dias, C., Saavedra, M. J., Borges, F., & Simões, M. (2016). New perspectives on the use of phytochemicals as an emergent strategy to control bacterial infections including biofilms. *Molecules*, *21*(7), 1–41. https://doi.org/10.3390/molecules21070877

Borges, A., Abreu, A. C., Ferreira, C., Saavedra, M. J., Simões, L. C., & Simões, M. (2015). Antibacterial activity and mode of action of selected glucosinolate hydrolysis products against bacterial pathogens. *Journal of Food Science and Technology*, *52*(8), 4737–4748. *https://doi.org/10.1007/s13197-014-1533-1*

Borges, A., Serra, S., Cristina Abreu, A., Saavedra, M. J., Salgado, A., & Simões, M. (2014). Evaluation of the effects of selected phytochemicals on quorum sensing inhibition and *in vitro* cytotoxicity. *Biofouling*, *30*(2), 183–195. *https://doi.org/10.1080/08927014.2013.852542*

Boucher, H. W., Talbot, G. H., Bradley, J. S., Edwards, J. E., Gilbert, D., Rice, L. B., Scheld, M., Spellberg, B., & Bartlett, J. (2009). Bad bugs, no drugs: No ESKAPE! An update from the Infectious Diseases Society of America. *Clinical Infectious Diseases*, *48*(1), 1–12. https://doi.org/10.1086/595011

Camele, I., Elshafie, H. S., Caputo, L., Sakr, S. H., & De Feo, V. (2019). *Bacillus mojavensis:* Biofilm formation and biochemical investigation of its bioactive metabolites. *Journal of Biological Research, 92*(1), 39–45. https://doi.org/10.4081/jbr.2019.8296

Chaudhary, M., & Payasi, A. (2012). Role of EDTA and CSE1034 in curli formation and biofilm eradication of *Klebsiella pneumoniae*: A comparison with other drugs. *Journal of Antibiotics*, *65*(12), 631–633. https://doi.org/10.1038/ja.2012.82

Chung, P. Y. (2016). The emerging problems of *Klebsiella pneumoniae* infections: Carbapenem resistance and biofilm formation. *FEMS Microbiology Letters*, *363*(20), 1–6. https://doi.org/10.1093/femsle/fnw219

Cosa, S., Chaudhary, S. K., Chen, W., Combrinck, S., & Viljoen, A. (2019). Exploring common culinary herbs and spices as potential anti-quorum sensing agents. *Nutrients*, *11*(4), 1–17. https://doi.org/10.3390/nu11040739

Cosa, S., Rakoma, J. R., Yusuf, A. A., & Tshikalange, T. E. (2020). *Calpurnia aurea* (Aiton) Benth extracts reduce quorum sensing controlled virulence factors in *Pseudomonas aeruginosa*. *Molecules*, *25*(10), 1–21. https://doi.org/10.3390/molecules25102283

De la Fuente-Núñez, C., Reffuveille, F., Fernández, L., & Hancock, R. E. W. (2013). Bacterial biofilm development as a multicellular adaptation: Antibiotic resistance and new therapeutic strategies. *Current Opinion in Microbiology*, *16*(5), 580–589. https://doi.org/10.1016/j.mib.2013.06.013

De Paula Ramos, L., Da Rocha Santos, C. E., Camargo Reis Mello, D., Nishiama Theodoro, L., De Oliveira, F. E., Back Brito, G. N., Campos Junqueira, J., Cardoso Jorge, A. O., & Dias De Oliveira, L. (2016). *Klebsiella pneumoniae* planktonic and biofilm reduction by different plant extracts: *In vitro* study. *Scientific World Journal*, 1–5. https://doi.org/10.1155/2016/3521413

Divakar, S., Lama, M., & Asad U., K. (2019). Antibiotics versus biofilm: An emerging battleground in microbial communities. *Antimicrobial Resistance and Infection Control*, *3*, 1–10.

Donlan, R. M. (2001). Biofilm formation: A clinically relevant microbiological process. *Clinical Infectious Diseases*, *33*(8), 1387–1392. https://doi.org/10.1086/322972

Dufrêne, Y. F. (2014). Atomic force microscopy in microbiology: New structural and functional insights into the microbial cell surface. *MBio*, *5*(4), 1–14. https://doi.org/10.1128/mBio.01363-14

Famuyide, I. M., Aro, A. O., Fasina, F. O., Eloff, J. N., & McGaw, L. J. (2019). Antibacterial and antibiofilm activity of acetone leaf extracts of nine under-investigated South African *Eugenia* and *Syzygium* (*Myrtaceae*) species and their selectivity indices. *BMC Complementary and Alternative Medicine*, *19*(1), 1–13. https://doi.org/10.1186/s12906-019-2547-z

Fils, P. E. L., Cholley, P., Gbaguidi-Haore, H., Hocquet, D., Sauget, M., & Bertrand, X. (2021). ESBL-producing *Klebsiella pneumoniae* in a university hospital: Molecular features, diffusion of epidemic clones and evaluation of cross-transmission. *PLoS ONE*, *16*(3), 1–9. *https://doi.org/10.1371/journal.pone.0247875*

Foroohimanjili, F., Mirzaie, A., Hamdi, S. M. M., Noorbazargan, H., Hedayati Ch, M., Dolatabadi, A., Rezaie, H., & Bishak, F. M. (2020). Antibacterial, antibiofilm, and antiquorum sensing activities of phytosynthesized silver nanoparticles fabricated from *Mespilus germanica* extract against multidrug resistance of *Klebsiella pneumoniae* clinical strains. *Journal of Basic Microbiology*, *60*(3), 216–230. https://doi.org/10.1002/jobm.201900511

Foschiatti, M., Cescutti, P., Tossi, A., & Rizzo, R. (2009). Inhibition of cathelicidin activity by bacterial exopolysaccharides. *Molecular Microbiology*, *72*(5), 1137–1146. *https://doi.org/10.1111/j.1365-2958.2009.06707.x*

França, A., Freitas, A. I., Henriques, A. F., & Cerca, N. (2012). Optimizing a qPCR gene expression quantification assay for *S. epidermidis* biofilms: A comparison between commercial kits and a customized protocol. *PLoS ONE*, *7*(5), 1–9. https://doi.org/10.1371/journal.pone.0037480

Gibbons, S. (2004). Anti-staphylococcal plant natural products. *Natural Product Reports*, *21*(2), 263–277. https://doi.org/10.1039/b212695h

Gopu, V., & Shetty, P. H. (2016). Cyanidin inhibits quorum signalling pathway of a food-borne opportunistic pathogen. *Journal of Food Science and Technology*, *53*(2), 968–976. https://doi.org/10.1007/s13197-015-2031-9

Gupta, A., Dwivedi, M., Mahdi, A. A., Gowda, G. A. N., Khetrapal, C. L., & Bhandari, M. (2012). Inhibition of adherence of multi-drug resistant *E. coli* by proanthocyanidin. *Urological Research*, *40*(2), 143–150. https://doi.org/10.1007/s00240-011-0398-2

Hachlafi, N. E. L., Aanniz, T., Menyiy, N. El, Baaboua, A. El, Omari, N. El, Balahbib, A., Shariati, M. A., Zengin, G., Fikri-Benbrahim, K., & Bouyahya, A. (2021). *In vitro* and *in vivo* biological investigations of camphene and its mechanism insights: A Review. *Food Reviews International*, *00*(00), 1–28. https://doi.org/10.1080/87559129.2021.1936007

Huang, Q., Wu, H., Cai, P., Fein, J. B., & Chen, W. (2015). Atomic force microscopy measurements of bacterial adhesion and biofilm formation onto clay-sized particles. *Scientific Reports*, *5*(6), 1–12. https://doi.org/10.1038/srep16857

Jabuk, S. I. A. (2016). *In vitro* and *in vivo* effect of three aqueous plant extract on pathogenicity of *Klebsiella pneumoniae* isolated from patient with urinary tract infection. *World Journal of Pharmaceutical Research, 3*, 160–179.

Kamiloglu, S., Sari, G., Ozdal, T., & Capanoglu, E. (2020). Guidelines for cell viability assays. *Food Frontiers*, *1*(3), 332–349. https://doi.org/10.1002/fft2.44

Karuppiah, P., & Mustaffa, M. (2013). Antibacterial and antioxidant activities of *Musa* sp. leaf extracts against multidrug resistant clinical pathogens causing nosocomial infection. *Asian Pacific Journal of Tropical Biomedicine*, *3*(9), 737–742. https://doi.org/10.1016/S2221-1691(13)60148-3

Kelmanson, J. E., Jager, A. K., & Staden, J. Van. (2000). Zulu medicinal plants with antibacterial activity. *Journal of Ethnopharmacology, 69*, 241–246.

Khan, J., Tarar, S. M., Gul, I., Nawaz, U., & Arshad, M. (2021). Challenges of antibiotic resistance biofilms and potential combating strategies: a review. *Biotech*, *11*(4), 1–15. https://doi.org/10.1007/s13205-021-02707-w

Kikuchi, T., Mizunoe, Y., Takade, A., Naito, S., & Yoshida, S. I. (2005). Curli fibers are required for development of biofilm architecture in *Escherichia coli* K-12 and enhance bacterial adherence to human uroepithelial cells. *Microbiology and Immunology*, *49*(9), 875–884. https://doi.org/10.1111/j.1348-0421.2005.tb03678.x

Kumar, A. S., Mody, K., & Jha, B. (2007). Bacterial exopolysaccharides - A perception. *Journal of Basic Microbiology*, *47*(2), 103–117. https://doi.org/10.1002/jobm.200610203

Lahiri, D., Dash, S., Dutta, R., & Nag, M. (2019). Elucidating the effect of anti-biofilm activity of bioactive compounds extracted from plants. *Journal of Biosciences*, *44*(2), 1–19. https://doi.org/10.1007/s12038-019-9868-4

Lebeaux, D., Ghigo, J.-M., & Beloin, C. (2014). Biofilm-related infections: Bridging the gap between clinical management and fundamental aspects of recalcitrance toward antibiotics. *Microbiology and Molecular Biology Reviews*, *78*(3), 510–543. https://doi.org/10.1128/mmbr.00013-14

Li, B., Zhao, Y., Liu, C., Chen, Z., & Zhou, D. (2014). Molecular pathogenesis of *Klebsiella pneumoniae*. *Future Microbiology*, *9*(9), 1071–1081. https://doi.org/10.2217/fmb.14.48

Lin, T. H., Huang, S. H., Wu, C. C., Liu, H. H., Jinn, T. R., Chen, Y., & Lin, C. T. (2013). Inhibition of *Klebsiella pneumoniae* growth and capsular polysaccharide biosynthesis by Fructus mume. *Evidence-Based Complementary and Alternative Medicine*, 1–10. https://doi.org/10.1155/2013/621701

Mamabolo, M. P., Muganza, F. M., Tabize Olivier, M., Olaokun, O. O., & Nemutavhanani, L. D. (2018). Evaluation of antigonorrhea activity and cytotoxicity of *Helichrysum caespititium* (DC) Harv. whole plant extracts. *Biology and Medicine*, *10*(1), 1–4. https://doi.org/10.4172/0974-8369.1000422

Mbaveng, A. T., Sandjo, L. P., Tankeo, S. B., Ndifor, A. R., Pantaleon, A., Nagdjui, B. T., & Kuete, V. (2015). Antibacterial activity of nineteen selected natural products against multi-drug resistant Gram-negative phenotypes. *SpringerPlus*, *4*(1), 1–9. https://doi.org/10.1186/s40064-015-1645-8

Mikei, L. A., Starki, A. J., Forsyth, V. S., Vornhagen, J., Smith, S. N., Bachman, M. A., & Mobley, H. L. T. (2021). A systematic analysis of hypermucoviscosity and capsule reveals distinct and overlapping genes that impact *Klebsiella pneumoniae* fitness. *PLoS Pathogens*, 17(3), 1–15. https://doi.org/10.1371/journal.ppat.1009376

Mombeshora, M., Chi, G. F., & Mukanganyama, S. (2021). Antibiofilm activity of extract and a compound isolated from *Triumfetta welwitschii* against *Pseudomonas aeruginosa. Biochemistry Research International*, 1–13. https://doi.org/10.1155/2021/9946183

Monte, J., Abreu, A. C., Borges, A., Simões, L. C., & Simões, M. (2014). Antimicrobial activity of selected phytochemicals against *Escherichia coli* and *Staphylococcus aureus* and their biofilms. *Pathogens*, *3*(2), 473–498. https://doi.org/10.3390/pathogens3020473

Moreira, J. M. R., Gomes, L. C., Araújo, J. D. P., Miranda, J. M., Simões, M., Melo, L. F., & Mergulhão, F. J. (2013). The effect of glucose concentration and shaking conditions on *Escherichia coli* biofilm formation in microtiter plates. *Chemical Engineering Science*, *94*, 192–199. https://doi.org/10.1016/j.ces.2013.02.045

Nirwati, H., Sinanjung, K., Fahrunissa, F., Wijaya, F., Napitupulu, S., Hati, V. P., Hakim, M. S., Meliala, A., Aman, A. T., & Nuryastuti, T. (2019). Biofilm formation and antibiotic resistance of *Klebsiella pneumoniae* isolated from clinical samples in a tertiary care hospital, Klaten, Indonesia. *BMC Proceedings*, *13*(11), 1–8. https://doi.org/10.1186/s12919-019-0176-7

Patole, S., Rout, M., & Mohapatra, H. (2021). Identification and validation of reference genes for reliable analysis of differential gene expression during antibiotic induced persister formation in *Klebsiella pneumoniae* using qPCR. *Journal of Microbiological Methods*, *182*(2), 1–7. https://doi.org/10.1016/j.mimet.2021.106165

Patro, L. P. P., & Rathinavelan, T. (2019). Targeting the sugary armor of *Klebsiella* Species. *Frontiers in Cellular and Infection Microbiology*, *9*(11), 1–23. https://doi.org/10.3389/fcimb.2019.00367

Rabin, N., Zheng, Y., Opoku-Temeng, C., Du, Y., Bonsu, E., & Sintim, H. O. (2015). Biofilm formation mechanisms and targets for developing antibiofilm agents. *Future Medicinal Chemistry*, *7*(4), 493–512. https://doi.org/10.4155/fmc.15.6

Ramanathan, S., Arunachalam, K., Chandran, S., Selvaraj, R., Shunmugiah, K. P., & Arumugam, V. R. (2018). Biofilm inhibitory efficiency of phytol in combination with cefotaxime against nosocomial pathogen *Acinetobacter baumannii*. *Journal of Applied Microbiology*, *125*(1), 56–71. https://doi.org/10.1111/jam.13741

Sánchez-López, J., García-Caballero, A., Navarro-San Francisco, C., Quereda, C., Ruiz-Garbajosa, P., Navas, E., Dronda, F., Morosini, M. I., Cantón, R., & Diez-Aguilar, M. (2019). Hypermucoviscous *Klebsiella pneumoniae*: A challenge in community acquired infection. *IDCases*, *17*, e00547. https://doi.org/10.1016/j.idcr.2019.e00547

Sánchez, E., Rivas Morales, C., Castillo, S., Leos-Rivas, C., García-Becerra, L., & Ortiz Martínez, D. M. (2016). Antibacterial and Antibiofilm Activity of Methanolic Plant Extracts against Nosocomial Microorganisms. *Evidence-Based Complementary and Alternative Medicine*,1–3. https://doi.org/10.1155/2016/1572697

Santana, H. F., Barbosa, A. A. T., Ferreira, S. O., & Mantovani, H. C. (2012). Bactericidal activity of ethanolic extracts of propolis against *Staphylococcus aureus* isolated from mastitic cows. *World Journal of Microbiology and Biotechnology*, *28*(2), 485–491. https://doi.org/10.1007/s11274-011-0839-7

Sarkar, R., Chaudhary, S. K., Sharma, A., Yadav, K. K., Nema, N. K., Sekhoacha, M., Karmakar, S., Braga, F. C., Matsabisa, M. G., Mukherjee, P. K., & Sen, T. (2014). Anti-biofilm activity of *Marula* - A study with the standardized bark extract. *Journal of Ethnopharmacology*, *154*(1), 170–175. https://doi.org/10.1016/j.jep.2014.03.067

Srinivasan, R., Mohankumar, R., Kannappan, A., Raja, V. K., Archunan, G., Pandian, S. K., Ruckmani, K., & Ravi, A. V. (2017). Exploring the anti-quorum sensing and antibiofilm efficacy of phytol against *Serratia marcescens* associated acute pyelonephritis infection in wistar rats. *Frontiers in Cellular and Infection Microbiology*, *7*(10), 1–18. *https://doi.org/10.3389/fcimb.2017.00498*

Tshikalange, T. E., & Hussein, A. (2010). Cytotoxicity activity of isolated compounds from *Elaeodendron transvaalense* ethanol extract. *Journal of Medicinal Plants Research*, *4*(16), 1695–1697.

Vasavi, H. S., Arun, A. B., & Rekha, P. D. (2016). Anti-quorum sensing activity of flavonoid-rich fraction from *Centella asiatica* L. against *Pseudomonas aeruginosa* PAO1. *Journal of Microbiology, Immunology and Infection*, *49*(1), 8–15. https://doi.org/10.1016/j.jmii.2014.03.012

Vestby, L. K., Grønseth, T., Simm, R., & Nesse, L. L. (2020). Bacterial biofilm and its role in the pathogenesis of disease. *Antibiotics*, *9*(2), 1–29. https://doi.org/10.3390/antibiotics9020059

Wang, J., Liu, Q., Dong, D., Hu, H., Wu, B., & Ren, H. (2020). *In-situ* monitoring of the unstable bacterial adhesion process during wastewater biofilm formation: A comprehensive study. *Environment International*, *140*(4), 1–8. https://doi.org/10.1016/j.envint.2020.105722

Wijesinghe, G. K., Feiria, S. B., Maia, F. C., Oliveira, T. R., Joia, F., Barbosa, J. P., Boni, G. C., & Höfling, J. F. (2021). *In-vitro* antibacterial and antibiofilm activity of *Cinnamomum verum* leaf oil against *Pseudomonas aeruginosa, Staphylococcus aureus* and *Klebsiella pneumoniae*. *Anais Da Academia Brasileira de Ciencias*, *93*(1), 1–11. https://doi.org/10.1590/0001-3765202120201507

Wijesundara, N. M., & Rupasinghe, H. P. V. (2018). Essential oils from *Origanum vulgare* and *Salvia officinalis* exhibit antibacterial and anti-biofilm activities against *Streptococcus pyogenes. Microbial Pathogenesis*, *117*(1), 118–127. https://doi.org/10.1016/j.micpath.2018.02.026

Wiskur, B. J., Hunt, J. J., & Callegan, M. C. (2008). Hypermucoviscosity as a virulence factor in experimental *Klebsiella pneumoniae* endophthalmitis. *Investigative Ophthalmology and Visual Science*, *49*(11), 4931–4938. https://doi.org/10.1167/iovs.08-2276

Yao, B., Xiao, X., Wang, F., Zhou, L., Zhang, X., & Zhang, J. (2015). Clinical and molecular characteristics of multi-clone carbapenem-resistant hypervirulent (hypermucoviscous) *Klebsiella pneumoniae* isolates in a tertiary hospital in Beijing, China. *International Journal of Infectious Diseases*, *37*, 107–112. *https://doi.org/10.1016/j.ijid.2015.06.023*

Yilmaz, A., Ilke, H., Alp, E., & Menevse, S. (2012). Real-Time PCR for gene expression analysis. In *polymerase chain reaction*, 1–27.https://doi.org/10.5772/37356

Zhao, D., Jiang, J., Du, R., Guo, S., Ping, W., Ling, H., & Ge, J. (2019). Purification and characterization of an exopolysaccharide from *Leuconostoc lactis* L2. *International Journal of Biological Macromolecules*, *139*, 1224–1231. *https://doi.org/10.1016/j.ijbiomac.2019.08.114*

CHAPTER FIVE

GENERAL CONCLUSIONS, RECOMMENDATIONS AND LIMITATIONS

5.1 OVERVIEW OF FINDINGS

The overall purpose of this research was to investigate the effectiveness of specific South African medicinal plants, which are traditionally used to treat infections caused by *K. pneumoniae*, in inhibiting its virulence. To assess the antivirulence properties of the plants and their phytochemical compounds, various techniques including *in-vitro, in-silico, in-situ* and molecular approaches were employed.

This study addressed the quest for understanding which South African medicinal plants possess the potential to manage *K. pneumoniae* infections by modulating its virulence factors. Additionally, the research aimed at determining how the SdiA transcriptional regulator protein, which encodes for QS and virulence in *K. pneumoniae* can be suppressed through phytochemical compounds using a molecular modelling approach. Furthermore, an inquiry was raised concerning the phytochemical compounds that may have the ability to decrease biofilm formation and associated virulence factors in *K. pneumoniae*. Afterwards, it became imperative to assess the impact of the active compounds on the expression and regulation of virulence genes in *K. pneumoniae,* as well as determine which of these phytochemicals are safe for use when evaluated for cytotoxic effects on non-malignant mammalian cells.

Findings from this study presented virulence factors' modulation in biofilm-forming *Klebsiella pneumoniae* via selected South African medicinal plants and phytochemical compounds, revealing an alternative strategy for the management of hypervirulent *K. pneumoniae* infections. Achievement of objectives, general conclusions, limitations of the study and recommendations are discussed below:

5.2 ACHIEVEMENT OF OBJECTIVES & GENERAL CONCLUSIONS

In this study, all specified objectives (chapter 1) were achieved, providing succinct answers to the research questions posed. Three South African medicinal plants namely *Carpobrotus dimidiatus, Helichrysum populifolium* and *Lippia javanica* that could be promising for the management of hypervirulent *K. pneumoniae* infections were identified and validated for their antibacterial activities. The studied plants revealed potentials as antibiofilm and anti-virulent agents against CBR and ESBL producing *K. pneumoniae* strains. *C. dimidiatus* (dichloromethane) showed notable

antibacterial activity revealing an MIC value of 0.78 mgmL, whereas *L. javanica* (ethyl acetate) was active against virulence factors such as biofilm formation and exopolysaccharide production at 67.25% and 36.95% respectively. *L. javanica* (ethyl acetate) also significantly reduced curli expression and hypermucoviscosity in the studied *K. pneumoniae* strains, hence, revealing it as a promising medicinal plant that can be investigated to develop alternative therapy for managing *K. pneumoniae* associated infections.

Furthermore, when *in-silico* techniques were employed in this study to validate the binding of some compounds in the studied plants; p-cymene, alpha-pinene, isoterpinolene, alpha-terpinene, phytol, 3-carene, beta-pinene, sabinene, camphene, fisetin, genistin, diadzein, quercetin, glycitein, phloretin, apigenin and biacalein (terpenes and flavonoids) were found to bind or modulate the SdiA's autoinducer binding site. The following criterion formed the basis of selecting the compounds as potential QS antagonistic compounds (i) structural similarity to the signal molecules; (ii) low molecular weight; (iii) hydroxyl group for a side chain compound; (iv) a five-membered lactone ring with an acyl group as a spacer and hydrophobic tail which enables binding to the active site by hydrogen bonding and hydrophobic interactions. Molecular dynamics simulations established the stability of the protein-ligand system, revealed the atomic and inter-atomic interactions of the protein-ligand complex and estimated the binding free energies of the compounds, indicative of drug potency. High binding free energies of -34.2996 and -43.2680 were obtained for biacalein (flavonoid) and phytol (terpene) respectively. The drug-likeness prediction of the selected compounds validated their drug potential conferring them as promising QSI drugs for *K. pneumoniae.*

In situ, AFM and SEM proved to be useful microscopy techniques for visualizing the effect of plant extracts and phytochemical compounds on biofilms and exopolysaccharides production, which helped to corroborate the *in vitro* findings. Amongst the phytochemical compounds evaluated in this study, phytol proved to be the most potent antivirulence antibiofilm agent, inhibiting initial cell attachment (54.71%) as well as exopolysaccharide production (65.91%), curli expression and hypermucoviscosity.

The expression level of selected virulence genes in hypervirulent *K. pneumoniae* strains following treatment with phytochemical compounds were quantified using the

quantitative real-time polymerase chain reaction (qPCR) assay. Phytol and camphene were shown to downregulate the expression of *mrkA* and *rcsA* genes respectively, which are responsible for biofilm formation and exopolysaccharide production in *K. pneumoniae.* Phytochemical compounds were also examined for safety through cell viability and cytotoxicity assessment where phytol revealed no cytotoxic effect on the Vero cells. Thus, these compounds can be suggested as safe, potential drug candidates for the development of alternative treatment options for *K. pneumoniae* infections.

5.3 CONTRIBUTION, LIMITATIONS AND RECOMMENDATIONS OF THE STUDY

5.3.1 Contribution of the study

This study contributes to scientific knowledge through a few published research articles and data has been disseminated through presentations at scientific conferences (highlighted in pages v-vi). In addition, the data provided from this research adds to the solutions required to lessen the MDR quandary, the lag in number of compounds documented as antipathogenic or antivirulence and to the threats posed by hypervirulent and multi-drug resistant *K. pneumoniae* strains through the exploration of plant extracts used in traditional medicine as well as their phytochemical compounds.

5.3.2 Limitations

A few limitations of this study are as follows:

- One of the studied medicinal plants (*Helichrysum populifolium*) is not available all year round. Its limited growth can be due to some significant factors such as drought, shade, temperature and nutrient scarcity. Hence, there is a need for a proper storage system to always ensure its availability for research.
- *MagA* virulence gene was not detected in the studied *K. pneumoniae* strains despite careful optimization of the PCR protocol in the laboratory and confirmation of the quality of primers using primer3plus and other primer designing software.
- The insolubility of some phytochemicals in water used for the preparation of 1% DMSO is a limitation in evaluating their bioactivities and testing for their

antivirulence activities. Low water solubility poses significant concerns for poor bioavailability, large dosage requirements, and undesirable side effects, which hampers the development of phytochemicals in the pharmaceutical sector and, in turn, the full utilization of these plant resources.

- Difficulty in detecting contamination issues when conducting highly sensitive PCR and qPCR assays. These contaminations and non-specific amplifications could result from the amplification of small quantities of DNA fragments from the laboratory environment, a DNA template amplified in a previous experiment or from contaminated reaction components. Some of the assays were repeated multiple times which resulted in an extended period of conducting the experiments as well as purchasing additional kits and primers in a bid to avoid contamination risks and misleading results.

5.3.3 Recommendations

This study should involve but not be restricted to the following:

- Determination of the initial safety of plant extracts and phytochemical compounds using different cell lines suitable to be used on human hosts.
- *In-vivo* studies to validate the *in-vitro* and *in-silico* drug-likeness findings of the selected compounds and to evaluate the side effects and safety of the compounds.
- Combining two or more phytochemical compounds to test for synergistic or antagonistic effects against the studied *K. pneumoniae* strains.
- Further exploration of the few unknown compounds revealed in the LC-MS mass spectra of the studied plants to fully unveil their identities and characterize them.
- Studying all the compounds separately with focus on other targets.

APPENDICES

Appendix 2.1: Ethics approval for the use of hypervirulent *K. pneumoniae* strains from the Faculty of Natural and Agricultural Sciences, University of Pretoria

UNIVERSITEIT VAN PRETORIA
UNIVERSITY OF PRETORIA
YUNIBESITHI YA PRETORIA

Faculty of Natural and Agricultural Sciences
Ethics Committee
E-mail: ethics.nas@up.ac.za

20 August 2021

ETHICS SUBMISSION: LETTER OF APPROVAL

Miss IJ Adeosun
Department of Microbiology and Plant Pathology
Faculty of Natural and Agricultural Science
University of Pretoria

Reference number: NAS157/2021
Project title: Anti-quorum sensing potential of selected South African medicinal plants on biofilm forming Klebsiella pneumoniae

Dear Miss IJ Adeosun,

We are pleased to inform you that your submission conforms to the requirements of the Faculty of Natural and Agricultural Sciences Research Ethics Committee.

Please note the following about your ethics approval:

- Please use your reference number (NAS157/2021) on any documents or correspondence with the Research Ethics Committee regarding your research.
- Please note that the Research Ethics Committee may ask further questions, seek additional information, require further modification, monitor the conduct of your research, or suspend or withdraw ethics approval.
- Please note that ethical approval is granted for the duration of the research (e.g. Honours studies: 1 year, Masters studies: two years, and PhD studies: three years) and should be extended when the approval period lapses.
- The digital archiving of data is a requirement of the University of Pretoria. The data should be accessible in the event of an enquiry or further analysis of the data.

Ethics approval is subject to the following:

- The ethics approval is conditional on the research being conducted as stipulated by the details of all documents submitted to the Committee. In the event that a further need arises to change who the investigators are, the methods or any other aspect, such changes must be submitted as an Amendment for approval by the Committee.
- **Applications using GM permits:** If the GM permit expires before the end of the study, please make an amendment to the application with the new GM permit before the old one expires
- **Applications using Animals:** NAS ethics recommendation does not imply that Animal Ethics Committee (AEC) approval is granted. The application has been pre-screened and recommended for review by the AEC. Research may not proceed until AEC approval is granted.

Post approval submissions including application for ethics extension and amendments to the approved application should be submitted online via the Ethics work centre.

We wish you the best with your research.

Yours sincerely,

Prof VJ Maharaj
Chairperson: NAS Ethics Committee

Appendix 3.1: Multiple sequence alignment result of SdiA (*Klebsiella pneumoniae*) with CviR (*Chromobacterium violaceum*), LasR (*Pseudomonas aeruginosa*) and SdiA (*Escherichia coli*)

```
2UV0_1|Chains             -------GAMALVDGFLELERSSGKLEWSA-----------------ILQKMASDLGFSK        36
tr|D3W065|D3W065_CHRVL    MVISKPINARPLPAGLT-ASQQWTLLEWIHMA----GHIETENELKAFLDQVLSQAPSER        55
tr|A6TB66|A6TB66_KLEP7    ------------------------------MLHQFQSMATGEEVYNLLQRETEALEYDY        29
sp|P07026|SDIA_ECOLI      -------------------MQDKDFFSWRRTMLLRFQRMETAEEVYHEIELQAQQLEYDY        41
                                                                    ::   .    .

2UV0_1|Chains             ILF--GLLPK-DSQDYENAFIVGNYPAAWREHYDRAGYARVDPTVSHCTQSVLPIFWEPS        93
tr|D3W065|D3W065_CHRVL    LLLALGRLNNQNQIQRLERVLNVSYPSDWLDQYMKENYAQHDPILRI-HLGQGPVMWEER       114
tr|A6TB66|A6TB66_KLEP7    YTL---CVRHPVPFTRPRVTFQSTYPRAWMSHYQAENYFAIDPVLRPENFMRGHLPWNDS        86
sp|P07026|SDIA_ECOLI      YSL---CVRHPVPFTRPKVAFYTNYPEAWVSYYQAKNFLAIDPVLNPENFSQGHLMWNDD        98
                            :    : :       .  :  .**  * . *   .:   ** :         : *:

2UV0_1|Chains             IYQTRKQ--HEFFEEASAAGLVYGLTMPLHGARGELGA-LSLSVEAENRAEANRFMESVL       150
tr|D3W065|D3W065_CHRVL    FNRAKGAEEKRFIAEATQNGMGSGITFSAASERNNIGSILSIA----GREPGRN--AALV       168
tr|A6TB66|A6TB66_KLEP7    LFRDAPA----LWDGARDHGLQKGVTQCLTLPNHAQGF-LSVS--ANNRLPGGYPEDELE       139
sp|P07026|SDIA_ECOLI      LFSEAQP----LWEAARAHGLRRGVTQYLMLPNRALGF-LSFS--RCSAREIPILSDELQ       151
                          :          :   *   *:  *:*      .   *  **.:    .          :

2UV0_1|Chains             PTLWMLKDYALQSGAGL-------AFEHPVSK----------------------------       175
tr|D3W065|D3W065_CHRVL    AMLNCLTPHLHQAAIRVANLPPASPSNMPLSQREYDIFHWMSRGKTNWEIATILDISERT       228
tr|A6TB66|A6TB66_KLEP7    LRLRTLTELSLLTLLR-LEDEMVMPPEMKFSRRELEILKWTAEGKTSAEVAMILSISENT       198
sp|P07026|SDIA_ECOLI      LKMQLLVRESLMALMR-LNDEIVMTPEMNFSKREKEILRWTAEGKTSAEIAMILSISENT       210
                            :  *      :            :  .*:

2UV0_1|Chains             ------------------------------------       175
tr|D3W065|D3W065_CHRVL    VKFHVANVIRKLNANNRTHAIVLGMHLAMPPSTVANE      265
tr|A6TB66|A6TB66_KLEP7    VNFHQKNMQRKFNAPNKTQIACYAVATGLI-------      228
sp|P07026|SDIA_ECOLI      VNFHQKNMQKKINAPNKTQVACYAAATGLI-------      240
```

Appendix 3.2: Prediction of the conserved domain

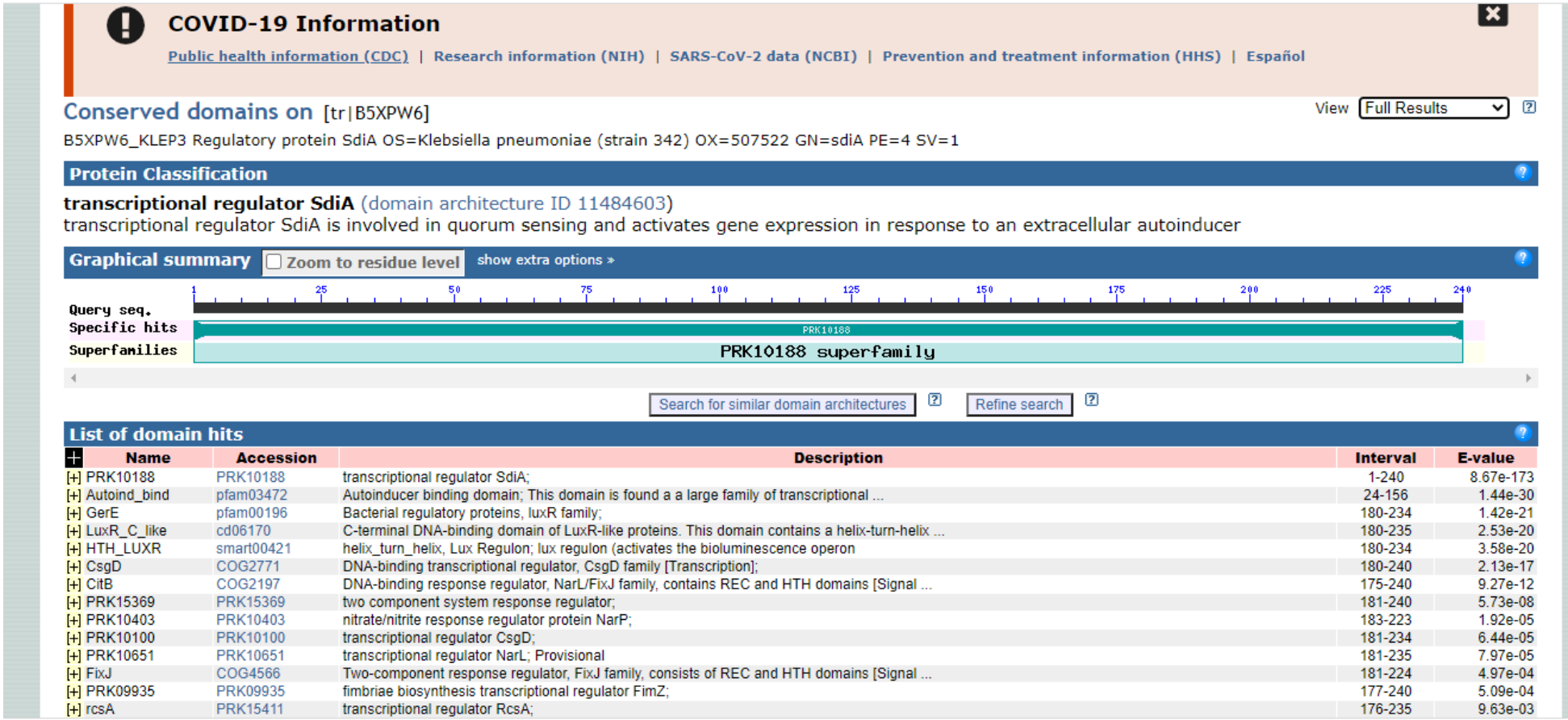

COVID-19 Information

Public health information (CDC) | Research information (NIH) | SARS-CoV-2 data (NCBI) | Prevention and treatment information (HHS) | Español

Conserved domains on [tr|B5XPW6]

View: Full Results

B5XPW6_KLEP3 Regulatory protein SdiA OS=Klebsiella pneumoniae (strain 342) OX=507522 GN=sdiA PE=4 SV=1

Protein Classification

transcriptional regulator SdiA (domain architecture ID 11484603)

transcriptional regulator SdiA is involved in quorum sensing and activates gene expression in response to an extracellular autoinducer

Graphical summary

Zoom to residue level | show extra options »

Search for similar domain architectures | Refine search

List of domain hits

Name	Accession	Description	Interval	E-value
[+] PRK10188	PRK10188	transcriptional regulator SdiA;	1-240	8.67e-173
[+] Autoind_bind	pfam03472	Autoinducer binding domain; This domain is found a a large family of transcriptional ...	24-156	1.44e-30
[+] GerE	pfam00196	Bacterial regulatory proteins, luxR family;	180-234	1.42e-21
[+] LuxR_C_like	cd06170	C-terminal DNA-binding domain of LuxR-like proteins. This domain contains a helix-turn-helix ...	180-235	2.53e-20
[+] HTH_LUXR	smart00421	helix_turn_helix, Lux Regulon; lux regulon (activates the bioluminescence operon	180-234	3.58e-20
[+] CsgD	COG2771	DNA-binding transcriptional regulator, CsgD family [Transcription];	180-240	2.13e-17
[+] CitB	COG2197	DNA-binding response regulator, NarL/FixJ family, contains REC and HTH domains [Signal ...	175-240	9.27e-12
[+] PRK15369	PRK15369	two component system response regulator;	181-240	5.73e-08
[+] PRK10403	PRK10403	nitrate/nitrite response regulator protein NarP;	183-223	1.92e-05
[+] PRK10100	PRK10100	transcriptional regulator CsgD;	181-234	6.44e-05
[+] PRK10651	PRK10651	transcriptional regulator NarL; Provisional	181-235	7.97e-05
[+] FixJ	COG4566	Two-component response regulator, FixJ family, consists of REC and HTH domains [Signal ...	181-224	4.97e-04
[+] PRK09935	PRK09935	fimbriae biosynthesis transcriptional regulator FimZ;	177-240	5.09e-04
[+] rcsA	PRK15411	transcriptional regulator RcsA;	176-235	9.63e-03

Appendix 4.1: Gel electrophoresis of PCR products showing the presence of virulence genes in genes in *K. pneumoniae* (**1**) DNA ladder (**2**) Negative control (**3**) *MrkA* (**4**) *LuxS* (**5**) *RcsA* and (**6**) *16srRNA*

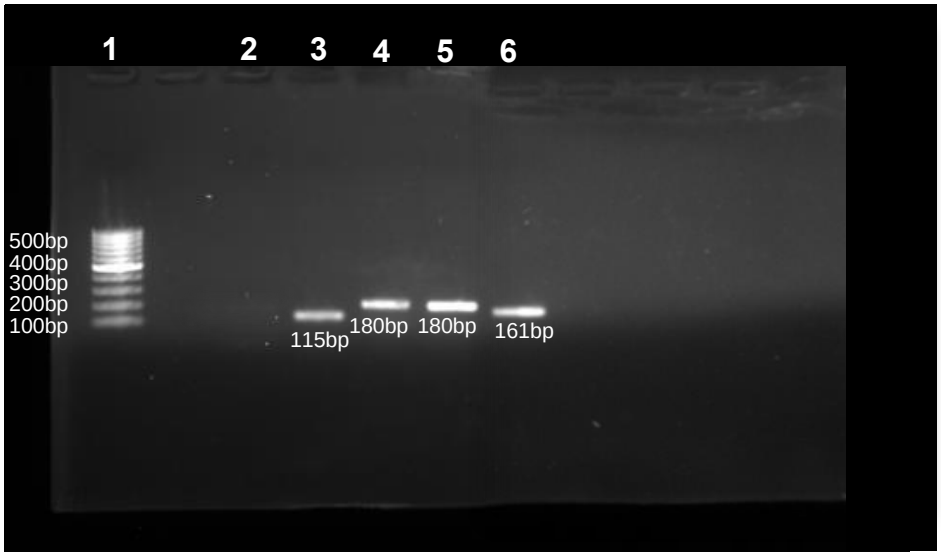

Appendix 4.2: Representative samples of RNA extracted from treated *K. pneumoniae* strains (**1**) DNA ladder (**2**) CBR-KP camphene (**3**) CBR-KP phytol (**4**) CBR-KP quercetin (**5**) CBR-KP ciprofloxacin (**6**) ESBL-KP camphene (**7**) ESBL-KP phytol

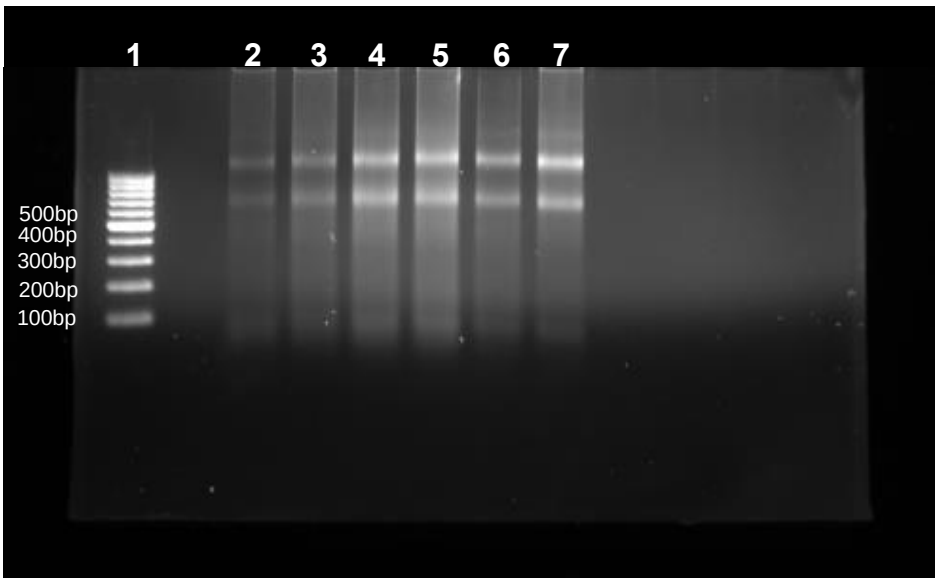

Appendix 4.3: Micrograph images displaying Vero cells exposed to compounds for 48 h at varying concentrations of 0.25 - 0.002 mg/mL. (A) Untreated Vero cells (B) Camphene (C) Phytol (D) Quercetin (E) Doxorubicin

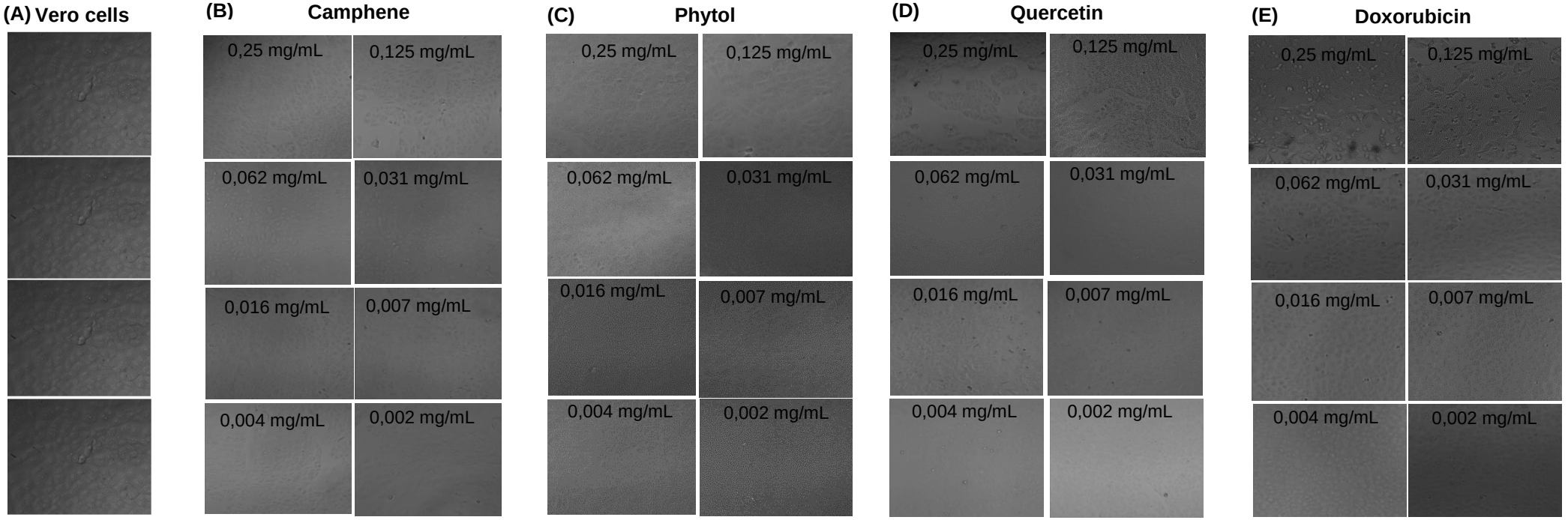

Appendix 5.1: Proof of manuscript submission to Evidence-Based Complementary and Alternative Medicine

Hindawi

Dear Dr. Cosa,

Congratulations, the manuscript titled "Extracts of selected South African medicinal plants mitigate virulence factors in multidrug-resistant strains of Klebsiella pneumoniae" has been successfully submitted to Evidence-Based Complementary and Alternative Medicine.

We will confirm this submission with all authors of the manuscript, but you will be the primary recipient of communications from the journal. As submitting author, you will be responsible for responding to editorial queries and making updates to the manuscript.

In order to view the status of the manuscript, please visit the manuscript details page.

Thank you for submitting your work to Evidence-Based Complementary and Alternative Medicine.